NASA CR-165515
PWA-5736-17

NASA

SENSOR FAILURE DETECTION SYSTEM

FINAL REPORT

by

E. C. Beattie (PWA-CPD)
R. F. LaPrad (PWA-CPD)
M. E. McGlone (PWA-GPD)
S. M. Rock (SCI)
M. M. Akhter (SCI)

August 1981

UNITED TECHNOLOGIES CORPORATION
Pratt & Whitney Aircraft Group
Commercial Products Division

Prepared for

NATIONAL AERONAUTICS AND SPACE ADMINISTRATION
NASA-Lewis Research Center
Contract NAS3-22481

1. REPORT NO.	2. GOVERNMENT AGENCY	3. RECIPIENT'S CATALOG NO.
NASA CR-165515		

4. TITLE AND SUBTITLE	5. REPORT DATE
SENSOR FAILURE DETECTION SYSTEM PROGRAM	6. PERFORMING ORG. CODE

7. AUTHOR(S)	8. PERFORMING ORG. REPT. NO.
E.C.Beattie (PWA-CPD), R.F.LaPrad (PWA-CPD), M.E.McGlone (PWA-GPD), S.M.Rock (SCI), M.M.Akhter (SCI)	PWA 5736-17

9. PERFORMING ORG. NAME AND ADDRESS	10. WORK UNIT NO.
UNITED TECHNOLOGIES CORPORATION Pratt & Whitney Aircraft Group Commercial Products Division	11. CONTRACT OR GRANT NO. NAS3-22481

12. SPONSORING AGENCY NAME AND ADDRESS	13. TYPE REPT./PERIOD COVERED
National Aeronautics and Space Administration Lewis Research Center 21000 Brookpark Road, Cleveland, Ohio 44135	Contractor Report 14. SPONSORING AGENCY CODE

15. SUPPLEMENTARY NOTES

Project Manager, Dr. Walter Merrill, NASA Lewis Research Center, Cleveland, Ohio 44135

16. ABSTRACT

Advanced concepts for detecting, isolating and accommodating sensor failures were studied in this program to determine their applicability to the gas turbine control problem. Five concepts were formulated based upon such techniques as Kalman filters and a screening process led to the selection of one advanced concept for further evaluation. The selected advanced concept uses a Kalman filter to generate residuals, a weighted Sum Square Residuals technique to detect soft failures, likelihood Ratio Testing of a bank of Kalman Filters for isolation, and reconfiguring of the normal mode Kalman filter by eliminating the failed input to accommodate the failure. The advanced concept was compared to a baseline parameter synthesis technique, which was also developed for this program. The advanced concept was shown to be a viable concept for detecting, isolating, and accommodating sensor failures for the gas turbine applications.

17. KEY WORDS (SUGGESTED BY AUTHOR(S))	18. DISTRIBUTION STATEMENT
Sensors, Failure Detection, Failure Isolation, Failure Accommodation, Filtering Techniques, Kalman Filters, Parameter Synthesis, Linear Modeling	UNCLASSIFIED - UNLIMITED

19. SECURITY CLASS THIS (REPT)	20. SECURITY CLASS THIS (PAGE)	21. NO. PGS	22. PRICE *
UNCLASSIFIED	UNCLASSIFIED		

* For sale by the National Technical Information Service, Springfield, VA 22161

FOREWORD

This document was prepared by United Technologies Corporation, Pratt & Whitney Aircraft Group, Commercial Products and Government Products Divisions and Systems Control, Inc. (Vt) to meet the requirements for a Final Report under Contract NAS3-22481, Sensor Failure Detection System.

TABLE OF CONTENTS

TABLE OF CONTENTS (Continued)

LIST OF ILLUSTRATIONS

LIST OF ILLUSTRATIONS (Continued)

LIST OF ILLUSTRATIONS (Continued)

LIST OF ILLUSTRATIONS (Continued)

LIST OF ILLUSTRATIONS (Continued)

LIST OF TABLES

LIST OF TABLES

SECTION 1

SUMMARY

The objective of this program was to develop an advanced concept for the Detection, Isolation, and Accommodation (DIA) of sensor failures in gas turbine engine control systems. Participants in the program were the Commercial Products Division and Government Products Division of Pratt & Whitney Aircraft Group, and Systems Control, Inc. (Vt.), with sponsorship provided by NASA Lewis Research Center.

Five advanced concepts were formulated from advanced techniques for detection, isolation, and accommodation of sensor failures. The concepts were evaluated by application in an F100 engine and Multivariable Control System simulation. The F100 Multivariable Control System was developed under Air Force Contract AFWAL-TR-80-2010. A simplified version of the simulation of the F100 engine and multivariable control system was used in a screening process to select one of these advanced concepts. This simplified simulation was also used as the model for the filters in the various advanced detection, isolation and accommodation concepts.

The selected advanced concept utilizes a Weighted Sum-Squared Residuals technique to detect soft failures. A normal mode Kalman filter; i.e., a filter designed to use all sensor inputs with no failure assumed on those inputs, is used to generate the residuals and the estimated measurements. Detection and isolation of hard-over failures is also accomplished with the normal mode filter by testing for large values of the individual residuals. Isolation of soft failures is accomplished by likelihood ratio based testing of innovations from a bank of Kalman filters, each designed with the assumption of one failed input. Accommodation is accomplished by reconfiguring the normal mode Kalman filter to eliminate the failed sensor from the input.

A baseline detection, isolation and accommodation concept was also developed based upon the conventional techniques of parameter synthesis. Performance of this concept and the selected advanced concept was evaluated in detail on the complete nonlinear dynamic simulation of the engine and control system.

Results of the detailed evaluation demonstrated that the advanced concept is a viable method for a sensor failure detection system. While performance was generally comparable to that of the parameter synthesis based concept, the advanced concept represents a more systematic design approach. Given a reasonably accurate plant model and sensor failure characteristics, the design of the various Kalman filters and detection and isolation tests is relatively straightforward. The parameter synthesis based concept requires significant trial and error analysis and refinement to develop useful gas generator relationships and associated logic for detecting, isolating, and accommodating sensor failures. The evaluation results did show that the simplified model used for the advanced concept was not accurate enough at a number of flight operating points. This was found to result from insufficient linearized data at these flight conditions to constrain the curve fits used in the implementation of the model. Additional refinement of the simplified model is expected to provide significant performance improvements of the advanced concept.

SECTION 2

INTRODUCTION

An orderly transition from hydomechanical control systems to full authority digital electronic control systems is currently in progress throughout the aircraft propulsion industry. Full authority means that all control logic functions are provided in the digital computer. The full authority digital electronic control system will provide increases in turbine life, elimination of ground trim requirements, improved engine performance, and reduced pilot workload as a result of the capability to implement accurate control of engine thrust and temperature ratings.

Other hardware and software features will include a modular construction approach, automatic trouble-shooting and self test devices, and fault tolerance logic. These features will simplify maintenance procedures and thereby reduce maintenance costs for the control system relative to current hydromechanical control systems. Paradoxically, present design philosophy emphasizes hardware redundancy to attain acceptable levels of mission reliability. This program addressed software, or analytical redundancy on measured parameters to provide acceptable mission reliability with minimal sensor hardware redundancy.

The logic programming capability of a full authority digital electronic control allows the incorporation of fault logic to accomplish three basic functions: 1) computer self-test; 2) actuator interface failure identification; and 3) sensor failure detection, isolation and accommodation (DIA). Fault tolerance logic can provide essentially fail operational control capability with a minimum number of parts and therefore contributes to a reduction in control related Mean Time Between In-Flight Shutdowns. For military aircraft, this means improved weapon system availability and mission effectiveness.

Over the past decade of electronic control system development, extensive work has been accomplished in the areas of developing comprehensive techniques for computer self-test and actuator interface failure identification. Relatively simplistic techniques have been applied to the sensor failure DIA problem.

Several techniques are available for the application to the sensor failure DIA task. For hard-over failures of sensors, simple range-check logic provides the simplest detection procedure, but redundant sensors, measurement synthesis, or control mode modification are required to accommodate the failed sensor. Soft failures, such as sensor drift, and sensor noise require more sophisticated logic or redundancy of sensors. With triple sensors, voting logic can be implemented to determine sensors with soft failures; however, these redundant sensors significantly increase control system cost, weight, complexity, and failure rate.

Therefore, to minimize the impact of hardware redundancy requires the development of a software detection, isolation and accommodation concept which can provide "analytical redundancy" equivalent to having multiple hardware sensors. The conventional approach for accomplishing this is to synthesize values

of measurements from other available parameters in the control system by using gas generator functional relationships, such as shown in Figure 1. Such synthesized measurements can be compared with single sensor measurements, or with dual measurements in a voting scheme, to evaluate the health of the sensors. A tolerance band must be established between synthesized and measured values to avoid false alarms due to:

- o Uncertainty in synthesis curves
- o Actuator failure impacts
- o Sensor tolerances
- o Engine-to-engine tolerances
- o Horsepower and bleed extraction variations in-service
- o Engine deterioration
- o Transient versus steady state conditions

The effort to develop the parameter synthesis technique and to minimize the required tolerance band to accommodate these effects can be substantial.

More sophisticated concepts such as the Kalman filter, whose typical implementation is shown in Figure 2, have also been suggested for the gas turbine sensor failure problem. Such techniques may offer a more systematic approach to the design of an effective sensor detection, isolation and accommodation concept and can automatically accommodate, in theory, many of the above variations which require a tolerance band for the parameter synthesis technique. However, basic research in this area has resulted in a proliferation of such advanced techniques. It is not obvious which of these techniques can be successfully applied to the gas turbine engine sensor problem and result in a sensor failure detection, isolation and accommodation concept which performs better than the conventional parameter synthesis approach.

To evaluate the applicability of the advanced detection, isolation and accommodation concepts to gas turbine engines, NASA Lewis Research Center sponsored the program which is the subject of this report. To accomplish the program goals, a team was established, consisting of Pratt & Whitney Aircraft Commercial and Government Products Division and Systems Control Inc. (Vt), (SCI) of California, with Pratt & Whitney Aircraft Commercial Products Division (CPD) being the prime contractor. Figure 3 shows the team members' primary responsibilities for this program. This program utilized the F100 engine and F100 Multivariable Control (MVC) logic (described in Section 3.1), developed under Air Force contract, as the test bed system for concept evaluation.

A summary of the complete program is presented in the following paragraphs:

The types of sensors to be used for the engine parameters required in the F100 Multivariable Control System were selected. Typical state-of-the-art transducers were selected to ensure a realistic definition of the sensor failure modes and characteristics. Sensor failure characteristics for the selected sensor types were defined and quantified according to the predominant failure categories of out-of-range, drift, and noise. This task is described in detail in Section 3.2.

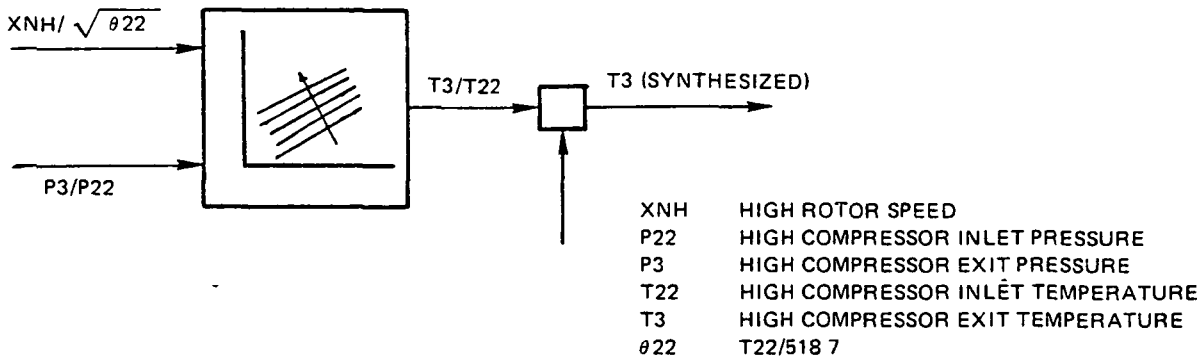

Figure 1 Examples of Synthesis of a Parameter from Gas Generator Characteristics - Compressor discharge temperature may be synthesized from a functional relationship between corrected rotor speed, pressure ratio, and compressor inlet temperature.

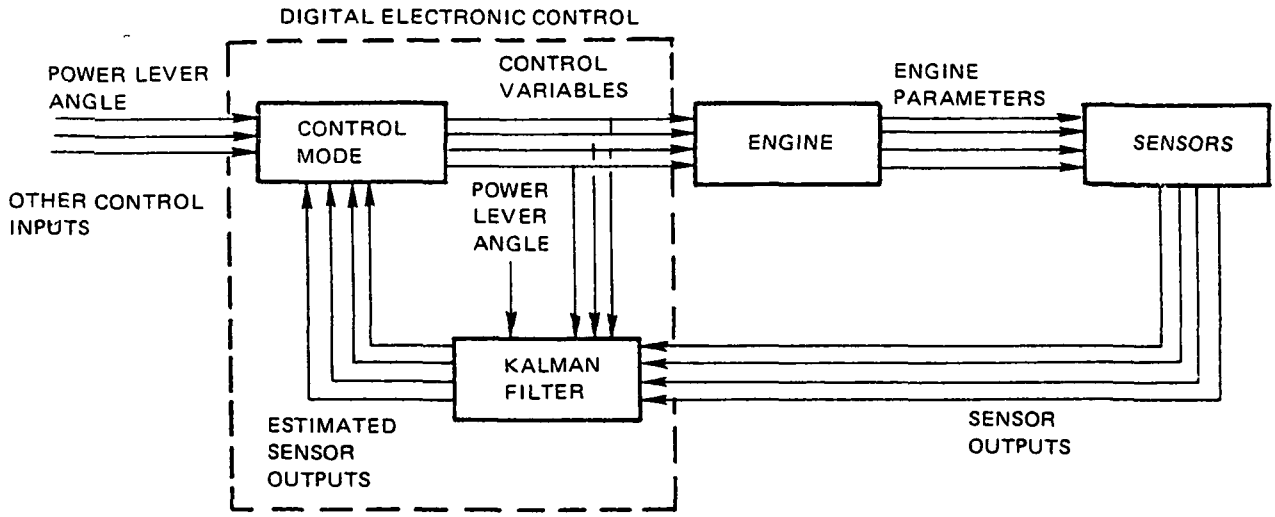

Figure 2 Typical Implementation of a Kalman Filter - Sophisticated logic may be implemented in the electronic control to estimate sensor outputs contaminated by noise or to synthesize a parameter when its sensor fails.

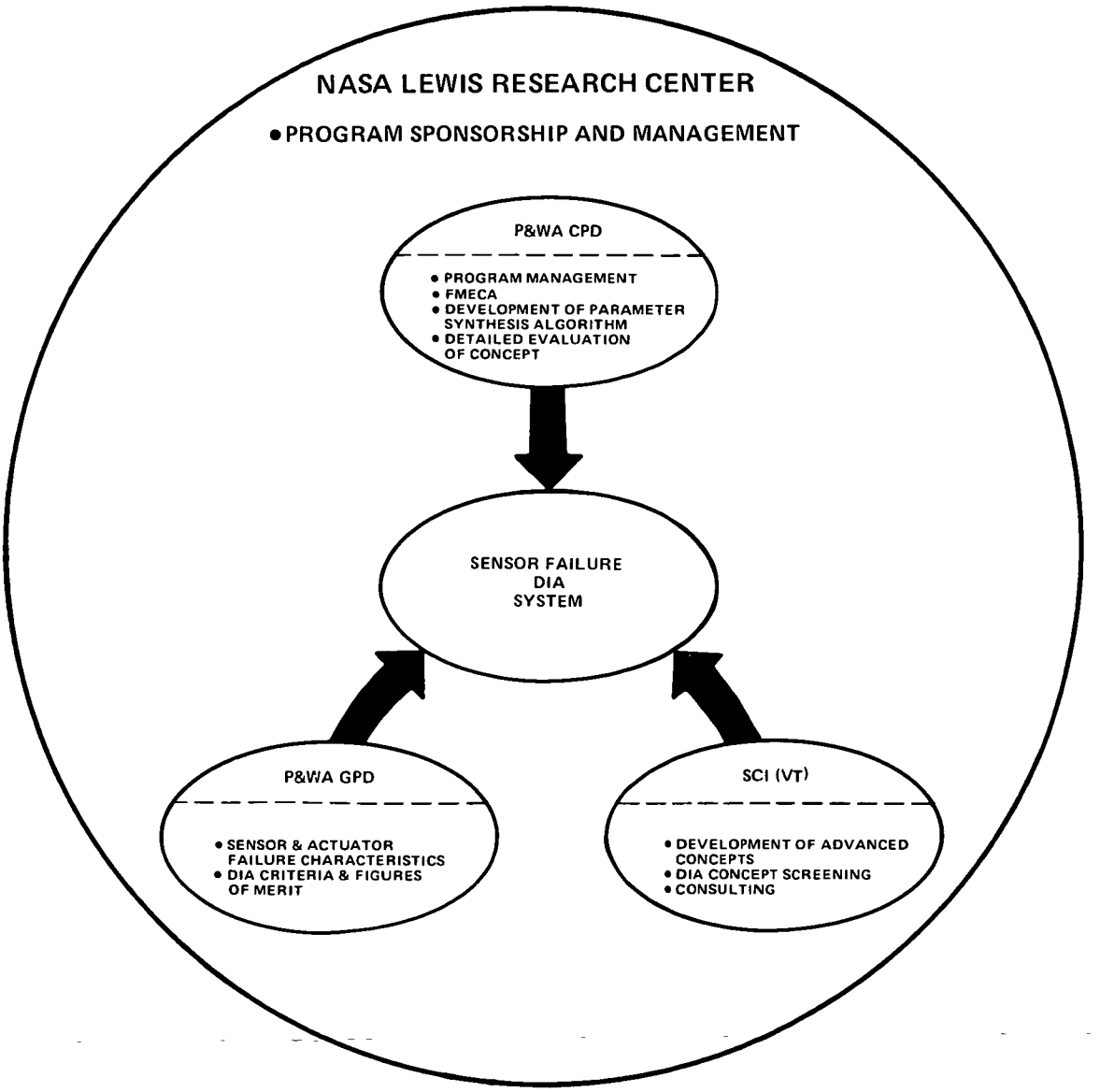

Figure 3 Team Members and Primary Responsibilities

A Failure Mode and Effects Criticality Analysis (FMECA) was conducted using the F100 Multivariable Control System simulation. Each sensor failure was evaluated at 15 flight operating points. This provided the necessary information to classify the various failure modes into categories of critical and non-critical failures. Critical failures are defined as any failure which results in a fan or compressor surge, excessive thrust variation (greater than 10%) or a rotor overspeed above the operating limits. A detailed description and the results of this study are included in Section 3.3.

A Detection, Isolation and Accommodation (DIA) concept scoring system was developed which quantitatively and qualitatively evaluates the candidate concept for:

1. DIA Criteria
2. DIA Detection Performance
3. DIA Figures of Merit

The DIA criteria are defined as the set of transient and steady state operational requirements which the propulsion system must satisfy in the event of various potential sensor failures in order to meet minimum aircraft operational requirements. DIA Detection Performance relates to how effective the concept is in terms of detecting and isolating a sensor failure. In other words, if the DIA concept has excellent accommodation capability, but cannot consistently detect failures, then it is not a good concept. The DIA figures of merit are more qualitative in nature, and are defined as the benefits of bettering DIA criteria in the event of single failures or meeting criteria in the event of multiple sensor failures. The details of the evaluation approach and the evaluation results are described in Section 3.4.

Available techniques for detection, isolation, and accommodation were reviewed to determine which techniques or combination of techniques yield detection, isolation and accommodation concepts having a theoretical basis applicable to the turbine engine sensor failure problem. From this review, a set of five candidate concepts was selected. These concepts were formulated to span as many of the applicable techniques as possible. The advanced detection, isolation and accommodation techniques which were reviewed are discussed in Section 4.3.

A simplified F100 engine simulation was constructed for use in screening the five concepts in order to minimize computer run times. The simplified simulation consists of a fourth order state variable model augmented with nonlinear steady state relationships to result in an accurate representation of nonlinear engine characteristics. The details of the development of the simplified nonlinear model are discussed in Section 4.2. The five candidate concepts were implemented in the simplified simulation and evaluated relative to performance for single sensor failures. Using the detection, isolation and accommodation scoring system, each candidate concept was quantitatively evaluated on its ability to detect, isolate and accommodate the single sensor failures as well as on their ability to satisfy the criteria as previously described. Two concepts were selected from this initial screening process. A more detailed analysis was conducted on these two concepts. This evaluation led to the selection of one concept for implementation and evaluation on the detailed nonlinear F100 engine. Results of the concept evaluation process are presented in Section 4.4.

In addition to investigating advanced detection, isolation and accommodation concepts, an algorithm, based upon conventional Parameter Synthesis techniques, was developed as a baseline system for evaluating the performance of the selected advanced concept. The parameter synthesis based algorithm is described in Section 4.1

A detailed evaluation of the parameter synthesis based algorithm and advanced concept detection, isolation and accommodation algorithm was conducted by simulating sensor failures for both steady state and transient operation at the 15 flight operating points, using the nonlinear F100 Multivariable Control System simulation. The evaluation results of the two algorithms were compared to determine the benefits of implementing advanced algorithms in production control systems, rather than the conventional parameter synthesis techniques currently used. The results of this comparison are presented in Section 5.

SECTION 3.0

PROBLEM DEFINITION

The initial portion of this program was concerned with defining and characterizing the subject engine control system sensor failures and developing a scoring system for evaluating advanced detection, isolation and accommodation concepts. This effort as shown in Figure 4 involved a review of the F100 Multivariable Control (MVC) System requirements, defining the sensor types to be used and determining the various failure modes of those sensors. A Failure Mode and Effects Criticality Analysis (FMECA) was performed to determine the impact of a sensor failure on engine operation and thereby establish which sensors are critical. Detection, isolation and accommodation criteria, figures of merit, and an overall evaluation methodology were established to provide a quantitative basis for concept selection.

The following paragraphs present a detailed description of this portion of the program.

3.1 F100 ENGINE AND MULTIVARIABLE CONTROL MODE DESCRIPTION

The engine selected as a testbed system for evaluating sensor failure Detection, Isolation, and Accommodation (DIA) concepts is a Pratt & Whitney Aircraft F100 afterburning turbofan, representative of current high technology engines. The F100 is low bypass ratio, twin-spool, axial-flow turbofan engine, consisting of the following components:

- Three-stage fan driven by a two stage turbine
- Ten-stage compressor driven by an aircooled two-stage turbine
- Main burner with an annular chamber
- Annular fan duct that surrounds the basic gas generator and discharges air in the mixed flow augmentor.
- Variable area nozzle

An inlet guide vane with a movable trailing edge to achieve variable airfoil camber is used ahead of the fan to improve inlet distortion tolerance and fan efficiency. The first three stators of the high compressor are variable to improve starting and high Mach number characteristics. Airflow bleed is extracted at the compressor exit for installation requirements and starting. The exhaust nozzle for the engine is a balance beam design with actuated divergent flap. The variable geometry of the balanced-beam nozzle enables all three nozzle performance parameters (nozzle area, expansion ratio, and boattail drag) to be simultaneously near optimum throughout the operating range.

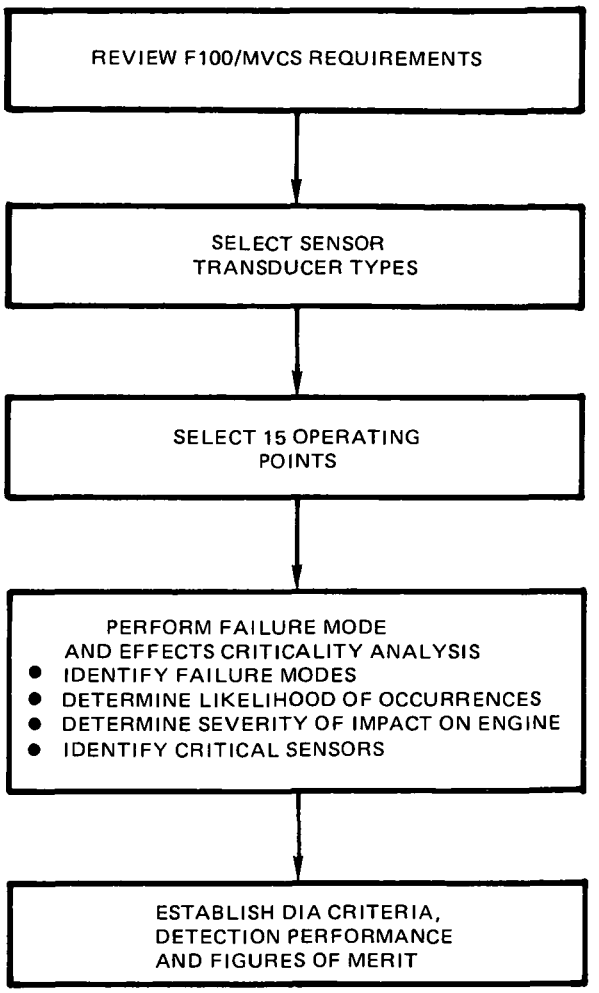

Figure 4 Task I Failure Definition Procedure

The engine simulation includes a simulation of the multivariable control mode. This control mode was developed by Systems Control, Inc. and Pratt & Whitney Aircraft under the F100 Multivariable Control Synthesis Program (Air Force Contract No. AFWAL-TR-80-2010) which was funded as a cooperative effort between the Air Force Aero Propulsion Laboratory and NASA Lewis Research Center.

A simplified block diagram of the F100 multivariable control system is shown in Figure 5. The control mode is basically proportional plus integral with a feed-forward path to provide rapid response. The proportional control action is provided by the Linear Quadratic Regulator, (LQR) with the regulator gains C_P able to affect changes in all of the available control variables U to reduce deviations in all of the state variables X relative to the specified reference point X_{nom}. The state, control, and output variables used in the multivariable control are as follows:

State Variables	Control Variables	Output Variables
Fan Speed	Fuel Flow	Thrust
Compressor Speed	Nozzle Area	Fan Airflow
Afterburner Pressure	Compressor Inlet Variable Vanes	Burner Temperature
Fuel Flow	Rear Compressor Variable Vanes	Fan Surge Margin
Burner Pressure	Bleed Flow	Compressor Surge Margin

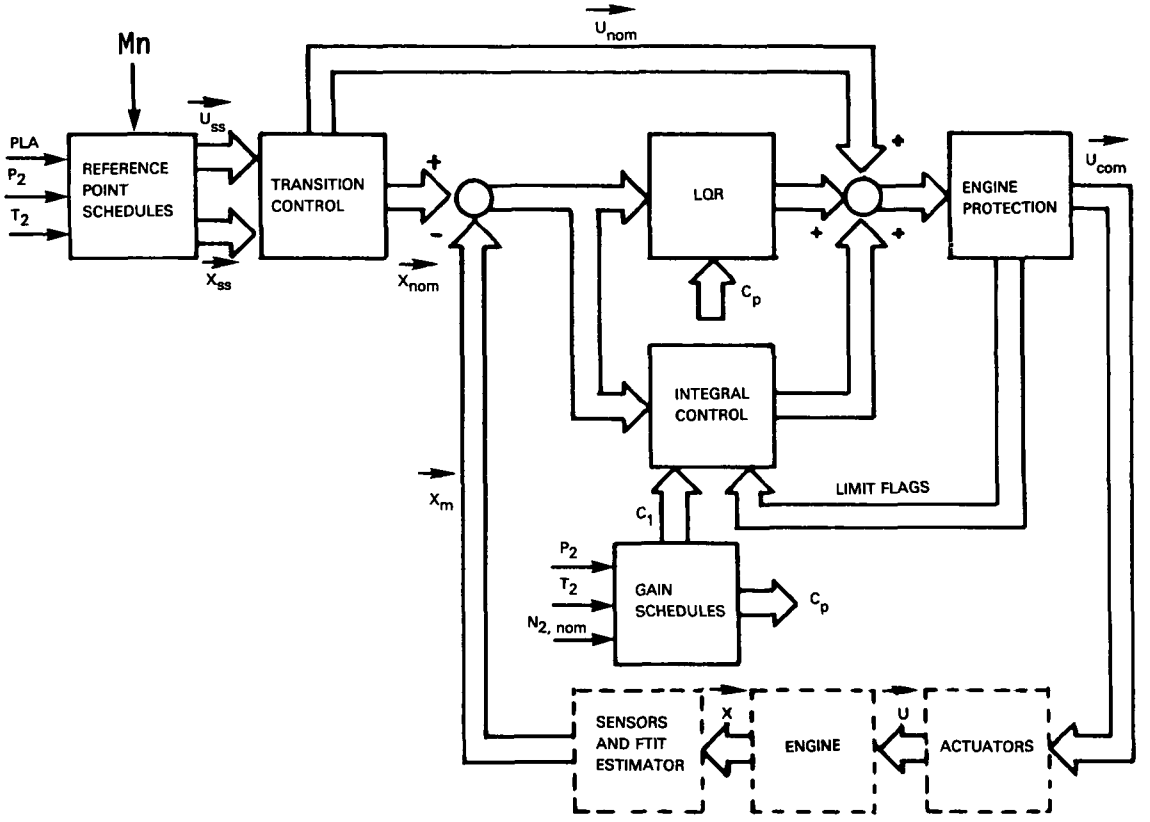

Figure 5 Simplified Block Diagram of F100 Multivariable Control System

The feedback law itself represents an optimal regulator structure with integral trims for steady-state accuracy and a model following implementation to prevent saturation during transients. Each element of the control law is described briefly below.

The control law is written for small perturbations of state and control variables about an equilibrium condition. The equilibrium conditions must be derived approximately by the controller given the requested power level, altitude, Mach number, engine face pressure and temperature. A functional (or tabular) description of these equilibrium conditions is a reference point schedule.

The reference schedules are produced by calculating the thermodynamic equilibrium associated with a given control vector at a representative group of subsonic and supersonic flight points. Nondimensionalized quantities were then utilized to fit approximate reference points with minimum complexity.

When a large transition in power is requested by the pilot, the small perturbation character assumed in the regulator design is lost. A large change in the reference state vector will cause large commanded inputs. This tends to saturate actuators and produce significantly nonlinear behavior unless a feed forward control input is provided. The transition control generates this signal. A regulator can then be used to track the compatible trajectory taking the system from one state to another.

The dynamic response of the engine is affected strongly by the air mass flow. Power level, altitude and Mach number determine this mass flow and the response. The linearized control synthesis procedure produces regulator gains that control the engine satisfactorily in the neighborhood of the design flight/power point. To implement a continuous envelope-wide controller, the gains are varied as the system makes the transition from one condition to another.

The gain scheduling adopted for the F100 implementation approximately fits important gain elements with univariate functions of the engine face density and rotor speed. The former variable accounts for altitude effects, while the latter schedules the power condition. Dominant gain elements were determined by assessing the closed-loop ergenvalue sensitivity of the system to each gain element and eliminating those that do not affect closed-loop response.

The engine set-point is a group of reference values of states and controls which the engine must attain exactly in steady-state. These values define the equilibrium point. Error terms are calculated between these reference values and corresponding sensed values. These error terms always are integrated unless the associated control variables are driven transiently into saturation. To avoid integrator wind-up due to this uncontrollable situation, the appropriate error is switched out until the transient command tends to cause the control to unsaturate. This switching logic provides smooth and controlled engine transition for changes in power and flight condition.

The engine protection logic provides hard limits on the commands to the control actuators. The engine protection logic includes fuel flow, variable vane, bleed air and exhaust nozzle area limits. Whenever a commanded actuator position exceeds a specified limit or when a control saturation is detected, a flag is set with the control logic. These flags send a signal within the logic to clamp and hold the appropriate trim integrator to prevent integrator wind-up.

Temperature limiting during transient and steady-state operation is a critical function of any turbine engine control system. For the F100, the maximum temperatures specified for compressor discharge and turbine inlet stations in the gas path are implicitly limited by the maximum fan turbine inlet temperature (FTIT). The fan turbine inlet temperature sensor output response is extremely slow relative to the temperature overshoot criteria, however. Compensation of this signal was, therefore, required to provide adequate temperature limiting during transient maneuvers. For the F100 Multivariable Control System program, this was implemented with a steady-state, third-order filter to estimate fan turbine inlet temperature. For the Sensor Failure Detection System program, this filter was eliminated since fan turbine inlet temperature was one of the variables used in the advanced detection, isolation, and accommodation algorithm.

3.2 SELECTED SENSOR SET AND FAILURE CLASSIFICATIONS

3.2.1 Selection of Sensor Set

A list of the required engine sensors and sensor types was compiled for F100 Multivariable Control (MVC) application.Typical state-of-the-art sensors were selected for the engine parameters to ensure the best chance of defining realistic sensor failure modes and characteristics. Sensor selection was also directed toward satisfying hardware requirements such as availability, cost, reliability, durability and system compatability. A list of the sensed variables and associated sensor types is shown in Table I.

The advanced Detection, Isolation and Accommodation algorithms and the parameter synthesis based algorithm developed for this program were designed to detect, isolate and accommodate failures of the PT6, PT4, N1, N2, and fan turbine inlet temperature sensors. These parameters were selected since they are basic feedback parameters in the Multivariable Control Mode.

3.2.2 Sensor Failure Classification

Sensor failure rates and failure modes were defined for the selected sensor set. The failure rates for each type of sensor and its associated electrical harness were obtained from historical U. S. Air Force records for the F100 military engine and from failure mode and effects analysis conducted by Pratt & Whitney Aircraft and component vendors in support of other electronic control development programs.

TABLE I

ENGINE PARAMETER SENSOR LIST
Multivariable Control for the F100 Engine

Sensed Variable	Symbol	Sensor Type
Engine Face Temperature	TT2	Thermocouple
Engine Face Pressure	PT2	Vibrating Cylinder
Fan Discharge Temperature	TT25	Thermocouple
Fan Speed	N1	Magnetic Pickup
Compressor Speed	N2	Alternator Winding
Burner Pressure	PT4	Vibrating Cylinder
Fan Turbine Inlet Temperature	FTIT	Thermocouples
Augmentor Total Pressure	PT6	Vibrating Cylinder
Jet Area Servo Stroke	AJ	Resolver
Compressor Inlet Variable Vane Angle	CIVV	Resolver
Rear Compressor Variable Vane Angle	RCVV	Resolver

In a military configuration, the typical short flight mission may not allow adequate time for an accurate diagnosis of control system problems. In addition, the increased complexity of the high performance control system required for an application such as the F100 engine can often result in misdiagnosis of system problems. Since the component is charged with a failure when it is removed and replaced, a misdiagnosis problem may unjustifiably increase the failure rate of an individual component in military records. In addition, the temperature and vibration environment experienced with a military application are more severe than with a commerical application. Therefore, the failure rates may differ from those recorded for commercial control systems.

The sensor failure rates were broken down into the predominant failure categories of out-of-range, drift, and noise. The failure category of noise consists of all unconfirmed in-range intermittent failures. Block diagrams of the sensor configurations and their associated failure rates are shown in Figures 6 through 10 and summarized in Table II. The predominant causes of in-range sensor failures are presented in Appendix A.

As shown on Table II, the total failure rate for one complete set of sensors required for the multivariable control application is 406 failures per million hours. To put this number in perspective, the failure rate of a total multivariable control system (including all control components such as pumps, ignition system, actuators, etc.) with sensor hardware redundancy is 3706 failures per million hours. By replacing one set of the redundant sensors with analytical redundancy (advanced concepts), the total system failure rate would be reduced from 3706 to 3300 failures per million hours. Therefore, incorporating advanced concepts to detect, isolate, and accommodate sensor failures has a potential for reducing the total control system failure rate by approximately 11%.

TABLE II

SENSOR FAILURE RATES

Sensor	Failure Rate/ Million Hours	Out of Range	Drift %	Noise %
N1	22	93	1	6
N2	22	80	10	10
TT2	43	87	12	1
FTIT	222	20	79	1
PT2	18	89	10	1
PT6	18	89	10	1
Pb	18	89	10	1
TT2.5	43	87	12	1
	406			

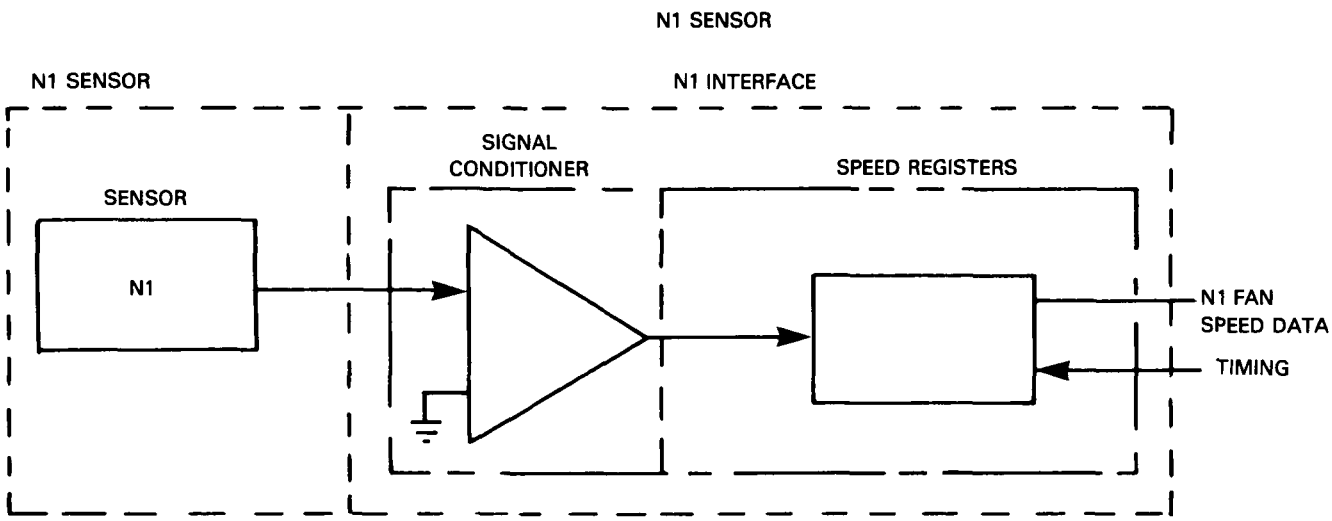

N1 SENSOR AND CABLE

λ^* = 17/MILLION HOURS

OUT-OF-RANGE	= 94%
DRIFT	= 0%
NOISE	= 6%

TOTAL SYSTEM

λ = 22/MILLION HOURS

MTB = 45,454

N1 INTERFACE

λ = 5/MILLION HOURS

OUT-OF-RANGE	= 90%
DRIFT	= 5%
NOISE	= 5%

*λ = FAILURE RATE IN TERMS OF NUMBER OF FAILURES PER MILLION OPERATIONAL HOURS

Figure 6 N1 Sensor configuration

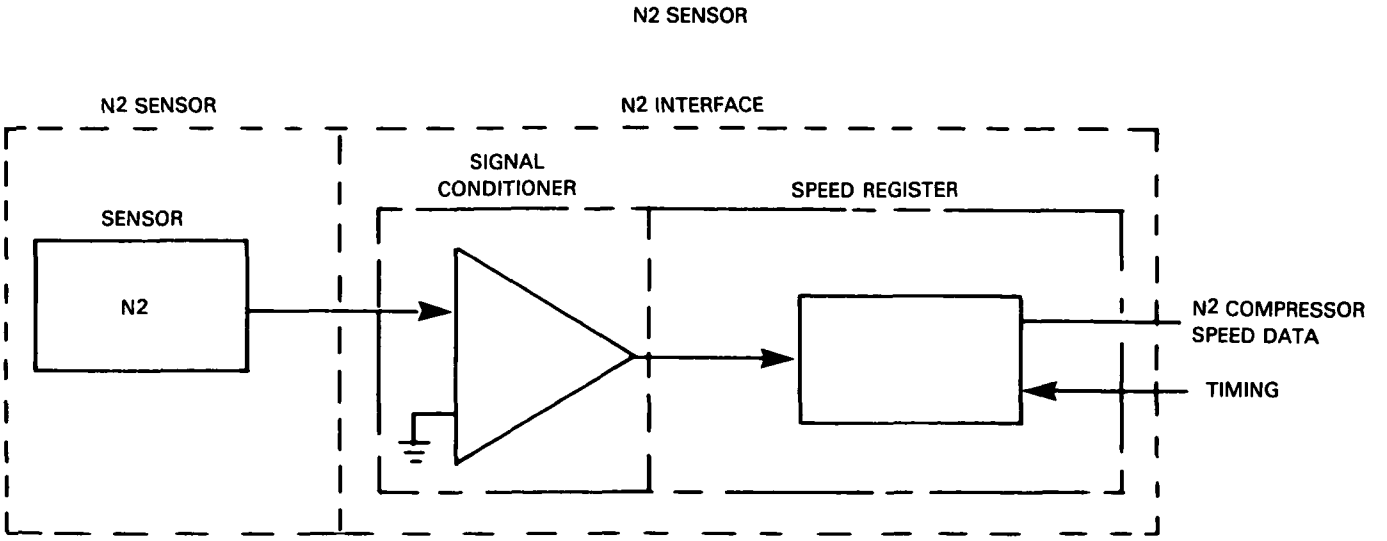

N2 SENSOR AND CABLE

λ^* = 17/MILLION HOURS

OUT-OF—RANGE	= 80%
DRIFT	= 10%
NOISE	= 10%

TOTAL SYSTEM

λ = 22/MILLION HOURS
MTB = 45,454

N2 INTERFACE

λ = 5/MILLION HOURS

OUT-OF-RANGE	= 90%
DRIFT	= 5%
NOISE	= 5%

*λ = FAILURE RATE IN TERMS OF NUMBER OF FAILURES PER MILLION OPERATIONAL HOURS

Figure 7 N2 Sensor configuration

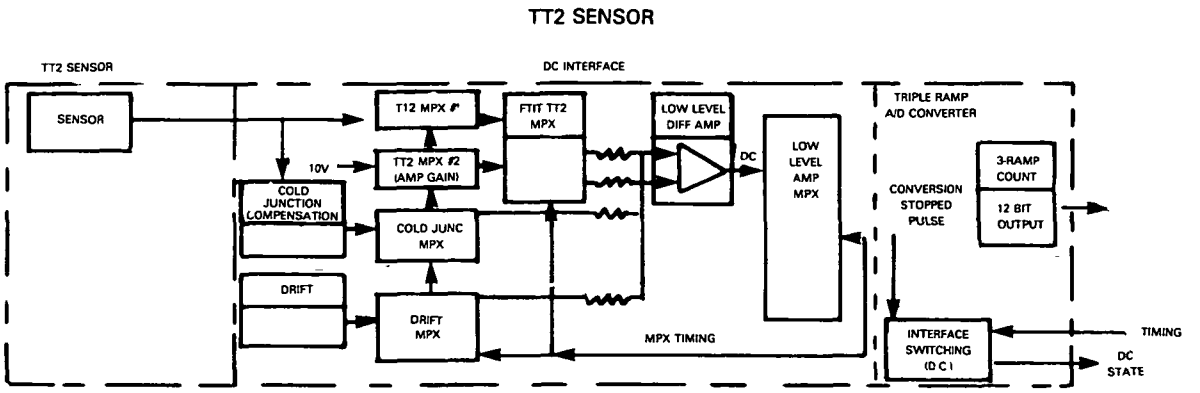

TT2 SENSOR AND CABLE

λ = 33/MILLION HOURS

OUT-OF-RANGE	= 90%
DRIFT	= 10%
NOISE	= 0%

TOTAL SYSTEM

λ = 43/MILLION HOURS
MTB = 23,255

TT2 INTERFACE

λ = 10/MILLION HOURS

OUT-OF-RANGE	= 75%
DRIFT	= 20%
NOISE	= 5%

*λ = FAILURE RATE IN TERMS OF NUMBER OF FAILURES PER MILLION OPERATIONAL HOURS

Figure 8 TT2 Sensor configuration

FTIT SENSOR

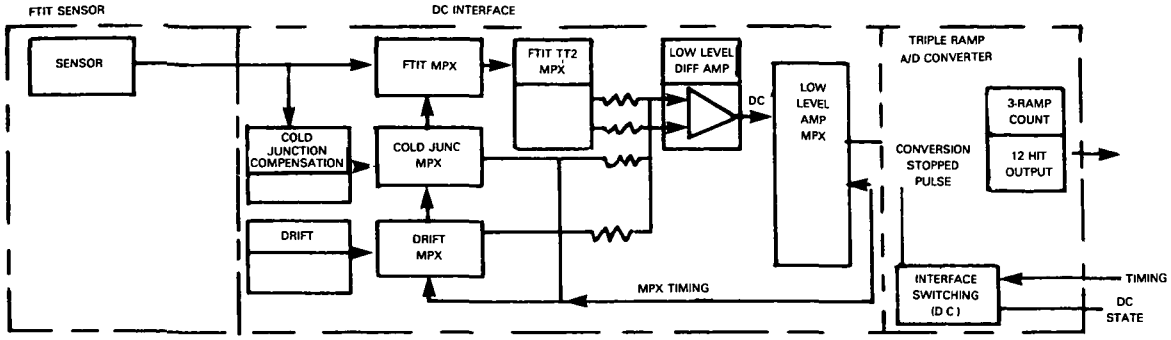

FTIT SENSOR AND CABLE

λ= 212/MILLION HOURS

OUT-OF-RANGE	= 18%
DRIFT	=82%
NOISE	= 0%

TOTAL SYSTEM

λ = 222/MILLION HOURS
MTB = 4500

FTIT INTERFACE

λ= 10/MILLION HOURS

OUT-OF-RANGE	=75%
DRIFT	=20%
NOISE	= 5%

*λ = FAILURE RATE IN TERMS OF NUMBER OF FAILURES PER MILLION OPERATIONAL HOURS

Figure 9 FTIT Sensor configuration

PT4 SENSOR

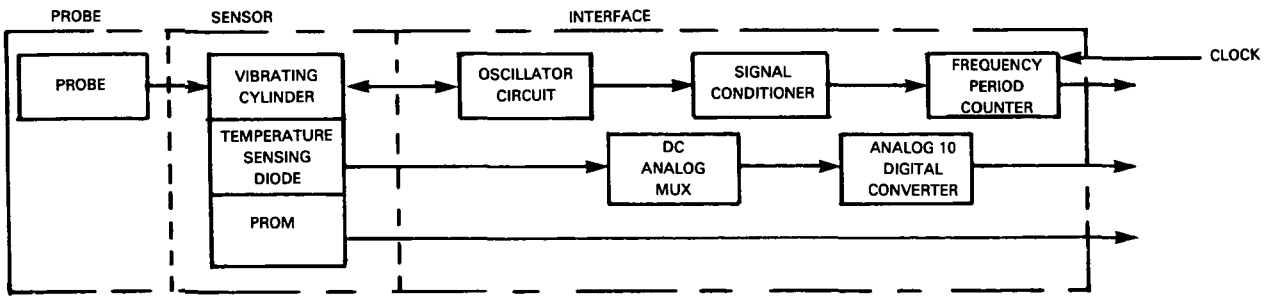

PROBE AND SENSOR

λ= 11/MILLION HOURS

OUT-OF-RANGE	= 88%
DRIFT	= 11%
NOISE	1%

TOTAL SYSTEM

λ = 18/MILLION HOURS
MTB = 55,000

INTERFACE

λ= 7/MILLION HOURS

OUT-OF-RANGE	=90%
DRIFT	10%
NOISE	= 0%

*λ = FAILURE RATE IN TERMS OF NUMBER OF FAILURES PER MILLION OPERATIONAL HOURS

Figure 10 PT4 Sensor configuration

3.3 FAILURE MODE AND EFFECTS CRITICALITY ANALYSIS

3.3.1 Introduction

An engine sensor Failure Mode and Effects Criticality Analysis (FMECA) was conducted with the objective of dividing the sensor set into critical and non-critical sensors. This allows proper emphasis to be placed upon developing concepts which can provide good detection, isolation and accommodation of failures of critical sensors.

A list of the required engine sensors and sensor types was compiled for F100 Multivariable Control (MVC) application as described in Section 3.2 The sensor types were selected to satisfy the accuracy and environmental requirements of the system. Using this selected sensor set, sensor failure characteristics were defined, including modes of failure, such as drift, out-of-range failures, and a failure category referred to as noise, which includes unconfirmed in-range intermittent failures. The magnitude of allowable sensor drift and the failure rates for the different failure modes were also determined during this study.

The impact of these sensor failure characteristics was evaluated on the nonlinear dynamic simulation of the F100 multivariable control system. This evaluation was accomplished at the fifteen (15) flight operating points selected for the detection, isolation, and accommodation concept evaluation to determine the impact on steady state and transient engine performance.

3.3.2 Impact of Out-of-Range Failures on Steady State Operation

Computer analysis, using the detailed nonlinear F100 multivariable control simulation, was conducted to determine the effects of out-of-range sensor failures on gas generator operation. Out-of-range sensor failures for each input sensor were simulated at the flight operating points by individually failing the sensors to their high and low range limits, and observing the steady state results. The results of this study are shown in Appendix A.

All out-of-range failures can exhibit critical failure characteristics at some of the flight operating points. Critical failures were defined as failures that result in a fan or compressor surge, excessive thrust variation (greater than 10%), or a rotor overspeed above the operating limits.

3.3.3 Impact of In-Range Sensor Failures on Steady State Operation

The impact of in-range sensor failures on steady state operation was also evaluated on the nonlinear simulation. As previously discussed, an in-range sensor failure can result in sensor drift anywhere between the accuracy of the sensor to the out-of-range limit. Therefore, a study was conducted to examine various levels of drift at each flight operating point, for each sensor, to determine the minimum drift which would cause a critical failure situation; i.e., the minimum drift that a detection, isolation and accommodation algorithm must be capable of detecting. The flight operating points reflect those conditions which exhibit the most severe consequences to out-of-range failures. The results are summarized in Table III.

TABLE III

MINIMUM SENSOR DRIFT FOR A CRITICAL FAILURE SITUATION

Sensor	Flight Operating Points	Minimum Drift (% of Point)
N2	20K ft/.30Mn, 83° PLA	3.4% (423 rpm)
T2	10K ft/.9Mn, 83° PLA	74% (76°F)
PT2	0 ft/1.2Mn, 83° PLA	16.9% (6 psi)
PT6	0 ft/0Mn, 20° PLA	113% (18 psi)
FTIT	65K ft/2.5Mn, 83° PLA	2.7% (45°F)
PT4	0 ft/0Mn, 83° PLA	22% (80 psi)
T25	0 ft/0Mn, 20° PLA	70% (70°F)

The N1 drifts were not considered in this study, since an in-range failure of this sensor is very unlikely (.22 failures/million hours). For a fan turbine inlet temperature in-range drift, critical failure characteristics will occur for all failures where the sensed temperature drifts to a fixed temperature above the control limit. This failure would result in a constant negative error term in the protection loop, causing fuel flow to drive down, resulting in excessive thrust loss.

A fan turbine inlet temperature in-range sensor drift could also exhibit critical failure characteristics for those failures where the sensed temperature drifts to a fixed temperature below the control limit. This failure mode would increase fuel flow and produce overtemperaturing of the turbine at the flight operating points in which the engine normally operates near the temperature limit.

3.3.4 Effect of Operating With Failures During Transient Operation

Power lever transients were run with out-of-range failures at those flight conditions where, in steady state, the failure produced marginally critical engine operation. These results showed more severe failure consequences transiently than in steady state. This reconfirmed the need to evaluate the detection, isolation and accommodation algorithms transiently, as well as in steady state. An example of transient operation is shown on Figure 11. The dashed line on this figure shows the effects on compressor surge margin resulting from failing the PT6 sensor out-of-range to its upper limit at idle power. The solid line shows the same failure at military power followed by a snap decel to idle occurring at five (5) seconds. This illustrates significantly greater loss of compressor surge margin during the snap decel to idle than in the steady state idle failure case.

3.3.5 Effects of Intermittent In-Range Sensor Failures

In-range intermittent sensor failure, which is referred to as noise for the purposes of this study, was considered for the failure mode and effects criticality analysis. However, upon examining field service data, it was found

that this failure category encompasses all unconfirmed intermittent failures reported mostly by pilot complaint. Therefore, very little quantitative data existed which made it very difficult to model. In addition, the failure rates for this category were shown to have a low probability of occurrence for the pressure and temperature sensors. It was therefore decided not to include this failure category in the analysis.

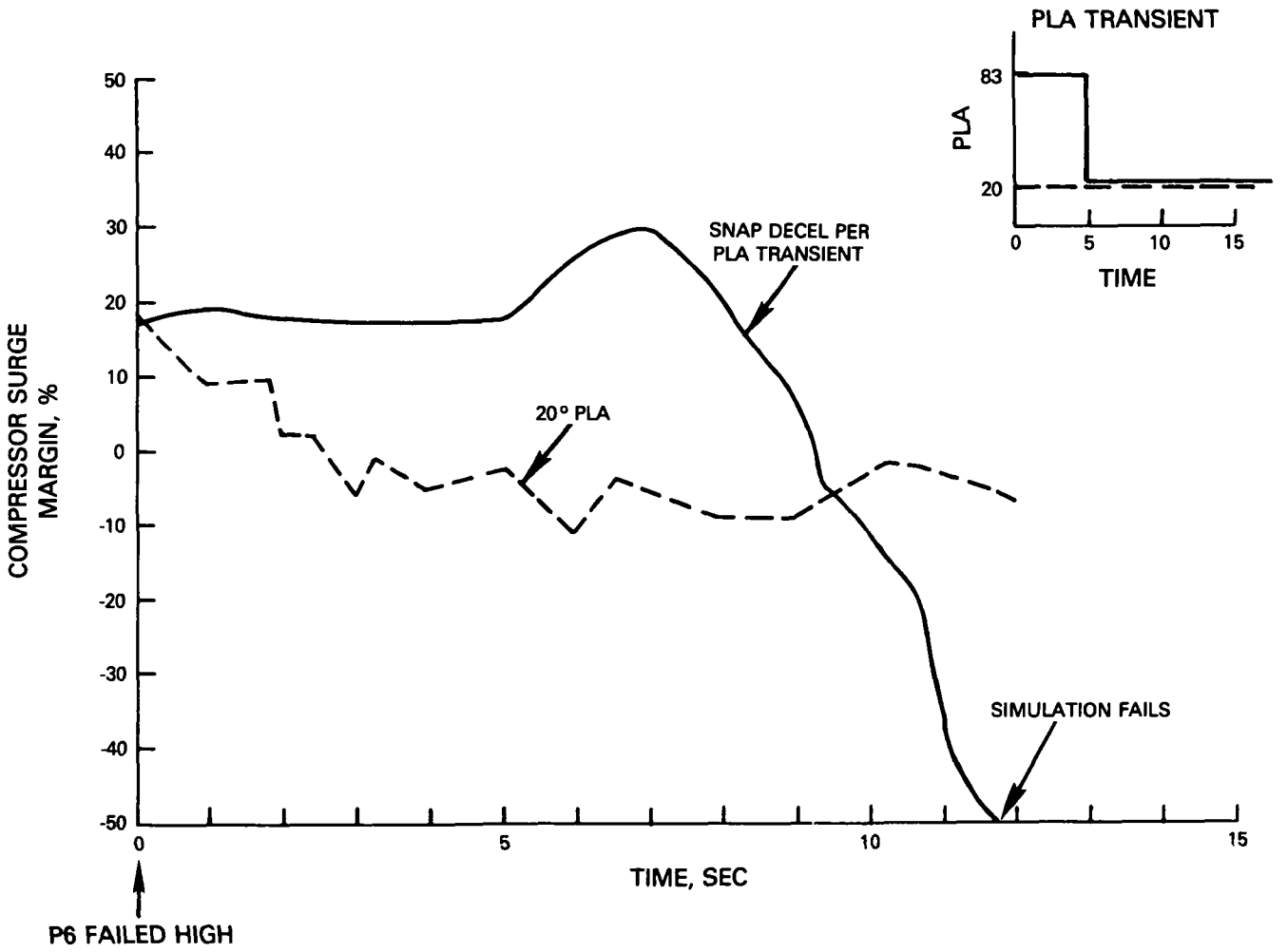

Figure 11 Typical Transient Operation - PT6 Sensor Failed Out-of-Range

3.3.6 Effects of Multiple Failures

After completing the single failure portion of the failure mode and effects criticality analysis, it was obvious that including multiple sensor failures would not be a meaningful addition to the study. This became apparent when all single sensor failures were shown to exhibit critical failure characteristics.

3.3.7 Summary of Results

A summary of the failure mode and effects criticality analysis results is shown in Table IV. This table illustrates that all out-of-range failures exhibit critical failure characteristics, where criticality is as defined in Section 3.3.2. In-range failures (drifts) of the N2, TT2, TT25, FTIT, PT2, PT6 and PT4 sensors are also shown to exhibit critical failure characteristics. The in-range failure rates of the N1 sensor and the pressure sensors are low. For out-of-range failures simple range tests can be used effectively for detection and isolation. For in-range failures, however, advanced detection, isolation and accommodation algorithms may be required to insure continued operation in the event of sensor failures. Therefore, less emphasis could be placed on developing in-range failure detection capability for these sensors than on the N2 sensor and the temperature sensors. In-range failures of the fan turbine inlet temperature sensor were shown to exhibit critical failure characteristics for the smallest magnitude of sensor drift, in addition to having the highest failure rate. Therefore, this sensor warrants an accurate algorithm.

TABLE IV
FMECA SUMMARY

	OUT-OF-RANGE FAILURES		IN-RANGE DRIFTS		
Sensor	Failure Rate /Mil Hrs	Failure Classif'n	Failure Rate Failure/Mil Hrs	Minimum Drift*	Failure Classif'n
N1	20.5	Critical	0.22	--	Unlikely
N2	17.6	Critical	2.2	3.4% (423RPM)	Critical
TT2	37.4	Critical	5.2	74% (76°F)	Critical
FTIT	44	Critical	175.4	2.7% (45°F)	Critical
PT2	16	Critical	1.8	16.9% (6 PSI)	Critical
PT6	16	Critical	1.8	113% (18.6 PSI)	Critical
Pb	16	Critical	1.8	22% (80 PSI)	Critical
TT2.5	37.4	Critical	5.2	70% (70°F)	Critical

* This is the minimum sensor drift in terms of % of point for which critical engine operation was observed.

For this program, the detection, isolation and accommodation algorithms were developed for the PT6, PT4, N1, N2, and fan turbine inlet temperature sensors to result in a sufficiently complex problem to be a good test of the advanced concepts.

3.4 DETECTION, ISOLATION AND ACCOMMODATION CRITERIA, DETECTION PERFORMANCE, AND FIGURES OF MERIT

3.4.1 Detection, Isolation and Accommodation Criteria

High performance turbine engines, such as the F100, operate at or near design limits with tight control of speed, pressure, temperature and airflow to achieve maximumm performance while maintaining engine durability. Basically, control requirements as applied to these engines consist of exhibiting desired

transient and steady-state responses while remaining within safe margins of engine thermal, aerodynamic and mechanical limits throughout flight envelope operation. These requirements were combined to create a design criteria list to apply in the design of detection, isolation, and accommodation concepts.

The criteria used in the design of the concepts include the following:

1. Maintaining critical engine parameter limits

    - o Maximum Fan Turbine Inlet Temperature
    - o Maximum High Rotor Speed
    - o Maximum Low Rotor Speed
    - o Maximum and Minimum Burner Pressure

2. Maintaining safe fan and compressor surge margins

3. Minimal steady state deviations from nominal

4. Acceleration requirement
    - o Minimize time to 90% thrust variation
    - o Minimize overshoot of Engine Pressure Ratio and Low Rotor Speed

The detection, isolation and accommodation criteria were incorporated in a scoring system (as described in Section 3.5) to quantitatively evaluate the candidate advanced concepts.

3.4.2 Detection, Isolation and Accommodation Detection Performance

The detection performance relates to how effective the concept is in detecting a sensor failure. For example, if a concept has excellent accommodation capacity but cannot consistently detect failures then it is not a good concept.

The response of the concept in detecting various induced failures was quantified in the following terms: Hit; Miss; False Alarm; and Response Time. The definitions of these terms are:

Hit:	A sensor failure(s) occurs and detection, isolation and accommodation are accomplished by the chosen concept;
Miss:	The concept detects no failure(s) for which it was programmed despite the fact that such a failure(s) was induced.
False Alarm:	A condition in which the concept incorrectly detects a sensor failure(s) when none has actually occurred.
Response Time:	Length of time after failure before detection of the failure occurs.

As with the detection, isolation, and accommodation criteria, mathematical equations were generated (as described in Section 3.5) to quantitatively evaluate the detection performance of the candidate advanced concepts.

3.4.3 Detection, Isolation and Accommodation Figures of Merit

The DIA figures of merit generated for the evaluation of the candidate concepts are more qualitative than the DIA Criteria or Detection Performance. The figures of merit are defined as the benefits of bettering the detection, isolation and accommodation criteria in the event of a single sensor failure or meeting the DIA criteria in the event of multiple sensor failures. The DIA figures of merit used in evaluating the concepts included the following:

1. Accommodation of multiple sensor failures

2. Complexity of software computation and implementation (core size, cycle time, control mode interactions and dependence, etc.)

3. Robustness (sensitivity to model errors)

4. Sensitivity to noise and disturbances

3.5 SCORING SYSTEM

A scoring system was developed for use in evaluation of the candidate detection, isolation, and accommodation concepts. The scoring system evaluates each concept on how well it detects, isolates, and accommodates sensor failures.

The accommodation criteria used in developing the scoring system was a set of transient and steady state operational requirements which the propulsion system must satisfy to meet minimum aircraft operational requirements in the event of various potential sensor failures. The accommodation criteria used in this study penalizes the concept for:

1. Exceeding critical engine protection parameter
   - o FTIT limit
   - o N2 speed limit
   - o N1 speed limit
   - o PT4 pressure limit

2. Decrease in fan compressor surge margins

3. Steady state accuracy deviations

4. Acceleration requirement
   - o Excessive time to 90% thrust variation
   - o Excessive Engine Pressure Ratio or Low rotor speed overshoot

The DIA detection performance relates to how effective the DIA concept is in detecting a sensor failure. This portion of the scoring system evaluates each DIA concept on time to detect a failure, the hit/miss ratio, and the number of false alarms.

Mathematical equations were derived which incorporate both the accommodation and detection criteria. These are presented in Appendix B. The scoring system was used in the initial detection, isolation and accommodation concept screening process to select the most desirable concept. The results of the scoring of the concepts are shown in Section 4.4.

3.6 SELECTION OF FLIGHT OPERATING CONDITIONS

A set of fifteen flight operating points were selected to be used as the evaluation conditions for the selected advanced detection, isolation, and accommodation algorithm and the baseline parameter synthesis algorithm. These flight operating points were chosen to span the F-15 aircraft flight envelope and to demonstrate the algorithm detection and accommodation performance at conditions where critical stability and engine parameter limits are encountered. The points were also selected to include, where possible, many of the NASA altitude stand test points which were run during previous programs. Table V shows the selected flight operating points and the criterion used to select the individual conditions. Figure 12 shows the flight operating points relative to an F-15 aircraft flight envelope and illustrates that the selected conditions span a considerable portion of the engine flight envelope.

TABLE V

FLIGHT OPERATING CONDITIONS

Point	Mach Number	Altitude x 10^{-3}Ft	PLA	Selection Criterion
1	0.0	0	20	Sea Level Operating Line
2	0.0	0	83	Sea Level Operating Line
3	0.0	0	130	Sea Level Operating Line
4	1.2	0	83	Max T4, q, PT4, N1, N2, P2
5*	0.9	10	83	Max T4
6	0.3	20	24	Lower PT4 Limit
7	0.3	20	83	Fan Stability Verification
8*	1.8	24	83	Max N1, T3, T4
9*	1.9	34	83	T4 Limit, Compressor Stability
10*	0.9	45	40	Min PT4, Low Power Altitude Operation
11*	0.9	50	83	Rating Point
12	2.2	54	130	Supersonic Cruise
13	1.2	65	83	Fan Stability Verification
14	2.5	65	83	Compressor Stability Verification
15	2.5	65	130	Max Augmentation

*NASA test points

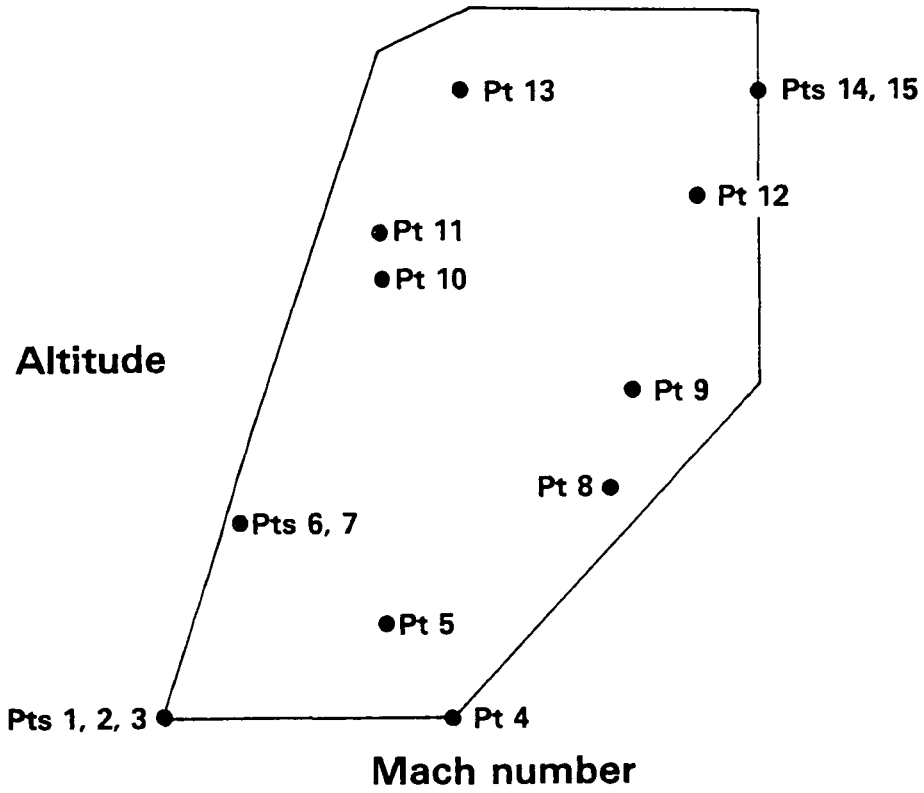

Figure 12 Selected Flight Operating Conditions

Section 4.0

CONCEPT FORMULATION

A survey was made of the available Detection, Isolation, and Accommodation techniques as described in technical literature. Five advanced sensor failure concepts, applicable to gas turbine engines, were formulated from the results of the survey. A simplified engine model was developed and used as a testbed for screening the candidate concepts. Various test cases were run to quantitatively evaluate the candidate concepts using the scoring system developed in section 3.5. This resulted in the selection of one concept for detailed evaluation. The detailed evaluation will be discussed in Section 5.

As a parallel effort to the development of the advanced detection, isolation and accommodation concepts, a baseline detection, isolation and accommodation algorithm was developed based upon conventional parameter synthesis techniques. The parameter synthesis based algorithm was evaluated in the same manner as the selected advanced detection, isolation and accommodation algorithm to provide a basis of comparison (as discussed in Section 6).

The development of the parameter synthesis concept, the simplified engine model, and the five selected advanced detection, isolation and accommodation concepts will be discussed in the following paragraphs.

4.1 PARAMETER SYNTHESIS

A sensor failure detection, isolation, and accommodation algorithm was developed based upon conventional parameter synthesis techniques. This algorithm was used as a baseline for comparison with the selected advanced algorithm. Comparing the performance of the two algorithms shows the value of using advanced concepts for production control systems. If the advanced DIA concept is of similar complexity to the parameter synthesis technique, but yields significantly better detection, isolation, and accommodation of failed sensors, then it would be desireable for implementation in production control systems. The results of this comparison are presented in Section 5.

The concept of parameter synthesis uses engine component relationships to compute synthesized values of measured parameters from other measured parameters. Generating these synthesized values provides the information to detect, isolate, and accommodate sensor failures. The following paragraphs describe the development of the engine component relationships and the design of the logic used to detect and isolate sensor failures.

Engine component relationships of the F100 engine were studied to obtain a set of curves potentially capable of synthesizing other measured parameters within the control system. The F100 engine and Multivariable Control (MVC) nonlinear simulation was programmed to run steady-state engine operating data from idle to full afterburner power at the flight operating conditions chosen for this study. Over sixty viable engine component relationships were computer plotted for all flight operating conditions to provide composite plots of the various

relationships. These plots were examined to eliminate those which did not form a relatively unique curve or a family of curves related by a bias measured within the control system, i.e., it is desireable to use simple curves to keep the algorithm complexity to a minimum. The remaining engine component relationships were judged for ease and accuracy of implementation, transient accuracy, and engine to engine variations and deterioration effects to arrive at the final curve set shown in Figure 13.

These engine component relationships can be used to detect, isolate, and accommodate PT6, PT4, N1, N2 and FTIT sensor failures. The detection and isolation functions are performed by comparing the difference between the synthesized values and measured values to predetermined tolerance bands; one or more of the synthesized values being out of tolerance with the measurements indicates (detects) a sensor failure.

The tolerance bands used for this study were derived by summing the production/deterioration variation of the relationship with the curve read inaccuracies. The production/deterioration portion of the tolerance band was derived by computer plotting actual engine data from sea level engine tests of seventy recent production engines in the same format as the parameter synthesis curves. This was done at five part power points to observe if the data scatter varies with power level. The tolerance bands were sized based upon a 2 sigma statistical variation applied to the results in units of the Y-Axis. Figure 14, is representative of the production/deterioration tolerance used for a typical parameter synthesis curve. The tolerance band arrived at by summing this production/deterioration spread with the curve read inaccuracies are as follows:

Curve 1 -- 0.15 PT4/PT2
Curve 1B -- 0.15 PT4/PT2
Curve 2 -- 300 RPM N2/$\sqrt{\theta}$ TT2
Curve 3 -- 0.35 PT6/PT2
Curve 4 -- 500 RPM N1/ $\sqrt{\theta}$ TT2
Curve 5 -- 150°F FT1T

These tolerance bands are increased by 50% during a power lever transient to avoid false alarms.

Logic was developed to incorporate the curve set and associated tolerance bands into a viable detection, isolation and accommodation concept, as shown in Figure 15 through 18. The failure detection logic, as shown in Figure 15, determines the general health of the five engine sensors. A comparison of the absolute value of the difference between the sensor measurements (Xsen(n)) and the corresponding synthesized value (Xsyn(n)) to the associated tolerance band is used to create a sensor fault word. This word varies uniquely between 0 to 31 depending on which curve or combination of curves are out of tolerance with their corresponding sensor measurements.

The sensor fault word is a 5 bit binary word, each bit being associated with one of the parameter synthesis curves. If a particular curve is out-of-tolerance, the polarity of the bit corresponding to the out-of-tolerance curve

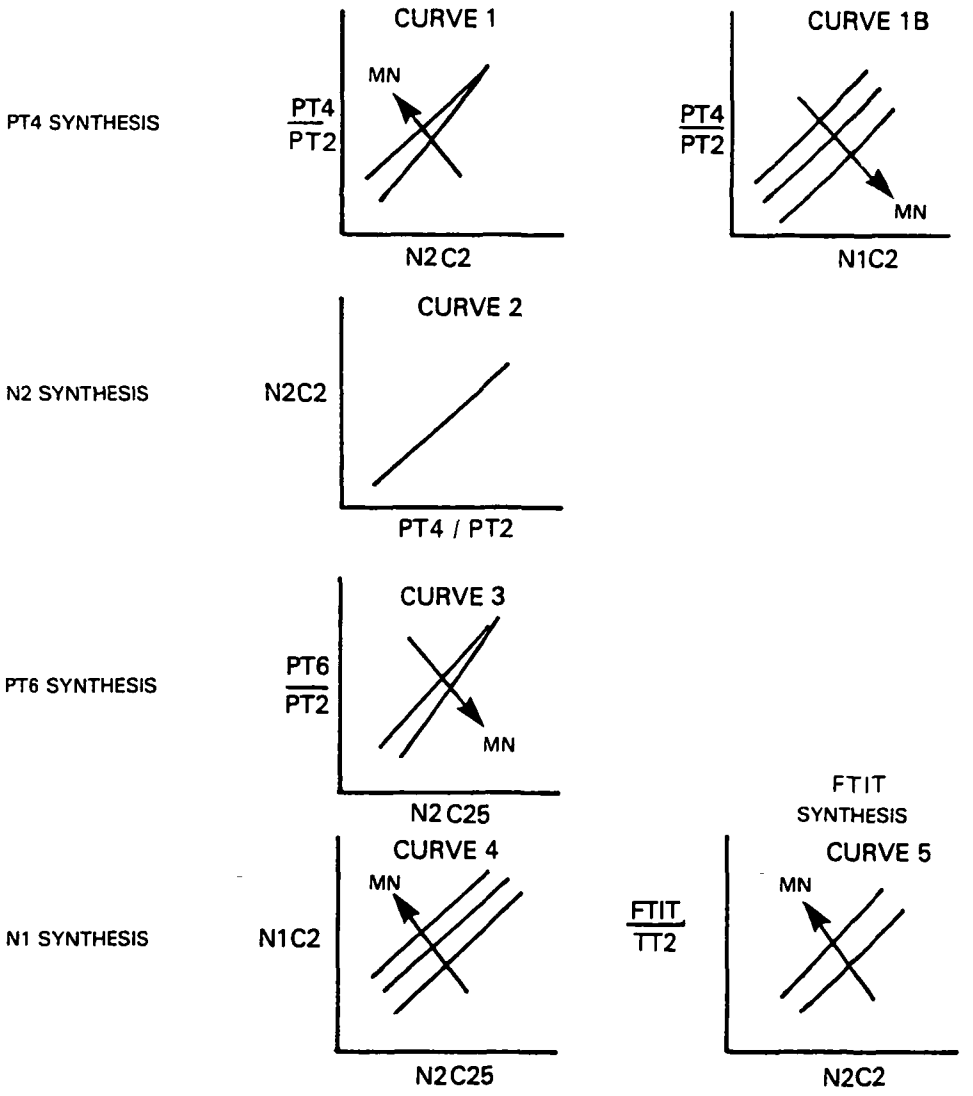

Figure 13 Final Curve Set for the Parameter Synthesis Algorithm

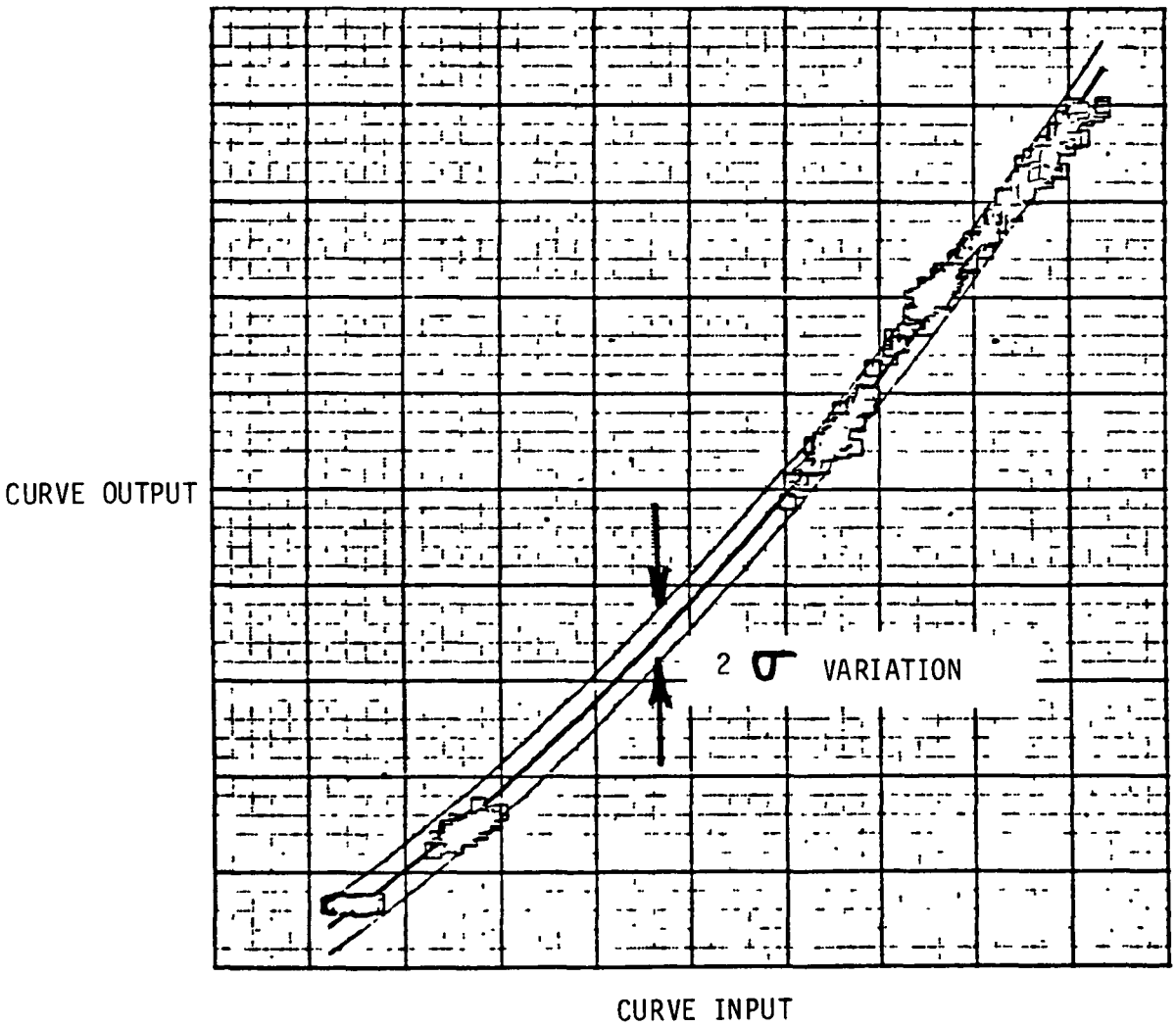

Figure 14 Typical Production Tolerance and Deterioration Bandwidth on a Parameter Synthesis Curve

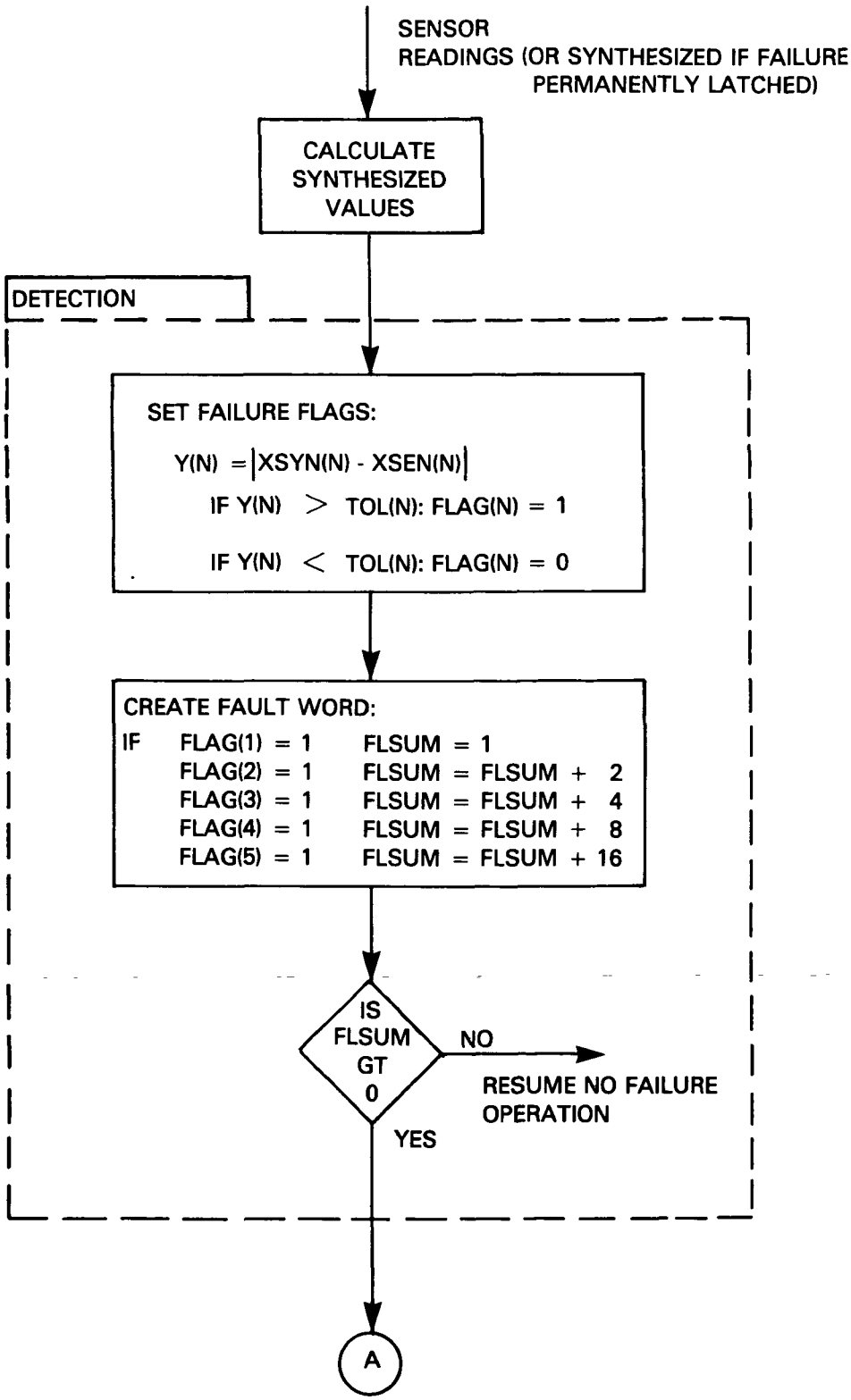

Figure 15 Parameter Synthesis Detection Logic

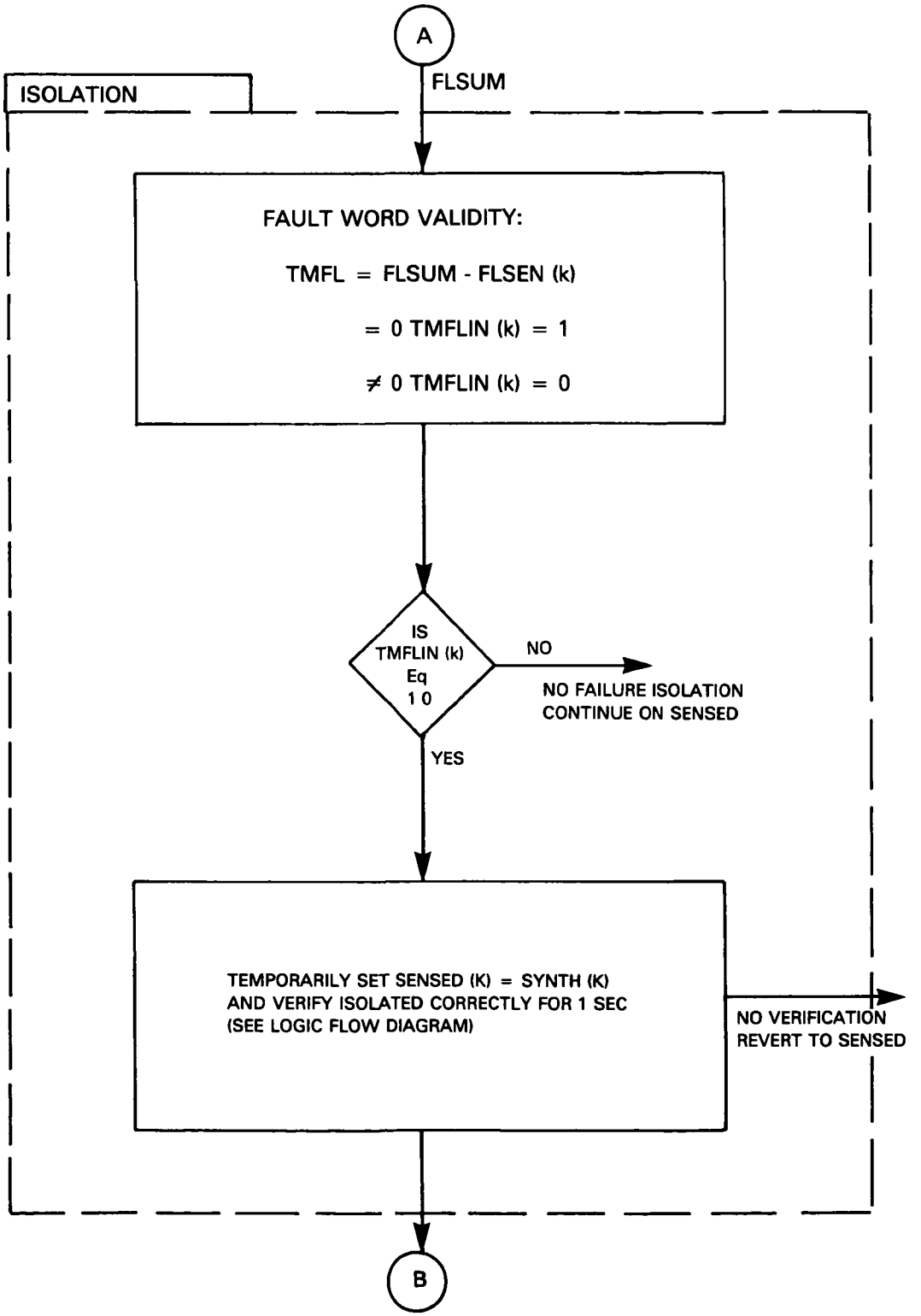

Figure 16 Parameter Synthesis Isolation Logic

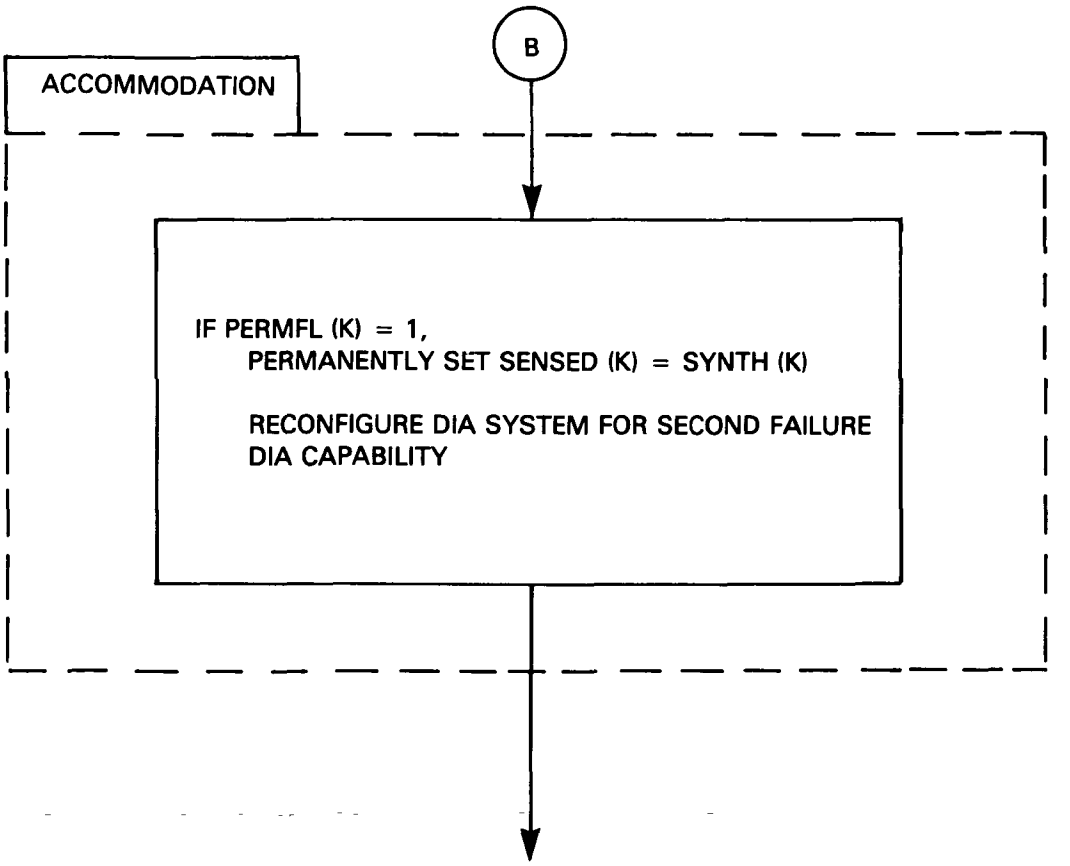

Figure 17 Parameter Synthesis Accommodation Logic

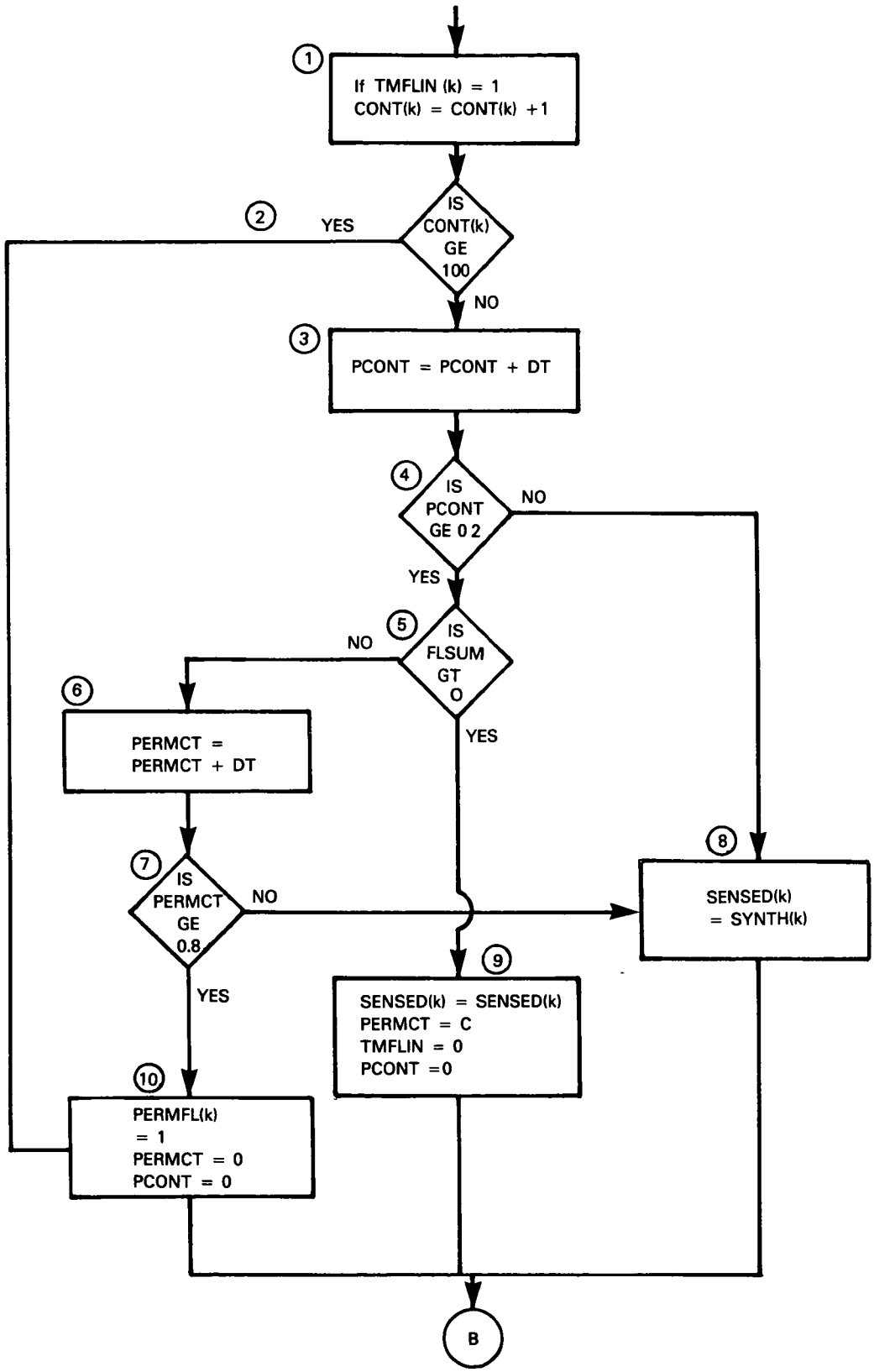

Figure 18 Parameter Synthesis Isolation Verification

changes from 0 to 1. The value of the binary bits that are set are then arithemetically summed to create the fault word. The calculation of the fault word is shown in Table VI.

If the fault word is zero, all curves are in tolerance with the sensor measurements, and, no failures are detected. A non-zero fault word indicates a sensor failure which requires exercising the isolation logic to pinpoint the failure to a particular sensor. The isolation and accommodation logic, as shown in Figures 16 and 17, compares the fault word (FLSUM) to a set of known fault words which are uniquely associated with particular sensor failures. The set of known fault words used to isolate the failure to a particular sensor measurement is shown in Table VII.

TABLE VI

PARAMETER SYNTHESIS FAULT WORD CALCULATION

Bit Number	1	2	3	4	5
Bit Value For Out-of-Tolerance Curves	1	2	4	8	16
Associated Curve	Curve 1	Curve 2	Curve 3	Curve 4	Curve 5

$$\text{Where: Fault word} = \sum_{\text{Bit 1}}^{\text{Bit 5}} \text{Bit values}$$

Note: If the curve is not out-of-tolerance with the sensor measurements; i.e., the bit polarities are all 0, the value of the bits are zero. For a no failure case, the fault word = 0.

TABLE VII

PARAMETER SYNTHESIS FAULT WORD ISOLATION SET

Sensor Measurement	Value of Known Fault Word
N1	1
N2	3,7,15,23,31
PT4	10, 8
PT6	4
FTIT	16

If the fault word generated is identical to one of the known fault words, the failure has been isolated to a given sensor and the sensed value is temporarily set equal to the synthesized value. A verification of the isolation validity is conducted for the next 1.0 second. The detailed verification logic is shown in Figure 18.

Blocks 1 and 2 in Figure 18 implement a counter to record the number of times a particular sensor has been isolated as a failed measurement during a flight or mission. This logic will permanently latch a sensor as failed if an intermittent failure occurs more than 100 control computation cycles. (This is based upon a 0.01 second computation cycle for the nonlinear simulation.) Blocks 3 and 4 delay further isolation verification for 0.2 second during which time any transient resulting from the switch over from sensed to synthesize would decay significantly. After the 0.2 second delay, if the failure was isolated properly, the fault word should be zero. A non-zero fault word indicates that the failure was incorrectly isolated and operation is reverted to the sensed measurements. If the fault word is zero for the next 0.8 seconds, the sensor failure has been properly isolated and the permanent failure flag is set for the failed sensor. If the failure fault word is non-zero during the 0.8 second interval, the failure was either incorrectly isolated or intermittent in nature. This logic assumes that a second failure would not occur during the one second time interval.

Once the permanent failure flag has been set, the parameter associated with the failed sensor is permanently set equal to the synthesized value, as shown on Figure 18. After the failure is permanently accommodated, the logic is reconfigured for second failure detection, isolation and accommodation capability. The reconfiguration process involves increasing tolerance bands and modifying the known fault words (FLSEN(k)) to account for the loss of the input signal.

The parameter synthesis logic was programmed in the F100 MVC simulation and was exercised over the selected flight operating conditions. Figures 19 and 20 show an example of the parameter synthesis algorithm response to an N1 sensor failure. The failure was simulated at sea level static, intermediate power and was induced at a time of 3.0 seconds. These figures show only a minor transient occurring when switching from sensed measurements to synthesized, with a minimal loss in steady state accuracy (-55. pounds loss in thrust). The detailed analysis of the parameter synthesis algorithm performance is included in Section 5.

4.2 SIMPLIFIED ENGINE MODEL

4.2.1 Introduction

A full envelope simplified nonlinear model of the F100 engine is required for two reasons when developing, evaluating, and implementing fault detection, isolation and accommodation (DIA) concepts. First, all of the techniques investigated in this program employ filters which require a real time micro-

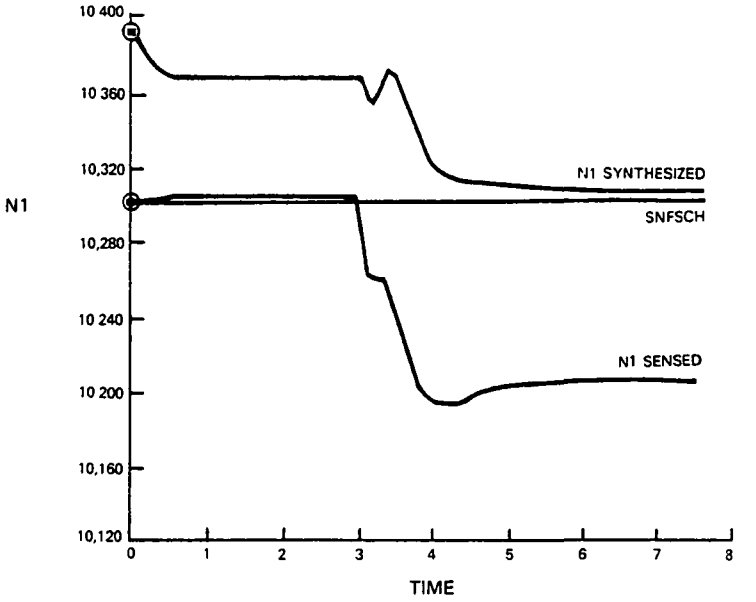

Figure 19 Parameter Synthesis Algorithm; Response of N1 With an N1 Sensor Failure

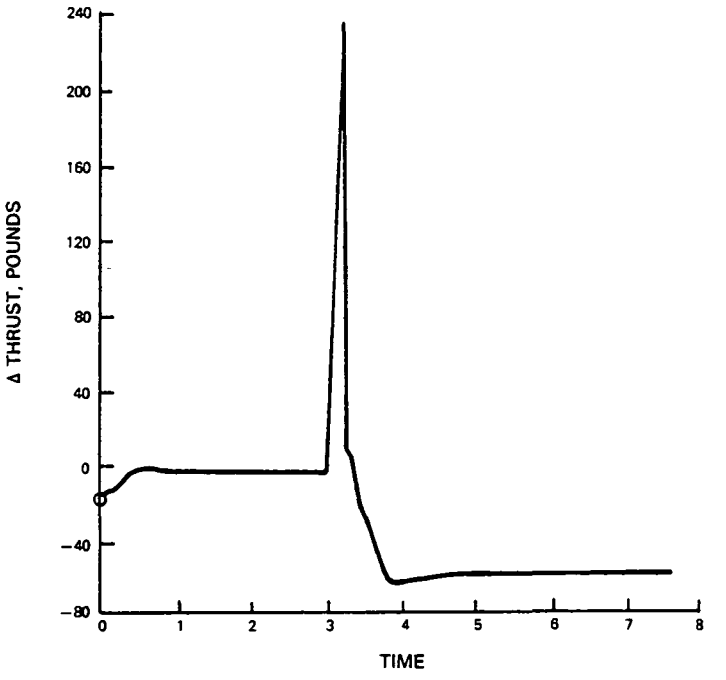

Figure 20 Parameter Synthesis Algorithm; Response of Thrust With an N1 Sensor Failure

processor implemented engine model. A simplified model minimizes hardware requirements. Second, evaluating the concepts involves many computer runs of an engine simulation. Using a simplified model (rather than a full nonlinear dynamic deck) during the initial evaluation process can greatly reduce cost.

A procedure for generating a full envelope, simplified nonlinear engine model is presented in this section. This model is developed from steady state operating line data and linear dynamic models generated about that operating line.

The simplified model generation procedure is summarized in Figure 21. Linear dynamic model generation techniques are described in detail in Reference 1 and summarized in Appendix C. Model reduction procedures, for reducing the number of state variables, are described in Reference 4 and summarized in Appendix D.

The form of the resulting model is shown in a block diagram in Figure 22, and described with the equations,

$$\dot{X} = F(X-X_{ss}) \qquad (1)$$

where

$$X_{ss} = X_b - F^{-1}G\cdot(U - U_b)$$

and

$$Y = Y_b + H\cdot(X - X_b) + D\cdot(U - U_b)$$

Here the state derivative, X, is being driven by the distance the state, X, is from its steady state value, X_{ss}. The subscript, b, denotes a base point obtained from the original steady state operating line data.

This model looks much like a linear model. Note, however, that the model matrices (F, $F^{-1}G$, H and D) are functions of the operating condition as are the base points (X_b, U_b, and Y_b). In general, the matrices used are formed by scheduling linear model matrices throughout the flight envelope. The base points are equivalent to the operating line data.

Section 4.2.2 presents a review of the original sixteenth order linear models, the simplified linear models, and the generation of the simplified nonlinear models. Section 4.2.3 discusses model validation.

4.2.2 Simplified Nonlinear Model Development

4.2.2.1 Engine Linear Models

The F100 nonlinear dynamic engine simulation was used to develop the steady state operating line data and linear engine models. Sixteenth order linear models were generated by Pratt and Whitney Aircraft Group using a full F100 nonlinear simulation during the F100 Multivariable Control Program (Contract F33615-75-C-2053). A description of the procedure and a complete set of dynamic models is listed in reference 3.

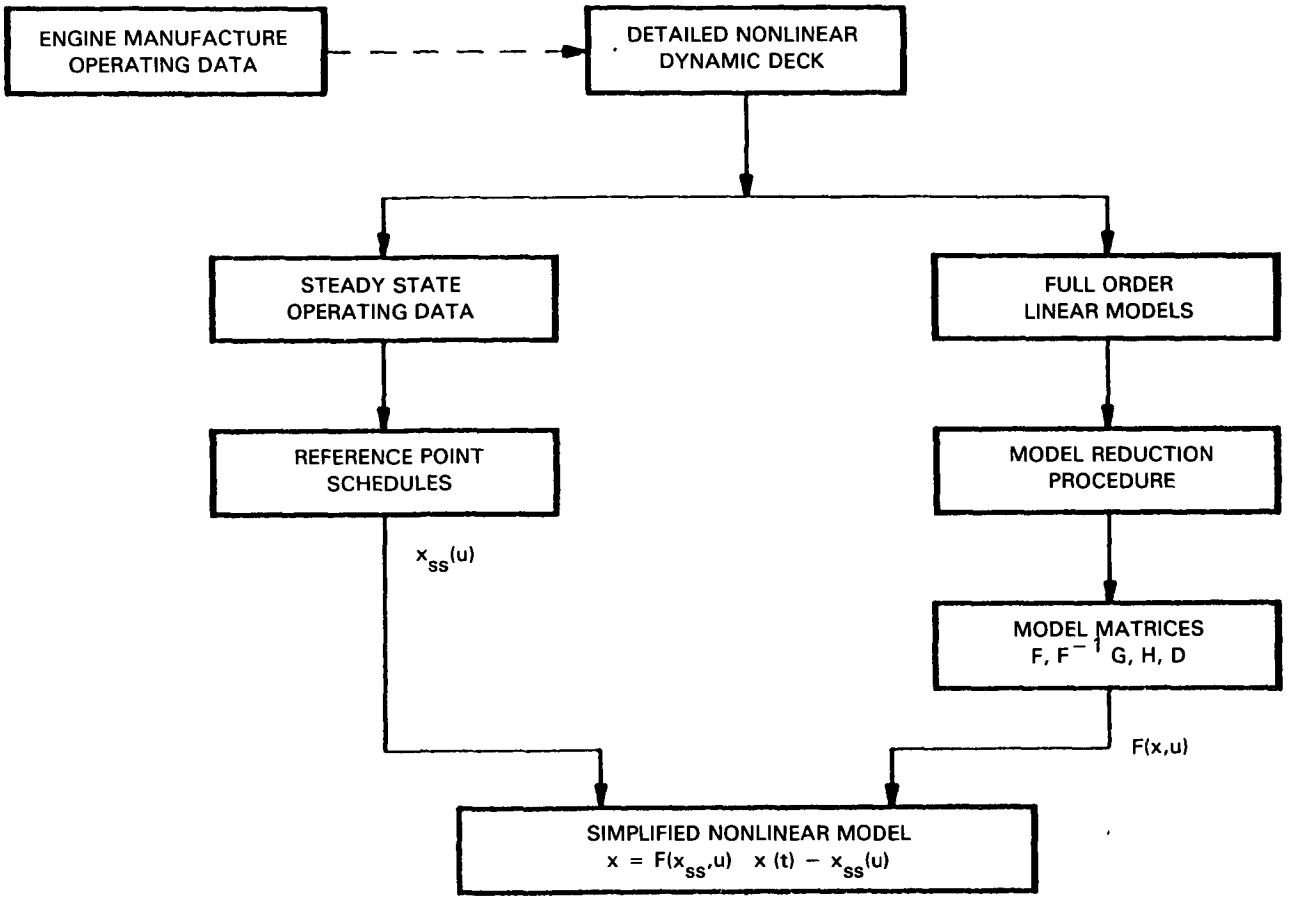

Figure 21 Development of A Simplified Nonlinear Model From Reference Schedules and Reduced Order Linear Models

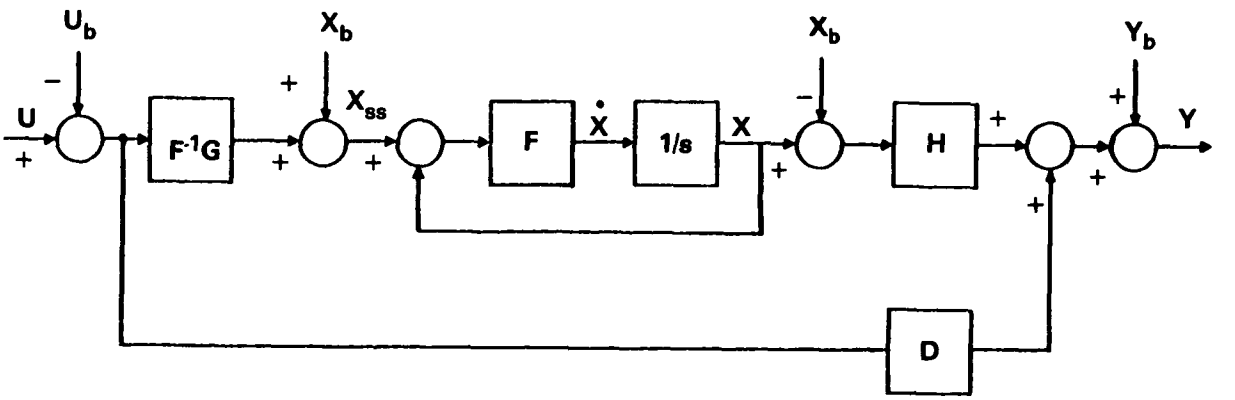

Figure 22 Simplified Nonlinear Model Implementation

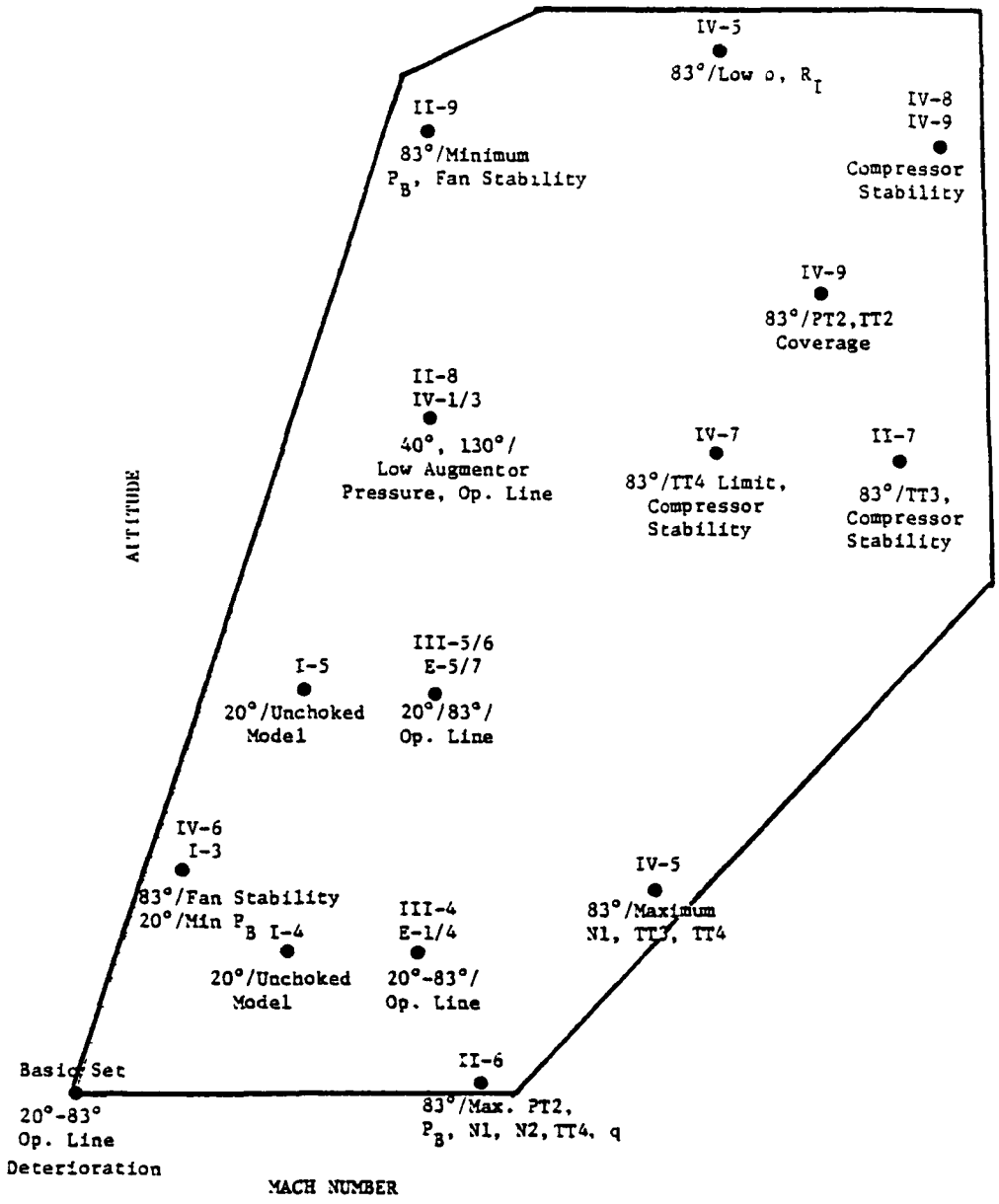

Figure 23 Relative Linear Model Operating Point Location Relative to the F-15 Aircraft Flight Envelope

Table VIII lists the state, input and output variables which constitute these linear models. Table IX lists the linear model operating points. Figure 23 shows the F-15 aircraft operating envelope spanned by the chosen set of linearization points.

TABLE VIII
ENGINE VARIABLES USED IN LINEAR MODELS

1. Engine State Variables

X_1 = Fan Speed, SNFAN (N_1) - rpm
X_2 = Compressor Speed, SNCOM (N_2) - rpm
X_3 = Compressor Discharge Pressure, P_{t3} - psia
X_4 = Interturbine Pressure, $P_{t4.5}$ - psia
X_5 = Augmentor Pressure, P_{t7m} - psia
X_6 = Fan Inside Diameter Discharge Temperature $T_{t2.5h}$ - °R
X_7 = Duct Temperature, $T_{t2.5c}$ - °R
X_8 = Compressor Discharge Temperature, T_{t3} - °R
X_9 = Burner Exit Fast Response Temperature, T_{t4hi} - °R
X_{10} = Burner Exit Slow Response Temperature, $T_{t4\ 10}$ - °R
X_{11} = Burner Exit Total Temperature, T_{t4} - °R
X_{12} = Fan Turbine Inlet Fast Response Temperature, $T_{t4.5hi}$ - °R
X_{13} = Fan Turbine Inlet Slow Response Temperature, $T_{t4.5lo}$ - °R
X_{14} = Fan Turbine Exit Temperature, T_{t5} - °R
X_{15} = Duct Exit Temperature, T_{t6c} - °R
X_{16} = Mixed Exhaust Stream Temperature, T_{t7m} - °R

2. Engine Inputs

U_1 = Main Burner Fuel Flow, WFMB - lb/hr
U_2 = Nozzle Jet Area, A_j - ft^2
U_3 = Compressor Fan Inlet Variable Vane, CIVV - deg
U_4 = Rear Compressor Variable Vane, RCVV - deg
U_5 = Customer Compressor Bleed Flow, BLC - %

3. Engine Outputs

Y_1 = Engine Net Thrust Level, FN - lb
Y_2 = Total Engine Airflow, WFAN - lb/sec
Y_3 = Turbine Inlet Temperature, T_{t4}
Y_4 = Fan Stall Margin, SMAF
Y_5 = Compressor Stall Margin, SMHC
Y_6 = Fan Exit $\Delta P/P$, $(P_{t2.5} - P_{S2.5})/P_{S2.5}$, based on test data
Y_7 = Fan Exit $\Delta P/P$, $(P_{t2.5} - P_{S2.5})/P_{S2.5}$ theoretical function of area and airflow

TABLE IX

LINEAR MODEL OPERATING POINTS

CODE	POINT NO.	MACH NO.	ALTITUDE FT. (000)	PLA (DEG)	COMMENTS
Basic	1	0	0.0	20	
Set	2	0	0.0	36	
	3	0	0.0	52	Sea Level Static Operating Line
	4	0	0.0	67	
	5	0	0.0	83	
Group I	1	0	0.0	24	Additional Unchoked Model
	2	0.9	10.0	83	Performance at Max. TT4
	3	0.3	20.0	24	PT4 Lower Limit
	4	0.6	10.0	20	Unchoked Model Behavior
	5	0.6	30.0	24	Unchoked Model Behavior
Group II	6	1.2	0.0	83	Maximum q, PT4, N1, N2, TT4
	7	2.2	40.0	83	TT3, TT4 Limit, Compressor Stab.
	8	0.9	45.0	130	Low Augmentor Pressure
	9	0.9	65.0	83	Fan Stability
	10	2.5	65.0	130	Maximum Augmentation
Extra(E)	1	0.9	10.0	36	
	2	0.9	10.0	52	
	3	0.9	10.0	67	
	4	0.9	10.0	83	Additional Operating Line
	5	0.9	30.0	36	Data for Engine Test
	6	0.9	30.0	52	
	7	0.9	30.0	67	
GroupIII	1	0.0	0.0	20	Minor Deck Modification
	2	0.0	0.0	20	With BLD/HPX Extraction
	3	0.0	0.0	83	Minor Deck Modification
	4	0.9	10.0	20	
	5	0.9	30.0	20	Additional Operating Line
	6	0.9	30.0	83	Data for Engine Test
Group IV	1	0.9	45.0	83	Rating Point
	2	0.9	45.0	52	Altitude Part Power Point
	3	0.9	45.0	40	Minimum Burner Pressure
	4	1.8	75.0	83	Low Density, Reynolds Index
	5	1.8	20.0	83	Maximum N1, TT3, TT4
	6	0.3	20.0	83	Fan Stability
	7	1.8	40.0	83	TT4 Limit, Compressor Stab.
	8	2.5	65.0	83	Compressor Stability
	9	2.15	58.5	83	PT2, TT2 Coverage

4.2.2.2 Reduced Order Linear Models

Simplified linear models were generated using the 16th order linear models and reducing the order of the system. A modal decomposition method was utilized for this purpose. A detailed description of this method is given in Appendix D. The reduced order models were then scheduled against engine parameters to obtain a simplified model operable over the entire flight envelope.

The reduction process allows important dynamic modes to be retained and important, measureable quanitities to be included as state variables in the system of equations. Four states which represented imporant engine parameter dynamics, were chosen as a result of dynamic response analysis. Table X lists the states and input and output variables which constitute the reduced order models. The two rotor speeds are an important part of engine dynamics at each flight condition. The other two states are slow response modes and lie within the bandwidth of interest.

TABLE X

ENGINE VARIABLES USED IN REDUCED ORDER MODELS

1. Engine State Variables

X_1 = Fan Speed, SNFAN (N_1) - rpm

X_2 = Compressor Speed, SNCOM (N_2) - rpm

X_3 = Burner Exit Slow Response Temperature, T_{t41o} - °R

X_4 = Fan Turbine Inlet Slow Response Temperature, $T_{t4.51o}$-°R

2. Engine Inputs

U_1 = Main Burner Fuel Flow, WFMB - lb/hr

U_2 = Nozzle Jet Area, A_j - ft^2

U_3 = Compressor Inlet Variable Vane, CIVV-deg

U_4 = Rear Compressor Variable Vane, RCVV-deg

U_5 = Customer Compressor Bleed Flow, BLC - %

3. Engine Outputs

Y_1 = Fan Speed, SNFAN (N_1) - rpm
Y_2 = Compressor Speed, SNCOM (N_2) - rpm
Y_3 = Burner Pressure, PT4 - psia
Y_4 = Augmentor Pressure, PT6 - psia
Y_5 = Fan Turbine Inlet Temperature, FTIT - °R

The simplified model must include burner pressure for use in the maximum and minimum burner pressure limiting loops in the control mode. However, the burner pressure flow dynamics have a time constant always less than 0.01 sec. Therefore, burner pressure is included only as an output variable, i.e., as a linear combination of the chosen state variables. Similarly, augmentor pres-

sure is required for calculating engine pressure ratio (EPR), but its associated time constant is small. Therefore, it is only included as an output variable. The maximum temperatures specified for compressor discharge and turbine inlet stations in the gas path are implicitly limited in the control mode by limiting the maximum fan turbine inlet temperature. Thus, Fan Turbine Inlet Temperature (FTIT) is also included as an output.

4.2.2.3 Simplified Nonlinear Model

The simplified, reduced order linear models discussed above were used to generate a simplified nonlinear model to operate over the flight envelope. Elements of the linear model matrices were scheduled using engine variables and ambient parameters.

The reduced order linear model is given by

$$\delta\dot{X} = F \cdot \delta X + G \cdot \delta U \tag{2}$$

$$\delta Y = H \cdot \delta X + D \cdot \delta U \tag{3}$$

where δX, δU, and δY are perturbational quantities given by

$$\begin{aligned} \delta X &= X - X_b \\ \delta U &= U - U_b \\ \delta Y &= Y - Y_b \end{aligned} \tag{4}$$

The quantities X_b, U_b, and Y_b are the steady state equilibrium points (base points) about which the small perturbation assumption is valid.

An alternative representation of a linear model can be written as follows. In steady state $\dot{X} = 0$, so that equation (3) becomes

$$0 = F \cdot \delta X_{ss} + G \cdot \delta U_{ss}$$

$$\delta X_{ss} = - F^{-1} G \cdot \delta U_{ss}$$

$$\text{or} \quad X_{ss} = X_b - F^{-1} G \cdot (U - U_b) \tag{5}$$

Using equations (4) and (5), equations (2) and (3) can be written as

$$\dot{X} = F \cdot (X - X_{ss}) \tag{6}$$

$$Y = Y_b + H \cdot (X - X_b) + D \cdot (U - U_b) \tag{7}$$

X_{ss} is defined as the reference schedule of the states given the control, when the system is in equilibrium. This formulation is valid if it is assumed that $U(t)$ is piecewise constant on an interval $[NT, (N + 1) T]$. The time interval T can be made small relative to the dynamics so that the constant

control assumption is valid. Equations (6) and (7) is an accurate model only if δX and δU are small. In steady state if the control reaches the base point; i.e. $U = U_b$, then it is guaranteed that the state and outputs will reach their base points, i.e. $X = X_b$ and $Y = Y_b$. This is true independent of F, $F^{-1}G$, H, and D provided F is stable.

The implementation of this simplified nonlinear model for operation over the flight envelope involves scheduling system matrices F, $F^{-1}G$, H, and D used in equations (5) thru (7). These matrices were scheduled as a function of ambient and engine variables. The ambient variables used were engine inlet total pressure (PT2) and temperature (TT2). The engine variables were low and high rotor speeds (N1, N2), burner and augmentor pressures (PT4, PT6), and compressor inlet and fan turbine inlet temperatures (TT25, TT45). A regression analysis was used to produce polynominal functions which fit the model matrix elements with operating variables. A typical matrix element looked like the following.

$$F(i,j) = a_1 (N1)^3 + a_2 (PT4 * PT6) + \ldots + a_n \qquad (8)$$

The number of terms in a model depended on the accuracy of the model desired. Polynominals for the matrix elements were generated using regression analysis software available in Systems Control Incorporated's software library.

Values for the engine variables used in the polynominals and the base point vectors X_b, U_b, and Y_b, were obtained from the steady state reference point schedules and the reference transition control in the Multivariable Control logic. The transition control in this logic essentially provides a "reasonable transient reference" for the linear quadratic regulator control to "regulate to". The transient low rotor speed reference from this transition control was used as the basic reference for the simplified model base point inputs and polynominal parameters. This was accomplished by reading the low rotor speed versus power lever angle steady state reference schedule "backwards" to define a power lever angle, or "virtual power code", corresponding to the trajectory value for low rotor speed. The "virtual power code" is then used to read all of the steady state reference schedules to obtain the base point references, X_b, U_b, and Y_b, and other engine variables required for the simplified nonlinear model calculations. Figure 24 presents the overall procedure. The fact that the base points and the system matrices vary as a function of operating conditions makes the engine model nonlinear.

4.2.3 Model Validation

The simplified engine model is incorporated in the filters employed by the various detection, isolation and accommodation concepts. The model was therefore implemented in the filter for validation. Filter gains were designed using simplified linear models at selected points in the envelope. These points correspond to the points at which regulator gains were designed for the F100 multivariable control. These filter gains were also scheduled against the ambient and engine variables over the flight envelope.

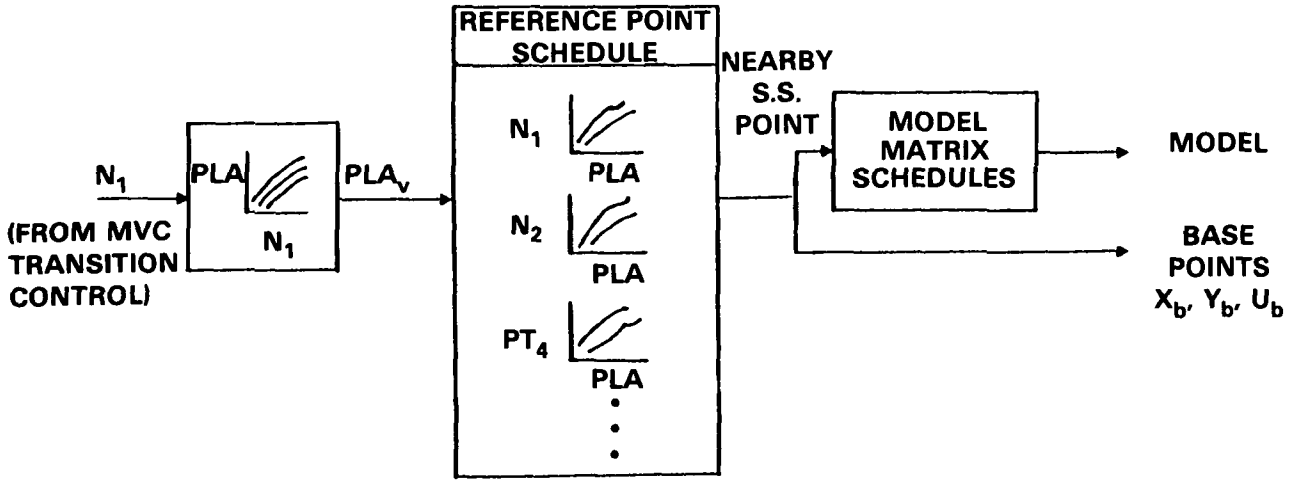

Figure 24 Scheduling of Base Points and Matrices for the Simplified Nonlinear Engine Model

The model validation was performed at the 15 selected flight operating points on the envelope. Figures 25 thru 33 show examples of the performance of the Kalman filters incorporating the simplified nonlinear model compared with the engine output.

While performance of the combined filter/model algorithm was quite good at the lower altitude and mach number flight conditions, some problems of steady state and transient mismatch were encountered at higher altitudes and mach numbers. These problems were found to result from not having a sufficient number of the original linear models available to constrain the curve fitting procedure for the matrix elements at these flight conditions to obtain a good accuracy of fit. Even though the Kalman filters did a commendable job of minimizing these mismatches, the effectivness of the detection, isolation and accommodation algorithms was reduced at these flight conditions. Additional work is required to generate more linear models and improve the curve fits for the simplified nonlinear models.

4.3 FORMULATION OF ADVANCED CONCEPTS

4.3.1 Introduction

A generalized form of a closed loop control system including sensor fault detection, isolation, and accommodation is shown in Figure 34. The system plant, actuators, and sensors are in the feedforward loop. All computations are performed in the feedback loop. These computations include evaluations of the commanded control, estimation of states, and detection, isolation, and accommodation of failures.

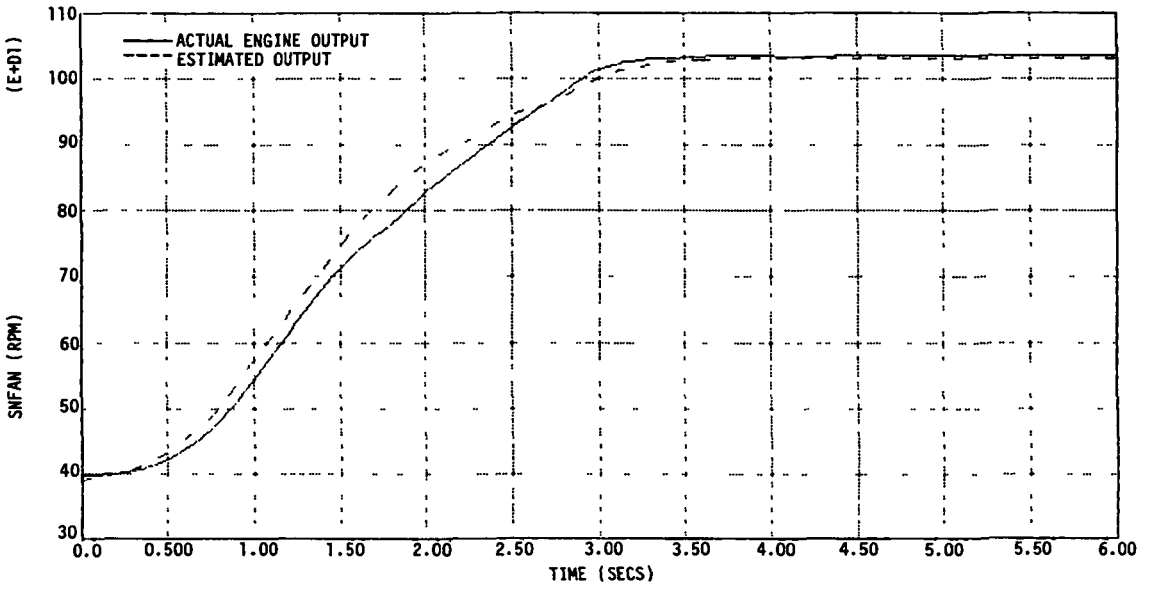

Figure 25 Actual and Estimated Fan Speeds (Flight Condition: Altitude = 0 Ft., Mach No. = 0, PLA Step From 20° to 83° at t=0.0 Seconds)

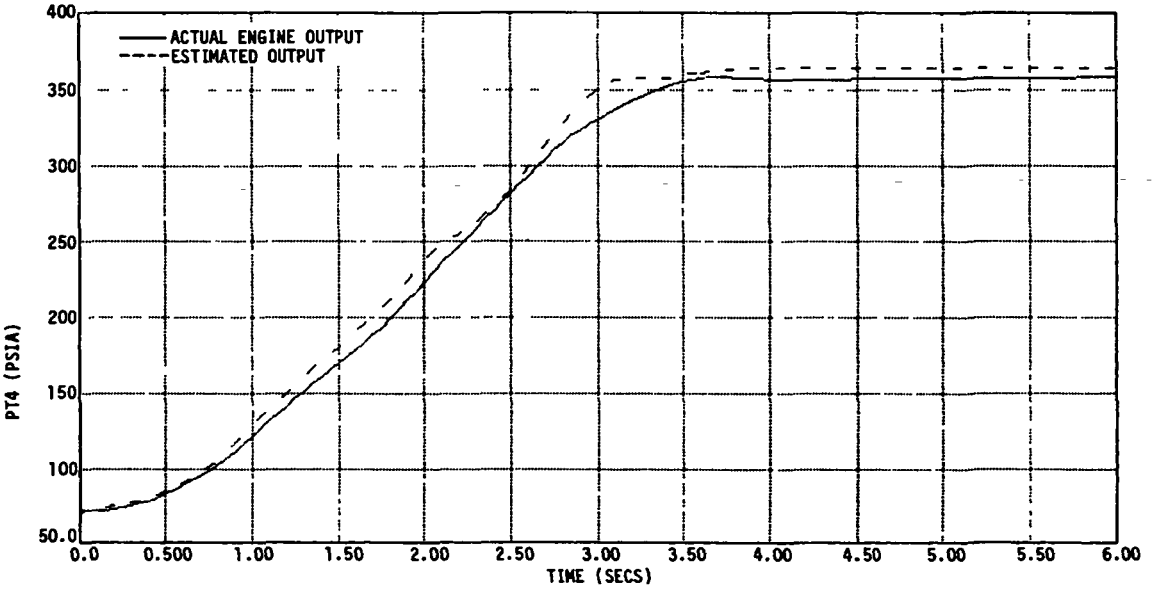

Figure 26 Actual and Estimated Burner Pressures (Flight Condition: Altitude = 0 Ft., Mach No. = 0, PLA Step From 20° to 83° at t=0.0 Seconds)

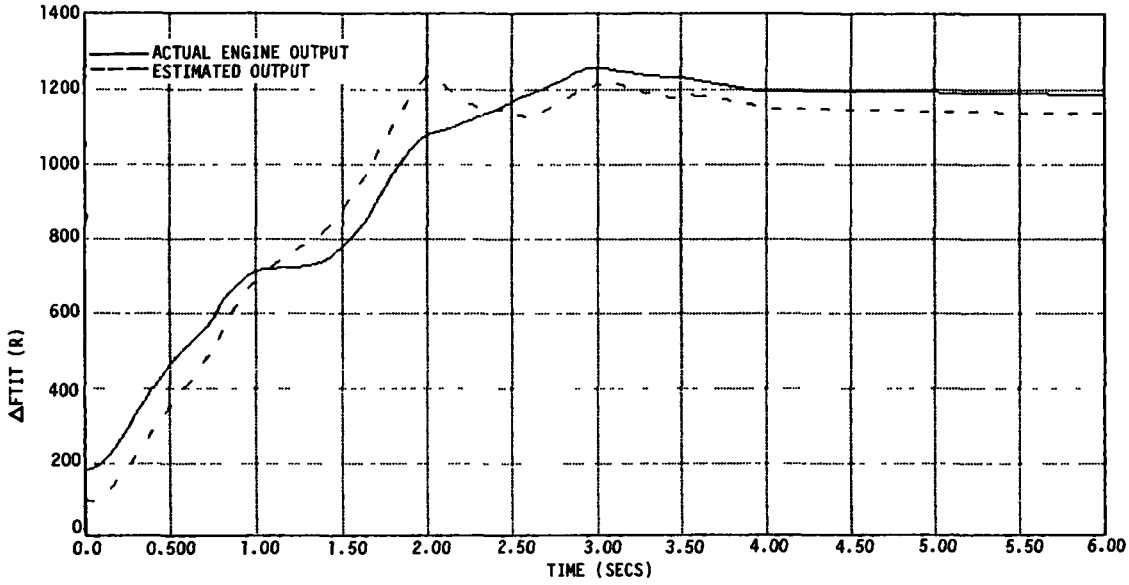

Figure 27 Actual and Estimated Fan Turbine Inlet Temperature (Flight Condition: Altitude = 0 Ft., Mach No. = 0, PLA Step From 20° to 83° at t=0.0 Seconds)

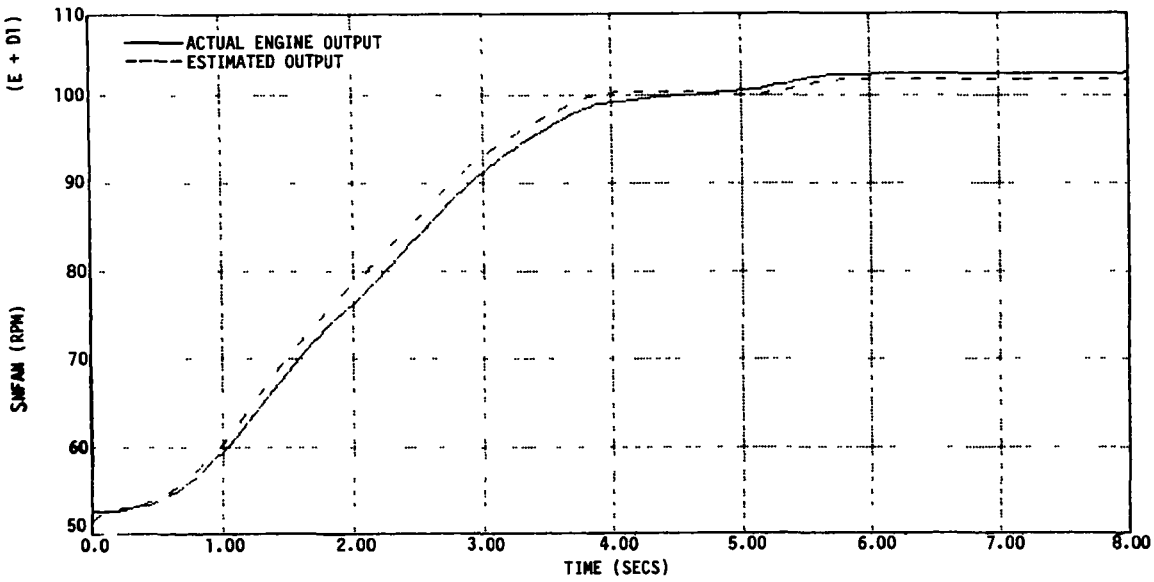

Figure 28 Actual and Estimated Fan Speeds (Flight Condition: Altitude = 20,000 Ft., Mach No. = 0.8, PLA Step From 20° to 83° at t=0.0 Seconds)

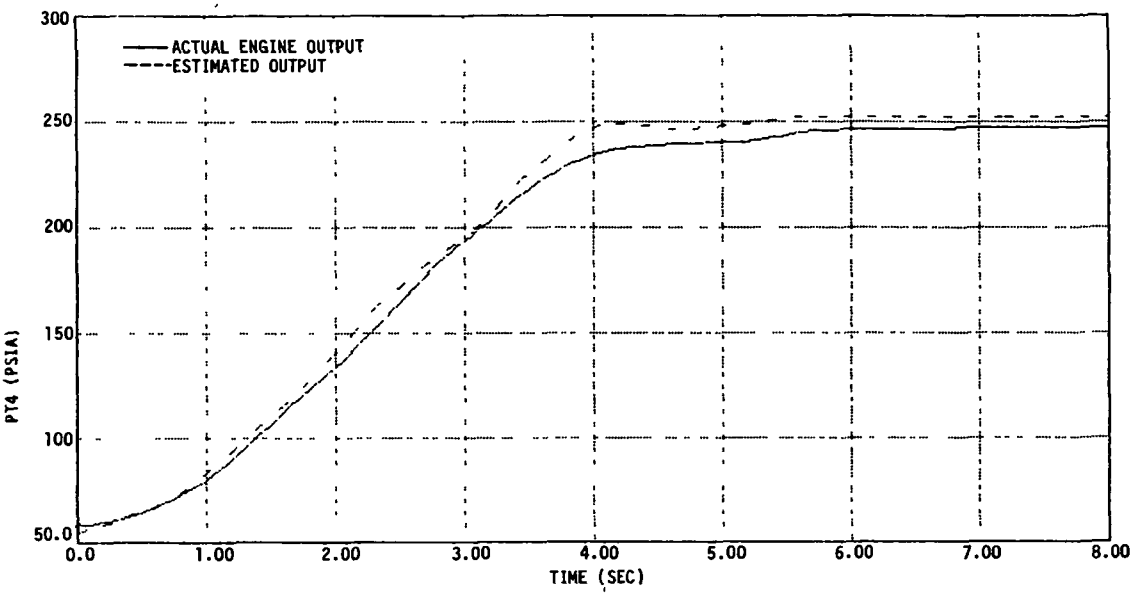

Figure 29 Actual and Estimated Burner Pressures (Flight Condition: Altitude = 20,000 Ft., Mach No. = 0.8, PLA Step From 20° to 83° at t=0.0 Seconds)

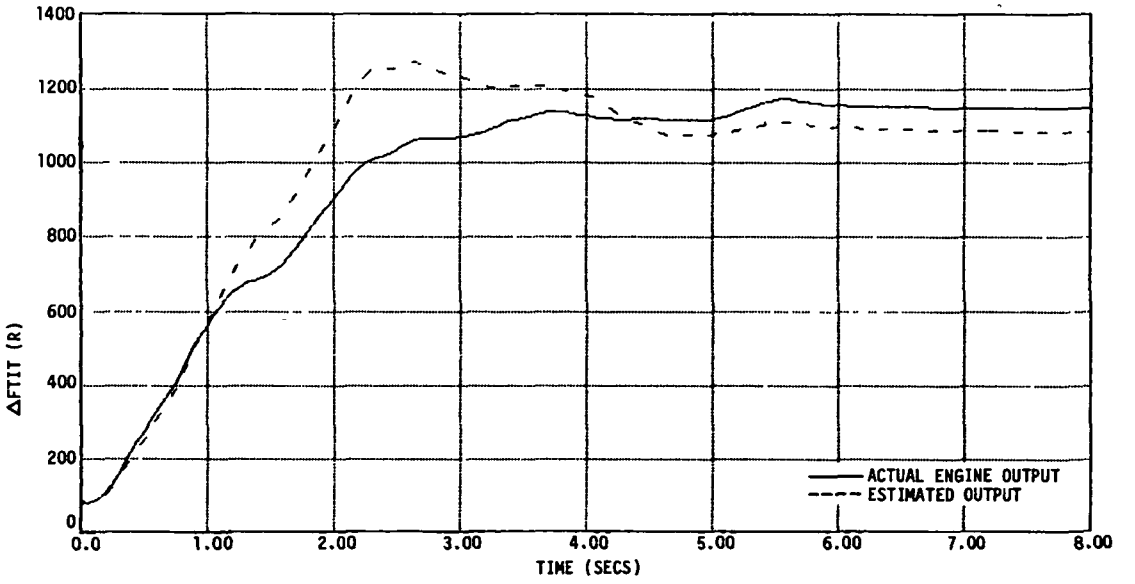

Figure 30 Actual and Estimated Fan Turbine Inlet Temperature (Flight Condition: Altitude = 20,000 Ft., Mach No. = 0.8, PLA Step From 20° to 83° at t=0.0 Seconds)

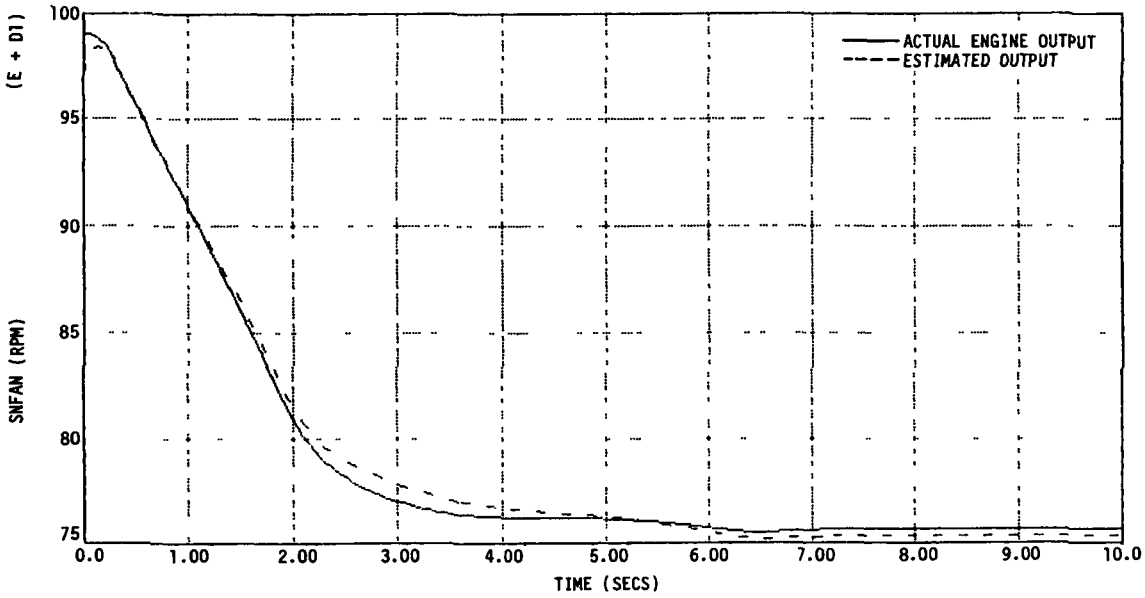

Figure 31 Actual and Estimated Fan Speeds (Flight Condition: Altitude = 45,000 Ft., Mach No. = 0.9, PLA Step From 83° to 20° at t=0.0 Seconds)

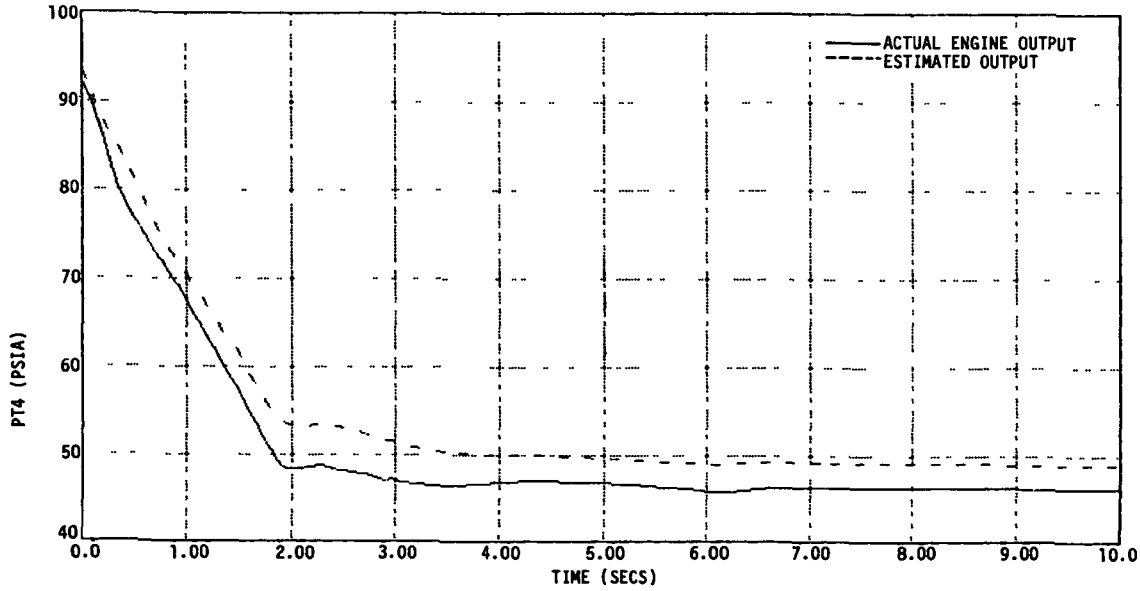

Figure 32 Actual and Estimated Burner Pressures (Flight Condition: Altitude = 45,000 Ft., Mach No. = 0.9, PLA Step From 83° to 20° at t=0.0 Seconds)

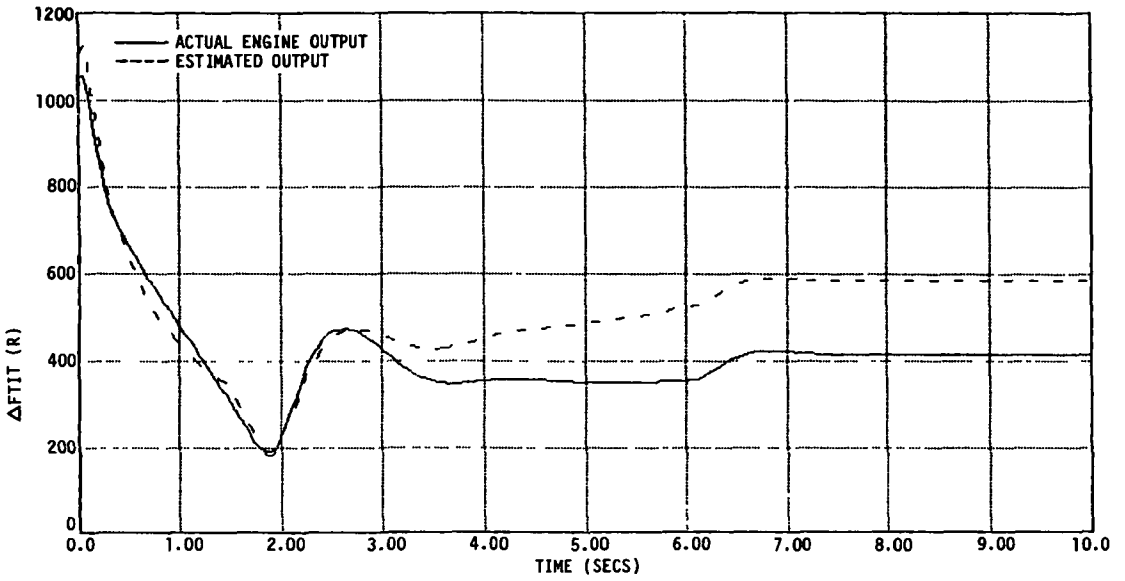

Figure 33 Actual and Estimated Fan Turbine Inlet Temperature (Flight Condition: Altitude = 45,000 Ft., Mach No. = 0.9, PLA Step From 83° to 20° at t=0.0 Seconds)

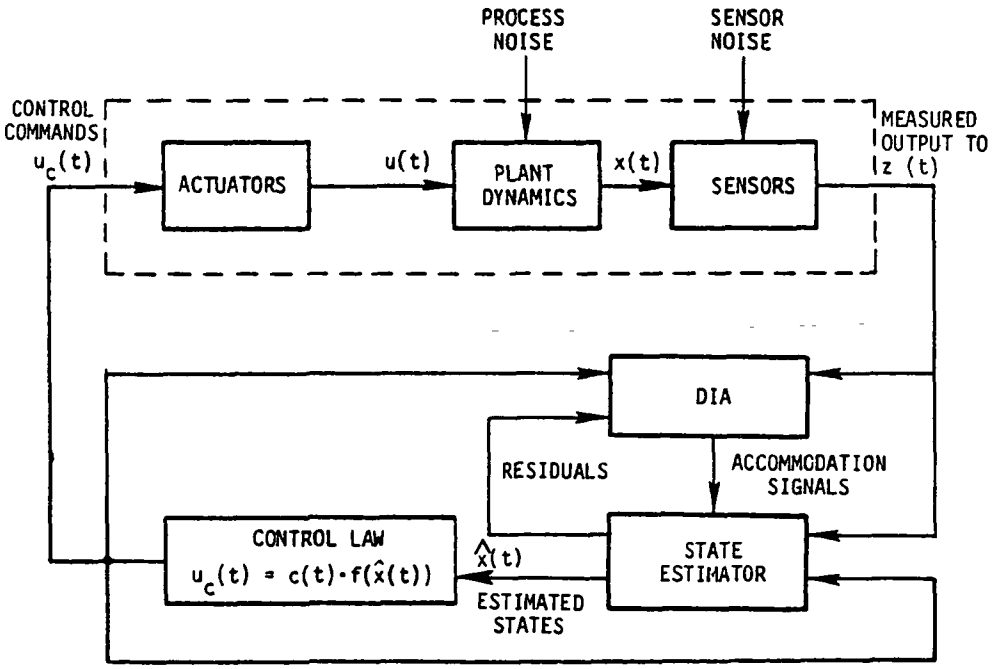

Figure 34 Generalized Block Diagram of Failure Detection, Isolation and Accommodation Logic

A spectrum of techniques for detecting, isolating and accommodating sensor failures have been reported in the literature (Reference 6 is a good summary article). This section contains a description of five detection, isolation, and accommodation strategies that were formulated during this program. The details of these concepts were developed specifically for the aircraft turbine engine system. Presented first is an overview of the general concepts from which a specific technique may be derived. This is followed by detailed discussions of the five concepts developed for this program.

4.3.2 Overview of Existing Techniques

Advanced techniques for detecting, isolating and accommodating sensor failures make use of classical statistical inference calculation and hypothesis testing applied to modern estimators and filters, and analytical redundancy available in unlike sensor channels. Table XI lists several viable techniques. Some of these techniques are capable of detection, isolation and accommodation, while others are only capable of one or two parts. Some techniques share a degree of commonality. Thus, individual techniques or combinations of techniques can be considered for formulating concepts.

TABLE XI

TECHNIQUES FOR DETECTION, ISOLATION, AND ACCOMMODATION

- Bank of Kalman Filters
- Failure Sensitive Filters
- Observers
- Voting Techniques
- Innovations Testing
- Modified Kalman Filters
- Parameter Estimation
- Jump Processes

This section reviews several detection, isolation, and accommodation techniques. All of these are based on the redundancy of information in unlike sensor channels (analytical redundancy). Traditional schemes of voting between redundant sensor hardware channels are only briefly reviewed. The advantage of analytical redundancy is that it avoids many of the size, weight, and cost penalties imposed by redundant hardware. The general disadvantage is computational complexity.

4.3.2.1 Bank of Kalman Filters

This technique employs a group ('bank') of Kalman filters to hypothesize each failure mode. Normal operation of the system is represented by the null hypothesis H_0. The failure hypotheses are labelled as H_i. The residuals of each filter are monitored and likelihood functions (e.g., probability density functions) are generated. Other statistical tests (7) can also be performed on the filter innovations. The hypothesis with the maximum likelihood of occurrence is then selected as representing the true failure mode. Concepts underlying the bank of filter's approach are discussed in references 8 and 9. Figure 35 demonstrates the concept.

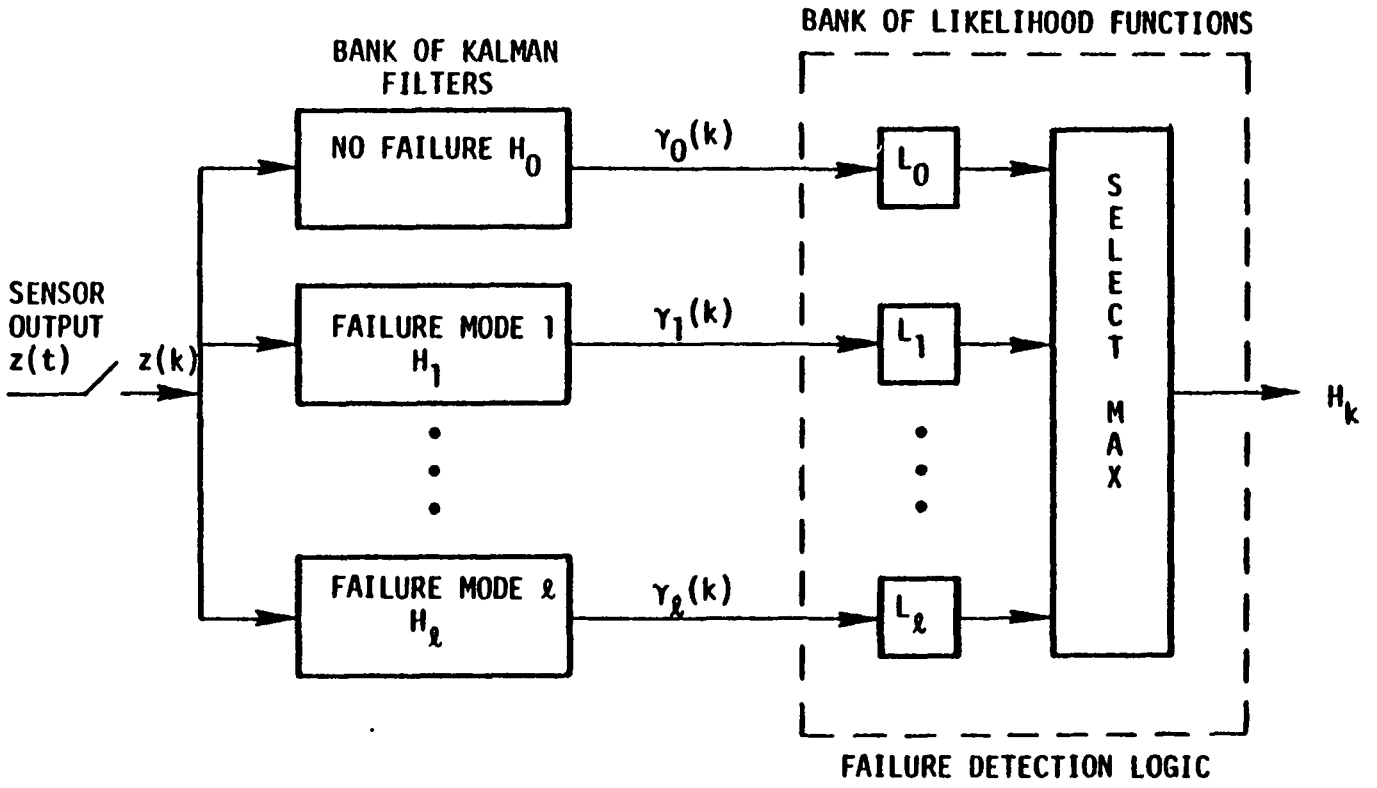

Figure 35 Bank of Kalman Filters Approach

The advantages of the bank of filters technique are; 1) It provides a good yardstick for comparison with simpler techniques, and 2) It allows insight into the failure propagation dynamics after failure detection. The disadvantages are 1) the bank of filters approach results in excessive computational complexity, and 2) there is the possibility of the bank of filters becoming oblivious and failures going undetected.

4.3.2.2 Failure Sensitive Filters

Failure sensitive filters can be classified as 1) filters using failure states in dynamics, and 2) detection filters. Figure 36 is a general block diagram of this technique.

4.3.2.2.1 Failure State Augmented Filters

This type of filter augments the state vector with failure states to form a higher dimensional system in state space. Several techniques which use these filters and are sensitive to specific types of failures have been developed. Kerr (10) discusses an approach where a bounded region is defined around the nominal and estimated trajectories and tests are performed to determine overlapping of the two regions. It is a geometrical approach and models failures as states for detection purposes. Figure 37 demonstrates this concept.

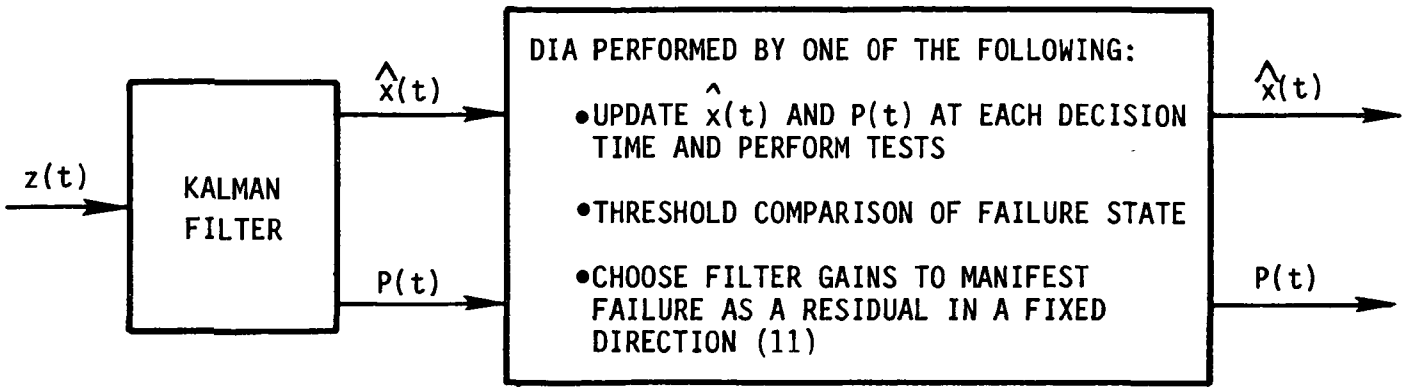

Figure 36 Failure Sensitive Filter Approach Overview

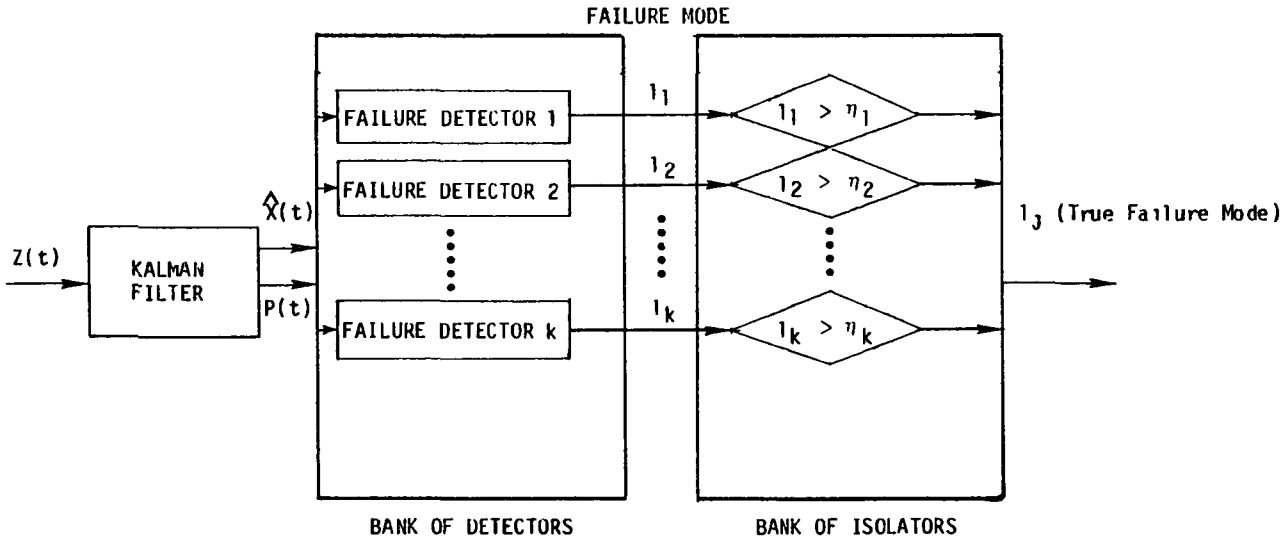

Figure 37 Failure Sensitive Filter Approach

A simple approach for detection and isolation is to compare the estimated failure modes against a predetermined threshold. An advantage is that accommodation can be performed by using the estimate of the failure mode itself. A disadvantage is the poor estimation due to increased order of the filter.

4.3.2.2.2 Detection Filters

Detection filters were developed by Beard (11) and Jones (12). The basic idea is to select the gain matrix such that filter innovations tend to zero in the no-failure state and give an indication of sensor failure in the failed state. Beard's (11) choice of gains is directed towards making the innovations point in a fixed direction in case of a failure. For example, it is easy to show that if the first sensor fails, the first component of filter residual vector is large relative to other components. In such cases, faults may be detected and some faults isolated uniquely.

The major advantage of detection filters is the simplicity with which they can be used. The disadvantages are 1) susceptibility to instrument errors and random disturbances, 2) applicable in theory only to linear regimes where the model structure does not change, 3) modelling errors may appear as soft failures, 4) criteria for declaring faults are hard to set, and 5) in general, this method requires measurements of all state variables.

4.3.2.2.3 Non-Oblivious Filters

If the mathematical model of a system is "close to" the actual physical system, Kalman filtering is the optimal technique for estimation. Performance may be degraded, however, due to modeling errors and the tendency of Kalman Filters to become "oblivious" to the sensor outputs. That is, as more and more information is received, the state estimation error covariance is decreased. Consequently, the filter gains are reduced and the filter bandwidth is reduced.

If a failure occurs early in the measurement sequence, while the filter gain and bandwidth are large, the filter can respond properly to the change. However, as the error covariance and gain decrease, the filter begins to "know the state too well." Thus, as time goes on, it becomes oblivious to incoming information and fails to track the actual system behavior. In fault tolerant systems it is desired to have filters which are sensitive to new data so that abrupt changes are reflected in the filter behavior.

Two techniques exist for avoiding the oblivious filter. They are the exponentially age weighted filtering and the limited memory filtering (13). Both techniques ensure that the filter gains on all failure modes never approach zero. Hence, the filters remain sensitive to failures.

4.3.2.3 Observers

A traditional scheme for protecting a system against failures in its feedback sensors is to provide the system with three (or more) sets of sensors, so that there is redundancy in the feedback information. A voting logic may then be used to identify a faulty instrument output. This approach works well in systems where redundant instrument sets do not cause cost, weight, or size problems.

The technique of using observers requires only one set of instruments. The redundancy provided by multiple sets of instruments is provided, artificially, in the control computer by a subsystem of multiple observers (Figure 38). It is assumed that the single set of instruments consists of three or more individual sensors. The output of each sensor is used to drive an observer, which is designed for that sensor. Thus, each sensor has its own observer. Each observer estimates the states, so there is redundancy in estimates. These observer estimates are compared in a voting manner. For perfect sensors and perfect system dynamics, the estimates will converge to the real state vector in a very short time.

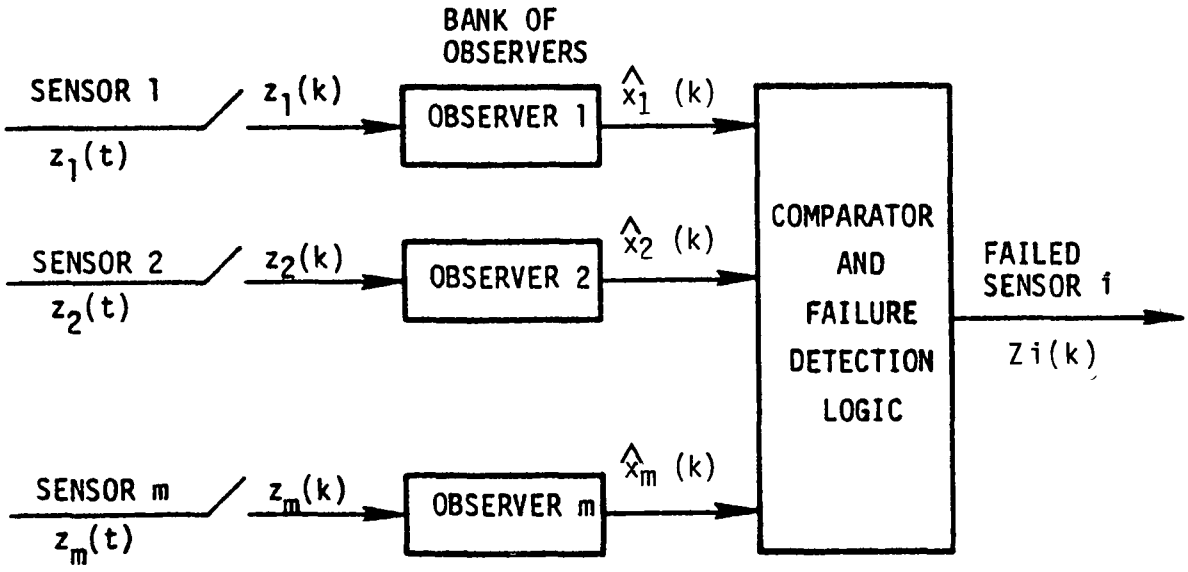

Figure 38 Bank of Observers Technique

If a sensor fails, however, the observer estimate, corresponding to that sensor, is in error and a comparison between the estimated states identifies the faulty sensor. Reference 14 discusses a scheme using multiple observers.

4.3.2.4 Voting Techniques

When redundant sensor channel information is available (analytic or hardware redundancy) voting techniques are useful. These methods work very well for hard failures and certain types of soft failures.

The standard voting process considers three (or more) "identical" signals. A marked deviation in one of the three redundant signals is sufficient to identify a failure. A recent voting scheme is presented in [15] by Broen.

The advantages of this technique are 1) it is simple to use, 2) not much computation is involved compared to other techniques, 3) it is easy to implement. The disadvantages include 1) detection of hard failure is possible, but only for systems with a high level of parallel redundancy; and 2) soft failures, like bias shifts, are hard to detect.

4.3.2.5 Innovations-Based Failure Detection Schemes

These schemes involve monitoring of the innovations of a filter based on the hypothesis of no-failure operation of the system. For a system described by a set of linear differential equations, a Kalman filter is often used to generate this innovation process (or sequence)*. Several detection schemes are discussed here.

4.3.2.5.1 Generalized Likelihood Ratio Test

The generalized likelihood ratio (GLR) technique requires existing functional redundancy to extract fault detection information. This technique monitors the output of one Kalman Filter (Figure 39). A bank of simple correlation operations and threshold comparisons is driven by the filter innovations. These correlations are very complex, however, as found in current literature [16], [17].

The generalized likelihood ratio technique detects the onset of abrupt changes in linear systems. It allows simultaneous detection of failure, the time of occurrence of failure and the extent of the failure. The failure of a sensor produces a non-white residual

$$\gamma(k) = \gamma'(k) + G_i(k\ ,\ \theta)\ \nu \qquad (9)$$

* Mehra and Peschon (7) have discussed various innovations in testing for failure detection and isolation.

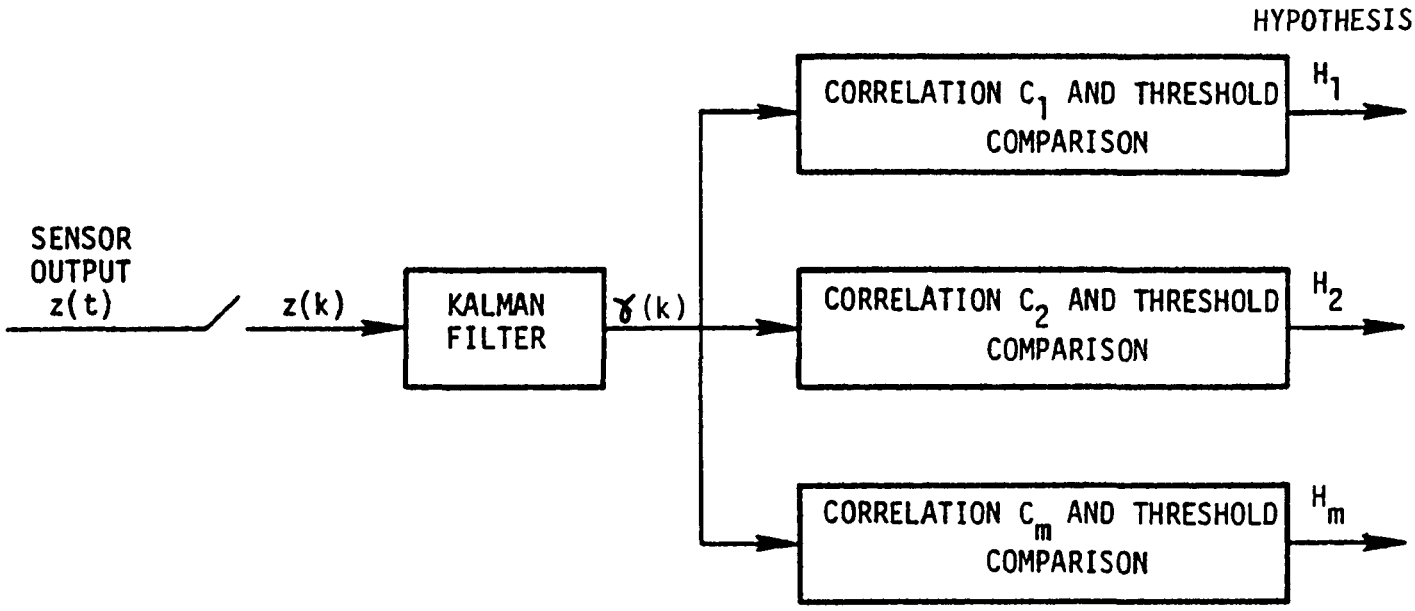

Figure 39 Innovations Based Detection and Isolation Scheme

where $\gamma'(k)$ is the residual for normal operating filter and $G_i(k,\theta)$ describes the effect of failure ν of type i occurring at a time θ on a residual at time k. A set of hypotheses are established to distinguish between failure and no failure modes, as follows:

H_0 = no failure mode
H_i = failure mode of type i (ν and θ unknown)

The Generalized Likelihood Ratio is defined as

$$L_i(k) = \frac{p(\gamma(1), \ldots, \gamma(k))/H_i, \theta = \hat{\theta}(k), \nu = \hat{\nu}(k)}{p(\gamma(1), \ldots, \gamma(k)/H_0)} \qquad (10)$$

where p is the probability density function of the innovations sequence $[\gamma(i)$ $i = 1,\ldots k]$, given the hypothesis H_i and given the maximum likelihood estimates of θ and ν .

When a failure occurs, the decision rule for choosing between a failure and no failure is

for H_i true: $L_i(K) > \lambda_D$ (11)

for Ho true: $L_i(K) < \lambda_D$

where λ_D is a predetermined threshold.

The advantages of this technique are: 1) built in functional relationships allow reduced requirements for multiple redundancy, 2) the technique is computationally feasible, 3) fast failure recovery is obtained since the time of failure occurrence is explicitly determined. The technique therefore does not have oblivious features.

The major disadvantage of this technique is that it is very sensitive to modelling errors. An accurate model is therefore required for a good estimate of failure parameters.

4.3.2.5.2 Likelihood Ratio Test

The likelihood ratio (LR) technique is in principle similar to the GLR technique except that it does not involve prediction of failure time or the extent of failure. The likelihood ratio is simply a ratio of two probabilities

$$L_j(k) = \frac{p\ (\ \gamma(1), \ldots,\ \gamma(k))/H_j}{p\ (\ \gamma(1), \ldots,\ \gamma(k))/H_0} \qquad (12)$$

where the probability density function in the numerator is calculated using the innovations $\gamma(j)$ from a filter designed on the basis of assumed failure (hypothesis H_j) and the denominator is calculated based on the assumption of no-failure (hypothesis H_0). The likelihood ratio is compared against a predefined threshold λ_D. If $L_j(k)$ is less than λ_D, a decision is made in favor of no failure hypothesis H_0; and if $L_j(k)$ is greater than λ_D, H_j is declared to be true, i.e., a failure is detected.

4.3.2.5.3 Sequential Probability Ratio Test

The sequential probability ratio test (SPRT) differs from the likelihood ratio test (LR) in that SPRT compares the likelihood ratio $L_j(k)$ (equation 12) against two thresholds λ_L, λ_u. If the ratio exceeds one threshold or falls below the other, a decision is made corresponding to the threshold that was crossed (see figure 40). The decision is, however, deferred until a threshold is crossed.

This technique was not applicable because a valid state estimate is required at each time step for the control logic. Therefore a decision on whether or not a failure has occurred has to be made. This reduces the SPRT to a simple hypothesis test.

4.3.2.5.4 Chi-Squared Test

The chi-squared test is a test on the whiteness of a residual sequence. Specifically, the covariance C of an innovation sequence γ_j, is given by (7)

$$C = \frac{1}{N} \sum_{j=1}^{N} (\gamma_j - \bar{\gamma}) \cdot (\gamma_j - \bar{\gamma})^T \qquad (13)$$

where N is the sample size. In case of no failure, C has a WISHART distribution. The trace of C has a chi-squared (χ^2) distribution (24), with (N-1) degrees of freedom. A failure decision is made when the probability of the innovation sequences being non-white exceeds a specified threshold.

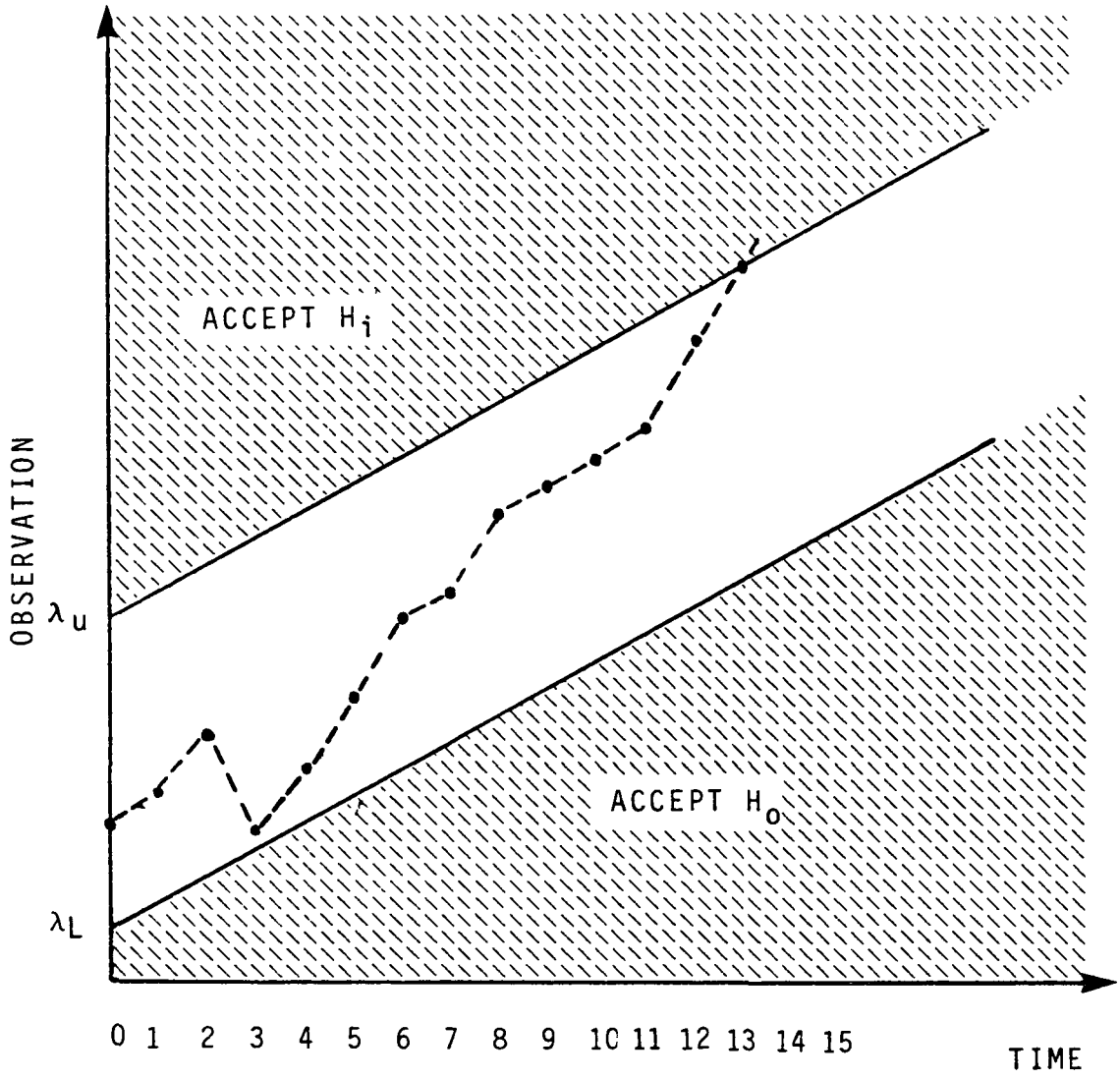

Figure 40 Sequential Probability Ratio Test

4.3.2.5.5 Modified Least Squares Criterion

This technique was devised to suppress extremely large residuals, obtained from bad sensor data, by modifying the least squares criterion. A very small weighting is given to large residuals. This method essentially involves performing a static test at each point in time, incorporating the new measurement and the predicted estimate of this measurement based on previous data. This criterion is also referred to as Weighted Sum Square Residual (WSSR) test [8].

4.3.2.5.6 Modified Kalman Filter Design

This procedure uses the functional redundancy in the system together with a modified Kalman filter as a means of fault detection. Several methods have been developed which modify the design of the kalman filter to achieve specific requirements. For example, a nonlinear single-stage filter algorithm

with filter gains calculated using a linearized system model is discussed in reference 25. This approach reduces the computational burden of a bank of Kalman filters running in parallel. A second example is the application of nonlinear filtering to failure detection in linear systems. This is discussed in reference 26. This approach derives linear optimal estimator equations using nonlinear filtering equations. Several other techniques are discussed in references 27 and 28. These techniques control the estimate error divergence in the case of a failure.

4.3.2.5.7 Parameter Estimation Technique

The failure modes (such as scale factor, failure parameters, and bias) are estimated from input and output data. These estimated values are compared with known values, and substantial differences between the two indicates a failure. Parameter estimation techniques are discussed in reference 18.

A simplified block diagram of the above concept is shown in Figure 41.

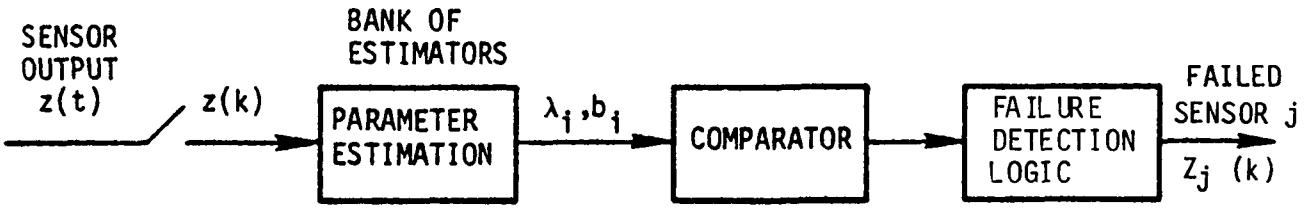

Figure 41 Parameter Estimation Technique

4.3.2.5.8 Jump Process Technique

This technique considers failures as jump processes with known probability distribution (19). It allows the formulation of failure sensitive control laws and computation of conditional probabilities of failure.

Another technique (20) based on nonlinear filtering theory reparameterizes the Kalman filter for both tracking the state and detecting a fault. It is, however, limited to specific types of failures.

This approach is still in early stages of theoretical development. The general concept is to represent randomly occurring failures as jump processes and to estimate time of occurrence and magnitude of jumps using optimal filtering theory. Solutions turn out to be infinite dimension filters. Research is being carried out to circumvent this problem without losing too much performance.

4.3.2.9 Accommodation of Failures

Two failure accommodation techniques were utilized for development of advanced detection, isolation, and accommodation concepts.

4.3.2.9.1 Accommodation Using Failure Parameter Estimate

Some of the detection and isolation techniques discussed above include the failure parameter (bias, drift) in the state vector for estimation purposes. Other techniques like maximum likelihood estimation (MLE) can also be used to estimate failure magnitude. The available failure parameter estimate can be subtracted from the measurement to produce an "unfailed" sensor reading. This technique requires a good estimate of the failure parameter. Once the failure is detected, accommodation could be delayed as much as the time involved in parameter estimation process.

4.3.2.9.2 Reconfiguration and Reinitialization of the Kalman Filter

If the Kalman Filter is being driven by faulty measurements, the state estimates wander off from their nominal values. Once a failure has been detected and isolated, the filter can be reconfigured so that the faulty measurement does not drive it. The reconfiguration involves using a new filter gain matrix designed with the assumption of one faulty measurement. This technique therefore requires as many gain matrices as there are failure modes.

Once the filter is reconfigured, it should be reinitialized since the state estimates are off-nominal. Estimates from a robust filter are needed for reinitialization. If, however, robust estimates are not available, reconfiguration is adequate and will bring the filter back to its nominal path. A small transient will result if the filter is only reconfigured since the filter starts out at some off-nominal point as its initial condition. Reinitialization will eliminate the transient.

4.3.3 Formulation of Advanced Sensor Failure Detection, Isolation and Accommodation Concepts

Five viable advanced concepts were developed based upon the techniques discussed in the last section. The available techniques were classified according to their functional features. Most techniques provide at least the detection capability with isolation and accommodation either implicitly (e.g., in a triplex voting scheme) or explicitly (e.g., in a bank of Kalman filters) addressed. A classification of the techniques based on the information processing structure, parameter on which tests are performed and decision techniques and logic used is presented in Table XII.

TABLE XII

CLASSIFICATION OF DETECTION, ISOLATION AND ACCOMMODATION TECHNIQUES

- o Logic Structure
  - On-line detection and isolation: detection and isolation are performed at each time step simultaneously
  - Off-line isolation: detection is always on-line but isolation is performed off-line, i.e., only after a failure is detected is isolation performed.
- o Parameters
  - Innovations based failure check
  - Failure state parameter
  - Statistical probability check
- o Decision Logic
  - Generalized Likelihood Ratio Testing (GLR)
  - Likelihood Ratio Testing (LR)
  - Sequential Probability Ratio Testing (SPRT)
  - Weighted Sum Square Residual (WSSR)
  - Voting
- o Decision Technique
  - Bank of Observers
  - Bank of Filters
  - Failure sensitive Filters
- o Accommodation Technique
  - Subtract estimated failure mode parameter (bias, drift) from the sensor measurement
  - Reconfigure (modify Kalman filter gains) and reinitialize (initialize to the filter corresponding to the isolated failure mode) the normal mode (no failure) filter.

The goal in selecting five candidate concepts was to span as many applicable techniques as possible. Thus, selected features of the above techniques have been blended together to formulate the five candidate concepts for evaluation. These concepts are:

1: Detection - Hypothesis testing using LR test
Isolation - Off-line isolation using bank of Kalman filters based on GLR technique
Accommodation - By "calculation" i.e., failure states are subtracted from the measurements.

2: Detection - Innovations testing based on WSSR technique for soft failure
- Innovations testing against thresholds for hard failure

Isolation - On-line isolation of hard failures using innovations testing; off-line isolation of soft failure using GLR technique. Both structures employ bank of Kalman filters.

Accommodation - Reconfiguration and reinitialization of normal mode filter.

3: Detection - Hypothesis testing using LR technique

Isolation - Off-line logic using failure-sensitive filter

Accommodation - By "calculation" i.e., failure states are subtracted from the measurements.

4: Detection & Isolation - Simultaneous detection and isolation using failure sensitive filter (on-line)

Accommodation - By "calculation" i.e., failure states are subtracted from the measurements.

5: Detection & Isolation - Simultaneous detection and isolation using bank of observers and voting technique

Accommodation - Computation of median of estimates from observers corresponding to unfailed measurements.

Figures 42 through 46 are block diagrams of the five concepts. Techniques and logic employed by each concept are found in Table XIII.

TABLE XIII

SELECTED FAILURE DETECTION, ISOLATION AND ACCOMODATION (FDIA) CONCEPTS

	DETECTION						ISOLATION												ACCOMMO-DATION	
	LOGIC STRUCTURE		PARAMETER		DECISION LOGIC		LOGIC STRUCTURE		PARAMETER			DECISION LOGIC				TECHNIQUE				
Concept	H_0	H_0 & H_I	Prob	Innov	LR	WSSR	ON-LINE	PARALLEL	FAILURE STATE	PROB	RESIDUAL	GLR	LR	THRES-HOLD	VOTING	BANK OF KF	BANK OF OBS	FAILURE SENSITIVE	R	R & I
1		X	X		X			X		X		X				X				X
2	X			X		X	X	X		X	X		X			X			X	
3		X	X		X			X	X					X				X	X	
4							X		X					X				X		X
5							X		X						X		X		X	

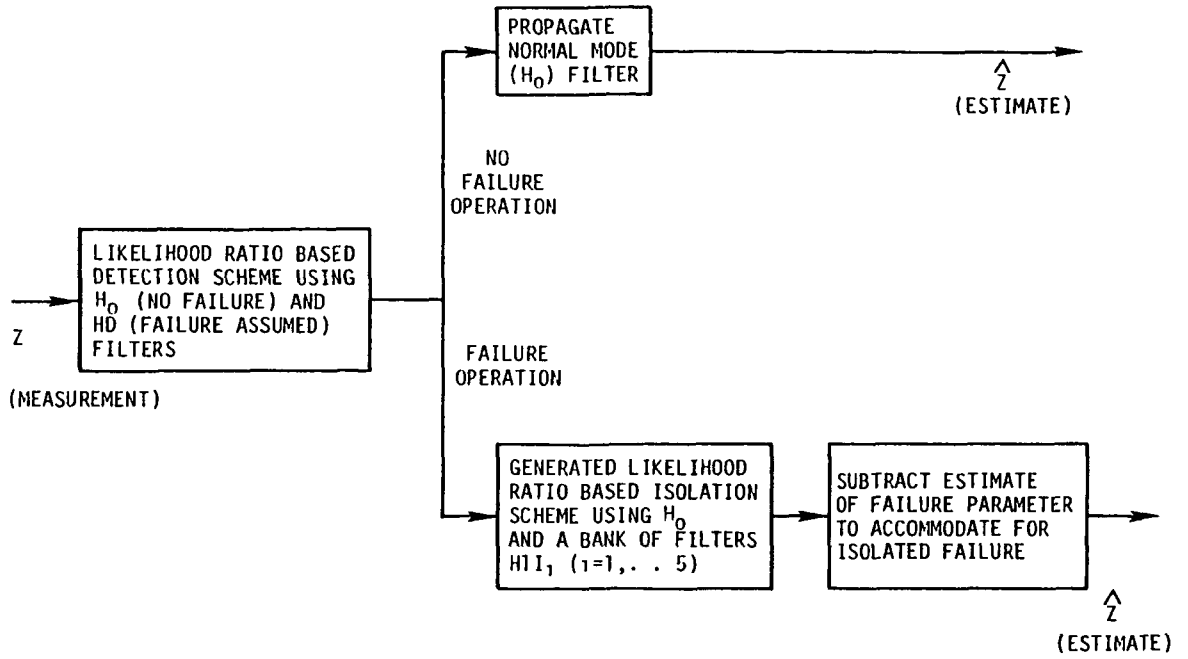

Figure 42 Detection, Isolation, and Accommodation Concept 1

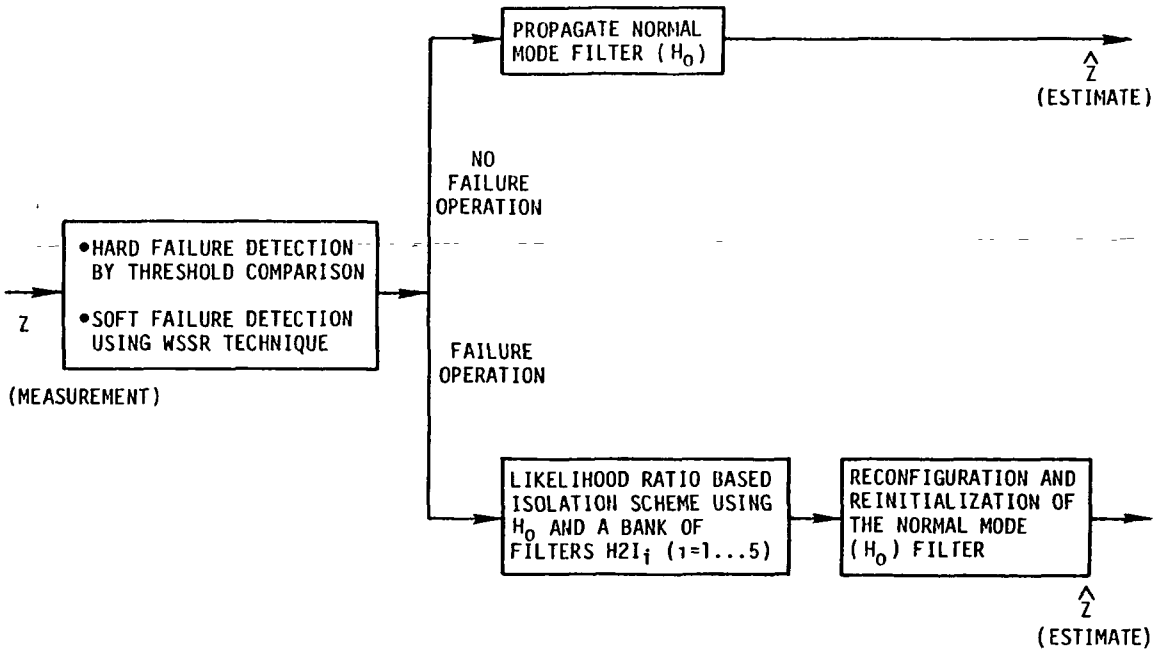

Figure 43 Detection, Isolation, and Accommodation Concept 2

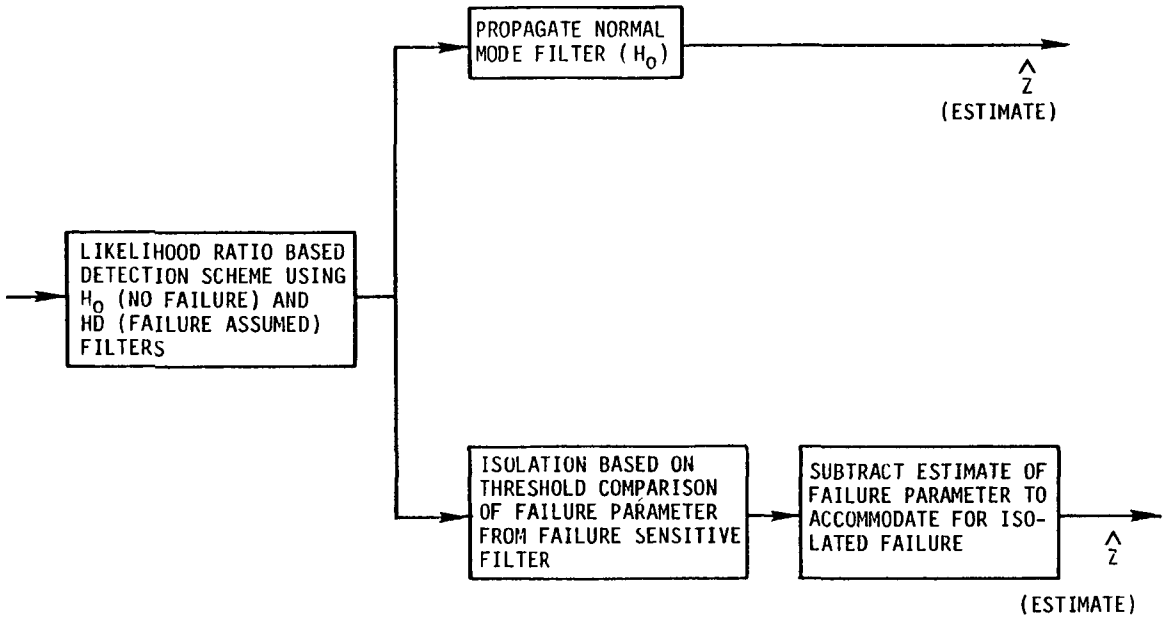

Figure 44 Detection, Isolation, and Accommodation Concept 3

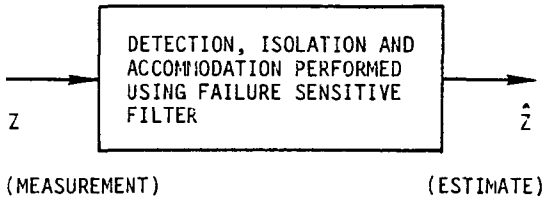

Figure 45 Detection, Isolation, and Accommodation Concept 4

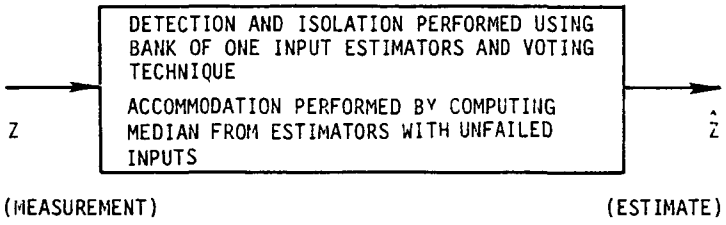

Figure 46 Detection, Isolation, and Accommodation Concept 5

4.3.3.1 Discussion of Detection, Isolation and Accommodation Concepts

The five concepts developed for preliminary evaluation are discussed in this section. A general formulation of the failure detection, isolation and accommodation problem is presented below and will be used to explain detection, isolation and accommodation concepts.

A linear dynamic system can be modelled as follows:

Plant Dynamics: $X(t) = F(t) \cdot X(t) + G(t) \cdot U(t) + W(t)$ (14)

Sensors: $Z(t) = H(t) \cdot X(t) + D(t) \cdot U(t) + V(t)$ (15)

Actuators: $U(t) = g \cdot (U_c(t))$ (16)

equations (14) through (16) can also be written in discrete form for linear stochastic systems as:

Plant Dynamics: $X(k+1) = \phi(k) \cdot X(k) + \Gamma(k) \cdot U(k) + W(k)$ (17)

Sensors: $Z(k) = H(k) \cdot X(k) + D(k) \cdot U(k) + V(k)$ (18)

Actuators: $U(k) = g \cdot (U_c(k))$ (19)

where W(k) and V(k) are zero-mean, independent, white Gaussian sequences with covariances given by:

$$E[W(j) \cdot W^T(k)] = Q \cdot \delta_{jk} \quad (20)$$

$$E[V(j) \cdot V^T(k)] = R \cdot \delta_{jk} \quad (21)$$

and where δ_{jk} is the Kronecker delta. Equations (17) through (21) describe a "no failure" model of the system. The optimal state estimator for this model is a discrete Kalman filter:

$$\hat{X}(k+1/k) = \phi(k) \cdot X(k/k) + r(k) \cdot U(k) \quad (22)$$

$$\hat{X}(k/k-1) = X(k/k-1) + K(k) \cdot Y(k) \quad (23)$$

$$\gamma(k) = Z(k) - H(k) \cdot X(k/k-1) - D(k) \cdot U(k) \quad (24)$$

Here $\gamma(k)$ is the zero-mean, Gaussian innovations process. The estimator gain matrix, K, is found from:

$$P(k+1/k) = \phi(k) \cdot P(k/k) \cdot \phi^T(k) + B(k) \cdot QB^T(k) \quad (25)$$

$$P(k/k) = P(k/k-1) - P(k/k-1)\, H^T(k) \cdot [H(k) \cdot P(k/k-1) \cdot H^T(k) + R]^{-1} H(k) \cdot P(k/k-1) \quad (26)$$

$$K(k) = P(k/k-1) \cdot H^T(k) \cdot [V(k)]^{-1} \quad (27)$$

$$V(k) = H(k) \cdot P(k/k-1) \cdot H^T(k) + R \quad (28)$$

where P(k) is the estimation error covariance of the estimate, $\hat{X}(k)$.

The above general formulation is the basis of the concepts described in the following section.

4.3.3.1.1 Detection, Isolation and Accommodation Concept 1

Detection: This concept employs hypothesis testing based on the likelihood ratio (LR) technique. For example, normal mode or no failure operation is termed null hypothesis, Ho. The failure modes are also hypothesized and are termed as failure hypothesis, H_1.

In a given system, each observation (measurement) has a hypothesis associated with it. The hypothesis cannot be observed directly. A probability transition mechanism separates the hypothesis from observations. Hypotheses are accepted on the basis of knowledge of a priori probabilities, some inherent conditional probabilities and access to observation space. Thus a failure is detected by choosing a hypothesis according to some decision logic. In the detection scheme used here the decision logic is the likelihood ratio test.

Let z be the observation at a decision time and z_t be the predefined threshold. A decision is then made by testing the hypothesis as follows,

$z < z_t$ H_0 is true

$z > z_t$ H_1 is true (29)

In the binary decision of Ho and H_1, a possibility of errors exists which are termed as "false alarm" and "miss". A false alarm is the condition when H_1 is false but is accepted to be true. Acceptance of Ho when it is false is called a miss. Let the probability density associated with the measurements under the hypotheses Ho and Hl be P(z/Ho) and $P(z/H_1)$ respectively. The object of the detection logic is to accept one of the two density functions. Figure 47 illustrates the hypothesis testing technique. A variety of threshold selection procedures exists which are given in Table XIV. Each of the minimization procedures results in the comparison of the ratio of two probability density functions to a given parameter. The resultant likelihood ratio test is then given by:

$$\frac{P(z/H_1)}{P(z/H_0)} \quad \begin{cases} < \lambda \text{ implies } H_0 \text{ true} \\ > \lambda \text{ implies } H_1 \text{ true} \end{cases} \qquad (30)$$

In Concept 1, Kalman filter innovations were obtained to formulate the H_0 hypothesis (assuming perfect modelling and random noise). Innovations from a "failure insensitive filter" were obtained to formulate hypothesis H_1. Probability density functions using innovations were calculated and the likelihood ratio test performed for failure detection.

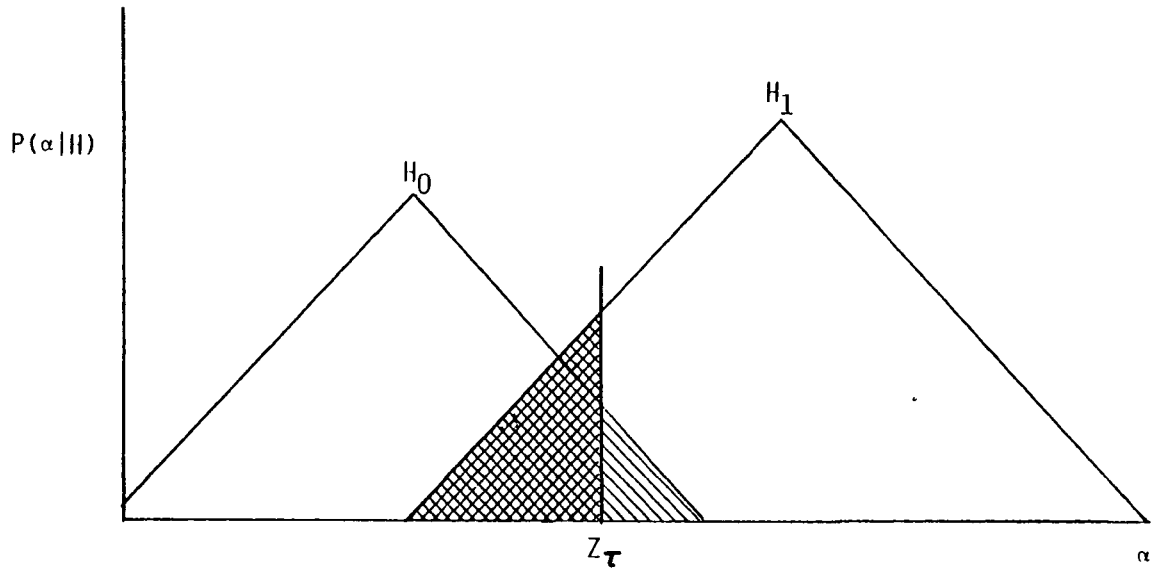

Figure 47 Hypothesis Testing Technique

TABLE XIV

THRESHOLD SELECTION

Minimize Miss Probability for a Fixed False-Alarm Rate
Minimize Sum of Miss and False-Alarm Probabilities
Minimize the Bayes Risk

$$B = C_{00} \cdot P(H_0,H_0) + C_{01} \cdot P(H_0,H_1) + C_{10} \cdot P(H_1, H_0) + C_{11} \cdot P(H_1,H_1$$

where:

$P(H_i,H_j) = P_{H_j} \quad (H_i/H_j)$

H_i hypothesis associated with failure mode i

C_{ij} cost of accepting H_i when H_j is true

P_{H_j} a-priori probability that H_j is true

$P(H_i/H_j)$ probability of accepting H_i given H_j is true

Isolation: Multiple hypothesis testing using the Generalized Likelihood Ratio test (GLR) was used for isolation of failures. This technique differs from the Likelihood Ratio (LR) technique in that the probability density functions associated with the hypotheses involved an estimated parameter. Maximum likelihood techniques was used to estimate the parameter and calculate the conditional densities. A bank of Kalman filters is used in parallel to produce innovations. Each filter is based on an assumed failure mode (hypothesis). The

maximum likelihood estimate of the failure parameter and the filter innovations are used to calculate the generalized likelihood ratio and test the hypothesis:

$$\frac{\max_{\theta_1} P(z/H_1, \hat{\theta}_1)}{\max_{\theta_0} P(z/H_1, \hat{\theta}_0)} \quad \begin{matrix} < \lambda \text{ implies } H_0 \text{ true} \\ > \lambda \text{ implies } H_1 \text{ true} \end{matrix} \qquad (31)$$

Accommodation: The filter which provides estimates to the control logic is the normal mode filter (Ho filter) and works directly with sensor measurements. In the event of a failure, the filter drifts while the failure is being isolated. After isolation the filter needs to be reinitialized. Isolation of a failure means acceptance of a hypothesis. The filter in the isolation scheme corresponds to the accepted hypothesis, and is used to reinitialize the normal mode filter. The filter must be reconfigured to avoid using the failed channel. This is done by subtracting the failure estimate (maximum likelihood estimate) from the failed channel. The resulting reinitialized and reconfigured filter is the accommodation filter.

A detailed flow chart of this concept is shown in Figure 48.

4.3.3.1.2 Detection, Isolation and Accommodation Concept 2

Detection: The sensor failures can be classified as soft or hard failures.

The detection scheme uses a simple threshold comparison check on the normal mode filter residuals to declare a hard failure. The Weighted Sum Square Residual (WSSR) test is used for soft failure detection. This technique, discussed in reference 8, uses filter innovations for decision making. The innovation sequence $\gamma(k)$ is white with known covariance if the model is perfect and there is no failure. In case of a failure the residual becomes

$$\gamma(k) = \text{white noise} + \text{effect of failure}$$

and the detector is used to identify the failure using a priori knowledge of white noise covariance and the new statistics. To detect a failure, one therefore has to compute the quantity, (k) over the last N observations,

$$1(k) = \frac{1}{N} \sum_{j = k - N + 1}^{k} \gamma^T(j) \cdot V^{-1}(j) \cdot \gamma(j) \qquad (32)$$

where V(j) is given by (28).

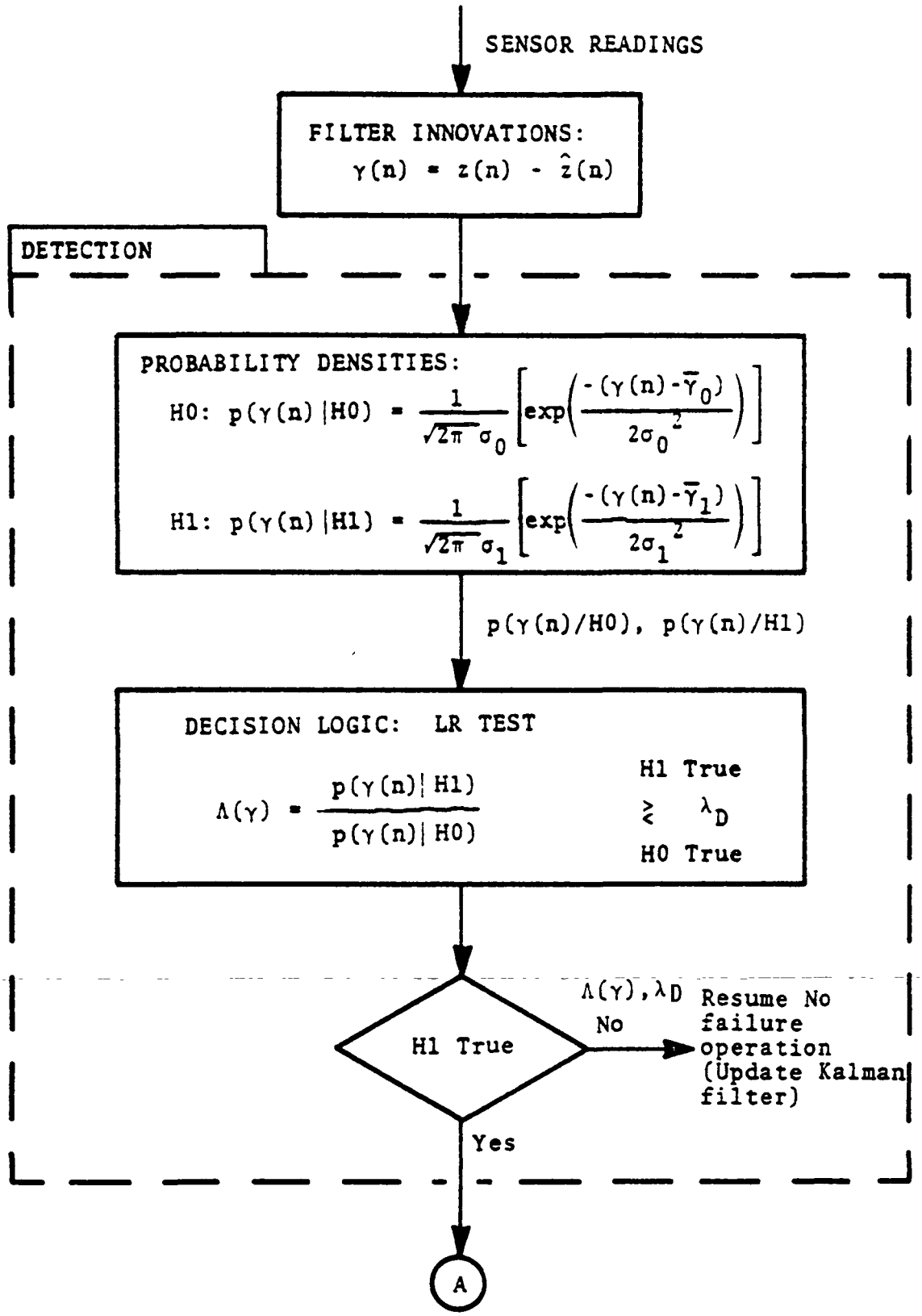

Figure 48 Flow Chart of DIA Concept 1

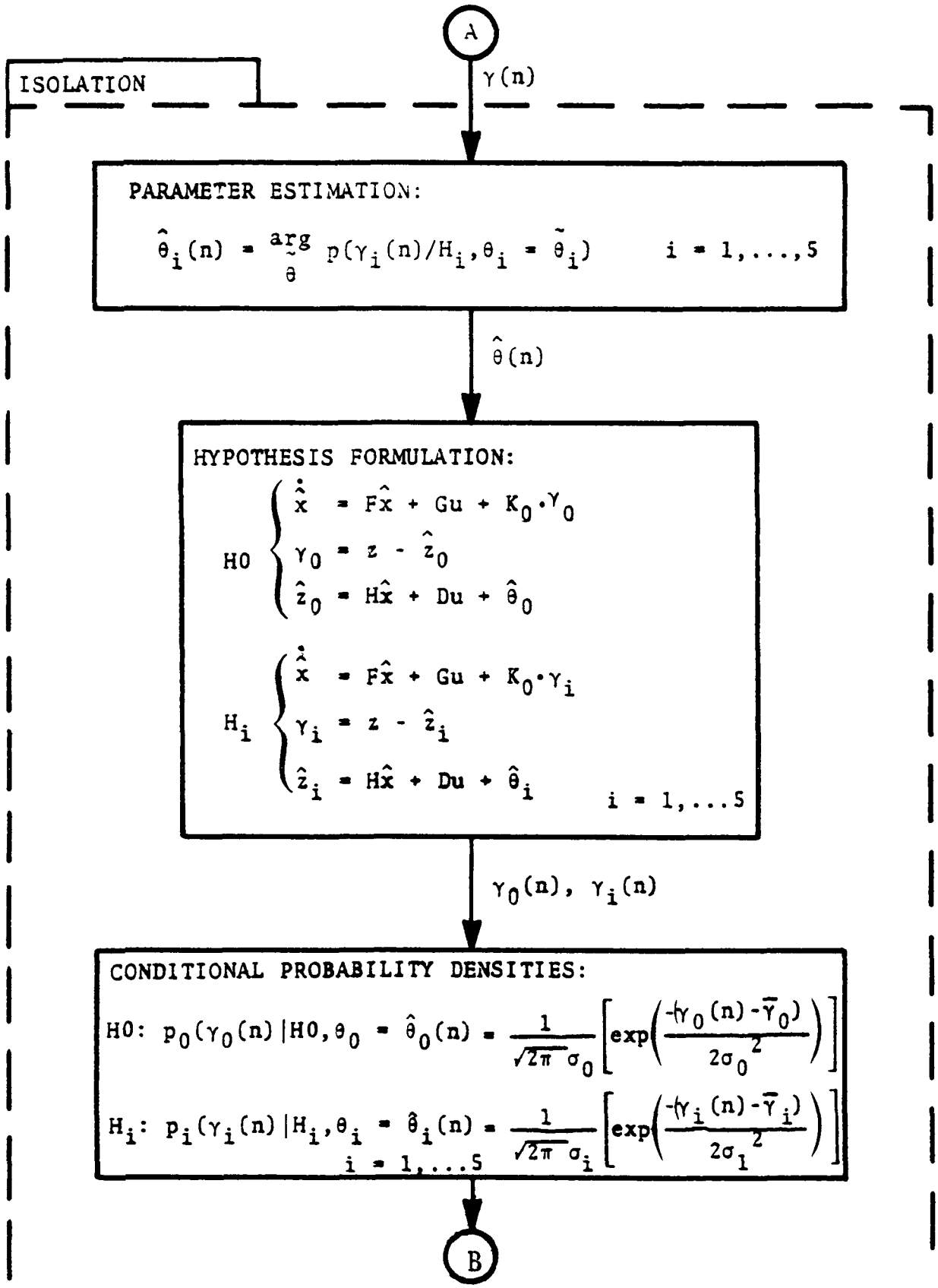

Figure 48 Flow Chart of DIA Concept 1 (Continued)

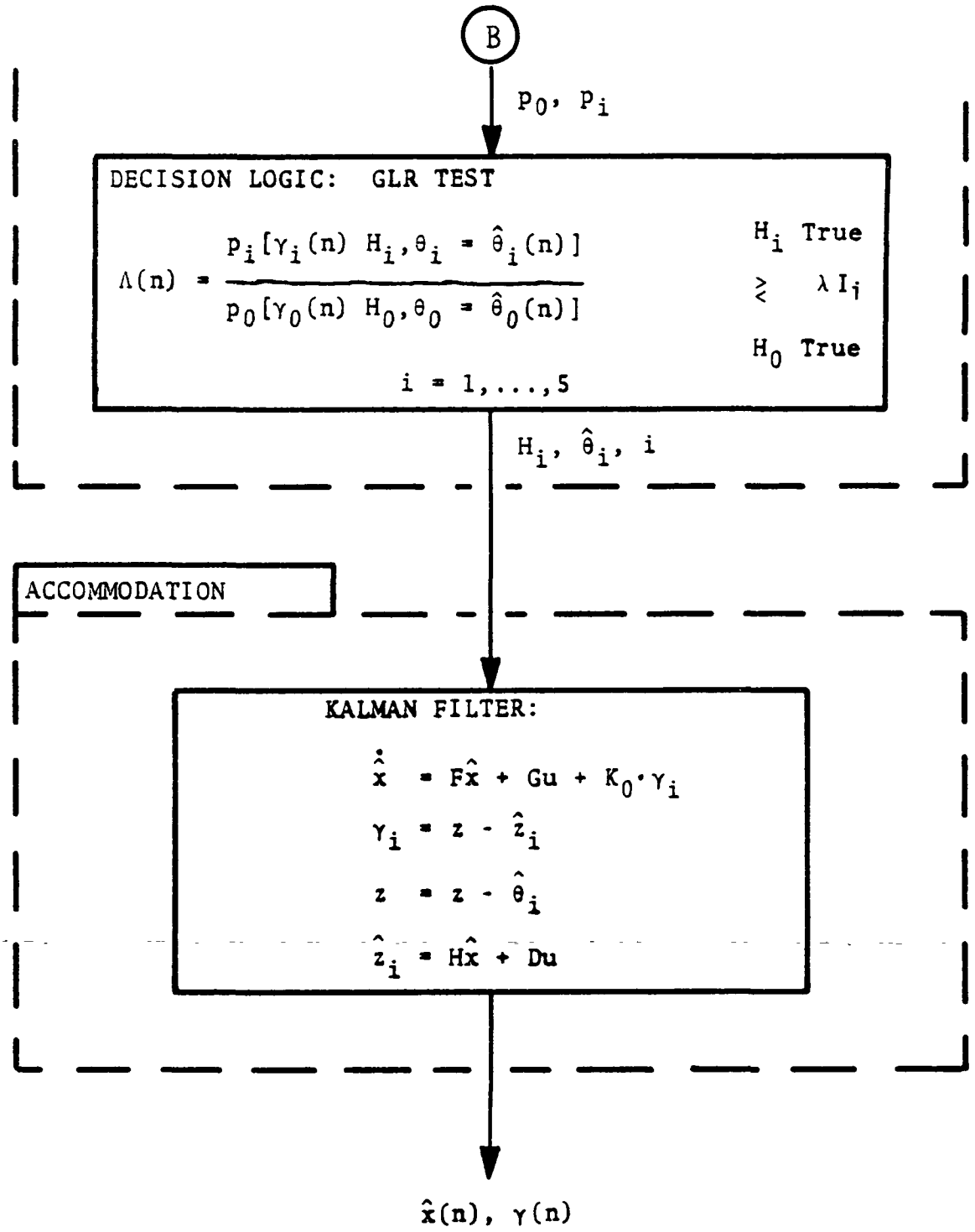

Figure 48 Flow Chart of DIA Concept 1 (Concluded)

The quantity $l(k)$ is called the Weighted Sum Square Residual. For normal (no-failure) operation, $l(k)$ is expected to remain small. However, in case of a failure, $l(k)$ will increase. If λ is the threshold value to make a decision between H_0 and H_1, we have

$$l(k) \begin{cases} < \lambda \text{ implies } H_0 \text{ true} \\ > \lambda \text{ implies } H_1 \text{ true} \end{cases} \qquad (33)$$

The size of N and λ are design parameters, chosen to provide acceptable tradeoff between false alarms and misses.

Isolation: In concept 2, isolation of soft failures is performed "off-line" using a likelihood ratio test. This procedure was discussed in the detection scheme of concept one. For isolation purposes, however, since M failure modes are hypothesized, M Kalman filters (bank of filters) are designed based on each failure mode. Each of the filters ignores one measurement and operates on the assumption that the channel containing the failure information has been ignored. When a failure occurs, the filter which ignores the failed channel stands out from all other filters and the likelihood ratio test is used to identify the failed channel filter.

The design parameters involved in this isolation process are the thresholds used to perform the likelihood ratio test. The techniques in Table XIV can be used for this purpose.

Accommodation: The normal mode filter serves as the accommodation filter for the no-failure case. In case of a hard failure, where the failure is detected and isolated simultaneously, the accommodation filter is reconfigured to eliminate the failed channel. One of the isolation filters which ignores the failed channel is used for this purpose. There may be small transients associated with switching filters. In case of soft failures, the normal mode filter provides estimates to the control logic while the failure is being isolated. After the isolation of the failure the accommodation filter; i.e., the normal mode filter, is reinitialized and reconfigured using the "isolated" filter.

Once a failure has been detected and isolated, further tests for additional failures are performed on the accommodation filter. Each time a failure is isolated, the accommodation filter is reinitialized and reconfigured.

A detailed flow chart of this concept is shown in Figure 49.

4.3.3.1.3 Detection, Isolation and Accommodation Concept 3

Detection: The likelihood ratio based detector, used in concept 1 is used for detection purposes.

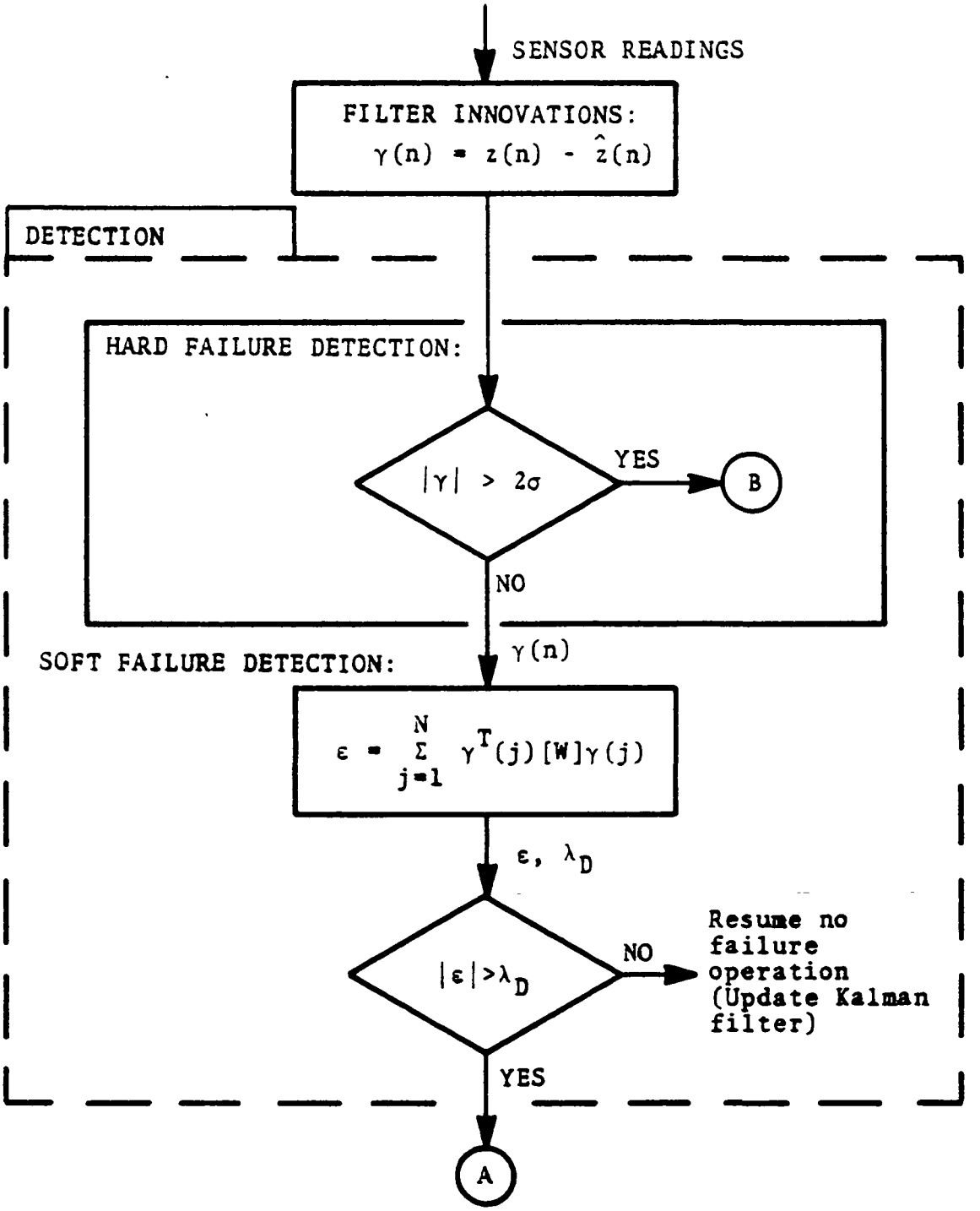

Figure 49 Flow Chart of DIA Concept 2

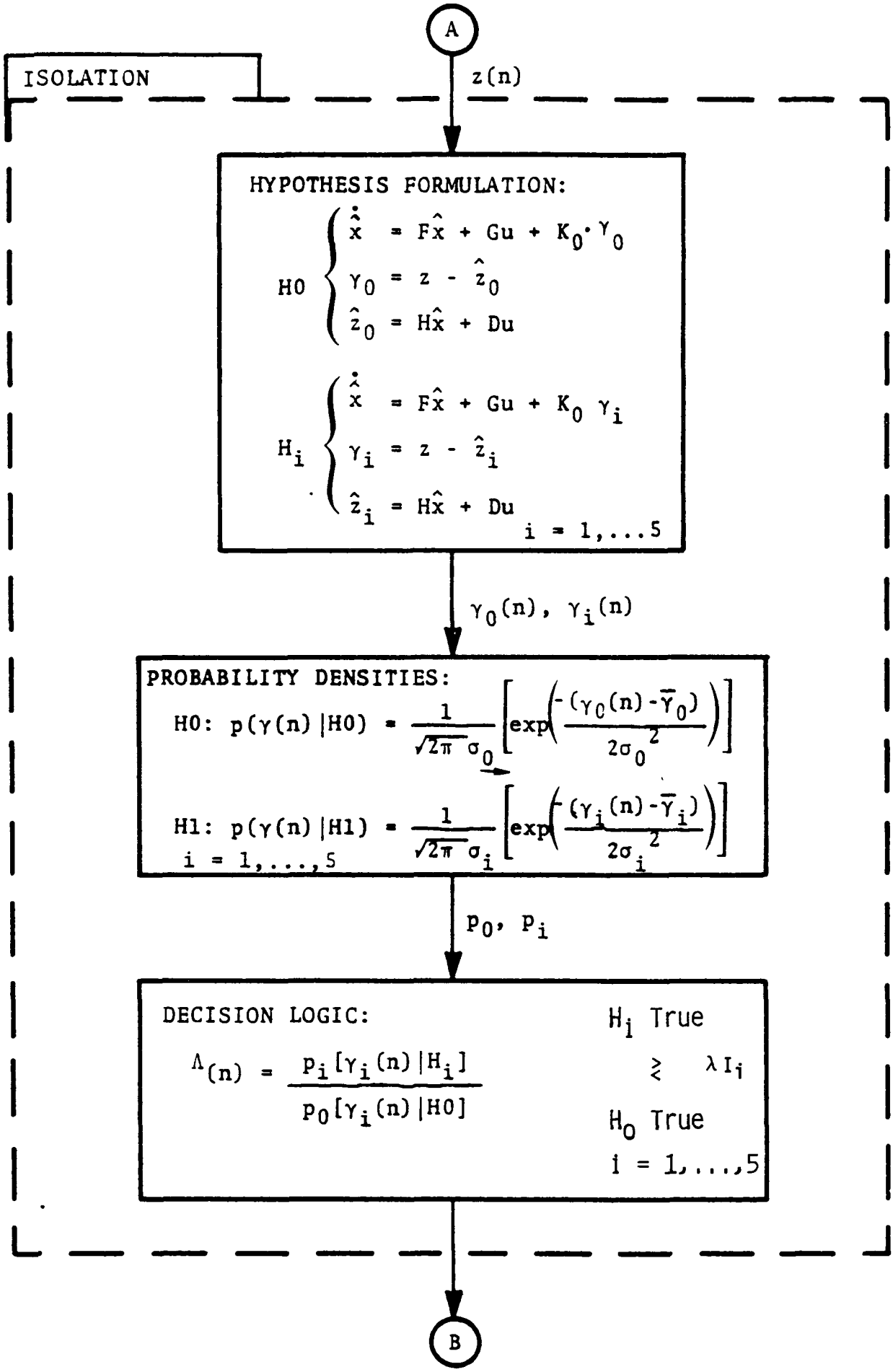

Figure 49 Flow Chart of DIA Concept 2 (Continued)

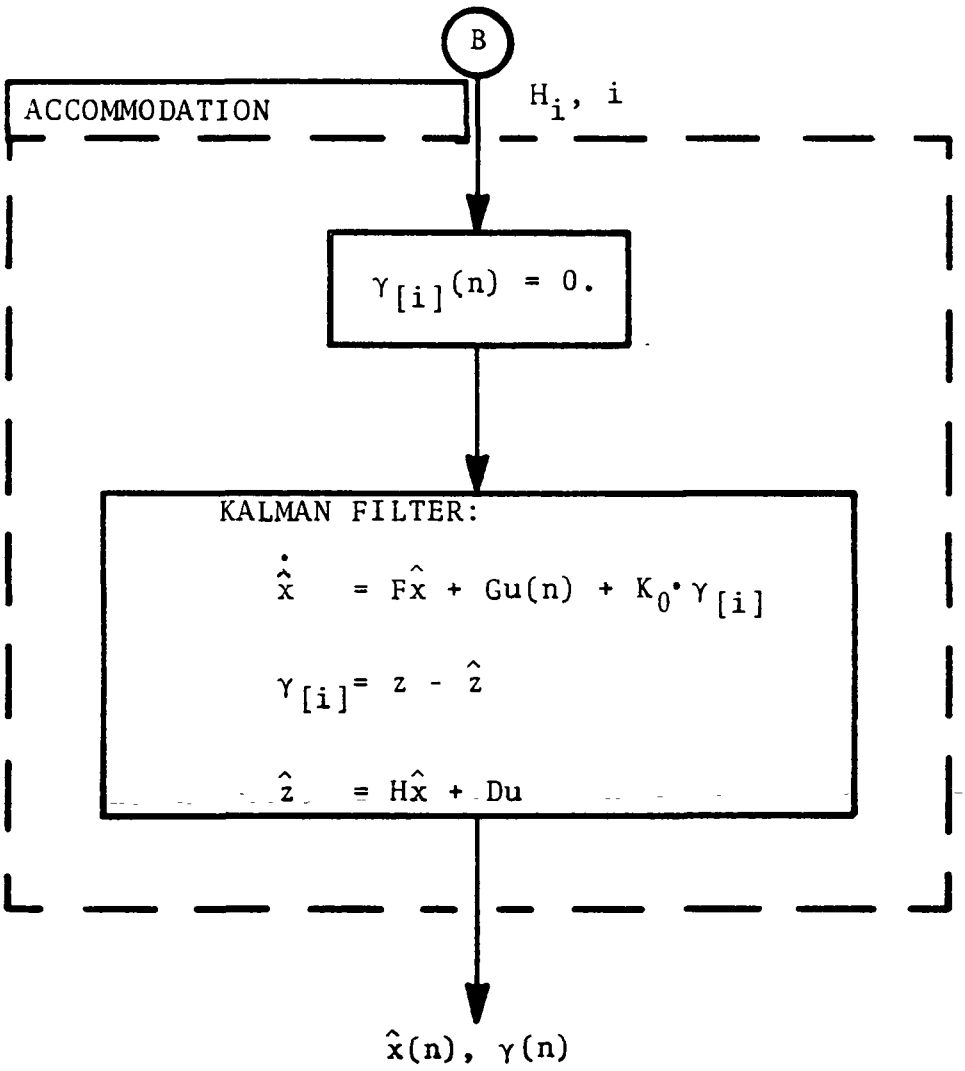

Figure 49 Flow Chart of DIA Concept 2 (Concluded)

Isolation: A failure sensitive filter is used for off-line isolation of failures. This filter models the failure parameters (biases, drifts, scale factor changes) as states and estimates these parameters. The failure magnitudes are compared to a threshold to isolate the failure. Note that the failure state is being used as a test parameter instead of filter innovations in previously discussed concepts.

Accommodation: The estimated failure state, using the failure sensitive filter in the isolation scheme, is subtracted from the isolated channel and used as the input to the normal mode filter. Since the estimate is updated at each time step, the normal mode filter receives the most current failure estimate. Thus the normal mode filter is always working with correct information (assuming perfect model and estimate). The accommodation filter (normal mode filter) requires no reinitialization or reconfiguration. However, a transient may be associated with subtracting the failure state because the filter may have drifted off while the failure was being isolated.

Figure 50 is a detailed flow chart of concept 3, where bias is shown as the assumed failure mode in the isolation scheme.

4.3.3.1.4 Detection, Isolation and Accommodation Concept 4

Detection, Isolation and Accommodation: Several well known techniques exist to design failure-sensitive filters [6, 8, 9, 16, 17]. The filter used in this concept is the same as the failure-sensitive isolation filter of concept 3. This single filter provides the three functions of detection, isolation and accommodation. Detection and Isolation are performed on-line simultaneously by comparing the estimated failure state against a threshold. Accommodation is performed by subtracting the failure state from the channel determined to be failed.

Figure 51 is a detailed flow chart of this concept. Bias is used as the assumed failure state to demonstrate the function of the DIA concept.

4.3.3.1.5 Detection, Isolation and Accommodation Concept 5

Detection and Isolation: A traditional scheme for failure protection of system is to provide redundant sensors and use voting logic to detect a failure. In the detection and isolation technique employed here, redundancy is provided by a bank of Luenberger observers [23]. The output from each sensor serves as input to an observer which estimates the state vector. The state estimates from each observer are voted on to detect and identify a faulty sensor.

The essence of this DIA concept was derived from Reference [14]. A detailed flow chart is given in Figure 52. A problem arises if small errors are present in the design coefficients of different observers or if small noise exists in the sensors. This is corrected by setting a threshold for each sensor and declaring a failure if the failure magnitude exceeds that threshold.

Accommodation: The accommodation scheme calculates a median of the estimates from the unfailed channels to feed them to the control logic.

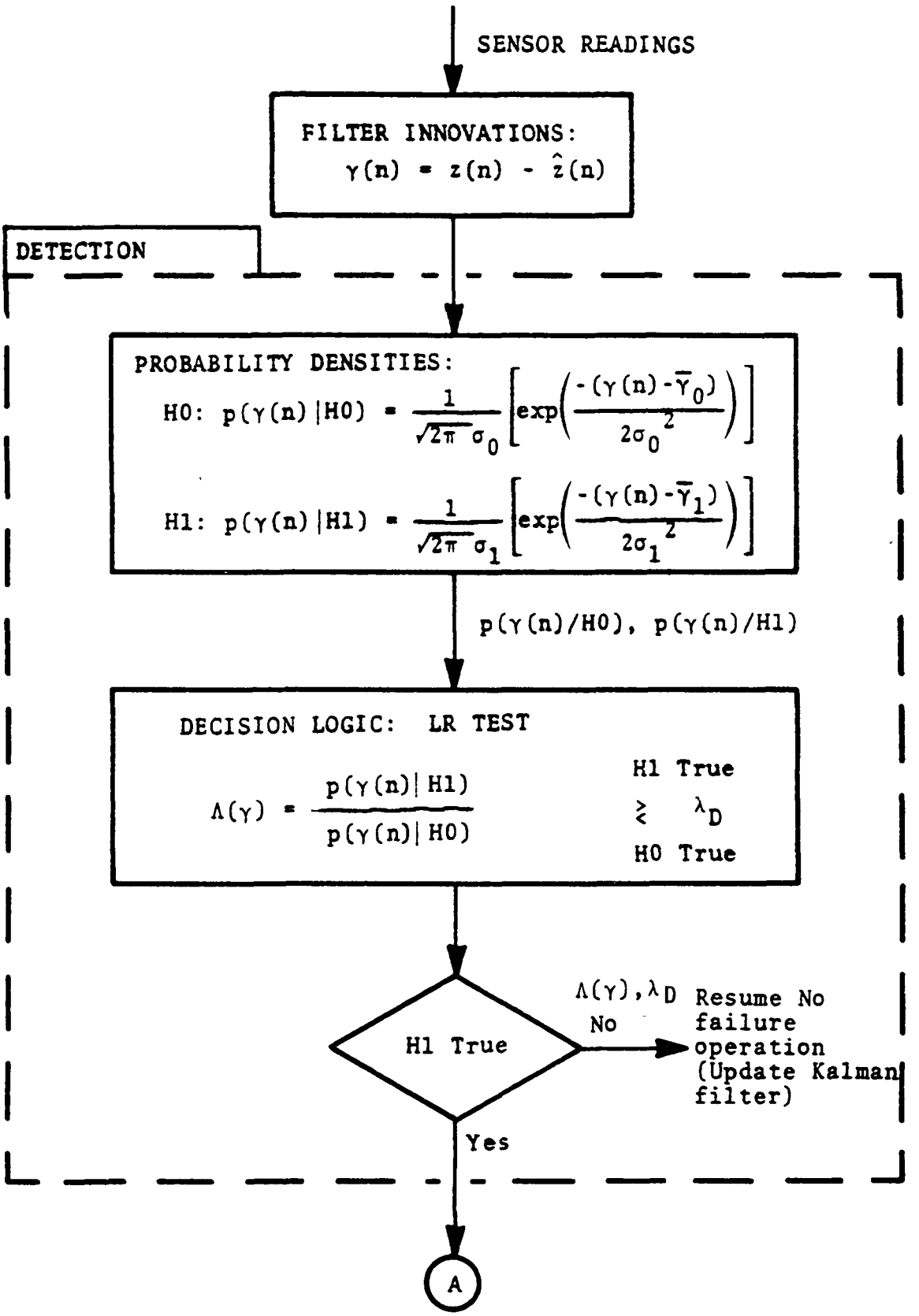

Figure 50 Flow Chart of DIA Concept 3

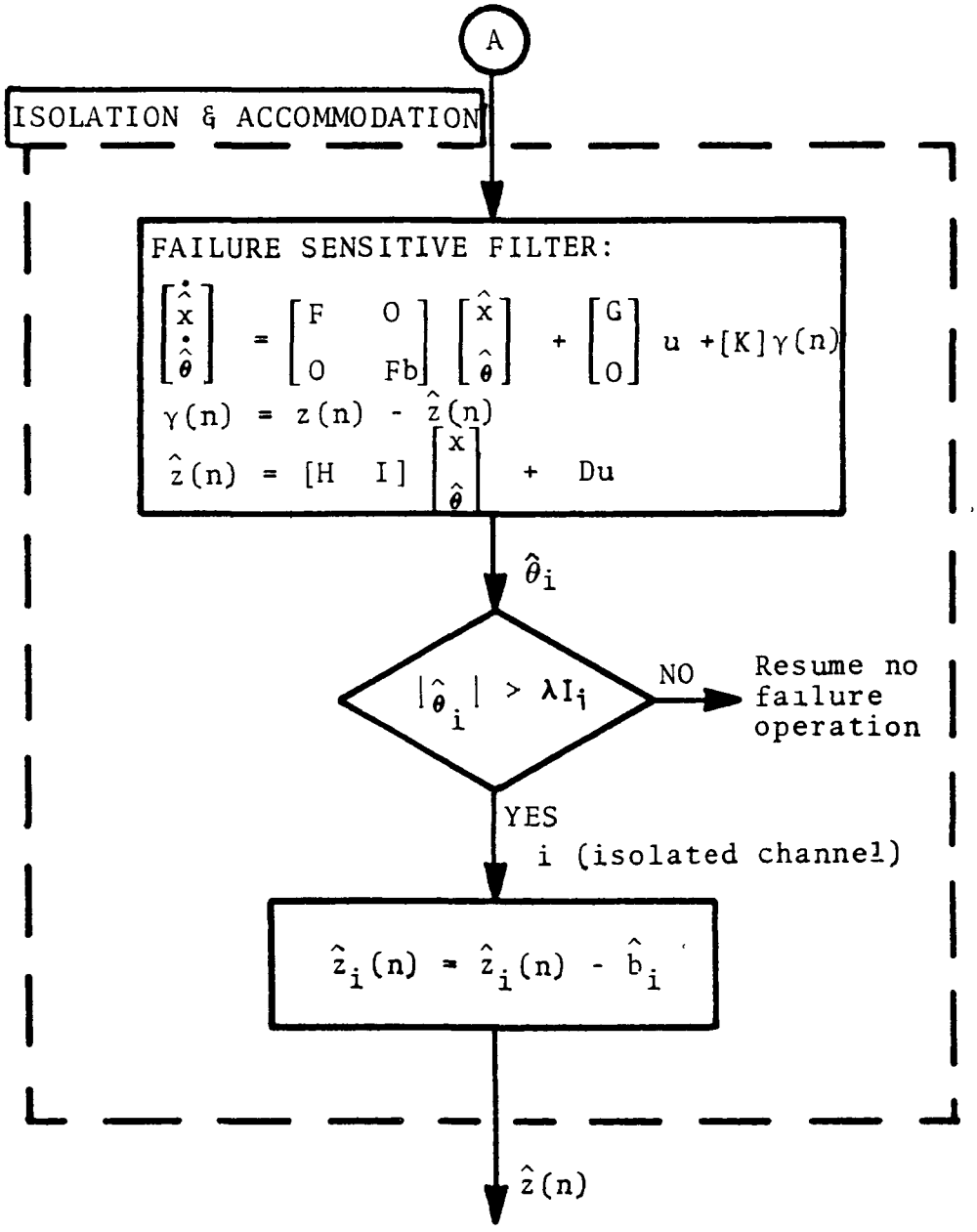

Figure 50 Flow Chart of DIA Concept 3 (Concluded)

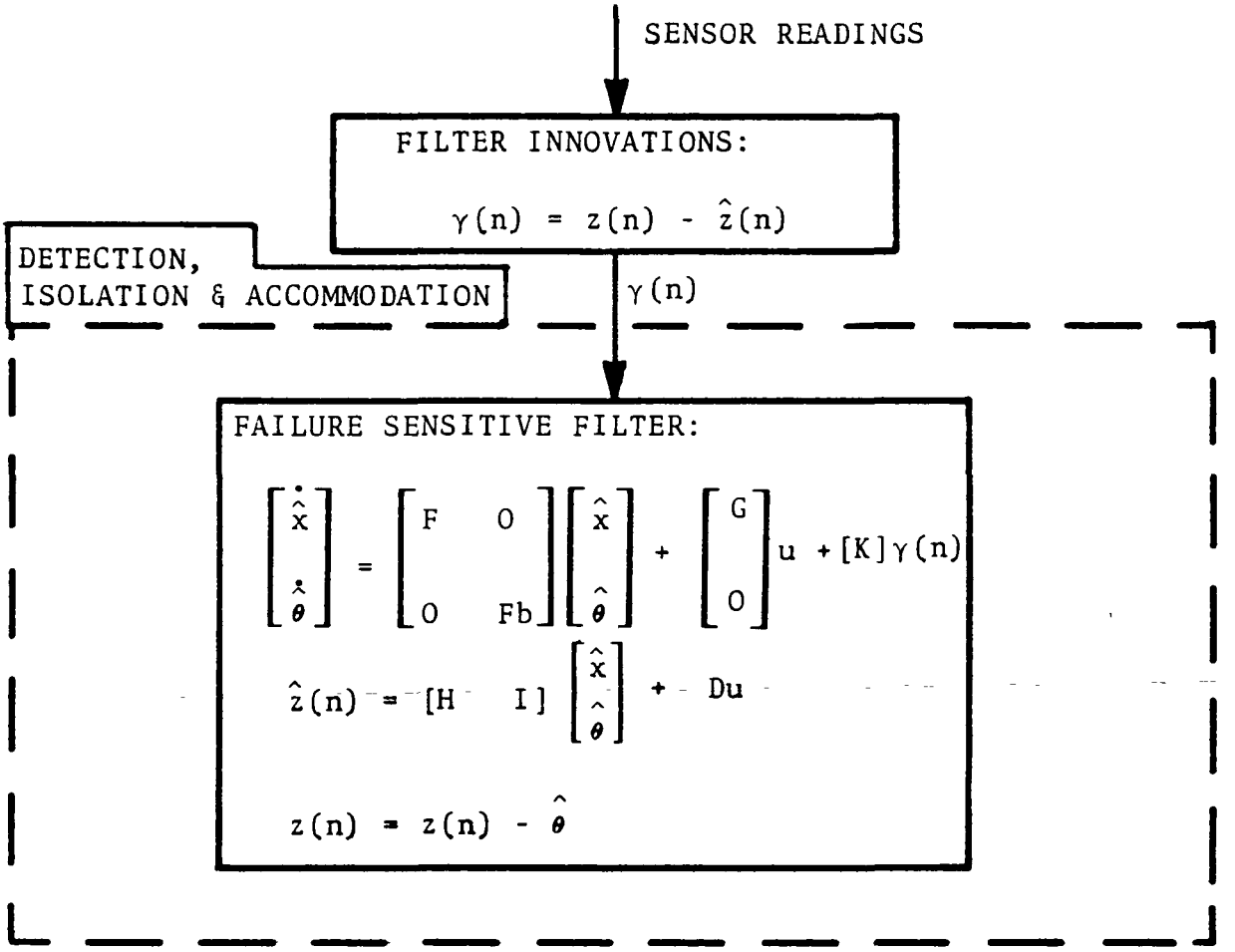

Figure 51 Flow Chart of DIA Concept 4

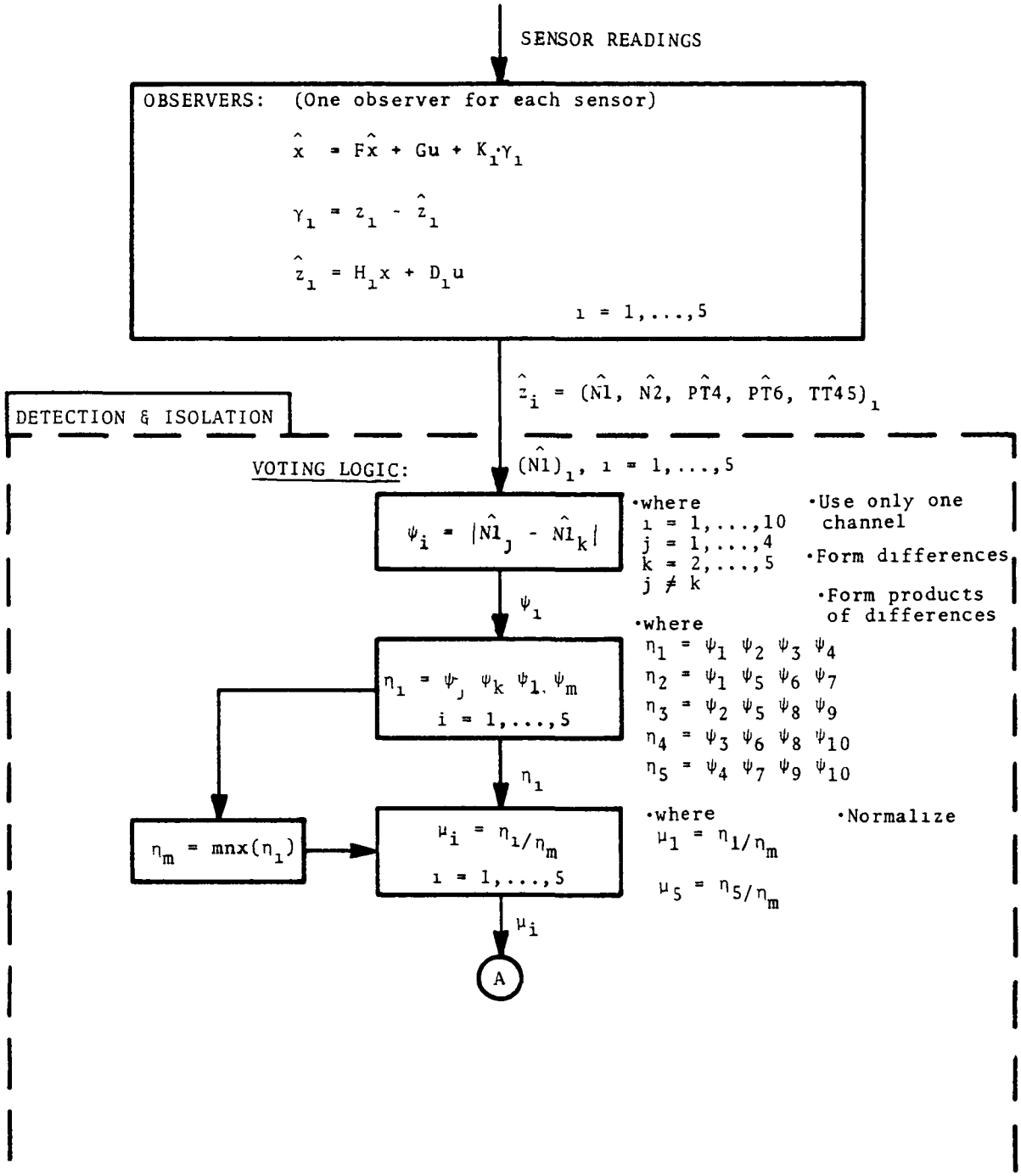

Figure 52 Flow Chart of DIA Concept 5

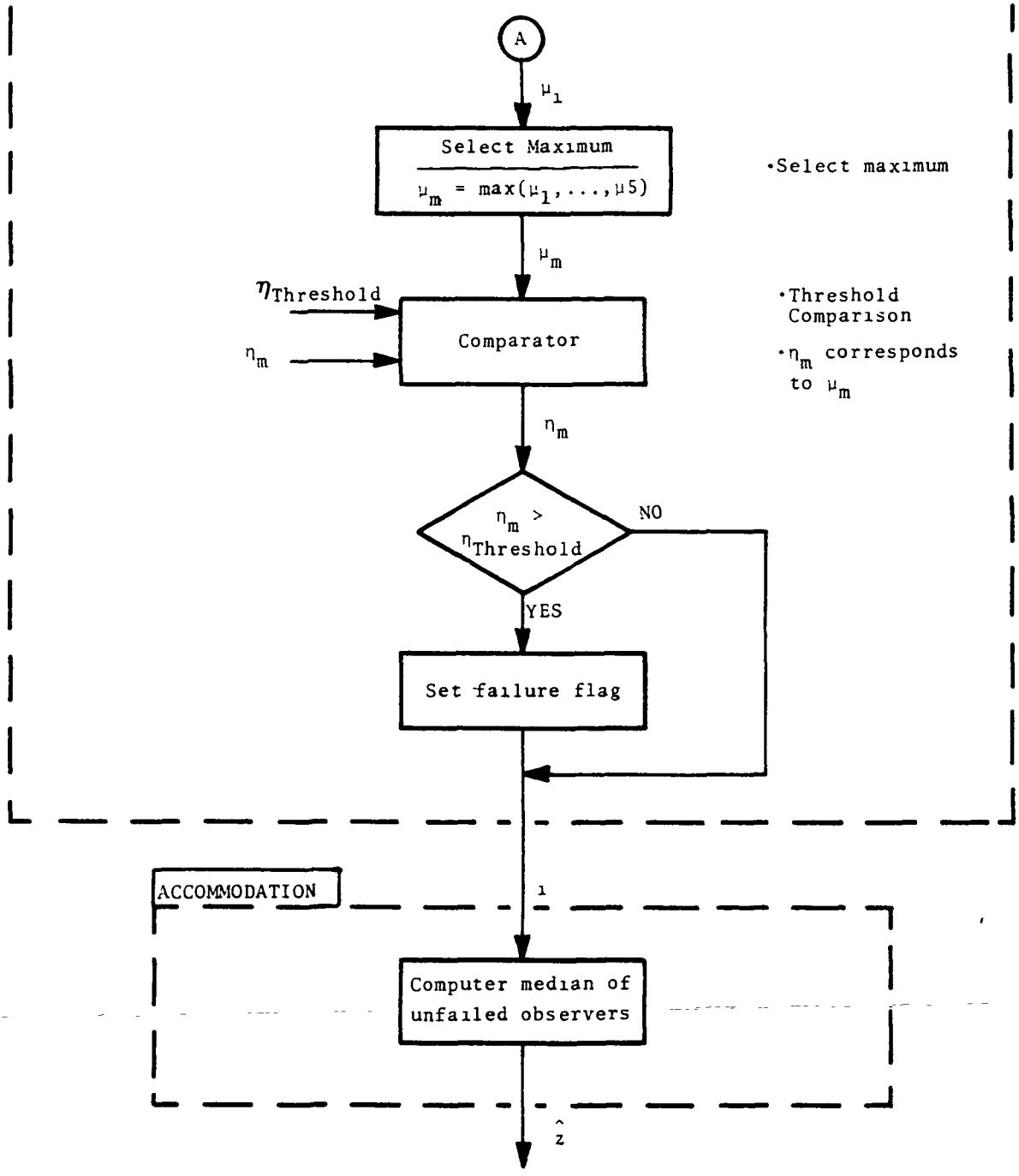

Figure 52 Flow Chart of DIA Concept 5 (Concluded)

4.4 RESULTS OF PRELIMINARY SCREENING PROCESS

4.4.1 Introduction

Advanced detection, isolation and accommodation techniques were reviewed and five viable concepts were formulated as discussed in the previous section. These concepts were implemented on the simplified simulation of the F100

engine and multivariable control. Using the scoring system discussed previously, a screening process evaluated performance of each concept for single PT6, PT4, N1, N2, and FTIT sensor failures at the sea level static operating condition. Each concept was awarded points in terms of its Detection performance and criteria. Results of this screening process are presented in this section. A schematic of the overall procedure is shown on Figure 53.

Two Concepts were selected for further evaluation as a result of this screening process. This evaluation also utilized the simplified model operational over the sea-level static operating line. Evaluation was performed for multiple sensor failures, noise, modelling errors and logic complexity. Results of the evaluation are also presented in this section.

Based on the detection, isolation and accommodation performance of each concept, one concept was chosen for implementation, validation and evaluation on the detailed nonlinear F100 engine and multivariable control simulation.

4.4.2 Sensor Model

A sensor model was developed for implementation on the engine simulation. This model simulates a wide variety of sensor failures.

The failed sensor model used was

$$Y_{SN} = K_{SF} * Y + K_{BI} + A * V \qquad (34)$$

where

Y_{SN} is the sensor output
K_{SF} is the scale factor
Y is the measured variable
K_{BI} is the bias
A is the noise amplification factor
V is the noise with normal distribution N (0,1); zero mean and unit variance

Hard failures, soft failures, biases and drifts can be simulated with this model.

4.4.3 Evaluation of Five Concepts

A comprehensive evaluation of the five detection, isolation and accommodation concepts was performed to determine the relative merits of each concept. The evaluation scored each concept for detection performance, engine protection limit exceedances, and steady state and transient performance using the scoring system described in Appendix B.

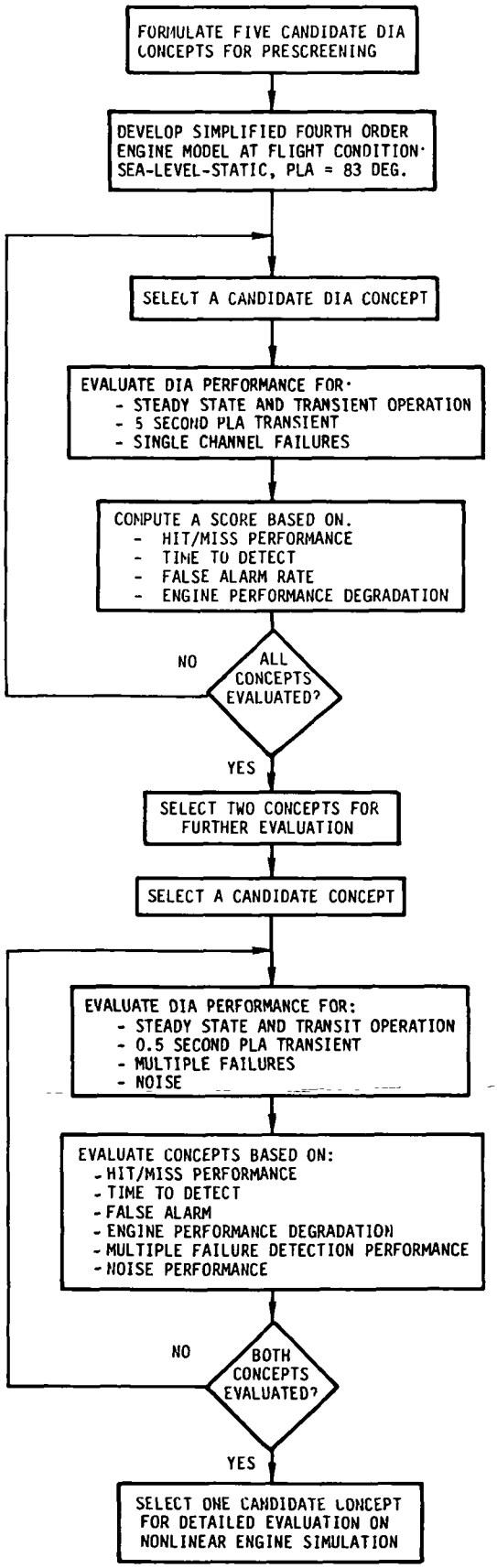

Figure 53 DIA Concept Evaluation and Selection Procedure

The flight point altitude = 0 ft, Mach No. = 0, and PLA = 83 degrees (Sea Level Static - Intermediate power) was chosen for this preliminary evaluation. A sixteenth order linear model was available and was reduced to fourth order linear model using the techniques discussed in Section 4.2. This simplified model was used both as the engine dynamic model and for filter update equations required by the DIA concepts.

Each concept was implemented as an independent software module which provided interchangeability and ease in modification. Each concept was evaluated and ranked based on its single failure capability. Table XV presents the results of the steady state performance of each concept when a soft failure (bias) of +50 RPM in fan speed measurement (N1) was introduced. The last column in Table XV lists the total score; the higher the total score, the worse the performance. The total score was calculated by summing the individual scores from the engine protection, steady state thrust variations, and time to detect portions of the scoring system. Note that for a case in which a concept was unable to isolate the failure properly, a maximum score of 15 was assigned to that concept. This steady state evaluation was of somewhat limited usefullness due to the fact that the simplified engine model was used both in the filters and as the engine simulation; i.e., perfect modelling. Several scores of zero were due to this perfect modelling. This was most evident in the engine protection portion of the score.

TABLE XV
SCORING RESULTS (SOFT N1 FAILURE)

FLIGHT CONDITION: ALT = 0, Mn = 0 PLA = 83 (STEADY STATE)
FAILURE TYPE: N1 BIAS (+50 RPM)

				SCORING								
CON-CEPT	TIME INDUCED	TIME DETECTED	TIME ISOLATED	ENGINE PROTECTION						SSFn*	TIME DETECT	TOTAL SCORE
				FTIT	N2	N1	PT4	SMF	SMC			
1	0.002	0.002	**							.006	4.0	15
2	0.002	0.002	0.016							0.0	ϵ***	ϵ***
3	0.002	0.002	0.514							0.1	10.0	10.1
4	0.002	0.516	0.516							0.01	10.0	10.0
5	0.002	0.02	0.02							.0001	0.0	ϵ***

*Steady State Thrust
**Since failure was not isolated, the maximum score of 15 was assigned to that concept
*** ϵ represents a very small non zero value

A hard failure (bias) of +300 RPM in fan speed measurement was induced and the steady state and transient performance of each concept was scored. A Power Lever Angle (PLA) step change from 35 degrees to 83 degrees was input at t=0 seconds and the failure induced at t=0.002 seconds to obtain the transient plots of Figures 54 through 58. The results of the scoring system are presented in Table XVI and XVII for steady state and transient performances, respectively.

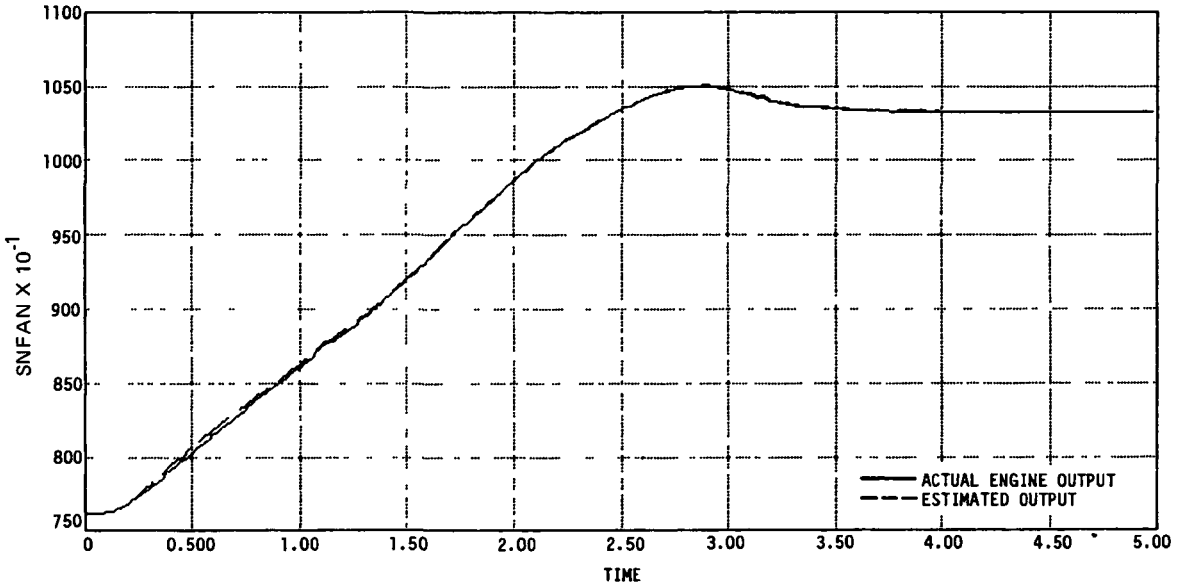

Figure 54 Concept 1; N1 Time History Resulting from a 35 to 83 PLA snap at t=0. Seconds With a Hard N1 failure (+300 RPM) at t = 0.002 Seconds.

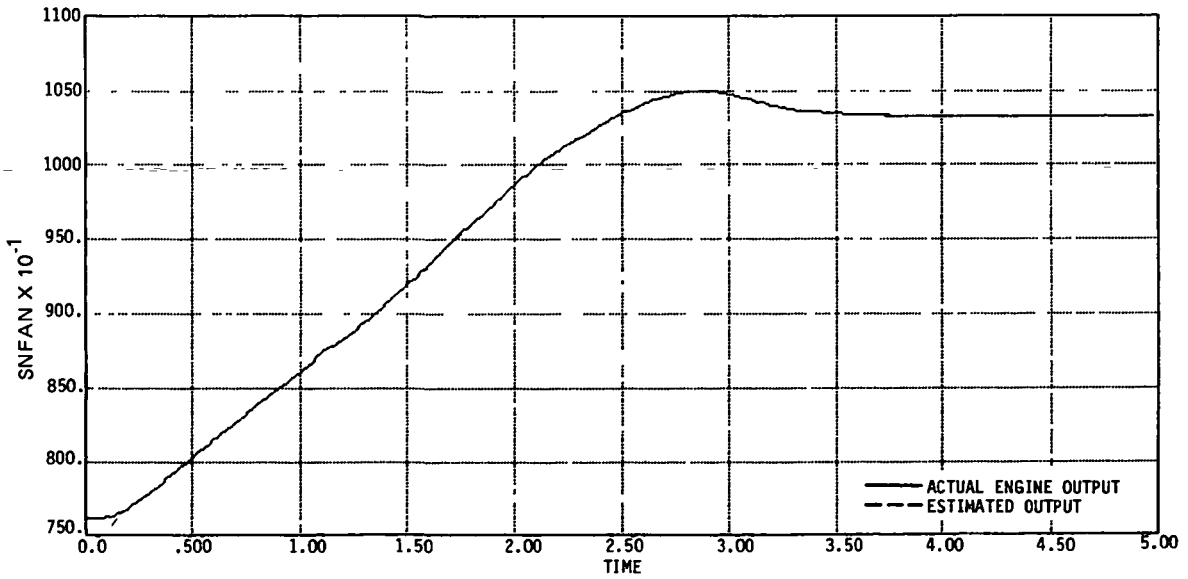

Figure 55 Concept 2; N1 Time History Resulting from a 35 to 83 PLA snap at t=0. Seconds With a Hard N1 failure (+300 RPM) at t = 0.002 Seconds.

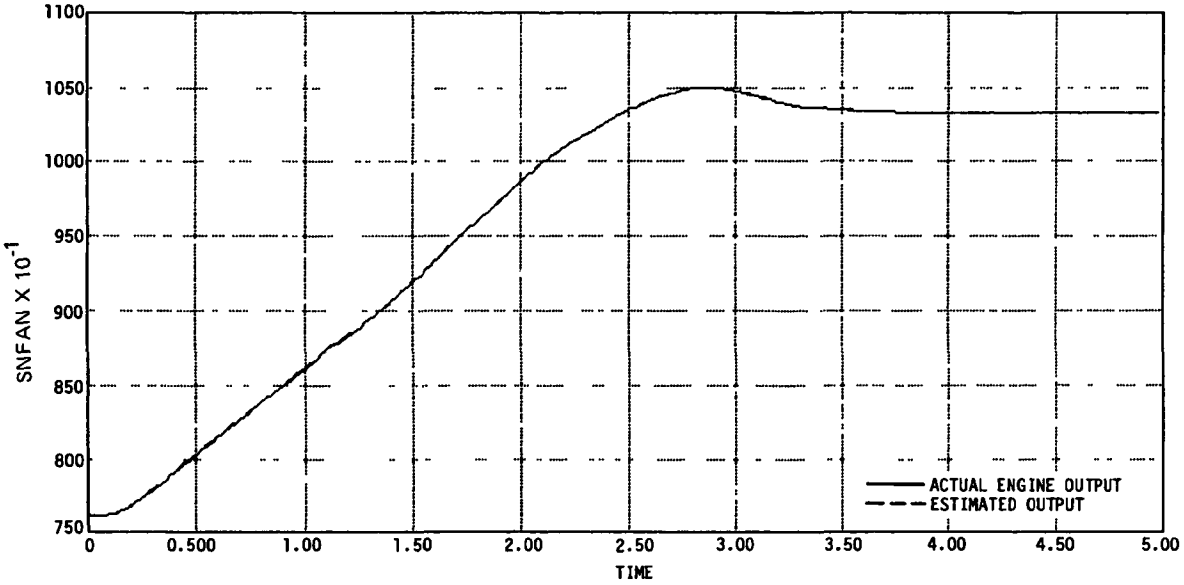

Figure 56 Concept 3; N1 Time History Resulting from a 35 to 83 PLA snap at t=0. Seconds With a Hard N1 failure (+300 RPM) at t = 0.002 Seconds.

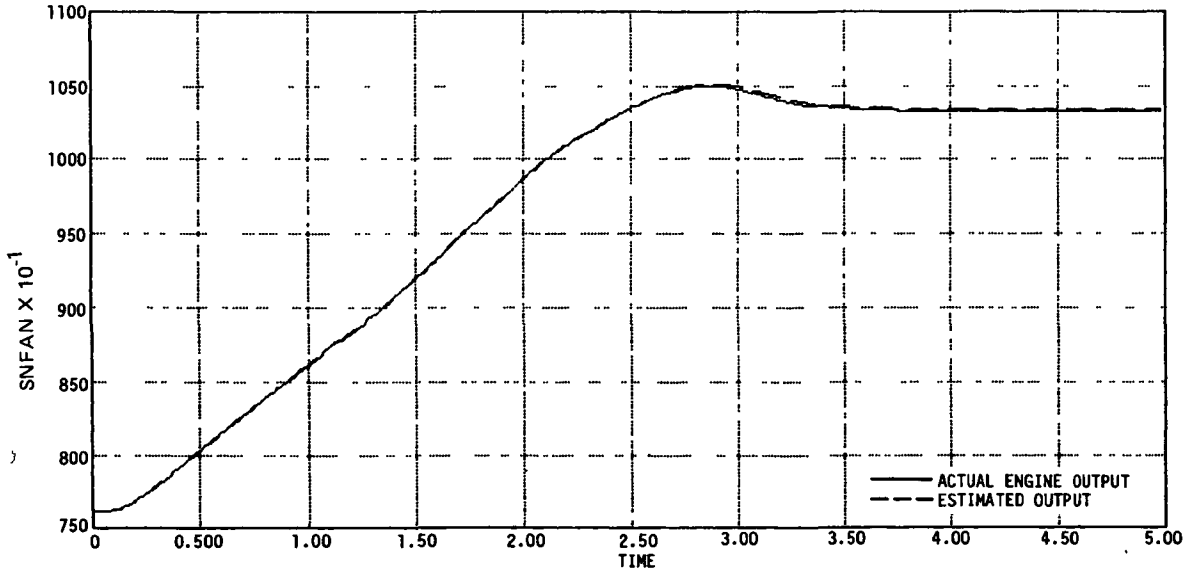

Figure 57 Concept 4; N1 Time History Resulting from a 35 to 83 PLA snap at t=0. Seconds With a Hard N1 failure (+300 RPM) at t = 0.002 Seconds.

C-2

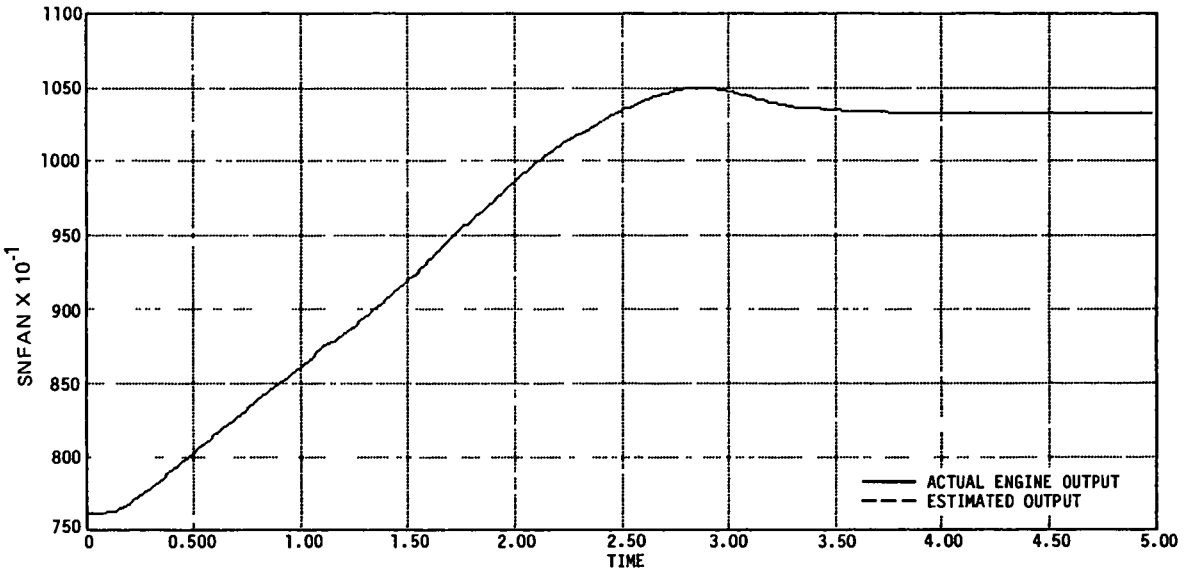

Figure 58 Concept 5; N1 Time History Resulting from a 35 to 83 PLA snap at t=0. Seconds With a Hard N1 failure (+300 RPM) at t = 0.002 Seconds.

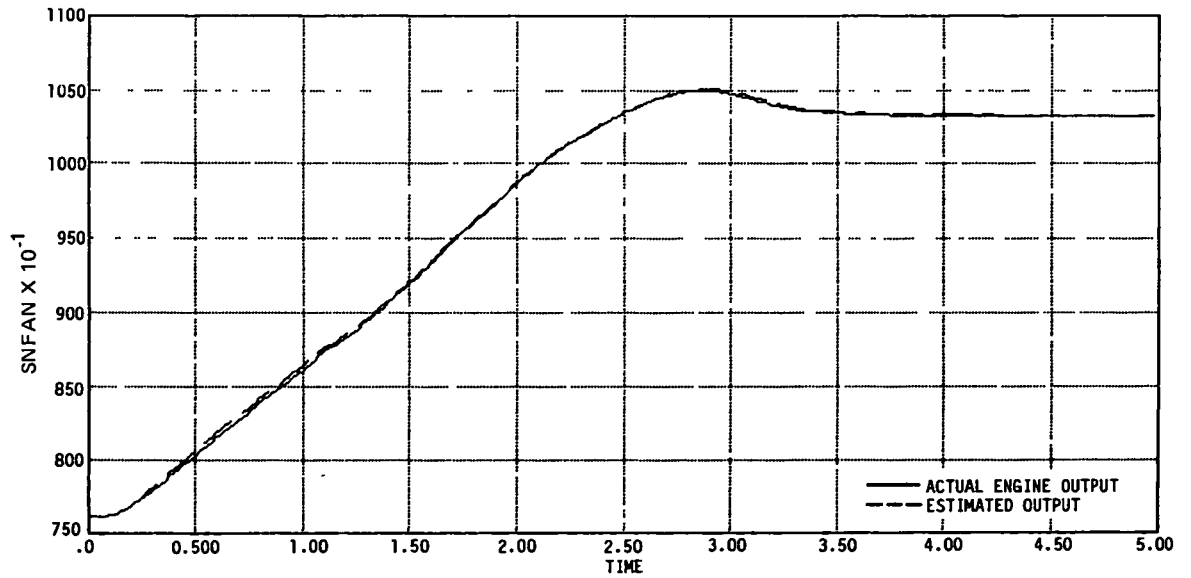

Figure 59 Concept 1; N1 Time History Resulting from a 35 to 83 PLA snap at t=0. Seconds With a Hard PT4 failure (+10 PSIA) at t = 0.002 Seconds.

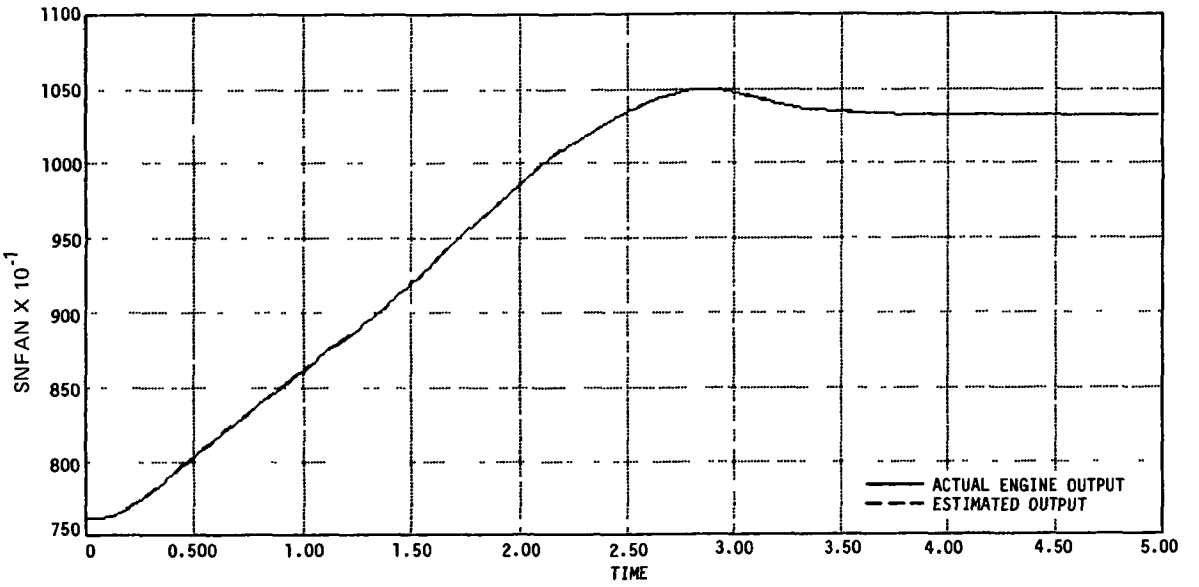

Figure 60 Concept 2; N1 Time History Resulting from a 35 to 83 PLA snap at t=0. Seconds With a Hard PT4 failure (+10 PSIA) at t = 0.002 Seconds.

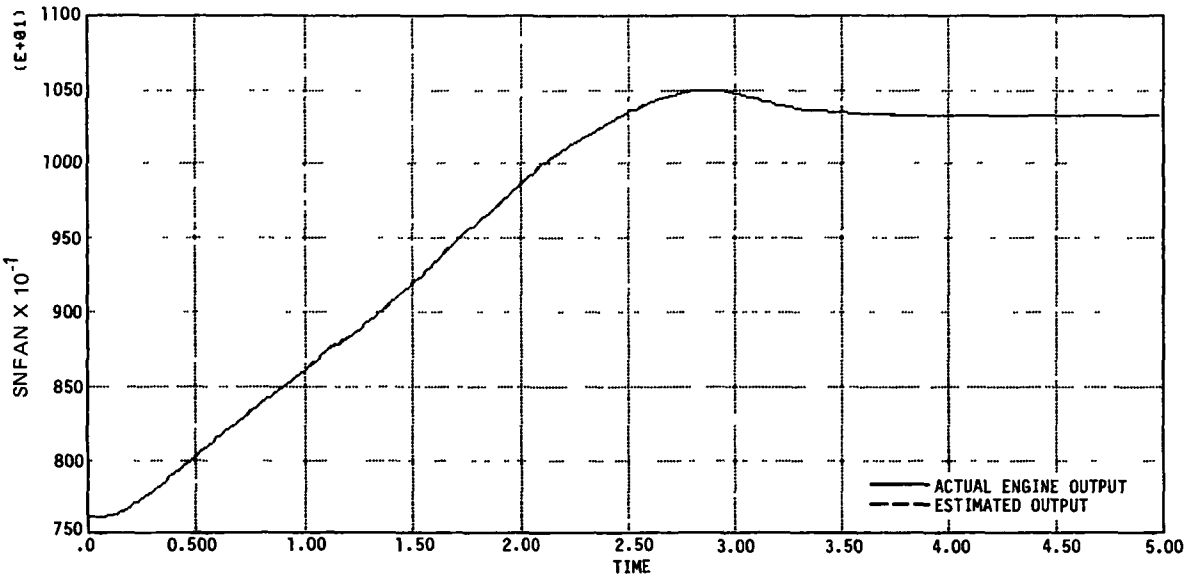

Figure 61 Concept 3; N1 Time History Resulting from a 35 to 83 PLA snap at t=0. Seconds With a Hard PT4 failure (+10 PSIA) at t = 0.002 Seconds.

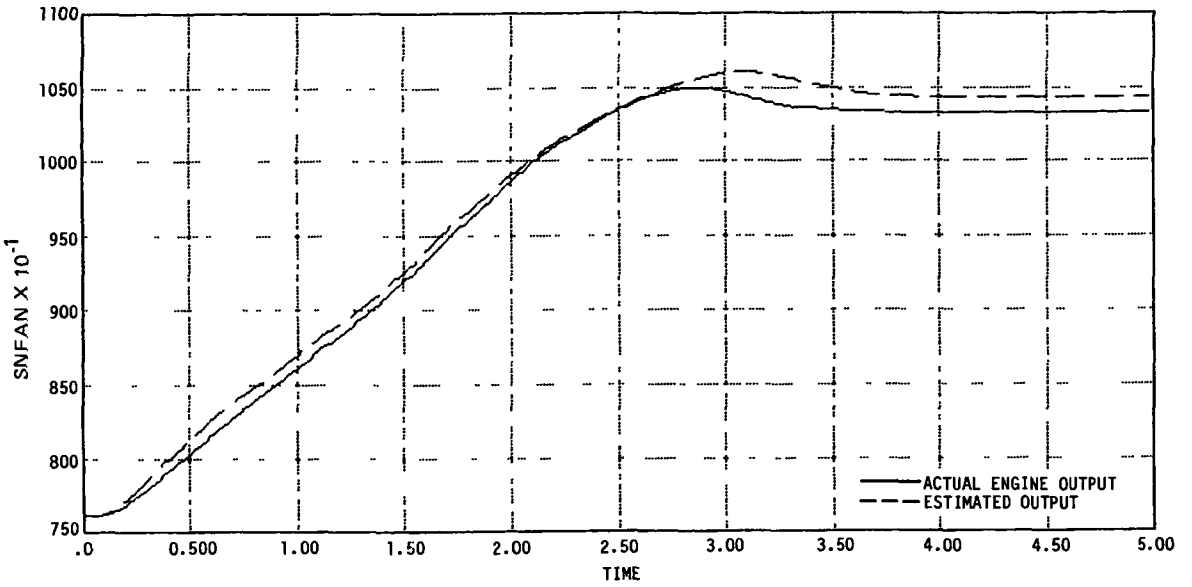

Figure 62 Concept 4; N1 Time History Resulting from a 35 to 83 PLA snap at t=0. Seconds With a Hard PT4 failure (+10 PSIA) at t = 0.002 Seconds.

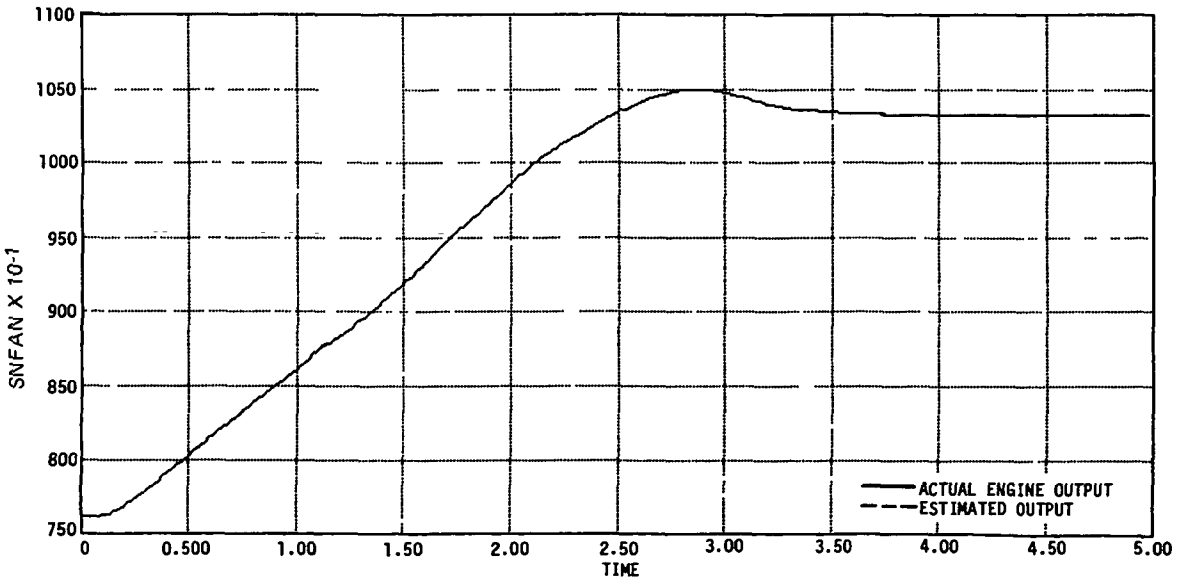

Figure 63 Concept 5; N1 Time History Resulting from a 35 to 83 PLA snap at t=0. Seconds With a Hard PT4 failure (+10 PSIA) at t = 0.002 Seconds.

TABLE XVI

SCORING RESULTS (HARD N1 FAILURE)

FLIGHT CONDITION: ALT = 0, Mn = 0 PLA = 83 (STEADY STATE)

FAILURE TYPE: N1 BIAS (+300 RPM)

				SCORING								
				ENGINE PROTECTION								
CON-CEPT	TIME INDUCED	TIME DETECTED	TIME ISOLATED	FTIT	N2	N1	PT4	SMF	SMC	SSFn	TIME DETECT	TOTAL SCORE
1	0.002	0.002	0.162							0.03	1.5	1.53
2	0.002	0.002	0.002							0.0	0.0	0.0
3	0.002	0.002	0.07							0.02	ϵ^{***}	0.02
4	0.002	0.108	0.108							0.05	0.02	0.07
5	0.002	0.01	0.01							0.0002	0.0	ϵ^{***}

TABLE XVII

SCORING RESULTS (HARD N1 FAILURE)

FLIGHT CONDITION: ALT = 0, Mn = 0 PLA = 35 TO 83 DEGREES (TRANSIENT)

FAILURE TYPE: N1 BIAS (+300 RPM)

				SCORING								
				ENGINE PROTECTION								
CON-CEPT	TIME INDUCED	TIME DETECTED	TIME ISOLATED	FTIT	N2	N1	PT4	SMF	SMC	TRAN-SIENT	TIME DETECT	TOTAL SCORE
1	0.002	0.002	0.162		.03				.005	.4	4.	4.43
2	0.002	0.002	0.002					ϵ^{***}		.0003	0	0^{+}
3	0.002	0.002	0.07		.05			ϵ^{***}		0.01	0	0.06
4	0.002	0.072	0.072		.06				.01	.08	0	.15
5	0.002	0.008	0.008							0	0	0

A hard failure bias of +10 PSIA in burner pressure measurement (PT4) was introduced at t = 0.002 seconds and detection, isolation and accommodation performance evaluated for a PLA transient from 35 degrees to 83 degrees t=0.0 seconds. Figures 59 through 63 are time history plots of fan speed and Table XVIII presents the scoring results.

TABLE XVIII

SCORING RESULTS (HARD PT4 FAILURE)

FLIGHT CONDITION: ALT = 0, Mn = 0 PLA = 35 TO 83 DEGREES (TRANSIENT)

FAILURE TYPE: PT4 BIAS (+10 PSIA)

				SCORING								
CON-CEPT	TIME INDUCED	TIME DETECTED	TIME ISOLATED	ENGINE PROTECTION						TRAN-SIENT	TIME DETECT	TOTAL SCORE
				FTIT	N2	N1	Pb	SMF	SMC			
1	0.002	0.002	**		0.05					0.5	4.0	15.0
2	0.002	0.002	0.002		0.02			ϵ^{***}	ϵ^{***}	0.002	0.0	0.02
3	0.002	0.002	0.008		0.01				ϵ^{***}	0.01	0.0^{+}	0.02
4	0.002	0.07	0.07		0.6				0.1	0.8	0.0	1.5
5	0.002	0.012	0.012		ϵ^{***}		ϵ^{***}	ϵ^{***}				0.0^{+}

Based on the scoring results the following order was established for performance of each concept:

- o FIRST - CONCEPTS 2 and 5
- o THIRD - CONCEPT 3
- o FOURTH - CONCEPT 4
- o FIFTH - CONCEPT 1

Thus concept 2 and 5 were chosen for further study. Details are presented in the following section.

4.4.4 Further Evaluation of Two Concepts

The operating region for evaluating the two selected concepts was extended for operation over the sea level static (altitude = 0 ft., Mach. No. = 0) operating line. The sixteenth order linear models were available for power points, PLA = 20, 36, 52, 67 and 83 degrees. These models were reduced to fourth order

models and parameterized over the sea level operating line to develop a simplified, reduced-order, nonlinear model. The same model was used for engine dynamics as well as filter update equations. Evaluation of concepts 2 and 5 was performed based on their single and multiple failure performance, effect of noise, and logic complexity. The relative advantages and disadvantages of each concept are summarized in Tables XIX and XX.

TABLE XIX

CONCEPT #2 SUMMARY

ADVANTAGES	DECISION FILTERS BASED ON MAXIMUM INFORMATION DECISIONS BASED ON STATISTICAL SIGNIFICANCE OF OUTPUT
DISADVANTAGES	STATISTICALLY SIGNIFICANT TESTS MORE DIFFICULT TO IMPLEMENT THAN SIMPLE THRESHOLD COMPARISON - DEPENDENT ON NOISE ASSUMPTIONS - DEPENDENT ON MODEL ACCURACY

TABLE XX

CONCEPT #5 SUMMARY

ADVANTAGES	DECISION TESTING IS SIMPLE DECISIONS BASED ON HIGHLY FILTERED SIGNALS LOGIC IS SIMPLE
DISADVANTAGES	DECISION FILTERS BASED ON MINIMUM INFORMATION

A soft N1 failure (bias) of +50 RPM and soft PT4 failure (bias) of + 3 PSIA were introduced at t = 0.1 and 0.2 seconds, respectively. A separate random noise signal was generated and superimposed on all five measurements with the same magnitude of noise amplification factor, A=1 (see equation 34). A step input from PLA = 30 to 83 degrees was commanded at t = 0.002 seconds. The transient response of N1 and PT4 are given in Figures 64 and 65 for concept 2 and in Figures 66 and 67 for concept 5. The solid line is the engine simulation output, the large broken line is the output of accommodation filter and the small broken line is the unfailed sensor measurement (including sensor lag). The failure detect and isolate events are registered along with the channel and the time on each plot.

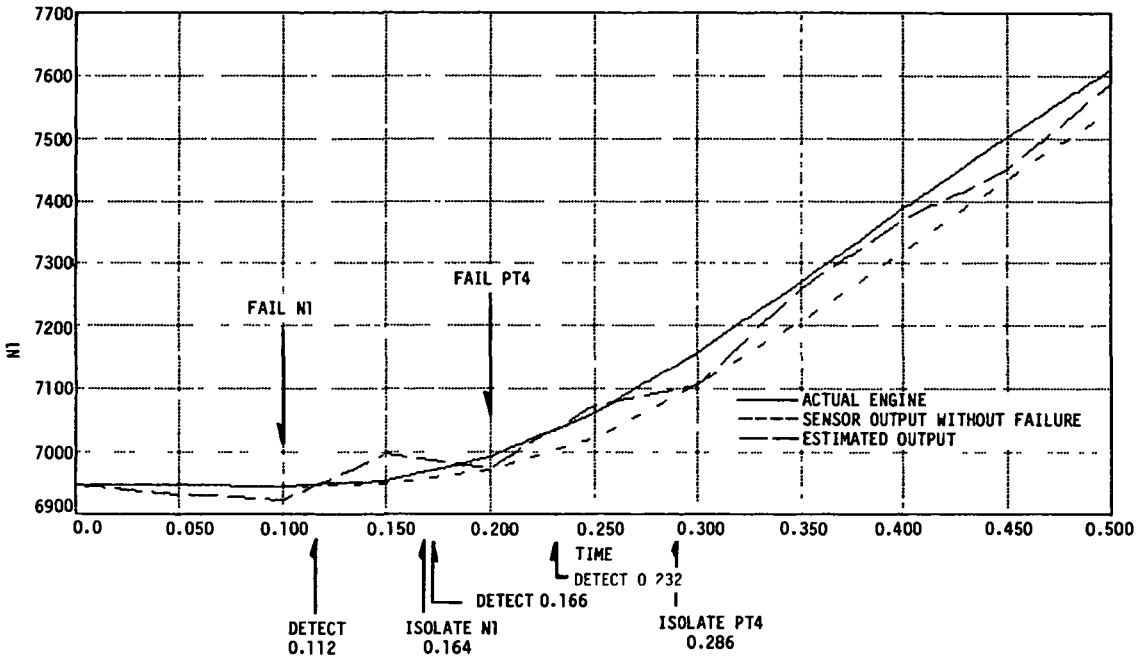

Figure 64 Concept 2; N1 Transient Response With N1 and PT4 Sensor Failures

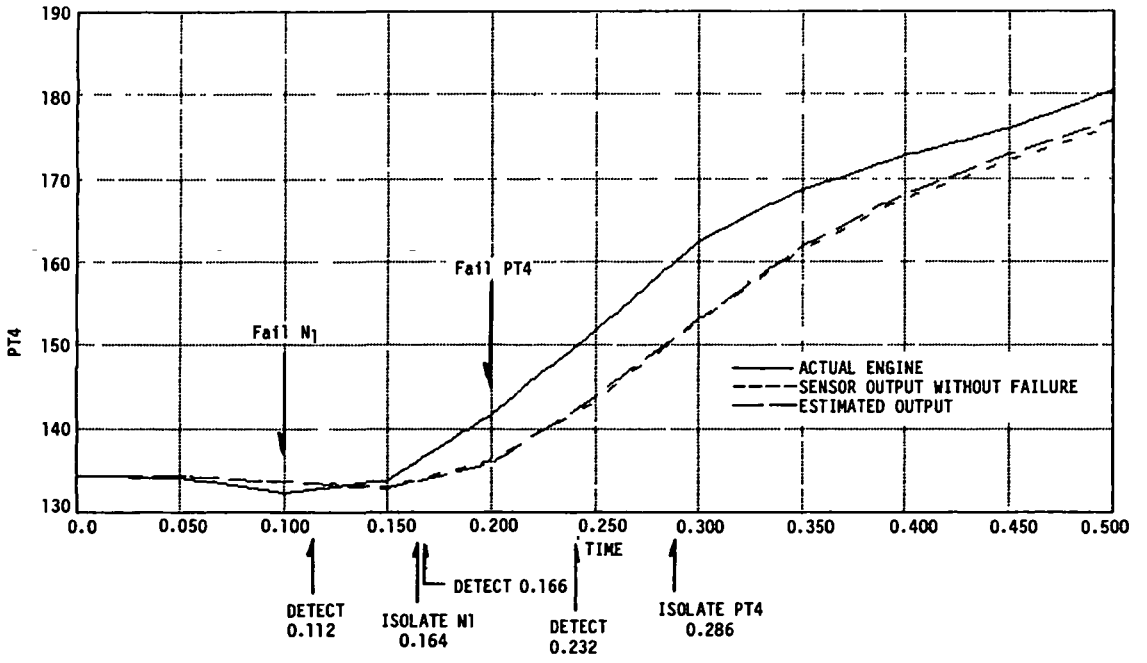

Figure 65 Concept 2; N1 Transient Response With N1 and PT4 Sensor Failures

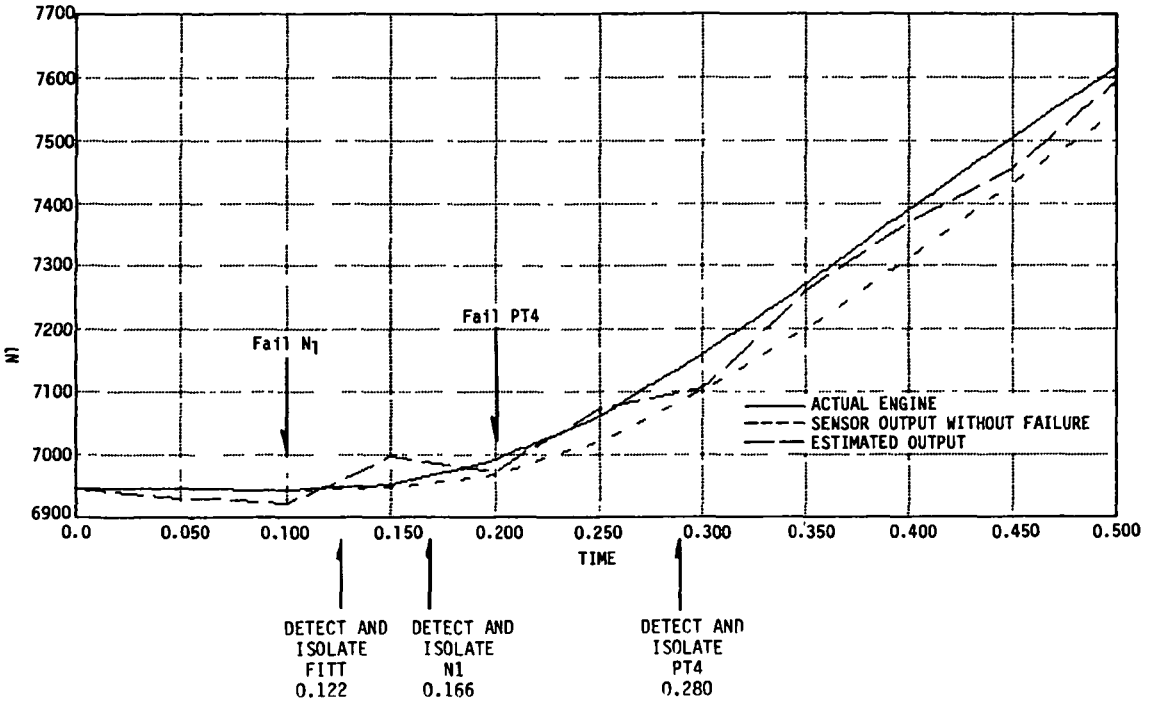

Figure 66 Concept 5; N1 Transient Response With N1 and PT4 Sensor Failures

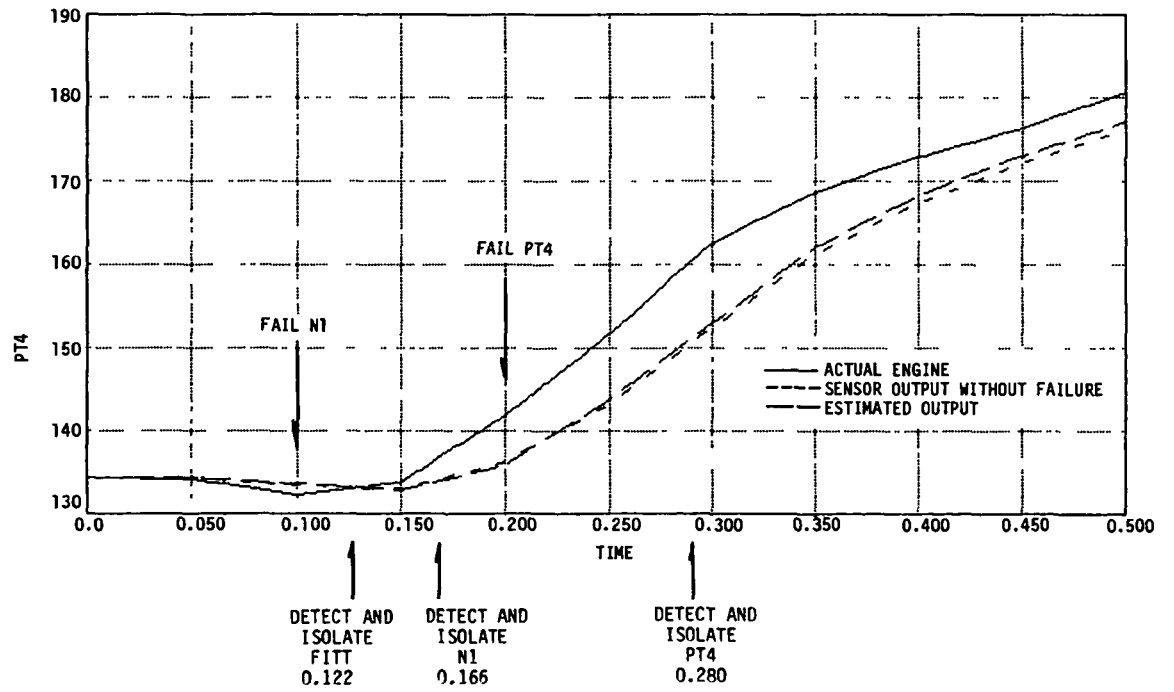

Figure 67 Concept 5; N1 Transient Response With N1 and PT4 Sensor Failures

Figures 68 through 73 are timing diagrams associated with other combinations of sensor failures. They register detect and isolate events and times. Concept 5 detected and isolated all failures correctly. However, it also falsely detected, and isolated fan turbine inlet temperature sensor failures when failures of other sensors were induced. This was attributed to the poor performance of the observer designed with FTIT as its only input. Since the time constant associated with fan turbine inlet temperature channel is slow, the estimates do not follow the measurement very well, causing the false failure detection. Concept 2 does very well in correctly detecting and isolating failures but also declared false alarms. This, in most cases, happened after two failures were detected and isolated and can be attributed to the performance of the accommodation filter after two failure accommodations. In figures 64, 65, 70 and 72 the false alarm was generated at the next time step after the isolation of a failure. In the detection technique, the weighted sum squared residual is averaged over last five measurements and then compared against the threshold for failure detection. After isolation of the failure the memory (past five measurements) should be erased (zeroed out) for a fresh start. It was not done so in the Concept 2 implementation. Therefore the residual remains high and allows generation of a false alarm right after failure isolation. This was observed every time a soft failure was isolated because WSSR technique is only used for soft failure detection. A summary of the detection, isolation and accommodation performance of the two concepts in given in Table XXI.

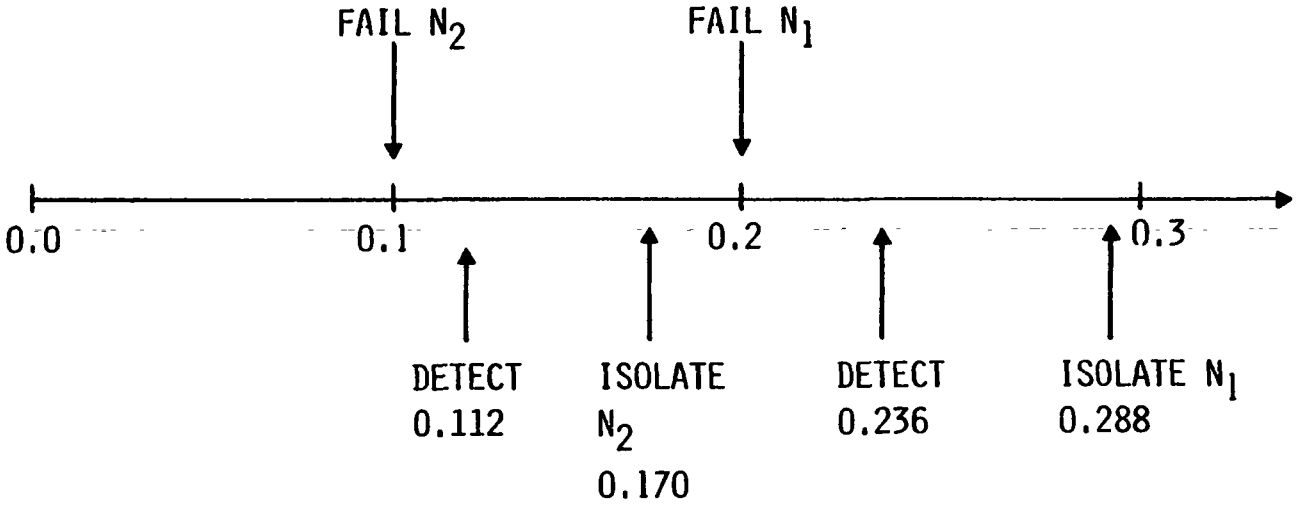

Figure 68 Concept 2 Detection and Isolation Timing Diagram, N1 and N2 Sensor Failures

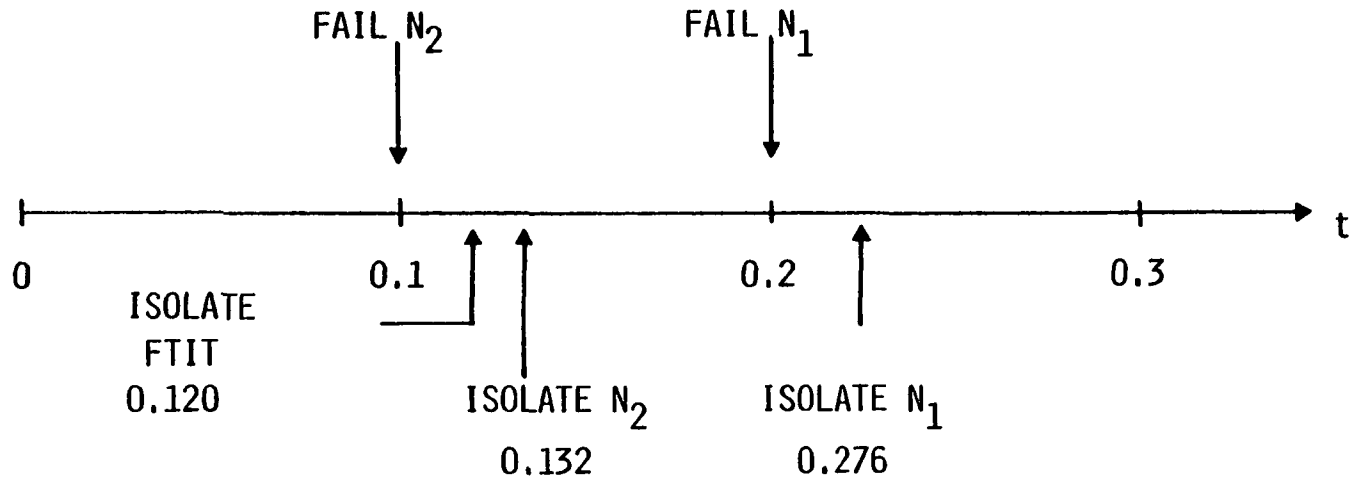

Figure 69 Concept 5 Detection and Isolation Timing Diagram, N1 and N2 Sensor Failures

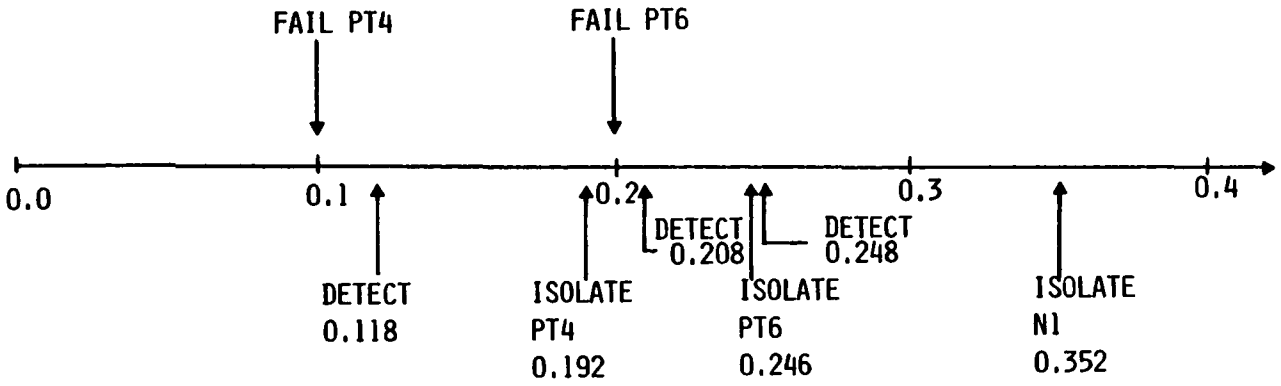

Figure 70 Concept 2 Detection and Isolation Timing Diagram, PT4 and PT6 Sensor Failures

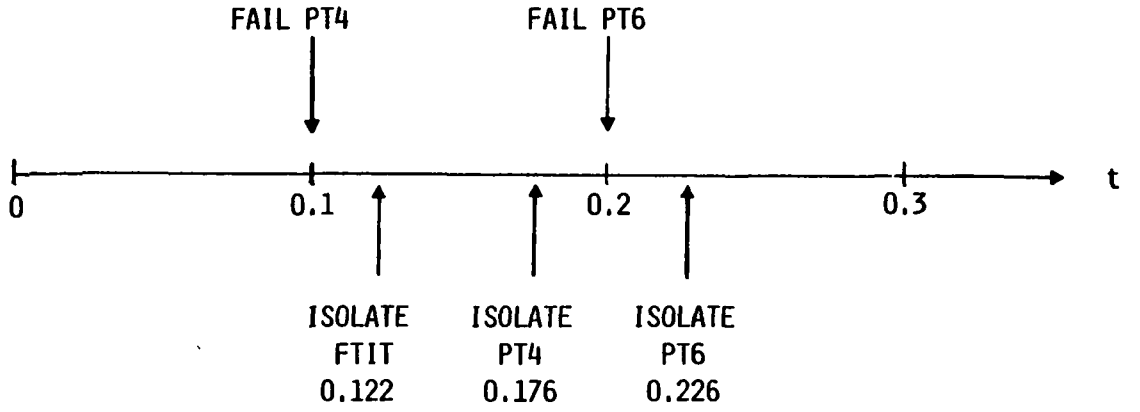

Figure 71 Concept 5 Detection and Isolation Timing Diagram, PT4 and PT6 Sensor Failures

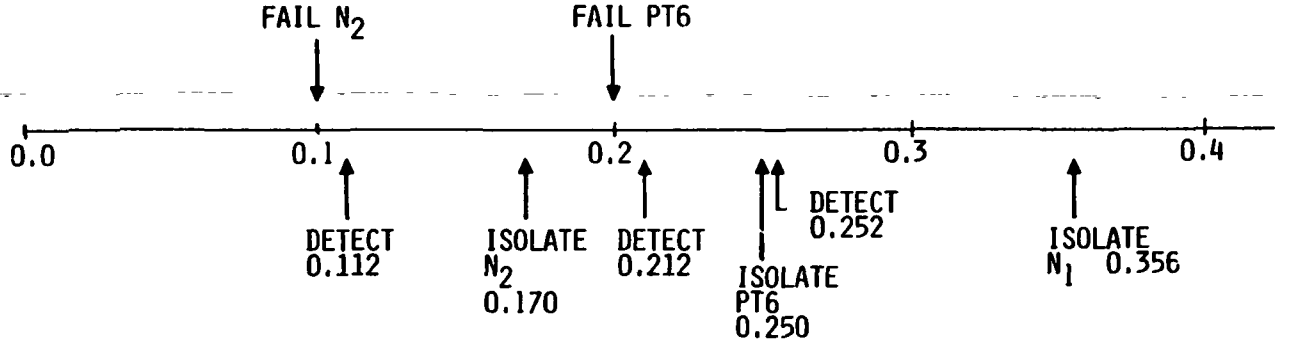

Figure 72 Concept 2 Detection and Isolation Timing Diagram, N2 and PT6 Sensor Failures

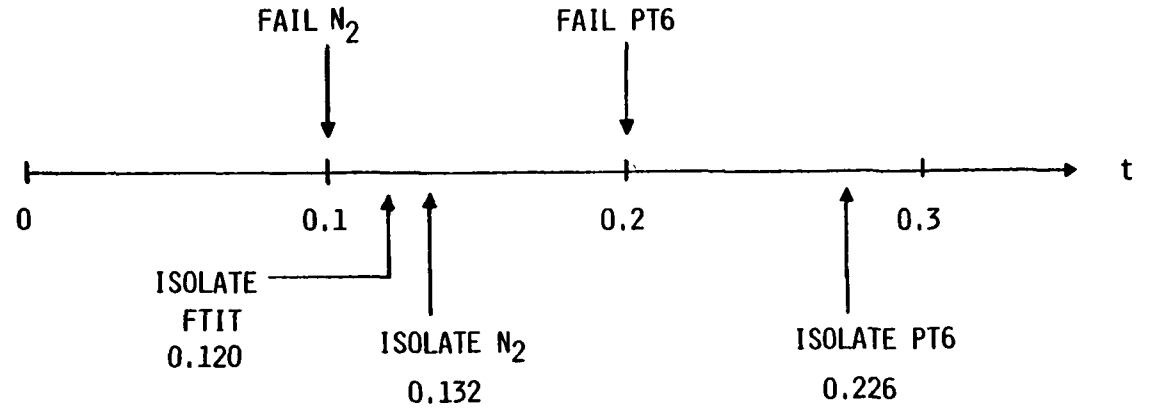

Figure 73 Concept 5 Detection and Isolation Timing Diagram, N2 and PT6 Sensor Failures

TABLE XXI

SUMMARY OF EVALUATION OF TWO CONCEPTS

CONCEPT 2	PERFORMANCE HIGHLY DEPENDENT ON THRESHOLD PARAMETERS NO MISSED FAILURES FOR ERRORS 2σ*
CONCEPT 5	ABLE TO ISOLATE FAILURES WITH ERRORS = 1σ* LOGIC SIMPLE TO IMPLEMENT SLOW FTIT OBSERVER

The two concepts look very promising. The logic complexity of concept 5 is relatively simpler than concept 2. Concept 2 treats hard and soft failures separately. Hard failure detection, isolation and accommodation logic of concept 2 involves less computation than concept 5. Soft failure logic of concept 2 is more complex than concept 5. Overall comparison reveals that the hard failure DIA performance of both concepts was very good. The soft failure DIA performance of Concept 2 was superior to concept 5. In the light of the above and Tables XIX to XXI, concept 2 was chosen as the final candidate concept for evaluation on the detailed nonlinear simulation of the F100 engine.

4.4.5 Final Concept Evaluation

The final concept selected was incorporated into the detailed nonlinear F100 engine and multivariable control simulation for detailed evaluation. A simplified nonlinear model was developed by reducing the available sixteenth order linear models to the fourth order linear models. The fourth order models span the entire flight envelope and were parameterized for operation over the flight envelope. This simplified nonlinear model was used to update filter equations of Concept 2. Note here that since the engine dynamic model and filter model were different, modelling errors were taken into account by increasing the detection and isolation thresholds.

* σ = Standard Deviation

5.0 COMPARISON OF PARAMETER SYNTHESIS AND ADVANCED ALGORITHMS FOR SENSOR FAILURE DETECTION, ISOLATION AND ACCOMODATION

5.1 INTRODUCTION

A detailed evaluation of the parameter synthesis based detection, isolation, and accommodation algorithm and advanced algorithm was conducted by simulating sensor failures for both steady state and transient operation at the 15 flight operating points, using the nonlinear F100 engine and Multivariable Control (MVC) simulation. The evaluation results of the two algorithms were compared to determine the benefits of implementing advanced algorithms in production control systems, rather than the conventional parameter synthesis techniques currently used. The following paragraphs present the results of the comparison.

5.1.1 Steady State Comparison

Steady State failure effects were evaluated for the two algorithms at the fifteen flight operating conditions selected for this program. The failures were induced by applying a constant bias to the sensor to be failed. The magnitude of the biases applied to the sensor values were:

N1	2000 RPM
N2	2000 RPM
PT6	35 psi
PT4	50 psi

Since the purpose of this test was to observe the accommodation accuracy of the algorithms, the biases were set arbitrarily large to insure failure detection. When the failure was induced, the resulting failure transients were observed and, after the transient effects decayed, pertinent steady state results were recorded. Tabulations of the resulting Steady State data for the PT6, PT4, N1, and N2 sensors failures are shown in Tables XXII through XXVI. These tabulations show the errors in PT4, N2, N2, fan turbine inlet temperature, thrust, and surge margins caused by using analytically generated inputs after any failure accommodation has taken place. The errors on the input signals (estimation errors) are calculated by taking the difference between the actual parameter value and the value being sent to the control laws. Variation in thrust is calculated as a function of the thrust that the engine is generating after the failure accommodation relative to the normal steady state thrust levels with perfect sensor feedback.

5.1.2 Comparisons With No Failures Induced

Table XXII shows the Steady State estimation errors and resulting thrust variations for the fifteen flight operating conditions with no failures induced. Since the parameter synthesis technique reverts to the synthesized signal only in the presence of a failure, the no-failure case results in no estimation errors. The advanced detection, isolation and accommodation concept feeds back the Kalman filter estimates to the control law. Therefore, estimation errors on the sensor inputs are present. The magnitude of estimation errors is a function of the accuracy of the model within the algorithm.

From Table XXII, it is seen that the estimation errors for the advanced algorithm vary as a function of flight condition. As noted in Section 4.1.3, increasing the linear data available for generating the model at the higher error flight conditions and improving modeling techniques could significantly reduce these estimation errors. This Table also shows that the fan turbine inlet temperature estimator is the driving force for the large estimation errors at many flight conditions. Therefore, additional work would be required on that portion of the estimator prior to implementing it in control system hardware. Since the fan turbine inlet temperature estimator was shown to be very inaccurate, it was not considered in the steady state comparison.

5.1.3 Comparisons With a PT6 Sensor Failure Induced

Steady State comparisons for the two detection, isolation and accommodation algorithms' accommodation of a PT6 sensor failure are shown on Table XXIII. This Table shows very good steady state PT6 failure accommodation for both the parameter synthesis and the advanced algorithm. The PT6 accommodation error for the parameter synthesis technique results in a maximum variation in thrust of 1.7% with very little variation in fan or compressor surge margins. The advanced algorithm shows estimation errors up to 50% thrust variation at the high altitude, high Mach number conditions. However, these errors are comprised of two portions: 1) the basic estimation errors with no sensor failures which were previously shown in Table XXII to be a function of modeling errors; and 2) the accommodation errors resulting from zeroing a column of the 'K' matrix in the Kalman filter.

To put the accommodation errors in perspective, one must examine the error shown on the sensor failure tables relative to the no-failure case. For example, for the sea level static, 83° PLA flight operating point, the total thrust variation when accommodating a PT6 failure with the advanced algorithm relative to the perfect sensor feedback case is shown to be -2.5%. On Table XXI, the no failure case was shown to result in a thrust variation of -3% relative to the perfect sensor feedback case. Thus accommodation of a PT6 failure actually reduced the total thrust variation from -3% to -2.5%.

Table XXIV shows a summary of the advanced detection, isolation and accommodation algorithm's estimation errors at sea level static, 83° PLA. The total estimation error is the sum of the basic estimator error with no sensor failures and the accommodation error which results from zeroing a column of the "K" matrix in the Kalman filter. This table shows little or no variation in the estimation error between the no failure case and the sensor failure cases. This illustrates that the algorithm's accommodation error is very small.

5.1.4 Comparisons With an N1 Sensor Failure Induced

Steady state comparison of the two algorithms accommodation for an N1 sensor failure is shown in Table XXV. This Table shows good steady state N1 failure accommodation for both the parameter synthesis and the advanced algorithm at most flight operating points. The parameter synthesis algorithm's worst negative thrust variations occur at low power conditions and the worst

TABLE XXII

PARAMETER SYNTHESIS/ADVANCED CONCEPT STEADY STATE COMPARISONS - NO FAILURES

Flight Operating Point		Steady State Estimation Errors - Parameter Synthesis									Steady State Estimation Errors - DIA Concept 2								
		PT4 (PSI)	PT6 (PSI)	N1 (RPM)	N2	FTIT °R	Thrust %CHANGE	SMF (%)	SMC (%)	Comments	P4 (PSI)	P6 (PSI)	N1 (RPM)	N2	FTIT °R	Thrust %CHANGE	SMF (%)	SMC (%)	Comments
0/0	20°	0	0	0	0	0	0	0	0		+ 0.8	.12	+ 22	- 35	+ 90	+ 1%	- .001	-.0029	
0/0	83°	0	0	0	0	0	0	0	0		- 6.6	-1.77	+ 6	+ 20	+ 47	- 3.7%	+ .021	-.0018	
0/0	130°	0	0	0	0	0	0	0	0		- 5.5	- 1.7	- 3	+ 20	+ 48	- 3.2%	+ .022	- .001	
0/1.2	83°	0	0	0	0	0	0	0	0		+ 3.3	+ 6.6	- 10	- 8	- 10	+ 6.1%	- .005	- .003	-0.073 TSFC
10K/0.9	83°	0	0	0	0	0	0	0	0		- 3.0	-1.08	- 10	+ 20	+ 32	- 2.1%	+ .011	-.0125	
20K/0.3	24°	0	0	0	0	0	0	0	0		- 5.1	- .49	+ 17	- 45	- 45	- 4.6%	- .005	+ .005	
20K/0.3	83°	0	0	0	0	0	0	0	0		- 3.0	- 1.7	+ 60	- 20	+105	- 5.5%	+ .058	- .005	
24K/1.8	83°	0	0	0	0	0	0	0	0		+ 4.7	+ 2.1	-123	- 8	- 9	- 3.4%	- .038	-.0014	
34K/1.9	83°	0	0	0	0	0	0	0	0		-13.0	+ .49	- 57	- 25	- 79	- 9.4%	- .04	+ .001	
45K/0.9	40°	0	0	0	0	0	0	0	0		- 2.5	+.184	+ 15	- 62	-118	+ 5.8%	- .008	+.0006	
50K/0.9	83°	0	0	0	0	0	0	0	0		-2.26	- .88	+ 27	- 25	- 69	- 1.9%	+ .027	- .003	
54K/2.2	130°	0	0	0	0	0	0	0	0		+ 8.0	+ .65	- 63	0	+ 49	+ 7.0%	- .005	- .005	
65K/1.2	83°	0	0	0	0	0	0	0	0		- 3.7	-0.19	+ 5	- 35	+110	+ 6.7%	+.0168	- .01	
65K/2.5	83°	0	0	0	0	0	0	0	0		+ 6.4	+1.85	+ 10	+ 50	+175	+49.7%	+ .003	+ .025	
65K/2.5	130°	0	0	0	0	0	0	0	0		+ 8.0	+ 1.6	- 35	+ 75	+169	+53.6%	+ .013	+ .028	

TABLE XXIII

PARAMETER SYNTHESIS/DIA CONCEPT STEADY STATE COMPARISONS - PT6 FAILED +30 PSI

Flight Operating Point		Steady State Estimation ERRORS - Parameter Synthesis									Steady State Estimation Errors - DIA Concept 2								
		PT4 (PSI)	PT6 (PSI)	N1 (RPM)	N2	FTIT °R	Thrust %CHANGE	SMF (%)	SMC (%)	Comments	PT4 (PSI)	PT6 (PSI)	N1 (RPM)	N2	FTIT °R	Thrust %CHANGE	SMF (%)	SMC (%)	Comments
0/0	20°	N.A.	- .0.5	N.A.	N.A.	N.A.	+ 0.8%	0	- .004		+.81	+ .1	+ 22	- 34	+ 90	+1.49%	0	- .005	
0/0	83°	N.A.	+ 0.95	N.A.	N.A.	N.A.	- 0.7%	-0.011	+ .001		-5.3	- 1.76	+ 5	+ 20	+ 47	- 2.5%	+ .02	- .002	
0/0	130°	N.A.	+ 0.85	N.A.	N.A.	N.A.	0	- .004	+.0005		-5.8	- 1.67	- 4	+ 20	+ 47	- 3.2%	+.018	-.0004	
0/1.2	83°	N.A.	+ 1.1	N.A.	N.A.	N.A.	+ 1.2%	- .001	- .002		+2.9	+ 4.5	- 7	- 6	- 10	+ 6.4%	-.006	+ .006	-0.168 TSFC
10K/0.9	83°	N.A.	- 0.85	N.A.	N.A.	N.A.	- 1.5%	+ .004	- .01		- 3	- 1.08	- 10	+ 20	+ 32	- 2.1%	+.008	- .009	
20K/0.3	24°	N.A.	- .15	N.A.	N.A.	N.A.	0	- .001	-.0025		-5.2	- 0.49	+ 16	- 42	- 45	- 4.9%	+.005	- .004	
20K/0.3	83°	N.A.	+ 1.24	N.A.	N.A.	N.A.	- 0.2%	+ .001	+ .003		- 3	- 1.7	+ 60	+ 20	+100	- 4.8%	+.051	- .01	
24K/1.8	83°	N.A.	+ 2.8	N.A.	N.A.	N.A.	- 1%	- .03	- .008		+4.5	+ 3	-130	- 5	- 8	- 3.7%	-.004	- .002	
34K/1.9	83°	N.A.	+ 1.47	N.A.	N.A.	N.A.	+ 1.7%	- .006	+.0035		-13.6	- 0.45	- 55	- 25	- 77	- 6.6%	- .04	+ .002	
45K/0.9	40°	N.A.	+0.076	N.A.	N.A.	N.A.	0%	- .001	+ .001		-2.53	+0.206	+ 15	- 60	-130	+ 5.8%	-.009	+ .002	-0.0187 TSFC
50K/0.9	83°	N.A.	+ 0.68	N.A.	N.A.	N.A.	+0.19%	- .004	+ .001		-2.26	- 0.91	+ 27	- 25	- 59	- 1.9%	+.025	- .002	
54K/2.2	130°	N.A.	+ 1.2	N.A.	N.A.	N.A.	- 0.8%	- .002	+ .005		+ 6	+ .67	- 66	- 25	+ 49	+ 7.6%+	-.006	+ .003	
65K/1.2	83°	N.A.	+ 0.47	N.A.	N.A.	N.A.	+ 0.4%	+ .004	- .006		-3.7	- 0.18	+ 5	- 40	+105	+ 7.1%	+.025	- .011	
65K/2.5	83°	N.A.	+ 0.38	N.A.	N.A.	N.A.	-	0	0	Unstable	+6.5	+ 2.05	0	+ 38	+180	+ 50%	+.008	+ .035	False Alarm before failure
65K/2.5	130°	N.A.	+ 1.38	N.A.	N.A.	N.A.	-0.49%	- .001	- .002		+ 8.0	+ 1.82	- 10	+ 30	+169	+ 53.6	+ .01	+ .03	False Alarm before failure

TABLE XXIV

ADVANCED DIA ALGORITHM
ESTIMATION ERROR

Sea Level Static 83° PLA

Sensor Failure	PT6 (psi) Estimation Error	PT4 (psi) Estimation Error	N1 (rpm) Estimation Error	N2 (rpm) Estimation Error	FTIT (°R) Estimation Error
No failure	-1.752	-5.32	+ 5	+20	+46
PT6	-1.752	-5.32	+ 5	+20	+46
N1	-1.714	-5.29	+12.0	+22	+45
N2	-1.761	+3.44	+35	+76	+43.6
PT4	-1.768	-5.41	+ 4	+16	+46.4

TABLE XXV

PARAMETER SYNTHESIS/DIA CONCEPT STEADY STATE COMPARISONS - N1 FAILED +2000 RPM

Flight Operating Point	Steady State Estimation ERRORS - Parameter Synthesis									Steady State Estimation ERRORS - DIA Concept 2								
	PT4 (PSI)	PT6 (PSI)	N1 (RPM)	N2	FTIT °R	Thrust %CHANGE	SMF (%)	SMC (%)	Comments	PT4 (PSI)	PT6 (PSI)	N1 (RPM)	N2	FTIT °R	Thrust %CHANGE	SMF (%)	SMC (%)	Comments
0/0 20°	NA	NA	-156	NA	NA	- 6.2%	+.0002	- .01		+1.98	+.188	+ 100	- 6	+ 81	+5.3%	-.0015	+ .012	
0/0 83°	NA	NA	-100	NA	NA	- .3%	- .017	+ .004		- 5.4	-1.72	+12.5	+22	+ 46	-3.1%	+.0215	- .002	
0/0 130°	NA	NA	-106	NA	NA	-1.45%	- .014	+.0018		- 5.7	-1.74	- 6.5	+25	+ 48	-3.2%	+ .022	- .001	
0/1.2 83°	NA	NA	+870	NA	NA	+ 5.8%	+ .01	- .021		+3.45	+ 4.3	- 20	-10	- 11	+6.4%	- .005	- .003	-0.0628 TSFC
10K/0.9 83°	NA	NA	-420	NA	NA	- 3.4%+	- .045	0		- 3.8	-1.18	+ 15	-19	+ 30	-2.2%	+ .01	- .013	Noisy After Accommodation
20K/0.3 24°	NA	NA	-440	NA	NA	-22.2%	+ .01	+ .008		-4.65	-0.43	+ 110	-30	- 57	- 1%	- .032	+ .021	
20K/0.3 83°	NA	NA	+ 18	NA	NA	- 0.1%	+.0005	+ .002		- 2.0	- 1.4	+ 160	+15	+ 90	- 4%	+ .071	- .012	
24K/1.8 83°	NA	NA	+440	NA	NA	- 3.2%+	- .01	- .01		+11.4	+1.85	- 350	-18	+ 8	-2.7%	- .036	+ .002	
34K/1.9 83°	NA	NA	+600	NA	NA	+11.3%	+ .024	- .008		- 13	0	- 160	-40	- 67	-5.6%	- .039	+.0035	
45K/0.9 40°	NA	NA	-124	NA	NA	-1.%	- .001	+ .001	-	-	-	-	-	-	-	-		Diverging Stability After Accom.
50K/0.9 83°	NA	NA	+ 40	NA	NA	+ 1.7%	+ .022	+ .004		-1.79	- .85	+ 172	+ 5	- 75	-0.2%	+ .04	- .002	
54K/2.2 130°	NA	NA	-195	NA	NA	0	-.0015	+ .005		+ 9.0	- .7	- 80	0	+ 90	+2.4%	+ .002	-.0055	Unstability After Accom.
65K/1.2 83°	NA	NA	- 7	NA	NA	0	- .002	+ .003		-3.55	-0.12	+ 28	-32	+100	+5.8%	+.0167	- .01	
65K/2.5 83°	NA	NA		NA	NA					+ 6.2	+ 1.8	- 10	+32	+175	+50.6%	+ .004	+ .03	FTIT False Alarm
65K/2.5 130°	NA	NA		NA	NA					+ 8.0	+1.54	- 40	+25	+176	+53.6%	+ .012	+ .027	FTIT False Alarm

* Problem with N1 synthesis due to multivariable control stability problem

positive errors occur at high power, both of which, could be reduced with minor power lever adjustments by the pilot. The parameter synthesis algorithm did not respond well at 65k/2.5 due to a multivariable control stability problem which resulted in exceeding the operating range of the N1 parameter synthesis curve. This could be rectified by extending the parameter synthesis curves, however, since the cause of the problem was a control stability problem, it was not felt to be worthwhile.

The advanced algorithm shows good accommodation to an N1 failure at most conditions where the fan turbine inlet temperature estimator is not the controlling loop (65k ft/1.2Mn, 65k ft/2.5Mn). At 10k ft/0.9Mn and 45k ft/0.9Mn, a control stability problem is experienced after the failure is accommodated. It is felt that this problem could be rectified by improving the Kalman filter gains. At the remaining conditions, the thrust variation is less than 6.5% with little variation in fan or compressor surge margin.

5.1.5 Comparisons With an N2 Sensor Failure Induced

A comparison of steady state accommodation of an N2 speed sensor failure for the two algorithms is shown in Table XXVI. Both algorithms accommodate an N2 failure with little variation in thrust, fan surge margin, or compressor margin. The parameter synthesis algorithm limits thrust variation for an N2 failure accommodation to 4.4% except at 65k ft/2.5Mn where the thrust variation is larger but still limited to less than 10%. At 24k ft/1.8Mn, the parameter synthesis algorithm does suffer a 5.4% loss in compressor surge margin, however, it still has adequate surge protection (9% compressor surge margin). The advanced detection, isolation and accommodation algorithm is shown to experience only minimal additional performance degradation when accommodating an N2 sensor failure. At 50k ft/.9Mn, the system was slightly unstable when accommodating an N2 sensor failure, however, the magnitude of the oscillation was minimal.

5.1.6 Comparisons With an PT4 Sensor Failure Induced

A comparison of the two algorithms' steady state accommodation to a PT4 sensor failure is shown in Table XXVII. This Table shows an acceptable amount of steady state thrust variation resulting from accommodation of the failure. At some conditions both algorithms experienced difficulty accurately detecting and isolating the PT4 failure. At four flight operating points (0 ft/0Mn 83° PLA; 0 ft/0Mn 130° PLA; 0 ft/1.2Mn 83° PLA; 10k ft/0.9Mn 83° PLA) the parameter synthesis algorithm detected a failure, but was unable to pinpoint the failure to the PT4 sensor. Referring to the parameter synthesis curve set shown in Figure 74, the four failure cases detected the failure by going out of tolerance on curve 2. Since curve 2 can be out of tolerance by itself for an N2 drift or a PT4 drift depending on the flight condition, it does not provide adequate information to isolate the sensor failure. To isolate a failure to PT4, curve 1 must also be out of tolerance with the sensed signal. Since the tolerance bands on curve 1 were sized to provide adequate margin for curve read errors at the higher altitude conditions, a large sensor drift is required at the lower altitude condition to drive the curve out of tolerance

TABLE XXVI

PARAMETER SYNTHESIS/DIA CONCEPT STEADY STATE COMPARISONS - N2 FAILED +2000 RPM

Flight Operating Point	Steady State Estimation ERRORS - Parameter Synthesis									Steady State Estimation ERRORS - FDIA Concept 2								
	PT4 (PSI)	PT6 (PSI)	NI (RPM)	N2 (RPM)	FTIT °R	Thrust %CHANGE	SMF (%)	SMC (%)	Comments	PT4 (PSI)	PT6 (PSI)	NI (RPM)	N2 (RPM)	FTIT °R	Thrust %CHANGE	SMF (%)	SMC (%)	Comments
0/0 20°	NA	NA	NA	+ 70	NA	+ 4.4%	-.0007	-.0005		- 0.2	- 0.1	+ 7	- 65	+ 98	+.095%	-.0005	- .003	
0/0 83°	NA	NA	NA	+ 22	NA	+0.04%	0	+ .003		+ 3.8	-1.73	+ 35	+ 76	+ 47	- 2.6%	+ .024	+ .002	
0/0 130°	NA	NA	NA	+ 50	NA	0	0	+ .001		- 4.0	- 1.7	+ 30	+ 80	+ 48	- 2.9%	+ .026	+ .002	
0/1.2 83°	NA	NA	NA	- 50	NA	+ 0.4%	0	0		+1.95	+4.45	- 55	- 45	- 4	+ 6.4%	- .006	+.0005	-0.068 TSFC
10K/0.9 83°	NA	NA	NA	+ 8	NA	- 0.8%	-.0001	+ .001		- 1.5	-1.13	+ 22	+ 58	+ 33	- 1.7%	+ .011	+ .001	
20K/0.3 24°	NA	NA	NA	+122	NA	- 1.2%	0	+ .028		- 7.1	-0.52	- 10	-132	- 31	- 6.1%	+ .002	-.0225	
20K/0.3 83°	NA	NA	NA	- 30	NA	-0.15%	+.0002	+ .003		- 3.5	- 1.7	+ 50	- 70	+100	- 5.5%	+.0423	- .013	
24K/1.8 83°	NA	NA	NA	-340	NA	- 4%+	- .028	- .054		+ 5.6	+ 2.1	-125	- 22	- 8	- 3.4%	- .04	+ .001	
34K/1.9 83°	NA	NA	NA	-115	NA	0%	+ .001	- .018		-19.7	+ .50	- 85	-140	- 74	- 9.5%	- .04	- .006	
45K/0.9 40°	NA	NA	NA	+ 66	NA	+ 2.5%	- .001	+ .006		- 3.3	+.174	0	-146	-114	+ 3.5%	- .006	- .001	
50K/0.9 83°	NA	NA	NA	- 20	NA	0%	+.0065	- .001		-2.68	- .88	+ 18	-113	- 67	- 2.7%	+ .003	- .001	Slightly Unstable after Accommodation
54K/2.2 130°	NA	NA	NA	-220	NA	- 1.7%	0	- .03		+ 6	+ .64	- 67	-130	+ 53	+ 7.7%	- .006	+ .001	
65K/1.2 83°	NA	NA	NA	- 25	NA	- .15%	+ .001	- .002		- 4.9	+ .20	- 5	-270	+120	+ 3.2%	- .012	- .04	
65K/2.5 83°	NA	NA	NA	-125	NA	+ 9%	- .005	0	Unstable before and after failure	+ 7.7	+ 1.8	- 25	+160	+180	+49.1%	+ .015	+ .046	FTIT False Alarm
65K/2.5 130°	NA	NA	NA	-200	NA	- 2.2%	- .004	- .04		+ 11	+ 1.7	+ 10	+120	+165	+53.2%	+ .013	+ .042	FTIT False Alarm

TABLE XXVII

PARAMETER SYNTHESIS/DIA CONCEPT STEADY STATE COMPARISONS - PT4 FAILED +50 PSI

Flight Operating Point	Steady State Estimation ERRORS - Parameter Synthesis									Steady State Estimation ERRORS - DIA Concept 2								
	PT4 (PSI)	PT6 (PSI)	N1 (RPM)	N2	FTIT °R	Thrust %CHANGE	SMF (%)	SMC (%)	Comments	PT4 (PSI)	PT6 (PSI)	N1 (RPM)	N2	FTIT °R	Thrust %CHANGE	SMF (%)	SMC (%)	Comments
0/0 20°	-1.45	NA	NA	NA	NA	- 6%	+.0025	- .006		+.75	+.08	+20	-41	+90	+1.14%	0	-.0002	FTIT False alarm @ time failure induced
0/0 83°	- 5.0	NA	NA	NA	NA	- 1.3%	+ .012	+ .005	Detection but no isolation	-5.5	- 1.7	+ 5	+17	+ 49	- 3.1%	+.021	-.0015	
20/0 130°	- 2.4	NA	NA	NA	NA	0%	0	0	Detection but no isolation	- 6	- 1.7	- 4	0	+ 50	- 3.8%	+.021	- .001	
0/1.2 83°	+ 5.0	NA	NA	NA	NA	- 0.4%	- .001	+.0025	Detection but no isolation	+2.8	+ 4.5	- 6	- 7	- 9	+ 6.5%	-.006	+.0045	-0.048 TSFC, P6 false alarm at time failure induced
10K/0.9 83°	- 1.5	NA	NA	NA	NA	- 1.2%	+ .006	+ .004	Detection but no isolation	-3.0	- 1.1	- 10	+17	+ 32	- 2.2%	+ .01	+ .001	
20K/0.3 24°	-0.15	NA	NA	NA	NA	+ 0.3%	+ .001	+.0002		-5.0	-0.45	+ 30	-46	- 60	- 5.2%	+.004	-.0045	
20K/0.3 83°	+ 1.3	NA	NA	NA	NA	+0.25%	+.0015	0		-2.8	-1.65	+ 60	-20	+100	- 5.8%	+.056	- .015	FTIT False Alarm at time Failure Induced
24K/1.8 83°	+ 5.0	NA	NA	NA	NA	-0.57%	- .002	- .008	Had Trouble did Isol. finally	+4.5	+ 3.1	-120	+ 5	- 80	- 4.9%	-.035	-.0005	P6 False Alarm
34K/1.9 83°	+ 6.0	NA	NA	NA	NA	0%	+ .001	0		- 13	+ 0.4	- 75	-20	- 77	- 6.6%	- .04	+.0015	
45K/0.9 40°	- 1.1	NA	NA	NA	NA	- 0.7%	+.0002	- .008		-2.6	+0.18	+ 12	-60	-120	+ 6.1%	-.011	0	-0.02 TSFC FTIT False Alarm When Failure Induced
50K/0.9 83°	+ 1.0	NA	NA	NA	NA	+ 0.9%	+.0247	+ .002		-2.2	- 0.9	+ 26	-28	- 70	- 1.1%	+.028	- .003	FTIT False Alarm When Failure Induced
54K/2.2 130°	+ 2.0	NA	NA	NA	NA	- 0.6%	+ .001	- .009	Transient FTIT Over Temp	+6.0	+0.65	- 61	0	+ 57	+ 7%+	-.004	- .009	FTIT False Alarm When Failure Induced
65K/1.2 83°	+ 0.7	NA	NA	NA	NA	0	0	0		-3.7	-0.19	+ 3	-35	+100	+ 7.1%	+.017	- .007	FTIT False Alarm When Failure Induced
65K/2.5 83°	+ 4.0	NA	NA	NA	NA	-	0	0	Simulation Unstable	+6.6	+ 1.8	- 10	+40	+122	+29.7%+	+ .01	+ .03	P6 & FTIT False alarm
65K/2.5 130°	0	NA	NA	NA	NA	+ 2%	+.0008	+ .001		+9.0	+ 1.6	0	+120	+167	+44.5%+	+ .01	+ .027	P6 & FTIT False Alarms

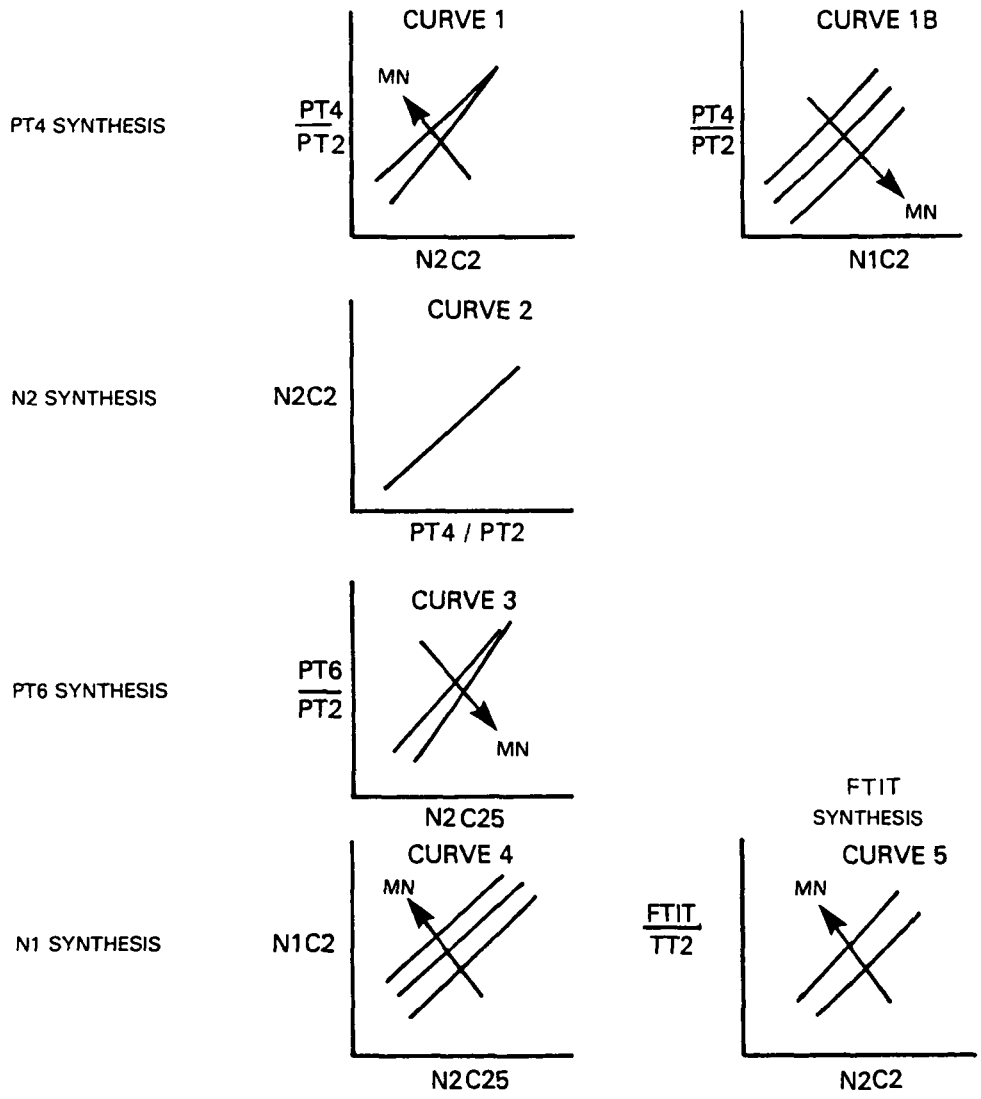

Figure 74 Parameter Synthesis Curve Set

with the sensor measurement. A biasing technique could be implemented (perhaps a PT2 bias) to reduce the tolerance band for curve 1 at the lower altitude conditions. However, since the non-isolated failure has only minimal effect on engine performance, the additional complexity of a biasing technique would be of questionable value.

The advanced algorithm also had difficulties isolating the PT4 failure at some flight operating conditions. This problem could be reduced by improving the simplified model's accuracy and redesigning the failure isolation tolerance bands.

5.1.7 Comparisons With a Fan Turbine Inlet Temperature Sensor Failure Induced

The two detection, isolation and accommodation algorithm's steady state accommodation to a fan turbine inlet temperature sensor failure was evaluated at a few flight operating points. It became evident that neither system provided adequate protection when operating on the synthesized or estimated value. These results are consistent with previous in-house studies which showed the accuracy of a synthesized signal to provide inadequate temperature limiting protection. With the advanced concept, however, improving the accuracy of the modeling approach within the algorithm may significantly improve the accuracy of the fan turbine inlet temperature estimate to insure adequate engine protection. This should be evaluated in future studies.

5.2 TYPICAL FAILURE TRANSIENTS

When the steady state sensor failures were induced, the resulting perturbation on engine performance was observed. For most conditions, there was less failure/accommodation transient with the advanced detection, isolation and accommodation algorithm than with parameter synthesis. This was expected since the parameter synthesis technique requires a switching from a sensor measurement to a synthesized signal to accommodate a sensor failure, whereas the advanced algorithm is always feeding back estimator values. To accommodate a sensor failure, the advanced failure detection, isolation and accommodation algorithm reconfigures the normal mode filter to eliminate the failed sensor from the computation of the estimated values.

Figure 75 compares the failure transients of pertinent engine performance parameter for a typical sensor failure. The time histories shown result from an N2 failure occurring at a time of 3.0 seconds at the sea level static, 83° PLA flight operating point. The parameter synthesis case shows a failure transient of 255 pounds thrust variation compared to the advanced algorithm's 60 pound thrust variation, however, after the failure transient decay, the parameter synthesis case shows 52 pounds of thrust less accommodation error.

5.3 DETECTION/ISOLATION ACCURACY

To compare the detection and isolation performance of the parameter synthesis and advanced algorithms, slow sensor drifts were simulated at the flight operating conditions shown to be the most sensitive to in-range failure in the

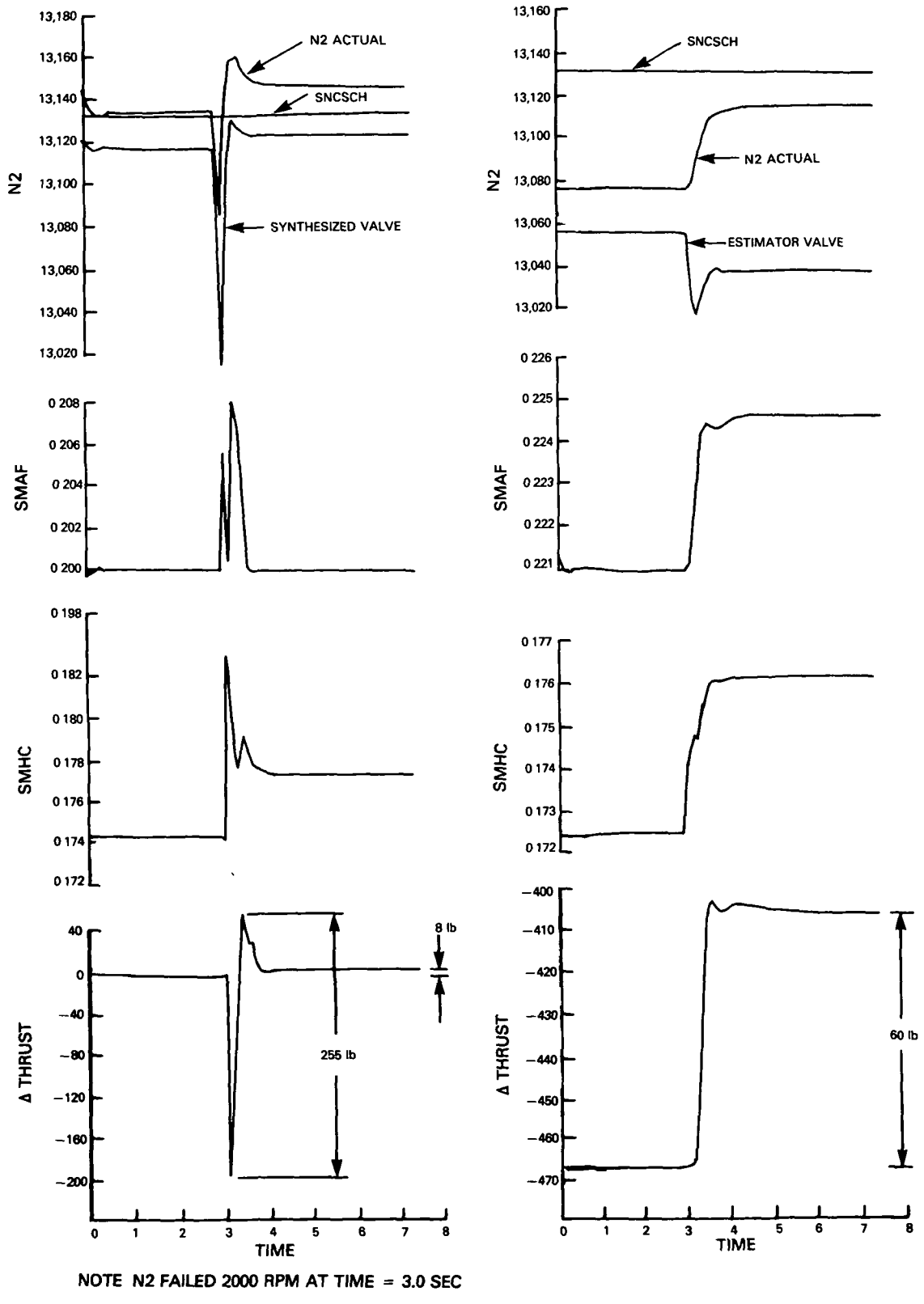

Figure 75 Failure Transient Comparisons for an N2 Sensor Failure at Sea Level Static Conditions and 83° PLA

Failure Mode and Effects Critical Analysis (FMECA). When the failure was detected and isolated, the magnitudes of the bias and thrust variation were recorded, as tabulated in Table XXVIII. N1 drifts were not included in this study since the analysis showed that in-range N1 failures rarely occurred.

As shown in Table XXVIII, the advanced algorithm is less sensitive to PT6, PT4, and fan turbine inlet temperature drifts than the parameter synthesis based algorithm. The PT4 drift, for example, is detected and isolated as a failure for smaller magnitudes of drift with the parameter synthesis technique (32 psi compared to 44.3 psi with the advanced concept). However, the parameter synthesis based on algorithm experienced a -5.4% larger thrust degradation prior to accommodation than was experienced with the advanced algorithm. The reduced performance degradation with the advanced concept results from the Kalman filter gains being sized to place the highest weighting on the N2 speed signal and considerably less weighting on the PT4, PT6, FTIT, and N1 signals. Therefore, when the PT4 signal was drifted, the estimated sensor values changed only slightly for a large magnitude of drift. Conversely, when the N2 signal was drifted, the estimated sensor values followed the N2 sensor drift resulting in significant performance degradation (greater than 10% thrust change) and difficulties in failure detection and isolation.

TABLE XXVIII
Parameter Synthesis/Detection, Isolation and Accommodation
Concept 2 Sensor Failure Detection Comparisons

Flight Operating Point	Sensor Drift	Parameter Synthesis Bias before DIA	Parameter Synthesis FNT before DIA	Parameter Synthesis Comments	DIA Concept 2 Bias before DIA	DIA Concept 2 FNT before DIA	DIA Concept 2 Comments
0/0 20° PLA	PT6 drifted Positive	+12.7 PSI	-3.5%		+5.68 PSI	+0.1%	
0/0 83° PLA	PT4 drifted Positive	+32 PSI	-5.6%		+44.3 PSI	-0.2%	
0/1.2 83°PLA	FTIT drifted Positive	+78°F	-20.3%		+114°F	0	
20k/0.3 83°PLA	N2 drifted Positive	+473 RPM	-3.2%		+1419 RPM	-6.5%	FTIT false occuring @ 666 RPM N2 Bias.
20k/0.3 83°PLA	N2 drifted Negative	-390	+2.3%		undetected	+10.5%	FTIT and N1 false alarms N1 and N2 overspeed

Figures 76 and 77 show time histories of pertinent engine and performance parameters responding to a PT4 drift with the parameter synthesis based algorithm and the advanced algorithm respectively. The thrust variations shown on these figures are calculated relative to the "perfect" sensor feedback case. As shown in Figure 77, the advanced algorithm's sensor estimates respond only slightly to the PT4 drift, resulting in only a minor performance degradation over no-failure operation. Figure 75 shows a similar failure scenario for the parameter synthesis based algorithm experiencing a larger performance degradation prior to isolation, however, after isolation, the parameter synthesis based algorithm accommodates the failure more accurately than the advanced algorithm.

Figures 78 and 79 show time histories of pertinent engine and performance parameters responding to an N2 drift with the parameter synthesis based algorithm and the advanced algorithm, respectively. The thrust variations shown on these figures are calculated relative to the "perfect" sensor feedback case. As shown in Figure 79, the advanced algorithm's sensor estimates respond considerably to the N2 sensor drift, and this results in significant performance degradation. For this particular failure case, the parameter synthesis algorithm's detection and isolation performance was shown to be more accurate than the advanced DIA algorithm. The parameter synthesis algorithm detected and isolated the N2 drift at time of 4.4 seconds, whereas, the advanced algorithm detected a failure at 5.656 seconds and isolated it to fan turbine inlet temperature at 5.664 seconds. A second failure was detected at 7.222 seconds and isolated to the N1 sensor at 7.230 seconds. Therefore, the advanced algorithm had two false alarms and never correctly isolated the failure to the N2 sensor.

This study showed that for all sensor failures, except PT6, the parameter synthesis algorithm detects and isolates the sensor failure for a smaller magnitude of drift than the advanced detection, isolation and accommodation algorithm. However, even with the larger magnitudes of drifts the effects on engine performance are smaller with the advanced algorithm for all sensor drifts with the exception of N2. Since the Kalman filter gains were sized to place the highest weighting on the N2 sensor input to improve filter response, the estimated values followed the N2 sensor drift thereby making it difficult to detect the failure. Therefore, the weighting on the other inputs should be increased to avoid the situation when a drift in one sensor can cause a significant decrease in engine performance and a drift in the remaining sensors has negligible effect.

5.4 TRANSIENT FAILURE COMPARISONS

Sensor failures were induced during large perturbation transients to compare the transient detection and isolation capability as well as observe the engine's transient behavior when operating with accommodation of failed sensors. All transient sensor failures were induced 1.0 second after the power lever snap. A summary of the results is shown in Table XXIX.

TABLE XXIX

TRANSIENT FAILURE COMPARISON

Flight Condition	Power Lever Transient	Sensor Failure	Parameter Synthesis Detection Isolation Performance	Parameter Synthesis Time to 90% Thrust Change	Parameter Synthesis Comments	Concept #2 DIA Algorithm Detection/Isolation Performance	Concept #2 DIA Algorithm Time to 90% Thrust Change	Concept #2 DIA Algorithm Comments
0/0	20°-83°	P6+35 PSI	P6 Detected & Isolated when induced	3.0 sec	60°F FTIT overshoot	Detected & Isolated P6 in 0.002 sec, Detected & Isolated N2 in 0.43 sec	3.0 sec	80° FTIT overshoot, N2 False Alarm
0/0	20°-83°	P4+50 PSI	P4 Detected & Isolated when induced	3.0 sec	90°F FTIT overshoot	Detected & Isolated P4 in 0.016 sec, Detected & Isolated N1 in 0.034 sec	3.05 sec	80° FTIT overshoot, N1 False Alarm
0/1.2	60°-83°	FTIT+300°F	FTIT Detected & Isolated when induced	1.4 sec	167°F Increase in FTIT	N1 & P6 Detected & Isolated before snap, FTIT Detected & Isolated in 0.616 sec then N1 & P6fault cleared	0.8 sec	60° PLA steady state level 1700 # thrust too high N1 + P6 false alarm
0/1.2	60°-83°	N1+2000 RPM	N1 Detected & Isolated when induced	1.3 sec	92°F Increase in FTIT	N1 & P6 Detected & Isolated before snap, Induced N1 failure detected and Isolated in 0.574 sec, P6 fault cleared	0.8 sec	60° PLA Case 1700 # thrust too high, N1 + P6 false alarm
20k/0.3	83°-24°	N2+2000 RPM	N2 Detected & Isolated when induced	3.3 sec		N2 Detected & Isolated in 0.004 sec, FTIT Detected & Isolated in 0.666 sec	2.8 sec	FTIT False Alarm
20k/0.3	83°-24°	P4+50 PSI	P4 Detected & Isolated when induced,cleared the fault, then detected + isolated 0.8 sec. later	3.9 sec		P4 Detected & Isolated in 0.012 sec, FTIT Detected & Isolated in 0.022 sec	2.85 sec	FTIT False Alarm
45k/0.9	40°-83°	N2+2000 RPM	N2 Detected & Isolated when induced	2.3 sec	120°F FTIT overshoot possible compressor surge	FTIT Detected & Isolated in 0.722 sec after PLA snap, N2 Detected & Isolated in 0.002 sec	4.7 sec	FTIT False Alarm
45k/0.9	40°-83°	N1+2000 RPM	N1 Detected & Isolated when induced	2.3 sec	130°F FTIT overshoot	FTIT Detected & Isolated in 0.722 sec after PLA snap, N1 Detected & Isolated in 0.002 sec	4.6 sec	FTIT False Alarm
45k/0.9	40°-83°	P4+50 PSI	P4 Detected & Isolated when induced	2.3 sec	110°F FTIT overshoot	FTIT Detected & Isolated in 0.772 sec after PLA snap, P4 Detected & Isolated in 0.012 sec,N2 Detected + Isolated in 0.024 sec	4.5 sec	FTIT + N2 False Alarm
45k/0.9	40°-83°	PT6+35 PSI	P6 Detected & Isolated when induced	2.3 sec	95°F FTIT overshoot	FTIT Detected & Isolated in 0.722 sec after PLA snap, PT6 Failure Detected & Isolated in 0.002 sec	4.4 sec	FTIT False Alarm
45k/0.9	40°-83°	FTIT+300	FTIT Detected & Isolated when induced	2.2 sec	105°F FTIT overshoot	FTIT Detected & Isolated in 0.278 sec before induced	4.4 sec	FTIT False Alarm

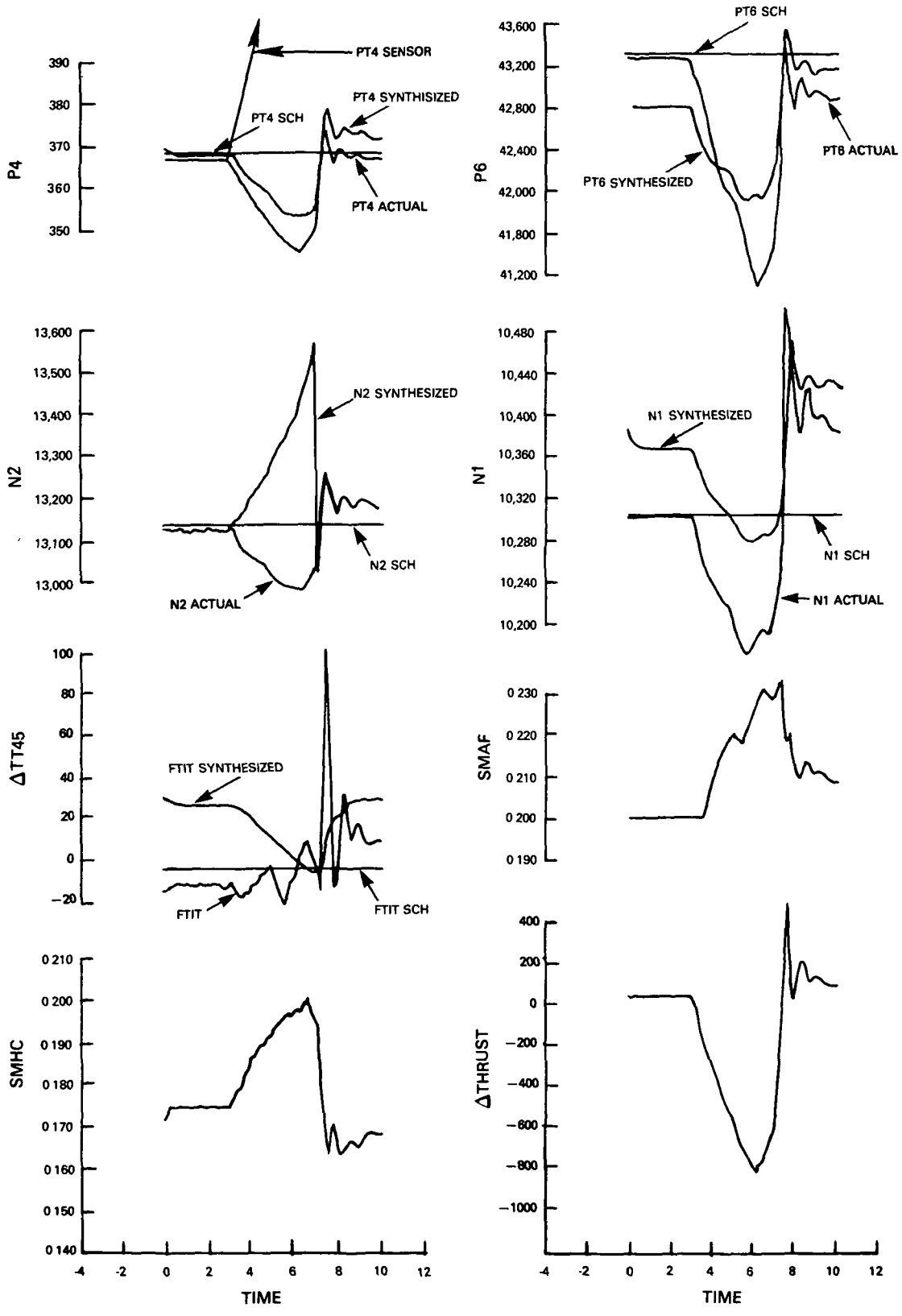

Figure 76 Transient Results With the Parameter Synthesis Algorithm for a PT4 Sensor Drift. (15PSI/sec) Sea Level Static 83° PLA

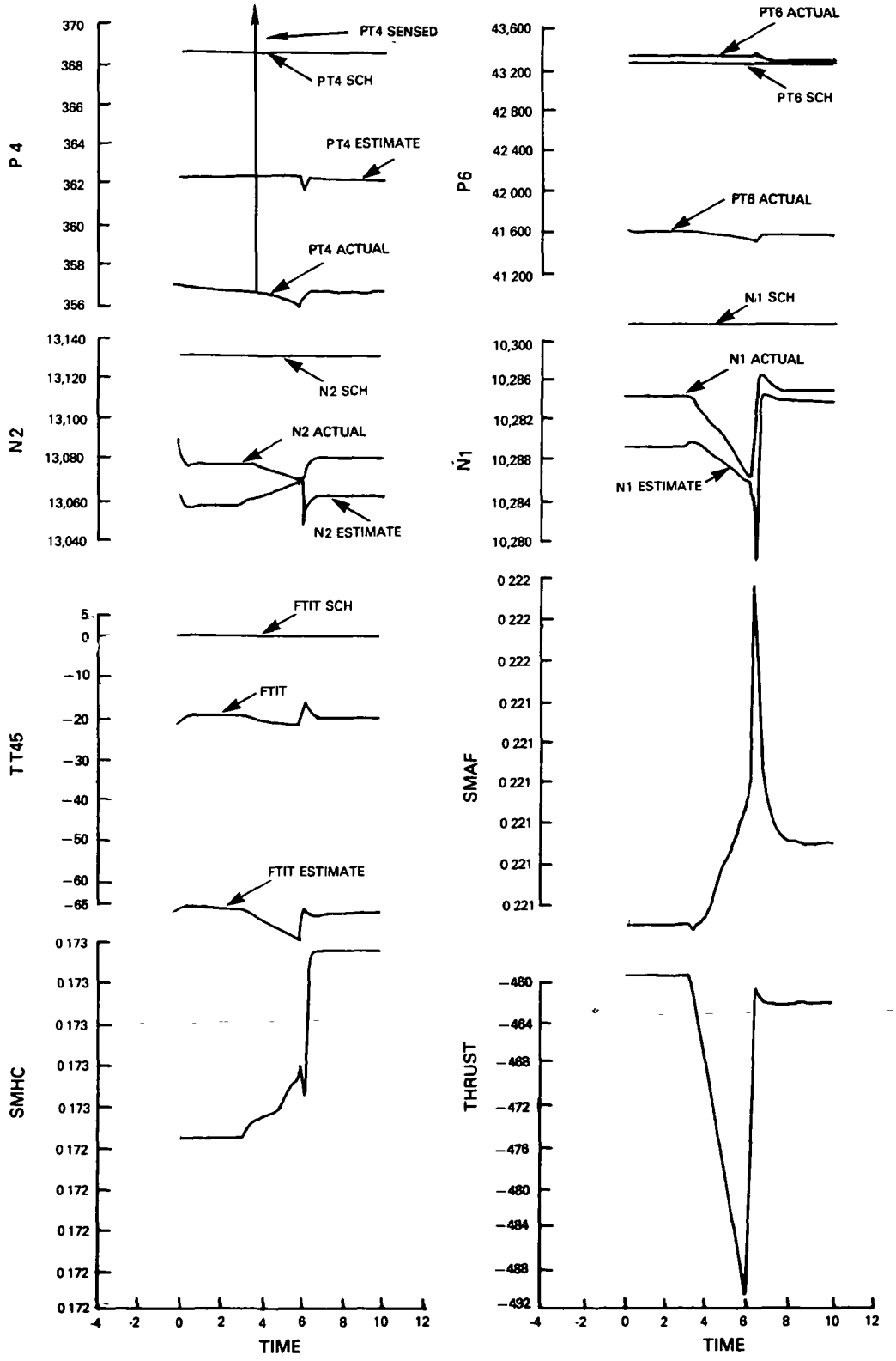

Figure 77 Transient Results With the Parameter Synthesis Algorithm for a PT4 Sensor Drift. (15PSI/sec) Sea Level Static 83° PLA

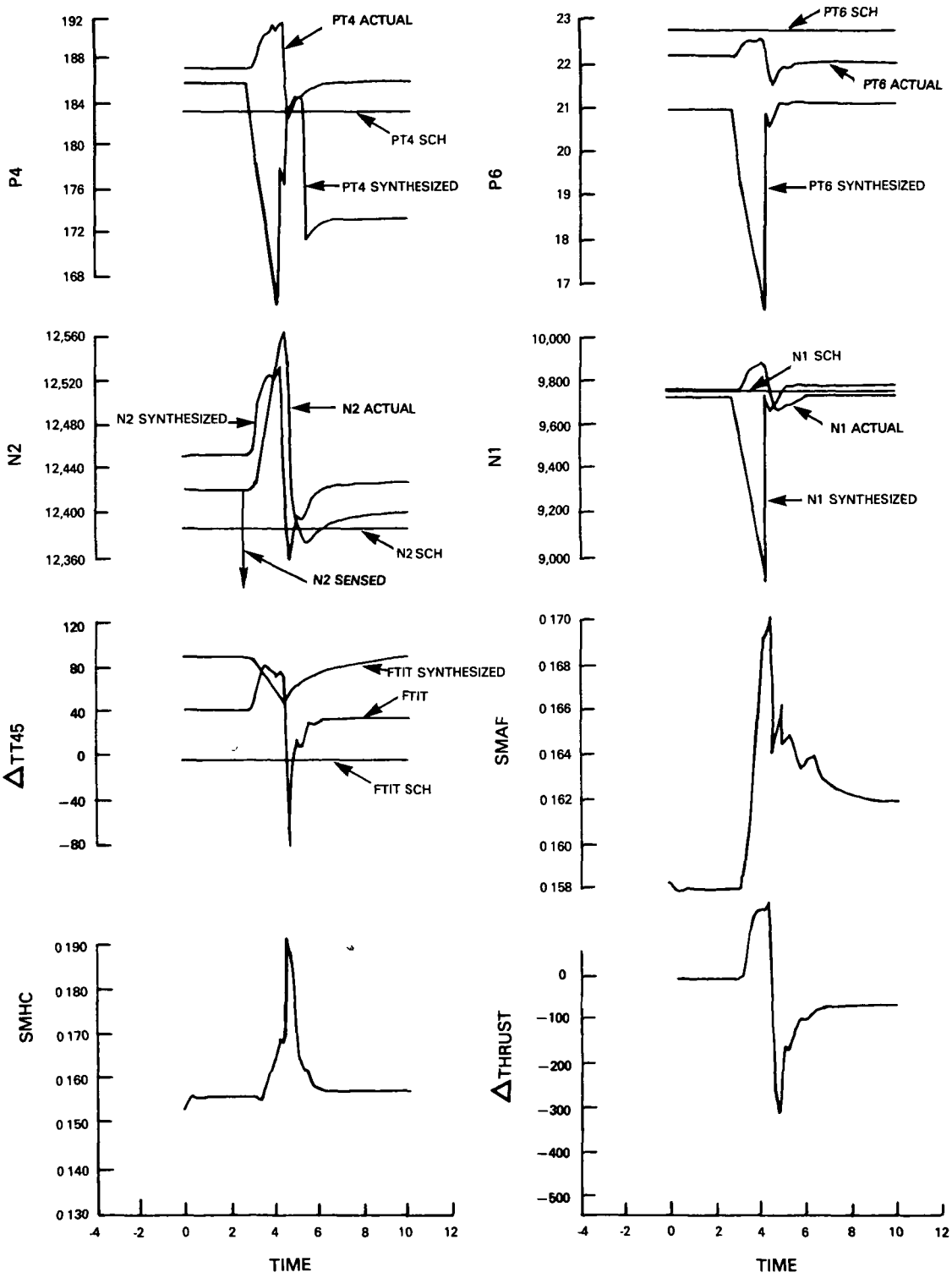

Figure 78 Transient Results With the Parameter Synthesis Algorithm for a PT4 Sensor Drift. (-400 RPM/sec) 20k/0.3Mn, 83° PLA

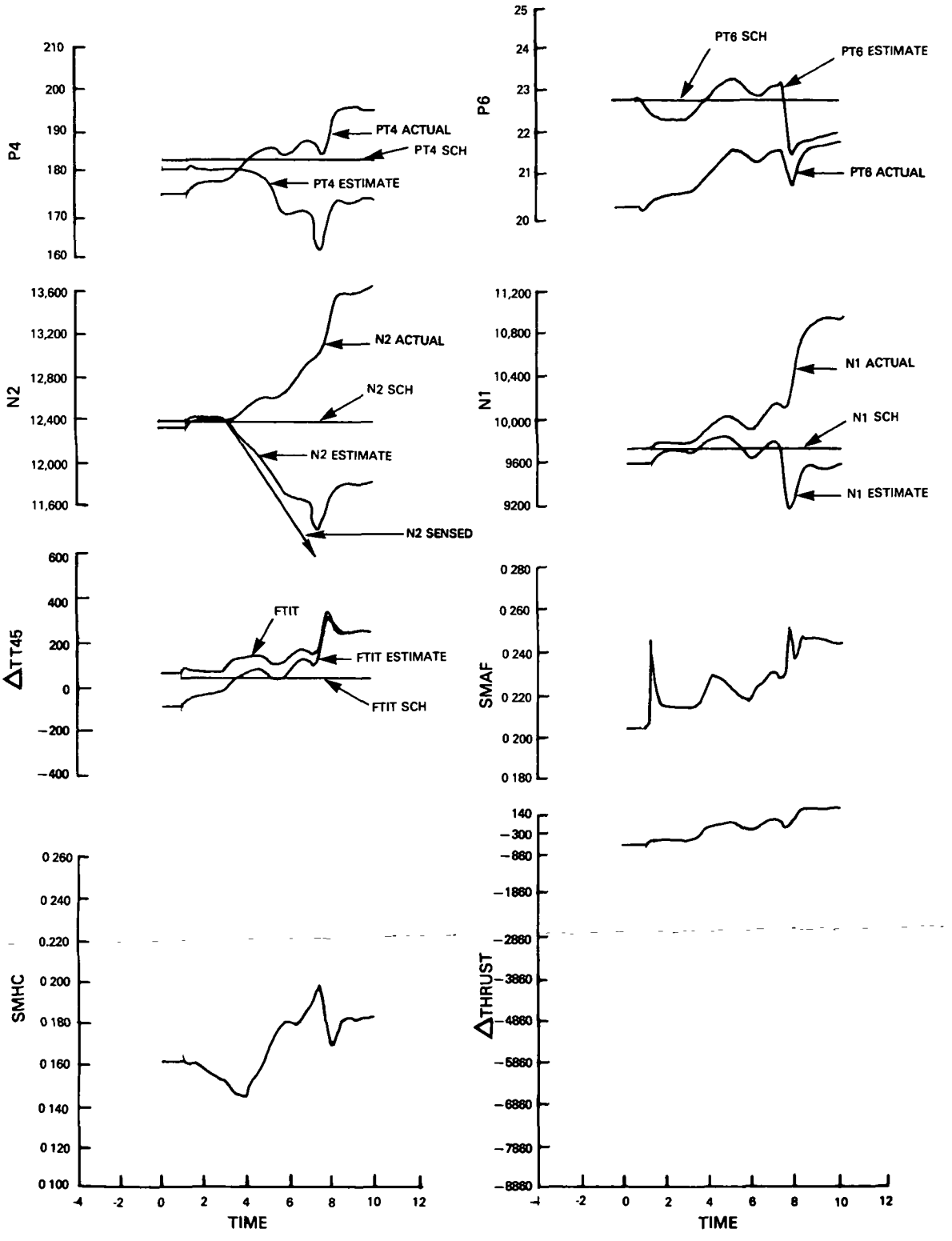

Figure 79 Transient Results With the Parameter Synthesis Algorithm for a PT4 Sensor Drift. (-400 RPM/sec) 20k/0.3Mn, 83° PLA

Table XXIX shows consistantly good transient detection and isolation with the parameter synthesis based algorithm. During the transient, fan turbine inlet temperature overshoots were observed. These overshoots result from operating on an uncompensated signal and are on the same order of magnitude as the no-failure case. At 0 ft/1.2Mn, when fan turbine inlet temperature is failed, a steady state over-temperature is observed. This results from synthesizing the signal to be lower than the reference.

The advanced detection, isolation and accommodation algorithm, as shown on this Table, has problems with false alarms. The fan turbine inlet temperature estimator consistently caused false alarms for most of the sensors failure cases examined. Therefore, additional refinements of the model and algorithm are required to correct this problem.

Generally, transients run with the advanced algorithm were slower. This results from the fan turbine inlet temperature estimator reducing fuel flow during the transient. The FTIT input signal used with the parameter synthesis algorithm is an uncompensated signal which allows fuel flow to accelerate faster, however, does result in more severe FTIT transient overshoots. A typical comparison of the two algorithms' transient behavior is shown on Figure 80. This figure shows good transient response when accommodating the PT4 failure with both algorithms despite the N1 false alarm which occurred with the advanced algorithm. Additional plots of pertinent engine and performance parameters for selected transient operation failure scenarios are included in Appendix E.

5.5 MULTIPLE SENSOR FAILURES

Multiple sensor failures were simulated at sea level static to compare the two algorithms capability to detect, isolate, and accommodate a second sensor failure. For the failure scenarios examined, the advanced detection, isolation and accommodation algorithm showed less performance degradation than the parameter synthesis algorithm. Figure 81 compares the thrust variations relative to perfect sensor feedback case for the parameter synthesis based algorithm and the advanced algorithm for a PT4/N2 multiple failure at sea level static, 83° PLA. As shown in this figure, the advanced algorithm suffers very little additional performance degradation with the second failure (57 pound thrust variation) whereas the parameter synthesis based algorithm shows a much larger performance degradation (2100 pounds thrust variation). Similar results were observed for the other multiple failure scenarios.

5.6 ACTUATOR FAILURES

The engine nozzle area actuator was slewed wide open at sea level static, 83° PLA, to simulate a hardover actuator failure. This test was conducted to verify that the two detection, isolation and accommodation algorithms would not confuse the actuator failure with a sensor failure. This test showed that neither the parameter synthesis algorithm nor the advanced algorithm falsely detected a sensor failure when the actuator failure was induced.

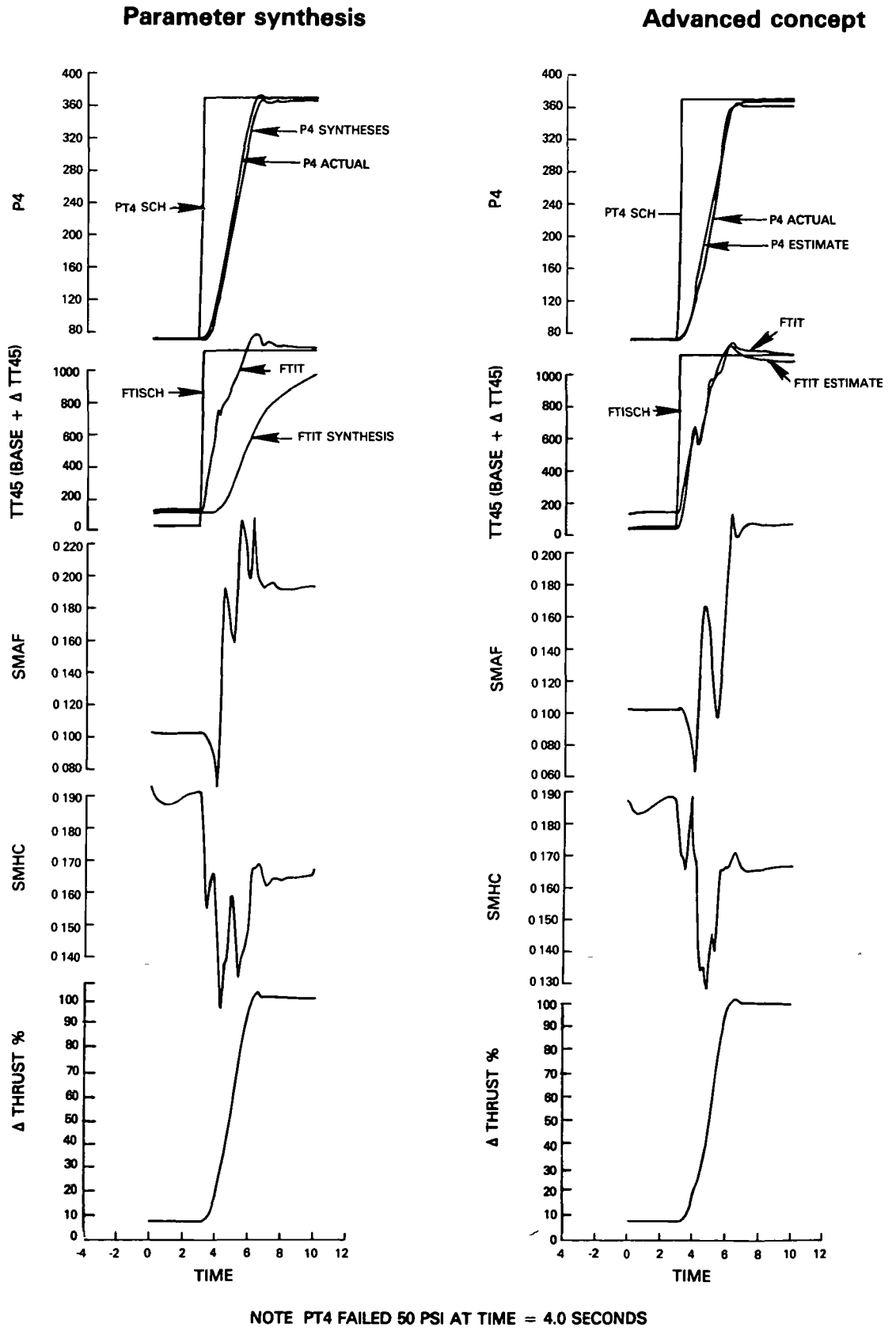

Figure 80 Failure Transient Comparisons for an PT4 Sensor Failure at Sea Level Static Conditions and 83° PLA

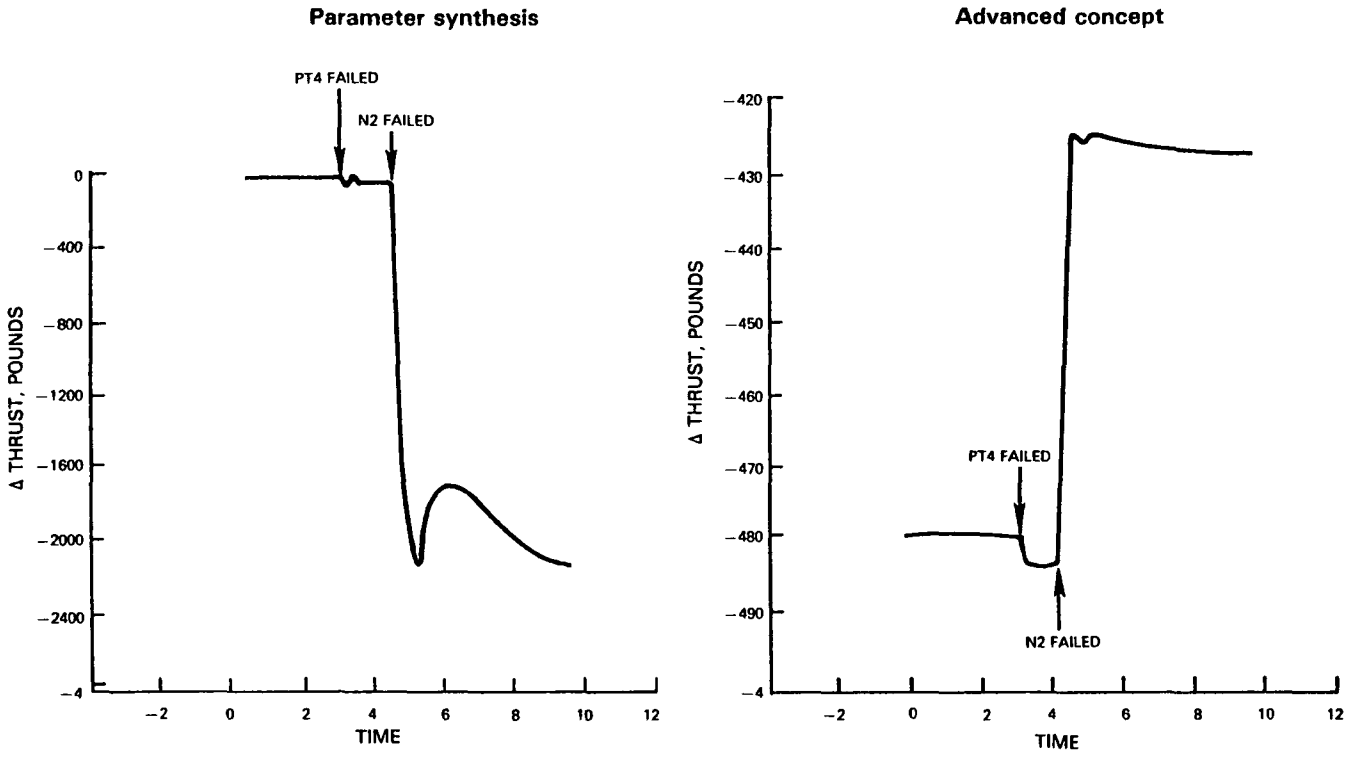

Figure 81 Thrust Transients Resulting From a Multiple Failure of the PT4 and N2 Sensors

SECTION 6.0

RESULTS AND CONCLUSIONS

The following results and conclusions result from this study:

1. Failure Mode and Effects Criticality Analysis Results:

   a. An analysis of failure characteristics for the state-of-the-art sensors selected for the F100 multivariable control mode showed that the majority of the sensor failures recorded were out-of-range failures (90 percent for speed sensors and pressure sensors and 75 percent for temperature sensors). Since 90% failure coverage is not satisfactory for most control applications, there is a need for detection, isolation, and accommodation algorithms to provide in-range failure coverage.

   b. All out-of-range sensor failures exhibit critical failure characteristics with the F100 multivariable control mode. Critical is defined as failures that result in a fan or compressor surge, excessive thrust variation (greater than 10%), or a rotor overspeed above the operating limits.

   c. In-range failures (drifts) of the N2, TT2, TT25, FTIT, PT2, PT6, and PT4 sensors are also shown to exhibit critical failure characteristics and therefore, require either sensor redundancy or analytical redundancy to ensure continued operation in the event of a sensor failure.

2. Simplified nonlinear engine models were developed for use in advanced algorithms for sensor failure detection, isolation, and accommodation. The models worked well except at high altitude (greater than 45K ft) or high Mach number conditions (greater than 1.2). The problems that arose at these conditions were found to result from an insufficient number of linear models available to constrain the curve fitting procedure for the matrix elements at these flight conditions. Therefore, it is concluded that generating more linear models and improving the curve fits will significantly improve the accuracy of the algorithm at the high altitude and high Mach number conditions.

3. Numerous advanced concepts for detecting, isolating and accommodating sensor failures can be developed based upon such techniques as Kalman filters. A screening process led to the selection in this program of an advanced concept which uses a Kalman filter to generate residuals, a weighted Sum Squared residual technique to detect soft failures, Likelihood Ratio testing of a bank of Kalman filters (each designed with one input missing) for isolation, and reconfiguring of the normal mode Kalman filter by eliminating the failed input to accommodate the failure. This was shown to be a feasible detection, isolation, and accommodation algorithm.

4. During the final screening process; the advanced DIA Concept 2, described in conclusion 3, was selected to be the most viable concept for detailed evaluation and comparison against the baseline parameter synthesis technique. The rationale for selecting Concept 2 are as follows:

   1. Since concept 2 uses maximum information (all other sensors) to generate estimates of each parameter it is least sensitive to model errors.

   2. The fault information is in the innovations. This allows concept 2 to respond quickly to sensor failures.

   3. Concept 2 provides good signal conditioning when no sensor failures are present.

5. The parameter synthesis concept developed under this program provided a viable baseline for comparison against the advanced concept. This comparison showed that the advanced concept was also a viable technique for detecting, isolating and accommodating sensor failures.

6. Parameter Synthesis/Advanced DIA Concept Comparisons:

   a. The advanced concept feeds back the estimator values to the control laws which result in a steady state hangoff (estimation error) with no induced sensor failures. This estimation error varies as a function of of flight condition due to the modelling errors previously noted in conclusion 2.

   b. Steady state comparisons between the parameter synthesis and the advanced concepts showed both to have very good detection, isolation, and accommodation for PT6, PT4, N1, and N2 sensor failures at most operating points.

   c. Neither the parameter synthesis nor the advanced concept provides ade quate FTIT protection when operating on the synthesized or estimated value. These results are consistent with previous in-house studies which showed the accuracy of a synthesized signal provides inadequate temperature limiting protection. With the advanced concept, however, improving the accuracy of the modeling approach within the algorithm may significantly improve the accuracy of the FTIT estimates.

   d. For most conditions evaluated, there was less failure/accommodation transient with the advanced concept than with the parameter synthesis concept.

f. With the exception of PT6, the parameter synthesis algorithm detects and isolates the sensor failure for a smaller magnitude of drift than the advanced detection, isolation and accommodation algorithm. However, even with the larger magnitudes of drifts the effects on engine performance are smaller with the advanced algorithm for all sensor drifts with the exception of N2. Since the Kalman filter gains were designed to place the highest weighting on the N2 sensor input, the estimated values tracked the drifted input signal which made the advanced concept unable to detect and isolate the sensor failure. Refinements to the algorithm are required to redistribute the weighting of the Kalman filter gains among the other inputs to avoid the situation when a drift in one sensor can cause a significant decrease in engine performance and a drift in the remaining sensors has negligible effect.

h. The advanced concept showed less performance degradation than the parameter synthesis concept for the multiple sensor failure scenarios examined.

7. The implementation of failure logic in a control system can have significant impact on computational requirements and, hence, the design of the digital control. Therefore, the control designer should evaluate the failure rates and failure modes of each sensor and apply sophisticated concepts only where warranted to insure the result is the simplest and most cost-effective control system which provides desired operational benefits and mission reliability.

Section 7.0

RECOMMENDATIONS

1. Refine the simplified simulation within the advanced DIA concept to improve the performance of the concept. Refinement to the simplified simulation should include: 1) improving the steady state accuracy by increasing the number of linear models used to constrain the curve fitting procedure for the matrix elements over the desired flight envelope, and 2) improving the dynamic portion of the simplified simulation to be comparable with the nonlinear simulation.

2. Develop refinements to the advanced DIA algorithm to: 1) insure that the logic is compatable with the revised simplified engine simulation, and 2) minimize the steady state estimator hangoff errors.

3. Develop algorithm simplifications to the DIA algorithm to reduce the complexity of a microprocessor based real-time control implementation of the DIA algorithm.

4. Implement the revised algorithm on a microprocessor for detailed evaluation utilizing a real-time engine model and eventual engine test.

APPENDIX A

FAILURE MODE AND EFFECTS ANALYSIS

The following paragraph summarizes the predominant causes of in-range sensor failures.

Speed Sensor Failure

In-range failures of the N1 system may be caused by the following:

- Failure of the Divide by 2 circuit causing a degredation in high speed range.
- Open circuit on an N1 connector pin resulting in loss of up to 1/2 word
- Failure in mux switch resulting in using high speed counter in low speed range.

N1 Accuracy	=	+3 rpm
N1 Operating Limits	=	4500 - 10200 rpm
N1 Range Limits	=	1300 - 13000 rpm

In-range failures of the N2 system may be caused by the following:

- Failure of the lamination stack or winding
- Failure in the Divide by a circuitry resulting in a division by 4 or 2
- N2 Period Counter and Control failures causes loss of 1/2 word, or random bit pattern, or counts for the wrong number of periods.

N2 Accuracy	=	+3 rpm
N2 Operating Limits	=	9000 to 13000 rpm
N2 Range Limits	=	1300 to 15000 rpm

Temperature Sensor System Failures

In-range failures of the TT2, TT2.5, and FTIT systems may be caused by the following:

- Open circuit in one or more of the probes, junctions of a probe or temperature measurement circuits of the control.
- Short circuit or ground in the TT2 or TT2.5 or FTIT probe or temperature measurement circuits of the control

- Failure of a particular gain amplifier

TT2 Accuracy	= ±7°F
TT2 Operating Limits	= -50 to +200°F
TT2 Range Limits	= -110 to +440°F
TT2.5 Accuracy	= ±7°F
TT2.5 Operating Limits	= -50 to +695°F
TT2.5 Range Limits	= -110 to 840°F
FTIT Accuracy	= ±12°F
FTIT Operating Limits	= $FTIT_{base}$ to $FTIT_{base}$ +1030°F
FTIT Range Limits	= -65°F to $FTIT_{base}$ +1999°F

Pressure Sensor Failures

In-range failures of the pressure sense systems PT2, PT4, and PT6 may be attributed to the following types of failures:

- Failure of the probe or pressure tubing
- In-range frequency shifts of the vibrating cylinder
- Loss of 1/2 word or random bit pattern from the Period Counter/Control
- Power strobe of only one PROM causing no effect on the signal which is properly strobed. The other signals are wrong, and possible in range.
- Power strobe two PROM's with results similar to above except that the unstrobed signal is wrong, possibly in range.

PT2 Accuracy	= ±.03 psi
PT2 Operating Limits	= 3 to 30 psia
PT4 Accuracy	= ±.4 psi
PT4 Operating Limits	= 40 to 500 psia
PT4 Range Limits	= 1 to 599 psia
PT6 Accuracy	= ±.07 psi
PT6 Operating Limits	= 6 to 60 psia
PT6 Range Limits	= 1 to 109.8 psia

Tabulation of the results of failing each sensor to their upper and lower out-of-range limits are shown on the following tables and are summarized on pages 150 and 151.

FMECA

FAILURE TYPE OUT-OF-RANGE FLIGHT CONDITION 0/0 20° PLA

SENSOR

		SM FAN	SM COMP	ΔFTIT*	PB	N1	N2
TT25C	Hi	.1055	.6073	-59	78.7	4124	11084
	Lo	.079	-.59	+325	68.3	3901	8305
N1	Hi	.13248	.00304	+101	48.6	2782	8536
	Lo	.19613	.16556	+152	135	6808	10310
N2	Hi						
	Lo	.113	.599	-83	67	3632	10548
FTIT	Hi	.101	.187	+6	70.1	3870	9191
	Lo	.192	.149	+9	70.7	3893	9204
PB	Hi	.248	.168	+556	252	9116	11871
	Lo	.054	-.193	+179	44.1	2840	7493
TT2	Hi	.245	.1722	+367	199	8645	11186
	Lo	.098	.1504	+21	61.2	3503	8976
PT2	Hi	.1148	.193	+112	118	6115	10086
	Lo	.0611	.151	+71	91.7	5755	9583
PT6	Hi	.0816	-.10836	+199	49.1	2977	8314
	Lo	.0908	.196	+9	70.7	3875	9202
Nominal		.102	.203	0	70.6	3894	9203

Simulation fails at 2 sec.; however, a Comp. Surge Observed

*From Nominal

FAILURE TYPE OUT-OF-RANGE FLIGHT CONDITION 0/0 83° PLA

SENSOR

		SM FAN	SM COMP	ΔFTIT*	PB	N1	N2
TT25C	Hi	.169	.293	+13	353	10102	14517
	Lo	.199	.168	+10	367	10307	13120
N1	Hi	.09606	.194	-129	303	9164	12423
	Lo	.2397	.155	+97	333	11221	13070
N2	Hi	.219	.166	+4	358	10260	13025
	Lo	.187	.370	+37	300	9481	16013
FTIT	Hi	.228	.232	-253	306	9583	12630
	Lo	.199	.174	+7	367	10304	13134
PB	Hi	.17548	.23428	-269	230	8699	11775
	Lo	.078	-.0815	-785	45.2	2942	7982
TT2	Hi	.298	.166	-390	227	9338	11521
	Lo	.06	.238	-275	242	8529	11973
PT2	Hi	.2085	.205	+313	386	10843	13507
	Lo	.3398	.1799	-536	185	8121	11066
PT6	Hi	.26174	.18155	-32	338	10317	12980
	Lo	.168	.162	+13	371	10222	13070
Nominal		.205	.174	0	365	10302	13131

*From Nominal

FMECA

FAILURE TYPE OUT-OF-RANGE FLIGHT CONDITION 0/1.2 83° PLA

SENSOR

		SM FAN	SM COMP	ΔFTIT*	PB	N1	N2
TT25C	Hi	.291	.30	+27	561	10492	14315
	Lo	.274	.005	+54	517	10219	12343
N1	Hi	.159	.23	+53	492	9416	12920
	Lo	.277	.027	+55	520	10266	12409
N2	Hi	.277	-.0045	+51	521	10261	12342
	Lo	.267	.434	+54	518	10149	15812
FTIT	Hi	.253	.233	-121	487	9908	12647
	Lo	.293	.167	+51	565	10502	13122
PB	Hi	.276	.159	-46	509	10118	12794
	Lo	.18	.237	-771	159	5696	10447
TT2	Hi	.255	.132	-181	417	9288	12161
	Lo	.117	.231	+71	473	8865	12922
PT2	Hi	.292	.168	+16	558	10492	13087
	Lo	.212	.211	-612	228	6959	11027
PT6	Hi	.292	.168	+39	556	10468	13080
	Lo	.279	.173	+46	574	10335	13261
Nominal		.295	.182	0	562	10507	13115

*From Nominal

FMECA

FAILURE TYPE OUT-OF-RANGE FLIGHT CONDITION 10K/0.9 83° PLA

SENSOR

		SM FAN	SM COMP	ΔFTIT *	PB	N1	N2
TT25C	Hi	.218	.308	-5	358	10033	14331
	Lo	.216	.143	-1	374	10302	13073
N1	Hi	.1204	.2322	+34	330	9512	12935
	Lo	.263	.143	+67	357	10930	13223
N2	Hi	.2066	.144	-5	377	10256	13069
	Lo	.1988	.38	+79	311	9555	15937
FTIT	Hi	.237	.194	-235	308	9554	12517
	Lo	.217	.175	+2	377	10348	13176
PB	Hi	.188	.189	-417	260	8861	12037
	Lo	.178	.214	-953	71.8	4631	9448
TT2	Hi	.254	.174	-469	232	9055	11635
	Lo	.102	.226	+14	317	9336	12712
PT2	Hi	.195	.207	+317	407	10608	13564
	Lo	.258	.18	-536	185	7954	11112
PT6	Hi	.257	.223	+14	330	10328	12964
	Lo	.1922	.148	+3	383	10239	13108
Nominal		.205	.177	0	382	10327	13196

*From Nominal

FMECA

FAILURE TYPE OUT-OF-RANGE FLIGHT CONDITION 20K/0.3 24° PLA

SENSOR

		SM FAN	SM COMP	FTIT	PB	N1	N2
TT25C	Hi	.097	.519	+15	53.	5247	10986
	Lo	.113	-.325	+57	54.3	5660	8847
N1	Hi	.119	.166	-77	30.2	3409	8442
	Lo	.223	.149	+318	101	7998	10612
N2	Hi	.1011	-1.38	+70	27	3057	5382
	Lo	.098	.57	-29	47	5084	10762
FTIT	Hi	.105	.195	-152	36.3	4272	8743
	Lo	.12	.175	+7	54.7	5646	9368
PB	Hi	.234	.147	+970	199	11033	12986
	Lo	.107	.176	-12	50.4	5373	9223
TT2	Hi	.298	.126	+925	123	9299	11132
	Lo	.09	.178	-36	45	4832	9018
PT2	Hi	.212	.167	+325	99	7803	10600
	Lo	.282	.1448	+396	122.2	8766	11057
PT6	Hi	.1026	.187	-28	48	5154	9153
	Lo	.117	.189	+16	54.7	5641	9372
Nominal		.13036	.188	0	53.8	5645	9346

*From Nominal

FMECA

FAILURE TYPE OUT-OF-RANGE FLIGHT CONDITION 20K/0.3 83° PLA

SENSOR

		SM FAN	SM COMP	ΔFTIT*	PB	N1	N2	
TT25C	Hi	.157	.285	+93	182	9644	14348	
	Lo	.158	.149	+13	187	9750	12408	
N1	Hi	.097	.173	-447	103	7420	10770	
	Lo	.233	.133		174	11791	12885	
N2	Hi	.216	.199	+42	178	10191	12559	
	Lo	.183	.37175	+177	174	9602	16946	
FTIT	Hi	.188	.184	-473	105.6	7865	10806	
	Lo	.157	.155	+1	187	9746	12420	
PB	Hi	.0988	.191	-781	50.66	5329	9242	
	Lo	.233	.190	+239	184	10332	12681	
TT2	Hi	.288	.086	-201	140	9568	11437	
	Lo	.116	.125	-316	156	8586	11597	
PT2	Hi							Fan Surge, failed simulated
	Lo	.284	.16	-325	122	8760	11079	
PT6	Hi	.247	.158	-37	167	9735	12210	
	Lo	.157	.161	+14	186.4	9736	12416	
Nominal		.183	.157	0	182	9745	12394	

*From Nominal

FMECA

FAILURE TYPE OUT-OF-RANGE FLIGHT CONDITION 24K/1.8 83° PLA

SENSOR

		SM FAN	SM COMP	ΔFTIT*	PB	N1	N2
TT25C	Hi	.26	.303	+16	430	10291	14325
	Lo	.24	-.03	+16	389	9896	12387
N1	Hi	.167	.143	-163	337	8644	12412
	Lo	.239	.017	+35	400	10009	12515
N2	Hi	.239	-.033	+16	401	10014	12434
	Lo	.24	.46	+37	395	9903	15724
FTIT	Hi	.255	.138	-130	366	9644	12602
	Lo	.277	.15	+51	444	10474	13177
PB	Hi	.257	.146	+15	425	10270	13039
	Lo	.178	.205	-721	139	5914	10765
TT2	Hi	.25	.144	-59	384	9822	12739
	Lo	.177	.138	-234	298	7713	11701
PT2	Hi	.231	.151	+39	428	10033	13127
	Lo	.224	.151	-521	206	7344	11342
PT6	Hi	.263	.158	+15	430	10321	13112
	Lo	.227	.148	+22	424	9920	13102
Nominal		.288	.181	0	443	10463	13207

*From Nominal

FMECA

FAILURE TYPE OUT-OF-RANGE FLIGHT CONDITION 34K/1.9 83° PLA

SENSOR

		SM FAN	SM COMP	ΔFTIT*	PB	N1	N2
TT25C	Hi	.269	.302	+32	326	10205	14174
	Lo	.247	-.0065	+79	314	10084	12355
N1	Hi	.164	.181	-217	199	8012	11723
	Lo	.253	.026	+70	314	10113	12425
N2	Hi	.238	-.015	+66	313	10025	12330
	Lo	.226	.449	+70	295	9584	15402
FTIT	Hi	.266	.129	-293	221	8507	11906
	Lo	.272	.154	+48	327	10225	12950
PB	Hi	.254	.133	-135	257	9027	12245
	Lo	.181	.232	-735	100	5749	10553
TT2	Hi	.247	.152	-8	303	9934	12713
	Lo	.189	.161	-324	180	7314	11507
PT2	Hi	.253	.16	+116	345	10177	13179
	Lo	.262	.135	-388	186	8022	11511
PT6	Hi	.272	.158	+18	322	10207	12912
	Lo	.241	.158	+65	339	10092	13121
Nominal		.274	.179	0	327	10222	12978

*From Nominal

FMECA

FAILURE TYPE OUT-OF-RANGE FLIGHT CONDITION 45K/0.9 40° PLA

SENSOR

		SM FAN	SM COMP	ΔFTIT*	PB	N1	N2	
TT25C	Hi	.216	.485	-117	34	6649	11558	
	Lo	.214	-.048	+31	47	7786	10018	
N1	Hi	.059	.172	-302	29.4	6059	9463	
	Lo	.232	.101	+641	84.5	11453	12579	
N2	Hi	.129	-.424	-196	23.1	5621	8600	
	Lo	.224	.458	-50	37.6	6934	11919	
FTIT	Hi	.225	.146	-308	29.5	6305	9492	
	Lo	.224	.128	+10	48.6	7855	10506	
PB	Hi							Compressor Surged, Failed simulation
	Lo	.226	.126	-110	41.2	7185	10142	
TT2	Hi	.277	.179	+435	67.7	10360	12032	
	Lo	.214	.128	-96	42	7172	10194	
PT2	Hi							Fan Surge, Failed simulation
	Lo	.221	.121	+395	79.2	9491	11947	
PT6	Hi	.227	.129	-11	49.2	7985	10519	
	Lo							Simulation Failed
Nominal		.214	.137	0	49.7	7851	10568	

*From Nominal

FMECA

FAILURE TYPE OUT-OF-RANGE FLIGHT CONDITION 50K/0.9 83° PLA

SENSOR

		SM FAN	SM COMP	ΔFTIT*	PB	N1	N2	
TT25C	Hi	.193	.202	+145	74.5	9883	14012	
	Lo	.133	.099	+17	73.1	9738	12318	
N1	Hi	.1099	.1295	+593	36.3	7120	10466	
	Lo	.226	.099	+224	67.1	11819	12825	
N2	Hi	.207	.075	+161	68.5	9760	12095	
	Lo	.176	.313	+164	62.9	9529	15752	
FTIT	Hi	.295	.145	-968	28	6901	9899	
	Lo	.133	.113	+3	73	9723	12336	
PB	Hi							Compressor Surge, Failed Simulation
	Lo	.209	.124	-524	38.1	7751	10522	
TT2	Hi	.2603	.145	-707	27.8	7127	9862	
	Lo	.211	.116	-583	33.6	7207	10238	
PT2	Hi							Compressor Surge, Failed Simulation
	Lo	.222	.106	-28	65.2	9714	12146	
PT6	Hi	.226	.105	-27	65.5	9738	12161	
	Lo	.133	.114	+8	72.7	9712	12326	
Nominal		.154	.115	0	71.3	9723	12315	

*From Nominal

FMECA

FAILURE TYPE OUT-OF-RANGE FLIGHT CONDITION 54K/2.2 130° PLA

SENSOR

		SM FAN	SM COMP	ΔFTIT*	PB	N1	N2
TT25C	Hi	.262	.302	+35	147	9581	14107
	Lo	.259	-.111	+46	142.4	9379	12428
N1	Hi	.137	.109	-553	53.7	5512	10884
	Lo	.252	.093	+104	158	10039	12959
N2	Hi	.256	-.175	+67	142.6	9463	12350
	Lo	.25	.495	+82	140.9	9430	15543
FTIT	Hi	.182	.107	-634	56.4	5948	10978
	Lo	.252	.094	+89	153.7	9743	12924
PB	Hi	.266	.184	+379	184	10805	13702
	Lo	.193	.055	+588	45.86	5270	10654
TT2	Hi	.262	.074	-48	135	9307	12557
	Lo	.164	.122	-410	55.2	5482	10952
PT2	Hi	.235	.191	+917	273	12214	15286
	Lo	.261	.048	-127	117	8802	12210
PT6	Hi	.259	.105	+38	150	9747	12901
	Lo	.248	.091	+43	144	9303	12767
Nominal		.261	.112	0	154	9746	12992

*From Nominal

FMECA

FAILURE TYPE OUT-OF-RANGE FLIGHT CONDITION 65K/1.2 83° PLA

SENSOR

		SM FAN	SM COMP	ΔFTIT*	PB	N1	N2	
TT25C	Hi	.201	.22	-90	36.2	9227	13414	
	Lo	.147	.041	0	43.8	9810	12398	
N1	Hi	.072	.098	-209	36.7	8866	11867	
	Lo	.239	.057	0	39.4	10198	12383	
N2	Hi	.227	-.101	-540	19.5	7467	10061	
	Lo	.207	.326	-2	35.6	9261	14668	
FTIT	Hi	.23	.116	-684	22.7	7770	10819	
	Lo	.141	.088	+34	44.9	9907	12569	
PB	Hi							Possible Prim. Burner Blowout. Fan and Compressor Surge
	Lo	.208	.089	-320	31.5	8896	11507	
TT2	Hi	.247	.12	-607	23.2	8195	10851	
	Lo	.083	.101	-159	38.6	9068	12014	
PT2	Hi							Compressor Surge, Failed Simulation
	Lo	.22	.1066	-507	25.5	8262	11048	
PT6	Hi	.228	.073	-140	37.4	9626	11985	
	Lo	.141	.083	-4	49.5	9824	12500	
Nominal		.139	.0844	0	44.8	9847	12524	

*From Nominal

FMECA

FAILURE TYPE OUT-OF-RANGE FLIGHT CONDITION 65K/2.5 83° PLA

SENSOR

		SM FAN	SM COMP	ΔFTIT*	PB	N1	N2
TT25C	Hi	.268	.239	-2	101	9204	13335
	Lo	.253	-.307	+53	94.7	9047	12354
N1	Hi	.159	-.003	-357	38.3	5215	10933
	Lo	.25	.015	+11	92.4	8867	12660
N2	Hi	.18	-.51	+7	76.7	8162	11858
	Lo	.255	.551	+74	99.2	9108	15665
FTIT	Hi	.196	-.00008	-410	39.5	5634	11042
	Lo	.262	.051	+154	107.6	9470	13087
PB	Hi	.2611	.176	+710	165	11515	14571
	Lo	.189	-.023	-293	41.6	5688	11103
TT2	Hi	.254	.013	+40	97.3	9036	12775
	Lo	.12	.026	+55	67.4	7051	12041
PT2	Hi	.24	.159	+628	145	10661	14153
	Lo	.247	.012	-15	89.8	8742	12586
PT6	Hi	.255	.015	+44	97.7	9058	12790
	Lo	.21	.0035	+8	87	8314	12516
Nominal		.274	.147	0	106	9421	13057

*From Nominal

SENSOR FAILURE DETECTION PROGRAM FMECA

STEADY STATE OUT-OF-RANGE FAILURES (LOW)

FLIGHT OPERATING CONDITION	TT25 FAILURE	N1 FAILURE	N2 FAILURE	FTIT FAILURE	P4 FAILURE	T2 FAILURE	P2 FAILURE	P6 FAILURE
0/0 PLA = 20°	Compressor Surge	Accels to a Higher Power	Excessive Thrust Loss	No Appreciable Effect	Compressor Surge	Slight Loss of Power	Accels to a High power	No Appreciable Effect
0/0 PLA = 83°	No Appreciable Effect	49°F Increase in FTIT	N2 Overspeed 2000 RPM Over Critical Limit	No appreciable effect	Compressor Surge	Excessive Thrust loss	Excessive Thrust Loss	No Appreciable Effect
0/0 PLA = 130°	See 0/0 83° PLA							
0/1.2 PLA = 83°	Possible Compressor Surge	Possible Compressor Surge; 54°F Increase in FTIT	N2 Overspeed 2100 RPM Over Critical Limit	+51°F Increase in FTIT	Excessive Thrust Loss	71°F Increase in FTIT; Excessive Thrust Loss	Excessive Thrust Loss	46°F Increase in FTIT
10K/0.9 PLA=83°	No Appreciable Effect	67°F Increase in FTIT	N2 Overspeed; 2217 RPM Over critical;88°F Increase in FTIT	No appreciable effect	Excessive Thrust Loss	10% Loss Fan S.M.; Excessive Thrust Loss	Excessive Thrust Loss	No Appreciable Effect
20K/0.3 PLA=24°	Compressor Surge	Accels to a High Power	1400 RPM Increase in N2 Excessive Thrust Loss	No appreciable Effect	Slight Thrust Loss	4% Loss Fan S.M Excessive Thrust Loss	Accels to a High Power	Slight Increase in Thrust
20K/0.3 PLA=83°	No Appreciable Effect	N1 Overspeed by 2046 RPM Over Nominal	3226 RPM N2 Overspeed Over Critical Design Limit	No appreciable Effect	600 RPM increase in N1 Slight Thrust Loss	Excessive Thrust Loss	Excessive Thrust Loss	Slight Thrust Loss
24K/1.8 PLA=83°	Compressor Surge	Possible Compressor Surge	2000 RPM N2 Overspeed	+51°F Incr. in FTIT	Excessive Thrust Loss	Excessive Thrust Loss	Excessive Thrust Loss	Slight Thrust Loss
34K/1.9 PLA=83°	Compressor Surge	Possible Compressor Surge	1622 RPM N2 Overspeed	+48°F Incr. in FTIT	Excessive Thrust Loss	Excessive Thrust Loss	Excessive Thrust Loss	65°F Increase in FTIT
45K/0.9 PLA=40°	Compressor Surge	Accels to a High Power	Excessive Thrust Loss 1400 RPM Incr in N2	No appreciable effect	Excessive Thrust Loss	Excessive Thrust Loss	Accels to a High Power	Simulation Fails
50K/0.9 PLA=83°	No Appreciable Effect	223°F Increase in FTIT	2000 RPM N2 Overspeed 164°F incr. in FTIT	No appreciable effect	Excessive Thrust Loss	Excessive Thrust Loss	Slight Thrust Loss	No Appreciable Effect
54K/2.2 PLA=130°	Compressor Surge	100°F Increase In FTIT	1100 RPM N2 Overspeed	+89°F Incr. in FTIT	Excessive Thrust Loss	Excessive Thrust Loss	Excessive Thrust Loss	Slight Thrust Loss
65K/1.2 PLA=83°	4% Loss in Compressor Surge Margin	3% Loss in Compressor S.M. Slight Thrust Loss	946 RPM N2 Over Critical Limit	+34°F Incr. in FTIT	Excessive Thrust Loss	Excessive Thrust Loss	Excessive Thrust Loss	No Appreciable Effect
65K/2.5 PLA=83°	Compressor Surge	Slight Thrust Loss	1943 RPM N2 Over Critical Limit	+154°F Increase in FTIT	Compressor Surge	Possible Comp. Surge;Excessive Thrust Loss	Excessive Thrust Loss	Possible Compressor Surge
65K/2.5 PLA=130°	See 65K/2.5 83° PLA							

SENSOR FAILURE DETECTION PROGRAM FMECA

STEADY STATE OUT-OF-RANGE FAILURES (HIGH)

FLIGHT OPERATING CONDITION	TT25 FAILURE	N1 FAILURE	N2 FAILURE	FTIT FAILURE	P4 FAILURE	T2 FAILURE	P2 FAILURE	P6 FAILURE
0/0 PLA=20°	1900 RPM Increase in N2	Possible compressor surge; 50°F increase in FTIT	Compressor Surge	Excessive Thrust Loss	Accel to a High Power	Accel to a High Power	Accel to a High Power	Compressor Surge
0/0 PLA=83°	1400 RPM Increase in N2	10% Loss Fan Surge Margin; Loss of Power	No Appreciable Effect	Excessive Thrust Loss	Excessive Thrust Loss	Excessive Thrust Loss	300°F FTIT Overtemp	Slight Loss in Thrust
0/0 PLA=130°	See 0/0 83° PLA							
0/1.2 PLA=83°	1200 RPM Increase in N2	14% Loss in Fan S.M.; 53°F increase in FTIT, loss of thrust	Compressor Surge	Excessive Thrust Loss	Slight Thrust Loss	Excessive Thrust Loss	16% Increase in FTIT	39% Increase in FTIT
10K/0.9 PLA=83°	1100 RPM increase in N2	8% Loss of Fan S.M.; 34°F Increase in FTIT, Excessive Thrust Loss	3% loss in Compressor Surge Margin	Excessive Thrust Loss	Excessive Thrust Loss	Excessive Thrust Loss	317°F Increase FTIT 364 RPM N2 Increase	14°F Increase in FTIT Slight Thrust Loss
20K/0.3 PLA=24°	1600 RPM increase in N2	Excessive Thrust Loss	Compressor Surge	Excessive Thrust Loss	Accels to Above Mil Power	Accels to a High Power	Accels to a High Power	Slight Thrust Loss
20K/0.3 PLA=83°	2000 RPM In crease in N2	8% Loss of Fan S.M. Excessive Thrust Loss	42°F Increase in FTIT 166 RPM Increase in N2	Excessive Thrust Loss	8% Loss Fan S.M. Decel to Power Slitly above Idle	Excessive Thrust Loss	Fan Surge	Slight Thrust Loss
24K/1.8 PLA=83°	1100 RPM Increase in N2	Excessive Thrust Loss	Compressor Surge	Excessive Thrust Loss	Slight Thrust Loss	Excessive Thrust Loss	29°F Increase FTIT Slight Thrust Loss	15°F Increase in FTIT Slight Thrust Loss
34K/1.9 PLA=83°	1200 RPM Increase in N2	11% Loss of Fan S.M. Excessive Thrust Loss	Compressor Surge	Excessive Thrust Loss	Excessive Thrust Loss	Slight Thrust Loss	116°F Increase FTIT 200 RPM Increase in N2	No Appreciable Effect
45K/0.9 PLA=40°	1000 RPM Increase in N2 Excessive thrust Loss	15% Loss Fan S.M. Excessive Thrust Loss	Compressor Surge	Excessive Thrust Loss	Compressor Surge	Accel to a High Power	Fan Surge	Slight Thrust Loss
50K/0.9 PLA=83°	1700 RPM Increase in N2	Excessive Thrust Loss	161°F Increase FTIT 4% Loss in Compressor Surge Margin	Excessive Thrust Loss	Compressor Surge	Excessive Thrust Loss	Fan Surge	Slight Thrust Loss
54K/2.2 PLA=130°	1100 RPM Increase in N2	Excessive Thrust Loss	Compressor Surge	Excessive Thrust Loss	380°F Increase in FTIT	Excessive Thrust Loss	FTIT Overtemp N2 Overspeed	Slight Thrust Loss
65K/1.2 PLA=83°	900 RPM Increase in N2	Excessive Thrust Loss	Compressor Surge	Excessive Thrust Loss	Burner Blowout Compressor and Fan Surge	Excessive Thrust Loss	Compressor Surge	Slight Thrust Loss
65K/2.5 PLA=83°	No Appreciable Effect	Compressor Surge Excessive Thrust Loss	Compressor Surge	Excessive Thrust Loss	849 RPM N2 Over Critical Limit	Slight Thrust Loss	430 RPM Over Critical Limit	44°F FTIT Increase Slight Thrust Loss
65K/2.5 PLA=130°	See 65K/2.5 83° PLA							

APPENDIX B

DIA SCORING SYSTEM

Mathematical equations which were derived to quantitatively score each candidate DIA algorithm for both detection and accommodation criteria are described in the following appendix.

ENGINE PROTECTION

Critical Design Limit Y_{CR}

Control Limit Y_{CL}

Threshold Y_{TH}

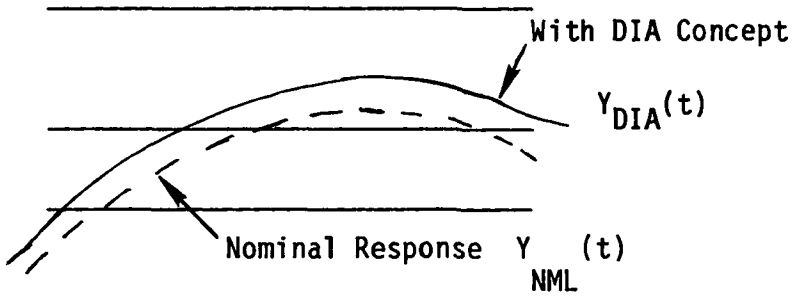

General Ground Rule: Decrease score for how much a limited parameter exceeds a limit due to sensor failures interacting with the control mode during transients and steady state operation.

General Scoring Formula:

$$\text{If } Y_{DIA}(t) > Y_{TH};$$

$$SCY(t) = [AMAX1(0.0, SGN * [Y_{DIA}(t) - Y_{NML}(t)])] * WTFC$$

Where: WTFC = Weighting Factor =

$$SGN * \left[\frac{WT2}{Y_{CR} - Y_{NML}(t)}\right] * [[AMAX1(0.0, SGN * [Y_{DIA}(t) - Y_{CL}])] *$$

$$SGN * \left[\frac{WT2}{Y_{CR} - Y_{CL}}\right] + 1.0]$$

SCY(t) = Time Varying Scoring

SGN = Sign (either +1 or -1)

$Y_{DIA}(t)$= Parameter Response With Dia Concept

$Y_{NML}(t)$= Nominal Parameter Response

WT1 = Weighting Constant

WT2 = Weighting Constant

Y_{CR} = Critical Operating Limit

Y_{CL} = Control Limit

Y_{TH} = Threshold, Above Which, Scoring Formula Is Executed

This equation will penalize a DIA concept if the engine protection parameter exceeds its respective nominal characteristics for operation above a threshold value. The scoring weighting factor (WTFC) is a function of the proximity of the nominal characteristics [$Y_{NML}(t)$] relative to the critical design limit (Y_{CR}).

This weighting factor is increased if the DIA concept exceeds the control limits. The weighting constants (WT1 and WT2) require different constant for steady state than transient operation. Since it is more critical to exceed the control limits in steady state than transiently, WT2 is weighed more heavily than WT1 in steady state. For transient operation, excursions above nominal operation is of more concern; therefore, WT1 is weighed more heavily.

Total Score (for each parameter)

$$TSCORE = \left(\sum_{0}^{N} SCY(t)\right) /N$$

Where N = Number of points run.

N is only increased by 1 for "quasi" steady state operation. It is therefore necessary to be aware if the system is in steady state for both the total score, and to determine the correct weighting factors. This may be done by either programming, as a function of time, a schedule indicating when steady state operation is expected (from the power lever profile), or, using simple logic, as shown on Figure 1. This figure shows simple logic which could be implemented; however, programming a steady state flag may be more desirable, since this type of logic could give erroneous results if the DIA concept was unresponsive to an input; i.e., transient should be occuring, yet the DIA algorithm results in steady state operation.

Constants (for engine protection parameters)

Note: Weighting factors designed to give a score of 5 at Y_{cr}

Temperature limits (FTIT)

	Steady State	Transiently
WT1	1.125	4.5
WT2	3.5	0.125

$Y_{CR} = Y_{TH} + 129°C$, $Y_{CL} = Y_{TH} + 25°C$, $Y_{TH} = FTIT_{base} + 563°C$

SGN = +1

Speed Limits

N2

	Steady State	Transiently
WT1	1.125	4.5
WT2	3.5	0.125

$Y_{CR} = 13720$, $Y_{CL} = f(T2)$, $Y_{TH} = Y_{CL} - 100$ RPM

SPN = +1

N1

	Steady State	Transiently
WT1	1.125	4.5
WT2	3.5	0.125

SGN = +1
$Y_{CR} = 12000$, $Y_{CL} = 11500$, $Y_{TH} = 11000$

Pressure Limits (Pb)

	Steady State	Transiently
WT1	1.125	4.5
WT2	3.5	0.125

Y_{CR} = TBD, $Y_{CL} = 580$, $Y_{TH} = 550$

SGN = +1

Engine Stability

Fan and Compressor Stall Margins

The ground rule for fan and compressor stability is to not allow fan stall margin to go below 0.15 or compressor stall margin to go below 0.05. Stall margin is defined by:

$$SM = \left[\frac{(\text{Pressure Ratio Stall} - \text{Pressure Ratio Operating})}{\text{Pressure Ratio Stall}}\right]$$ At constant airflow

The same equation set is used as was used for engine protection. Note: The value of "SGN" is -1.0 to reflect that a higher surge margin is more desirable.

Note: Weighting factor designed to give a score of 7.5 at SM = 0.

Fan

	Steady State	Transiently
WT1	1.25	1.25
WT2	5	5

$Y_{CR} = 0$, $Y_{CL} = 15$, $Y_{TH} = 18$

SGN = -1

Compressor

	Steady State	Transiently
WT1	1.25	1.25
WT2	5	5

$Y_{CR} = 0$, $Y_{CL} = 5$, $Y_{TH} = 8$

SGN = -1.0

Steady State Performance and Accuracy

Variation from nominal thrust will be scored for steady state operation at fixed PLA.

$$SCY(t) = \left|\frac{F_{NNML} - F_{NDIA}}{F_{NNML}}\right| * MLSS$$

10% variation in thrust from nominal will score 15 pts.

	Steady State	Transiently
MLSS =	150	0

Transient Requirements

- o Based on time to 90% thrust change (assumes only perform tests for parts of the PLA profile where 90% thrust change occurs)
- o 10% overshoot over references (N1, EPR) considered critical (only performed during parts of the PLA transient where referenced value is exceeded)

$$SCY(t) \quad [AMAX1\ (0.0,\ [TR_{DIA} - TR_{NML}])] * MLTR$$

$$+ [AMAX1\ (0.0,\ [OS_{DIAN} - OS_{NMLN}]) / (0.1 * N1REF)]$$

$$* MLNOS + [AMAX1\ (0.0,\ [OS_{DIAE} - OS_{NMLE}]) / (0.1 * EPRREF)]$$

$$* MLEOS$$

Where:

TR_{DIA} = Time to 90% Thrust Change for DIA Concept

TR_{NML} = Time to 90% Thrust Change for Nominal Response

OS_{DIAN} = N1 Overshoot, DIA Concept

OS_{DIAE} = EPR Overshoot, DIA Concept

OS_{NMLN} = Nominal N1 Overshoot

OS_{NMLE} = Nominal EPR Overshoot

		Steady State	Transiently
MLTR	=	0	5
MLNOS	=	0	5
MLEOS	=	0	5

For total score for steady state accuracy and transient response, use same TSCORE equation used in engine protection and engine stability.

DIA Detection Performance (50 PTS)

Hit/Miss Ratio

50% will score 20 PTS

$$DSCORE = \frac{NIF - NOH}{NIF} * 40$$

Where:

NIF = Number of induced failures
NOH = Number of Hits

Time to Detect (15 PTS Score)

Rational: The advanced electronic control design for the F100 engine takes 108 ms to detect a failure; therefore, the concept is penalized for times greater than this. A 300 ms detect time results in the worst score.

The concept is penalized for excessive thrust change between when the falure was induced to when the failure was detected for steady state operation. A 10% thrust variation results in worst score.

Scoring Equation:

$$DSCORE = [AMAX1 [0., (TFD - TFI - 108)]) / 192] * WTTD + \frac{FNTI - FNTD}{FNTI} * WTF$$

Where:

TFD = Time Failure Detected
TFI = Time Failure Induced
FMTI = Thrust When Failure Induced
FNTD = Thrust When Falure Detected

	Steady State	Transiently
WITD	5	15
WTF	100	0

Number of False Alarms

Ground Rule:
for every 10 hits, one false alarm is tolerable, three false alarms scores 15 PTS

Scoring: $\frac{NOFA}{NOH} * 50 = DSCORE$

Where:
NOFA = Number of False Alarms
NOH = Number of Hits

APPENDIX C

LINEAR MODEL DEVELOPMENT

A representative model should describe engine behavior over the entire flight envelope. The flight envelope was parametrically investigated (Reference 1) to identify portions where limiting boundaries were approached. The envelope was then partitioned into linearization regions, wherein each region shares boundaries with other regions and the envelope boundary. These linearization regions encompassed a region where operating characteristics were critical to some limiting variable. Model generation points were chosen to span the envelope and center on the linearization regions. A set of linear equations models the important dynamics in a linearization region and about an equilibrium point. For the locally linear models to operate throughout the flight envelope adaptability to ambient parameters is required.

The thermodynamic equations which describe turbine engines are nonlinear, and in general may be written as

$$\dot{x} = f\,[x(t)\ ,\ u(t)\ ,\ \theta(t)] \tag{1}$$

where x(t) represents the dynamic variables, u(t) represents the controls, and (t) represents ambient parameters. Relationships of non-dynamic variables can be represented as nonlinear, static equations as follows:

$$y(t) = h\,[x(t)\ ,\ u(t)\ ,\ \theta(t)] \tag{2}$$

The nonlinear equations (1) and (2) describe state and ouput time histories, x(t), y(t) for given control and ambient inputs, u(t), o(t); where t t_0, and initial state, $x_0 = x(t_0)$. Simultaneously solving equations (1) and (2) typically require high computational capability. In addition, even large-scale digital or hybrid simulations do not produce observed behaviour exactly. A simplified model reduces the computational burden considerably while still representing acceptable engine behaviours. A detailed description of model development is given in reference (1). Utilizing the perturbational quantities to equations (1) and (2) the following linear equations result:

$$\delta\dot{x} = F(t)\ \delta x + G(t)\ \delta u + \theta(\delta^2) \tag{3}$$

$$\delta y = H(t)\ \delta x + D(t)\ \delta u + \theta(\delta^2) \tag{4}$$

where

$$F(t) = \left.\frac{\delta f\,[x(t),\, u_0(t),\, \theta(t)]}{\delta x}\right|_{x\,=\,x_0(t)}$$

$$G(t) = \left.\frac{\delta f\,[x(t),\, u_0(t),\, \theta(t)]}{\delta u}\right|_{u\,=\,u_0(t)} \tag{5}$$

The term δx is an n x 1 vector of states, δu is an m x 1 vector of controls, and δy is a p x 1 output vector. The F, G, H, and D terms in δy representing the compatibly dimensioned state dynamics matrix, control distribution matrix, and output distribution matrices, respectively. Ignoring second order perturbational quantities and assuming that the dynamics matrices are constant within a region of state space, then equations (3) and (4) reduce to linear constant coefficient, differential equations:

$$\delta\dot{x} = F\,\delta x + G\,\delta u \tag{6}$$

$$\delta y = H\,\delta x + D\,\delta u \tag{7}$$

The linear models are valid in the neighborhood of an equilibrium point (x_0, u_0, θ_0) and describe perturbational motion δx, δy away from equilibrium.

APPENDIX D

MODAL DECOMPOSITION

Simplified, low order, linear models are derived from the high order linear models using a modal reduction procedure discussed in reference (1). Highlights of the procedure are discussed below.

The linear equations (6) and (7) (Appendix C) can be transferred to block diagonal form assuming the n x n dynamics matrix, F, has no repeated eigen values:

$$\delta x = Tz \tag{8}$$

which gives

$$\dot{z} = \Lambda z + \Sigma \delta u \tag{9}$$

$$\delta y = HTz + D\delta u \tag{10}$$

where Λ is an $n \times n$ block diagonal matrix, T is an $n \times n$ matrix composed of the column eigenvectors F; z is an n x 1 modal coordinate vector; and Σ is the n x 1 modal control distribution matrix. The system of equations (8) through (10) can be partitioned into a set of q states and of q eigenvalues and n - q states and eigenvalues as follows:

$$\begin{bmatrix} \delta x_1 \\ \cdots \\ \delta x_2 \end{bmatrix} = \begin{bmatrix} T_{11} & \vdots & T_{12} \\ \cdots & & \cdots \\ T_{21} & \vdots & T_{22} \end{bmatrix} \begin{bmatrix} z_1 \\ \cdots \\ z_2 \end{bmatrix} \tag{11}$$

$$\begin{bmatrix} \dot{z}_1 \\ \cdots \\ \dot{z}_2 \end{bmatrix} = \begin{bmatrix} \Lambda_1 & \vdots & 0 \\ \cdots & & \cdots \\ 0 & \vdots & \Lambda_2 \end{bmatrix} \begin{bmatrix} z_1 \\ \cdots \\ z_2 \end{bmatrix} + \begin{bmatrix} \Sigma_1 \\ \cdots \\ \Sigma_2 \end{bmatrix} \delta u \tag{12}$$

where δx_1, and z_1, are q x 1 vectors partitioning the state and modes and δx_2 and z_2 are (n-q) x 1 vectors partitioning the remaining states and modes.

If within the time frame of interest, the following relatonship is true:

$$\dot{z}_2 \approx 0 \tag{13}$$

then the following reduction can be made

$$\delta\dot{x}_1 = F_r\ \delta x_1 + G_r\ \delta u \tag{14}$$

where x_1, is now the q x 1 state vector, F_r is the q x q dynamics matrix, and G_r is the q x m control distribution matrix. Also:

$$\delta y = \left[H_1 \vdots H_2\right] \begin{bmatrix} \delta x_1 \\ \vdots \\ \delta x_2 \end{bmatrix} + D\delta u \tag{15}$$

$$\begin{bmatrix} \delta x_2 \\ \vdots \\ \delta y \end{bmatrix} = \begin{bmatrix} H^* \\ \vdots \\ H_r \end{bmatrix} \delta x_1 + \begin{bmatrix} D^* \\ \vdots \\ D_r \end{bmatrix} \delta u \tag{16}$$

where x_2 is treated as an additional (n-q) x 1 output vector with a (n-q) x q state distribution matrix H* and a (n-q) x m control distribution matrix D*. The original output distribution matrices, H and D, are modified to H_r and D_r respectively. The equations for these matrices in terms of model decomposition are:

$$F_r = T_{11}\ \ \Lambda_1\ \ T_{11}^{-1} \tag{17}$$

$$G_r = T_{11}\ (\Lambda_1\ T_{11}^{-1}\ T_{12}\ \Lambda_2^{-1}\ \Sigma_2 + \Sigma_1) \tag{18}$$

$$H^* = T_{21}\ T_{11}^{-1} \tag{19}$$

$$D^* = (T_{21}\ T_{11}^{-1}\ T_{12} - T_{22})\ \Lambda_2^{-1}\ \Sigma_2 \tag{20}$$

$$H_r = H_1 + H_2\ H^* \tag{21}$$

$$D_r = D + H_2\ D^* \tag{22}$$

Thus by assuming (n-q) modes are equilibrated, the nth order system (6) is reduced to the qth order system (14) with q state and B+n-q outputs.

A block diagram of the model reduction process is shown in Figure D-1

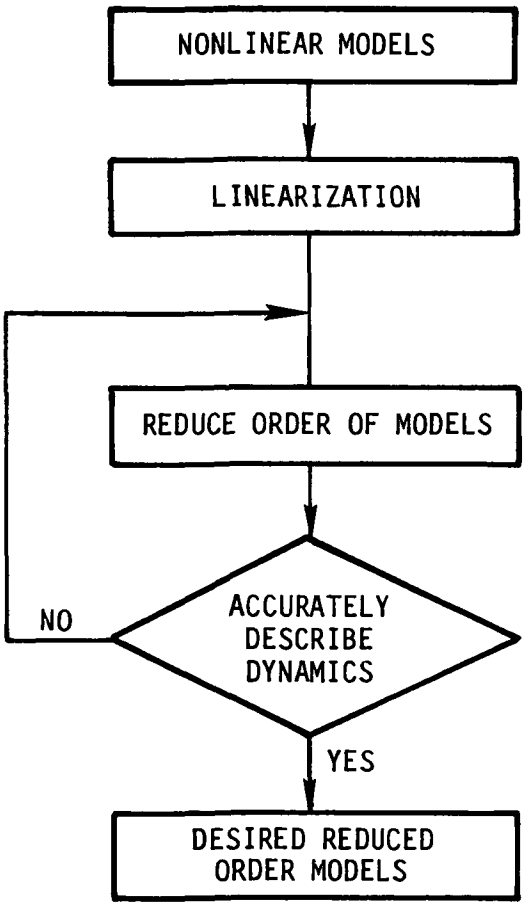

Figure D-1 Generation of Design Models

APPENDIX E

TYPICAL TRANSIENT OPERATION COMPARISONS

The following figures present additional transient failure operation scenarios comparisons between the selected advanced concept and the baseline parameter synthesis concept.

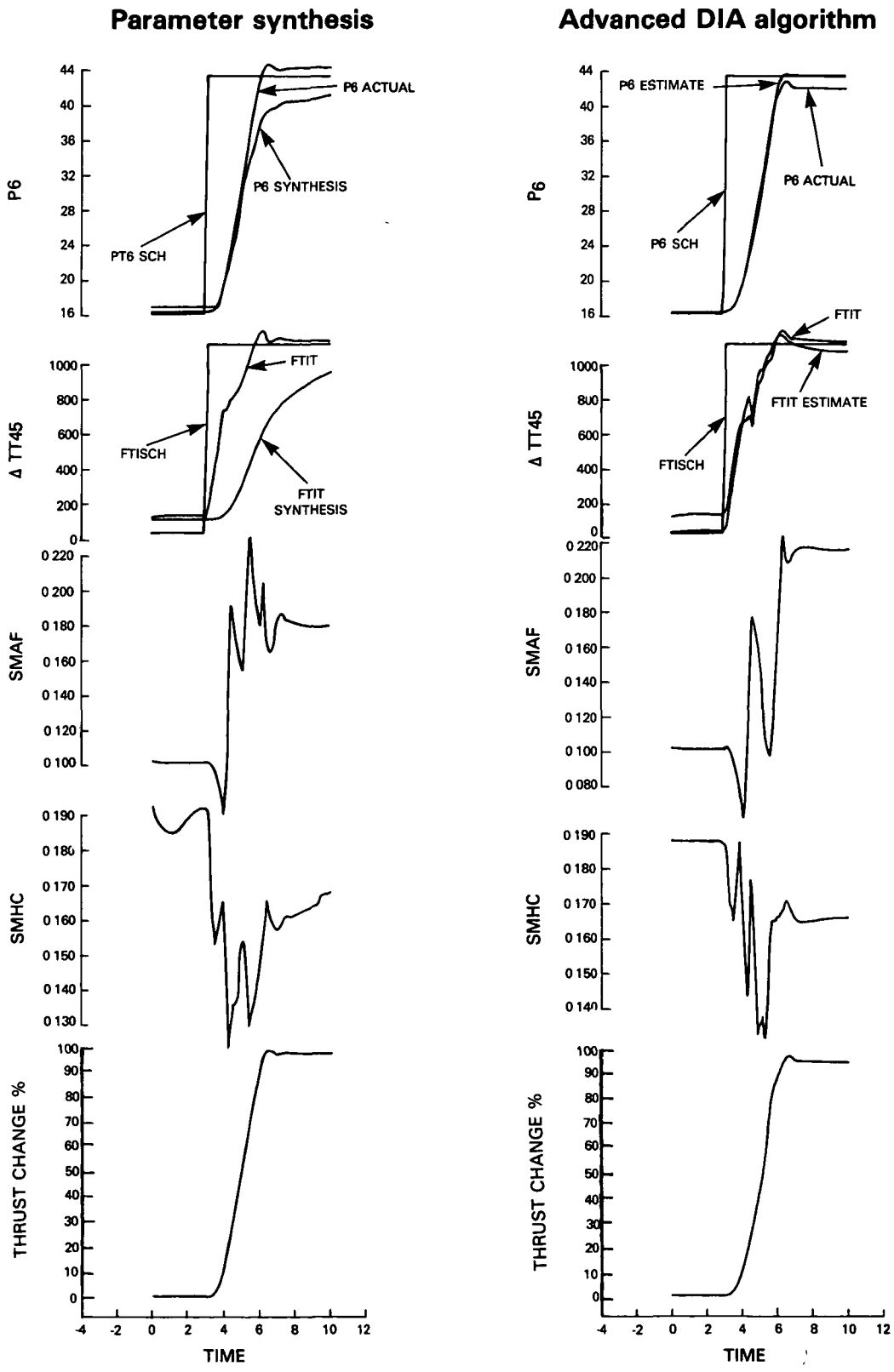

NOTE PT6 FAILED 30 PSI AT TIME = 4 SEC

Figure E-1 Failure Transient Comparisons at Sea Level Static Conditions and 20° to 83° PLA Snap PT6 Sensor Failed

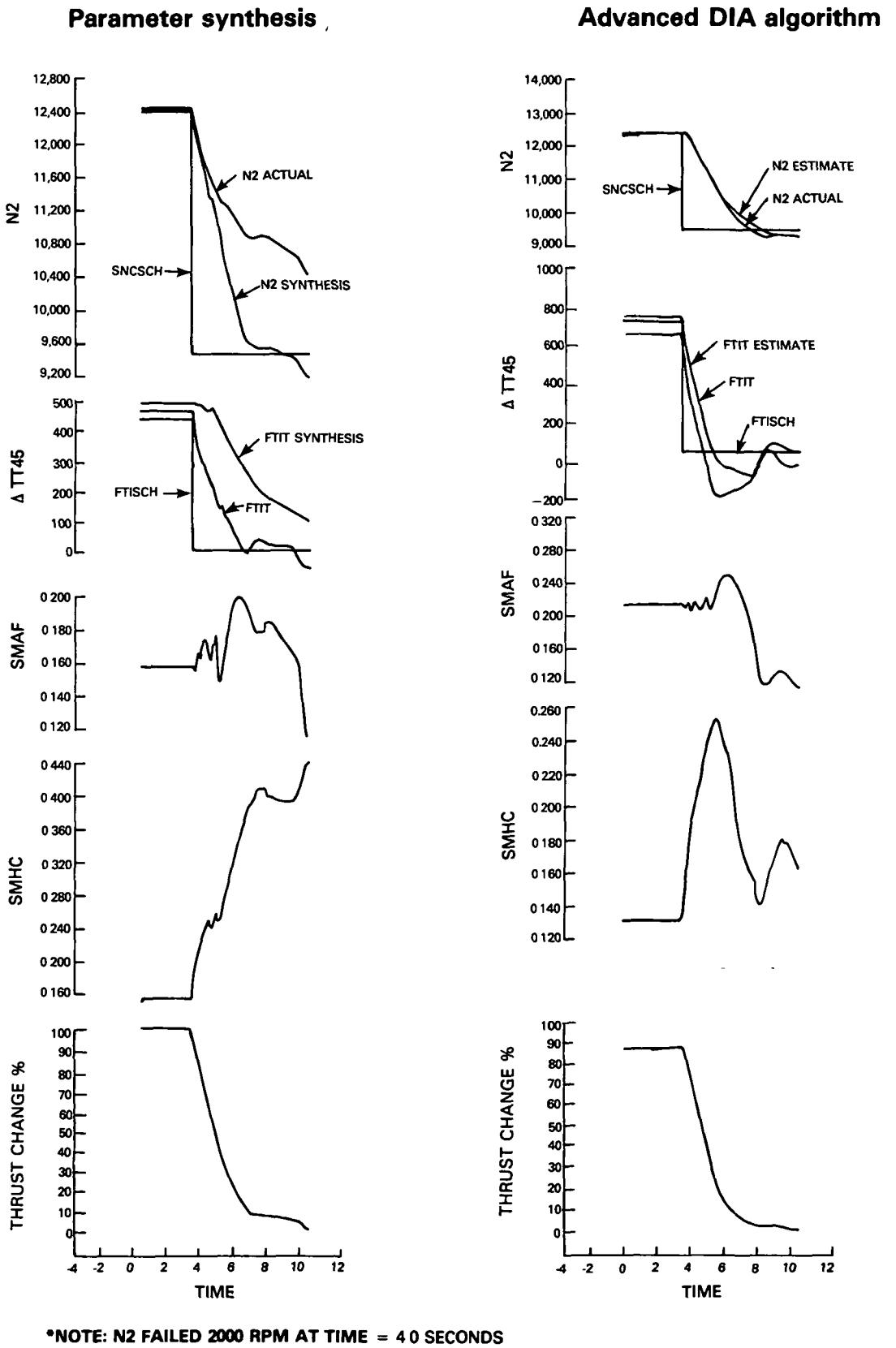

*NOTE: N2 FAILED 2000 RPM AT TIME = 4 0 SECONDS

Figure E-2 Failure Transient Comparisons at 20,000 ft/0.3 Mn Conditions and 83° to 24° PLA Snap Decel. at Time = 3.0 Seconds N2 Sensor Failed

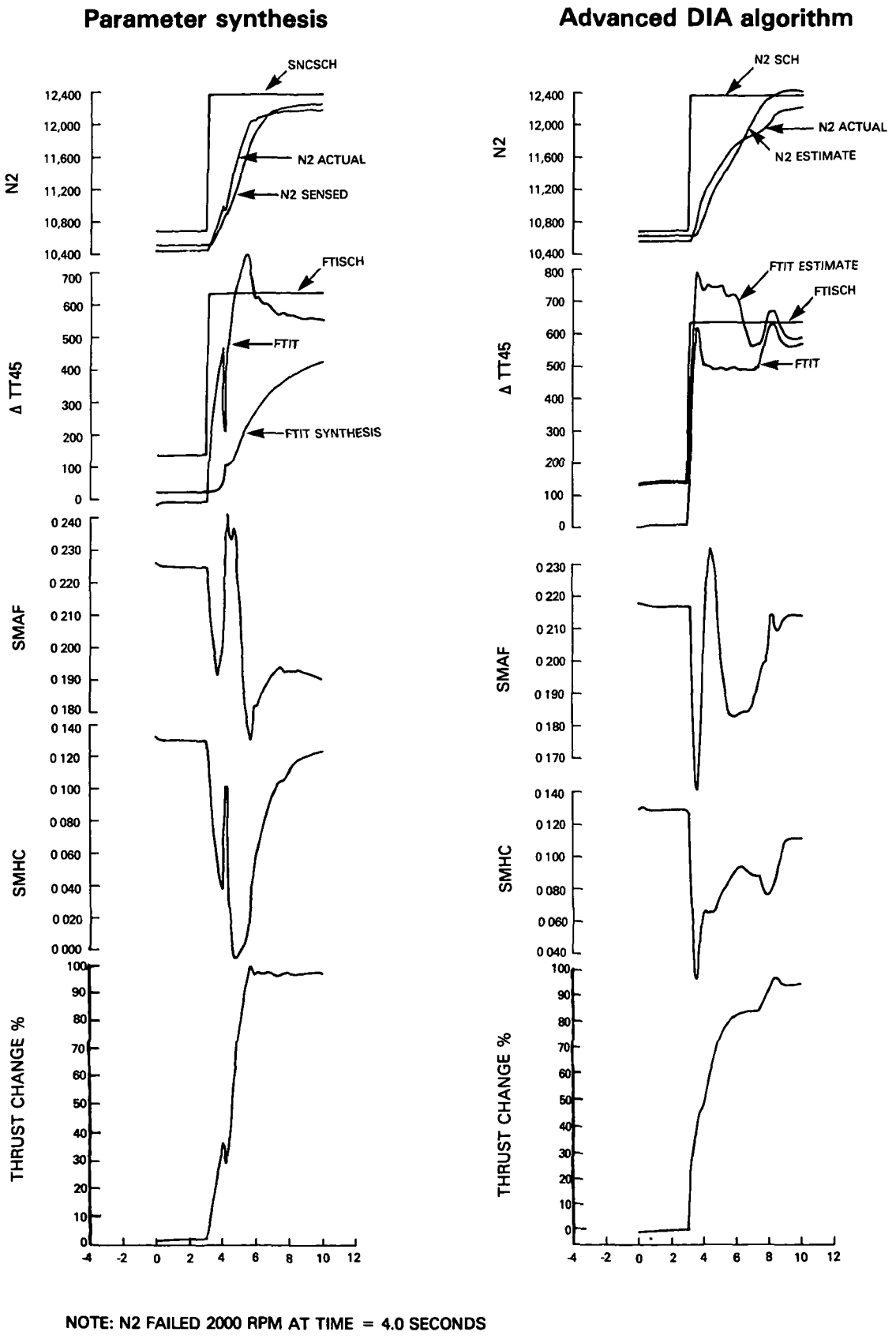

Figure E-3 Failure Transient Comparisons at 45,000 ft/0.90 Mn Conditions and 40° to 83° PLA Snap at Time = 3.0 Seconds N2 Sensor Failed

References

1. DeHoff, R.L., Hall, W.E., Adams, R.J., and Gupta, N.K., "F100 Multivariable Control Synthesis Program--Volume 1, Developement of F100 Control System", AFAPL-TR-77-35, 1977.

2. DeHoff, R.L., Hall, W.E., Adams, R.J., and Gupta, N.K., "F100 Multivariable Control Synthesis Program--Volume II, Appendices A through K", AFAPL-TR-77-35, 1977.

3. Miller, R.J., and Hackney, R.D., "F100 Multivariable Control System Engine Models/Design Criteria", Pratt & Whitney Aircraft Group, Government Products Division, AFAPL-TR-79-44, Nov. 1979.

4. Rock, S.M., and DeHoff, R.L., "Variable Cycle Engine Multivariable control Synthesis, Interim Report - Control Structure Definition," AFAPL-TR-79-2043, Feb., 1979.

5. Akhter, M. M., Rock, S.M. and DeHoff, R.L., "Trajectory Generation Techniques for Multivariable Control of Aircraft Turbine Engines", Thirteenth Asilomar Conference on Circuits, Systems and Computers, Pacific Grove California, Nov. 5 - 7, 1979.

6. Willsky, A. S., "A Survey of Design Methods for Failure Detection in Dynamic Systems", Automatica, Volume 12, PP 601-611, 1976.

7. Mehira, R. K., and Peschon, J., "An Innovations Approach to Fault Detection and Diagnosis in Dynamic Systems", Automatica, Volume 7, PP 637-640, 1971.

8. Willsky, A. S., Deyst, J. J. and Crawford, B. S., "Adaptive Filtering and Self Test Methods for Failure Detection and Compensation", Proc. of the JACC, Austin, Texas, June 1974.

9. Montgomery, R. C., and Price, D. B., "Management of Analytical Redundancy in Digital Flight Control Systems for Aircraft", AIAA Mechanics and Control of Flight Conference, Anaheim, CA, August 5-9, 1974.

10. Kerr, T. H., "A Two Ellipsoid Overlap Test For Real Time Failure Detection And Isolation By Confidence Regions", Paper No. FA5.2, IEEE Conf. on Decision and Cointrol, Phoenix, Arizona, November 1974.

11. Beard, R. V., "Failure Accommodation in Linear Systems Through Self Reorganization" Report. MVT-71-1, Man Vehicle Laboratory, Cambridge, Mass., Feb. 1971.

12. Jones, H. I., "Failure Detection in Linear Systems", Ph.D. Thesis, Dept. of Aeronautics and Astronautics, M.I.T., Cambridge, Mass., Sept. 1973.

13. Jazwinski, A. H., "Limited Memory Optimal Filtering", IEEE Trans. Aut. Control, Vol.13, 558 to 563 (1968).

14. Clark, R. N., Fosth, D. C., and Walton, V. M., "Detecting Instrument Malfunctions in Control Systems", IEEE Transactions on Aerospace and Electronic Systems, Vol. AES 11, No. 4, July 1975.

15. Broen, R. B., "A Nonlinear Voter Estimator for Redundant Systems", Proc. 1974, IEEE Conf. on Decision and Control, Phoenix, Arizona, pp. 743-748.

16. Bueno, R., "Performance and Sensitivity Analysis of the GLR Method for Failure Detection", S.M. thesis, Dept. of Aero. and Astro., M.I.T., 1976.

17. Chow, E. Y., "Analytical Studies of the Generalized Likelihood Ratio Technique for Failure Detection", SmM. thesis, Dept. of Elec. Eng. and Comp. Sci., M.I.T., Feb. 1976.

18. Gupta, N. K., Hall, W. E., "System Identification Methodology for Fault Detection and Isolation in Dynamics Systems", Interim Report for period January 1, 1976 to May 1, 1977, Prepared for Office of Naval Research, Report ONR-CR-215-245-2, February 1, 1978.

19. Van Trees, H. L., Detection, Estimation and Modulation Theory, Part III: Radar Sonar Signal Processing and Gaussian Signals in Noise, Wiley, New York (1971).

20. Davis, M. H. A., "The Application of Nonlinear Filtering to Fault Detection in Linear Systems", IEEE Transactions on Automatic Control, April 1975.

21. Fagin, S. L., "Recursive Linear Regression Theorgy, Optimal Filter Theory, and Error Analysis of Optimal Systems", IEEE Int. Conv. Record, March 1964.

22. Tarn, T. J., and Faborszky, J., "A Practical Non-diverging Filter", AIAA Journal 8, 1970.

23. Luenberger, D. G., "An Introduction to Observers", IEEE Transactions on Automatic Control, Vol. AC-16, No. 6, December 1971.

24. Papoulis, A., "Probability, Random Variables and Stochastic Processes", McGraw Hill Book Company, New York (1965).

25. Montgomery, R.C., and Price, D.B., "Failure Accommodation in Digital Flight Control Systems Accounting for Nonlinear Aircraft Dynamics", AIAA Mechanics and Control of Flight Conference, Paper 74-887, Anaheim, CA., August 5-9, 1974.

26. Davis, M.H.A., "The Application of Nonlinear Filtering to Fault Detection in Linear Systems", IEEE Transactions on Automatic Control, April, 1975, pp 257-259.

27. Schlee, F.H., Standish, C.J., and Toda, N.F., "Divergence in the Kalman Filter", AIAA Journal, Vol. 5, June 1967, pp 1114-1120.

28. Fitzgerald, R.J., "Error Divergence in Optimal Filtering Problems", 2nd IFAC Symposium on Automatic Control in Space, Vienna, Austria, September 1967.

LIST OF SYMBOLS

DIA	Detection, Isolation and Accommodation
D_i	Control to output distribution matrix corresponding to ith failure
F	System Dynamics Matrix
FMECA	Failure Mode and Effects Criticality Analysis
FTIT	Fan Turbine Inlet Temperature (°R)
G	Control to state distribution matrix
$G_i\ (k, \theta)$	Effect of a failure of type; at time θ on residual at time k
GLR	Generalized Likelihood Ratio
HO	Filter designed on the assumption of no failure
HD	Filter designed on the assumption of failure present
$\gamma(.)$	Innovations process
λI_i	Threshold for isolation corresponding to ith channel
Z	Measurement output vector
$\hat{Z}$	Estimated output vector
$p(\gamma(.)/H_i)$	Probability density function corresponding to $\gamma(.)$ assumming hypothesis H_i is true
P (0, 1)	Normal density with zero mean and unit variance
λ_D	Threshold for failure detection
X	State vector
$\hat{X}$	Estimated state vector
θ	Failure parameter or failure state
$\hat{\theta}$	Estimated value of failure parameter
X_{ss}	Steady state value of state vector
Hi	Hypothesis corresponding to ith failure
HlI_i	Bank of filters used in Concept 1 isolation technique; designed on the assumption (hypothesis) of a bias present in ith measurement

$H2I_i$	Bank of filters used in Concept 2 isolation technique; designed on the assumption (hypothesis) that ith measurement is faulty and is ignored as the input to the filter
LR	Likelihood Ratio
$\gamma_i(.)$	Innovations produced by filter corresponding to i^{th} failure
$\vec{\gamma}$	Mean value of innovations
σ	Standard deviation
Mn	Mach number
MVC	Multivariable Control
N1	Fan Speed (rpm)
N1C2	Corrected low rotor speed
N2	Compressor Speed (rpm)
N2C2	Corrected high rotor speed
PLA	Power Lever Angle (degrees)
PT2	Engine Face Pressure (psia)
PT4	Burner Pressure (psia)
PT6	Augmentor Total Pressure (psia)
q	Dynamic pressure
TT2	Engine Face Temperature (°R)
TT25	Fan Discharge Temperature (°R)
T3	Compressor discharge temperature
T4	Burner exit temperature
U	Control or input vector
X_b, U_b, Z_b	Base points vectors of state, control and measurement

DISTRIBUTION LIST

Walter Merrill
NASA LeRC
Cleveland, OH 44135
MS 100-1

20 Copies

Al Puher
NASA LeRC
Cleveland, OH 44135
MS 501-11

NASA Scientific and Technical
Information Facility
P.O. Box 8757
B.W.I. Airport, MD 21240

25 Copies

M. R. Adams
Airesearch Manufacturing Co.
402 S. #6 St. P.O. Box 5217
Phoenix, AZ 85010

William Aiken RJ-2
NASA Headquarters
Washington, DC 20546

Dr. Sheldon Baron
Bolt Beranek and Newman, Inc.
50 Moulton Street
Cambridge, MA 02138

ASD/YZE
Joe Batka
Wright Patterson AFB, OH 45433

Dorothy Brown
Technical Information Center
GM Technical Center
Warren, MI 48090

Roy Bruno Dept. 3324 Zip (AD)
Allis-Chalmers
P.O. Box 512
Milwaukee, WI 53201

F. W. Burcham
NASA DFRC
P.O. Box 273
Edwards, CA 93523

DISTRIBUTION LIST (CONT'D)

Chris Carlin
Boeing Aerospace Co.
P.O. Box 3999
Seattle, WA 98124

A. Caglayan
Bolt, Beranek, and Newman, Inc.
50 Moulton Street
Cambridge, MA 02138

Raymond Colladay RTP-6
NASA Headquarters
Washington, DC 20546

Dr. Ralph Corley
G.E. Company
Aircraft Engine Group
Cincinatti, OH 45215

David Cormier
Davy McKee Corp.
6200 Oak Tree Blvd.
Cleveland, OH 44131

DISTRIBUTION LIST (CONT'D)

Arlan Dabling
Airesearch Mfg. Co. of Arizona
111 S. 34th St. P.O. Box 5217
Phoenix, AZ 85010

Dr. John Deyst
C. Stark Draper Lab., Inc.
68 Albany Street
Cambridge, MA 02139

J. G. Elliott
Bendix Research Laboratories
Bendix Center
Southfield, MI 48076

Roger Furgurson
U.S. Army Applied Technology Labs
Ft. Eustis, VA 23604

Terry L. Greenlee, PhD
Jaycor
P.O. Box 370 1401 Camino DelMar
Delmar, CA 92014

DISTRIBUTION LIST (CONT'D)

Dr. Sol W. Gully
Alphatec
6 Iroquois Ave.
Andover, MA 01810

Dr. Thomas Houlihan
Propulsion Dynamics, Inc.
2200 Somerville
Annapolis, MD 21401

Dr. Jack Kerrebrock R
NASA Headquarters
Washington, DC 20546

Dr. Gary Leininger
Purdue University
School of Mechanical Engineering
West Lafayette, IN 47907

Jack Levine RJH-2
NASA Headquarters
Washington, DC 20546

DISTRIBUTION LIST (CONT'D)

Dr. Kenneth A. Loparo
Case Western Reserve University
Dept. of Systems Engineering
Cleveland, OH 44106

Dr. R. C. Montgomery MS 152A
NASA LaRC
Hampton, VA 23665

William F. Powers
Ford Motor Company
P.O. Box 2053
Dearborn, MI 48121

Dr. Herman A. Rediess RTE-3
NASA Headquarters
Washington, DC 20546

Charles Ryan
AFWAL/POTC
Wright Patterson AFB, OH 45433

DISTRIBUTION LIST (CONT'D)

Charles Skira
AFWAL/POTC
Wright Patterson AFB, OH 45433

Dr. Gary Slater
University of Cincinnati
Dept. of Aeronautics
Cincinnati, OH 45221

Lester Small
AFWAL/POTC
Wright Patterson AFB, OH 45433

Dr. H. Austin Spang III
G.E. Corp. Reserch & Development Center
P.O. Box 43
Schenectady, NY 12345

James Stewart E-EDC
Hugh L. Dryden FRC
Edwards, CA 93523

DISTRIBUTION LIST (CONT'D)

C. R. Stone M.S. A2340
Honeywell
2600 Ridgeway Road
Minneapolis, MN 55413

Kenneth Szalai E-EDC
NASA DFRC
Edwards, CA 93523

R. W. Vizzini
Naval Air Propulsion Test Center
Trenton, NJ 08628

Dennis Warner
Detroit Diesel Allison
P.O. Box 894
Indianapolis, IN 46206

Dr. William R. Wells
Wright State University
Chairman, Dept. of Engineering
Dayton, OH 45235

DISTRIBUTION LIST (CONT'D)

Gerald Cook
Vanderbilt University
Nashville, TN 37240

Eli Gai
CS Draper Lab
555 Technology Square
Cambridge, MA 02139

Mike Lodaya
Bendix ATC
9140 Old Annapolis RD
Columbia, MD 21045

Robert N. Clark FT-10
University of Washington
Dept. of Electrical Engineering
Seattle, WA 98195

Dr. Bernard Friedland
Kearfott Division
1150 McBride Ave.
Little Falls, NJ 07424

DISTRIBUTION LIST (CONT'D)

Pierre Mereau
Adersa/Gerbios
2 Av du 1er Mai
91120 Palaiseau FRANCE

Frank Niessen MS 1A-3-2
Hamilton Standard
Windsor Locks, CT 06096

J. Louis Tylee
EG&G Idaho, Inc.
P.O. Box 1625
Idaho Falls, ID 83415

Allen Thomas
P.O. Box 5928
Union Carbide Corp.
Greenville, SC 29606

Hugh VanLandingham
VPI & SU
Blacksburg, VA 24061

DISTRIBUTION LIST (CONT'D)

Dr. M. K. Sain
Notre Dame University
Dept. of Electrical Engineering
South Bend IN 46556

Dr. Joseph Peczkowski
Bendix Energy Controls Div.
717 N. Bendix Drive
South Bend, IN 46620

Cecil Rosen RTP-6
NASA Headquarters
Washington, DC 20546

Joe Osoni
P.O. Box 81186
Cleveland, Ohio 44181